

LEWIS ACID CATALYSED REARRANGEMENT OF EPOXIDES: A MECHANISTIC STUDY

A thesis
submitted in partial fulfilment
of the requirements for the Degree
of
Doctor of Philosophy in Chemistry
in the
University of Canterbury
by
James R. A. Cambridge

University of Canterbury

2004

WORK IN THIS THESIS HAS APPEARED IN THE FOLLOWING PUBLICATIONS

"NMR Separation of β -Prochiral Protons to the Ether Oxygen of Chiral Esters with Lanthanide Shift Reagents.", Coxon, James M.; Cambridge, James R. A.; Nam, Shayne G. C. *Org. Lett.* **2001**, 3, 4225-4227.

"Identification of β -Prochiral Protons to the Ether Oxygen of Chiral Esters of 2-Arylethan-1-ols with d -Yb(hfc)₃ Shift Reagents.", Coxon, James M.; Cambridge, James R. A.; Nam, Shayne G. C. *Synlett* **2004**, 8, 1422-1424.

Table of Contents

Abbreviations	iv
Abstract	v
Acknowledgements.....	viii
Chapter 1 - Introduction.....	1
1.1 Epoxide Structure.....	2
1.2 Rearrangement of Epoxides.....	2
1.3 Rearrangement of Symmetrically 1,1-Disubstituted Epoxide	4
1.4 BF ₃ Catalysed Rearrangement of 2,3,3-Trimethyl-1-butene Oxide.....	6
1.5 BF ₃ .OEt ₂ Catalysed Rearrangement of 1-Octene Oxide.....	8
1.6 LiClO ₄ and BF ₃ .OEt ₂ Catalysed Rearrangement of Styrene Oxide.....	9
1.7 Rearrangement of <i>p</i> -Methoxystyrene Oxide	11
1.8 BF ₃ .OEt ₂ Catalysed Rearrangement of Optically Active 1,1-Disubstituted Epoxide	13
1.9 <i>Ab Initio</i> Molecular Orbital Calculations	15
1.10 Fluorohydrin in BF ₃ Catalysed Epoxide Rearrangements	24
1.11 The Hammett Equation.....	25
1.12 Lewis Acid Catalysts for Epoxide Rearrangements ...	26
1.13 Deuterium Isotope Effects	30
1.14 Work Carried Out in this Thesis	30
Chapter 2 – NMR Determination of Prochiral Deuterium and Hydrogen Populations	33
2.1 Introduction.....	34
2.2 NMR Separation of the Prochiral Protons β- to an Ester Oxygen.....	38
2.3 Assigning the Prochiral Protons β- to an Ester Oxygen in a ¹ H NMR Spectrum	48
2.4 Relationship Between the Relative Integrals and the Delay Between Pulses in the ¹ H NMR.....	51

2.5 Integration of the ^1H NMR Spectrum Using MATLAB.....	53
Chapter 3 – Synthesis and Lewis Acid Catalysed Rearrangement of <i>p</i>-Methylstyrene Oxide	56
3.1 Introduction.....	57
3.2 Synthesis of <i>p</i> -Methylstyrene Oxide.....	58
3.3 $\text{BF}_3\cdot\text{OEt}_2$ Catalysed Rearrangement of <i>p</i> -Methylstyrene Oxide.....	69
3.4 LiClO_4 Catalysed Rearrangement of <i>p</i> -Methylstyrene Oxide.....	79
3.5 Summary of Results	88
3.6 Discussion of Errors	90
3.7 Discussion.....	90
Chapter 4 – The Role of Fluorohydrin in the Rearrangement of <i>p</i>-Methylstyrene Oxide	100
4.1 Introduction.....	101
4.2 Synthesis of Fluorohydrin	101
4.3 Conversion of Fluorohydrin to Aldehyde with $\text{BF}_3\cdot\text{OEt}_2$	105
4.4 Conclusion	106
Chapter 5 – Synthesis and Lewis Acid Catalysed Rearrangement of <i>m</i>-Methoxystyrene Oxide.....	108
5.1 Synthesis of <i>m</i> -Methoxystyrene Oxide	109
5.2 $\text{BF}_3\cdot\text{OEt}_2$ Catalysed Rearrangement of <i>m</i> -Methoxystyrene Oxide.....	117
5.3 LiClO_4 Catalysed Rearrangement of <i>m</i> -Methoxystyrene Oxide.....	123
5.4 Discussion.....	129
5.5 Implications and Major Results of this Study. The Mechanism of Epoxide Rearrangement with $\text{BF}_3\cdot\text{OEt}_2$ and LiClO_4	134
Chapter 6 – Computational Study into the Li^+ and BF_3 Catalysed Rearrangement of Styrene Oxides	136
6.1 Introduction.....	137
6.2 Li^+ Catalysed Rearrangement of Styrene Oxides	137

6.3 Geometry of Epoxide Opening	146
6.4 BF ₃ Catalysed Rearrangement of Styrene Oxides	149
6.5 Comparison to Experiment	150
Chapter 7 – BF₃ Catalysed Rearrangement of 2,3,3-Trimethyl-1,2-epoxybutane	153
7.1 Mechanism of the BF ₃ Catalysed Rearrangement of 1,1-Disubstituted Epoxide	154
7.2 B3LYP/6-31G* Density Functional Calculations	155
7.3 Rearrangement of 2,3,3-Trimethyl-1,2-epoxybutane with BF ₃ Coordinated to the More Hindered Face of the Epoxide	157
7.4 Conclusion	159
Chapter 8 – Synthesis of 1-Substituted and 1,1-Disubstituted Epoxides	160
8.1 Introduction	161
8.2 Synthesis of <i>p</i> -Methoxystyrene Oxide	161
8.3 Synthesis of Octene Oxide	164
8.4 Synthesis of 2,3,3-Trimethyl-1-butene Oxide	165
Chapter 9 – Intramolecular Acetate Attack on 1,2-Substituted Epoxide	167
9.1 Introduction	168
9.2 Molecular Modelling	169
9.3 Synthesis of 1-(2-Acetoxyphenyl)propene Oxide	170
9.4 Synthesis of 2-(3-Methyloxiranyl)-phenol Benzoate	170
9.5 Rearrangement of Epoxides with Lewis Acid	171
Summary and Future Work	172
Chapter 10 - Experimental	173
10.1 Experimental Work Described in Chapter Two	174
10.2 Experimental Work Described in Chapter Three	193
10.3 Experimental Work Described in Chapter Four	210
10.4 Experimental Work Described in Chapter Five	213
10.5 Experimental Work Described in Chapter Eight	228
10.6 Experimental Work Described in Chapter Nine	242
Appendices	249

ABBREVIATIONS

The following abbreviations are used in this thesis:

AD-mix α	Sharpless asymmetric dihydroxylation α mix
AD-mix β	Sharpless asymmetric dihydroxylation β mix
Ar	aromatic
DFT	density functional theory
Eu(dcm) ₃	tris-(d,d-dicampholylmethanato) europium(III)
Eu(dpm) ₃	(dipivalomethanato)europium(III)
Eu(hfc) ₃	europium tris[3-(heptafluoropropylhydroxymethylene)-(+)-camphorate
HF	Hartree Fock consistent field
HPLC	high performance liquid chromatography
HRMS	high resolution mass spectrometry
IRC	intrinsic reaction coordinate
MABR	methylaluminium bis(4-bromo-2,6-di- <i>tert</i> -butylphenoxide)
MTPACl	α -methoxy- α -(trifluoromethyl)phenylacetyl chloride, Mosher's acid chloride
<i>m</i> CPBA	<i>meta</i> -chloroperbenzoic acid
MP2	second order Moeler-Plesset perturbation theory
NMR	nuclear magnetic resonance spectroscopy
PES	potential energy surface scan
PIE	primary isotope effect
SCI-PCM	self-consistent isodensity polarizable continuum model
SCRF	self-consistent reaction field
SIE	secondary isotope effect
THF	tetrahydrofuran
TLC	thin layer chromatography
Yb(hfc) ₃	ytterbium tris[3-(heptafluoropropylhydroxymethylene)-(+)-camphorate

ABSTRACT

The Lewis acid catalysed rearrangement of optically active, deuterium labelled styrene oxide derivatives to aldehydes is studied experimentally and the mechanism is further elucidated by *ab initio* molecular orbital and density functional calculations. The Lewis acid catalysed rearrangement of styrene oxide derivatives is shown to occur *via* a carbocation intermediate. Opening of the epoxide ring occurs with rotation of the Lewis acid coordinated oxygen either towards or away from the aryl group to form either the *cis* or *trans* carbocation. Calculations indicate that conversion between the *cis* and *trans* cations will only occur via ring closure back to the epoxide. The selectivity for hydride migration is controlled by the preferred geometry of the carbocation intermediate, specifically whether the C-O bond prefers to adopt an eclipsed conformation relative to the adjacent cation substituent or whether the stabilisation of the cation is obtained from hyperconjugation of a terminal hydrogen to the cation centre.

Chapter One contains a review of the relevant literature and the results of previous mechanistic studies into the Lewis acid catalysed rearrangement of epoxides are discussed.

In *Chapter Two*, a methodology is developed to measure the relative amounts of hydrogen or deuterium in each position of the aldehyde produced by hydride or deuteride migration in the rearrangement of a styrene oxide derivative. The aldehyde product is reduced to an alcohol and reacted with a chiral acid chloride. The resulting ester can be analysed by ^1H NMR in the presence of $\text{Yb}(\text{hfc})_3$ or $\text{Eu}(\text{hfc})_3$ chiral shift reagents so that the full stereochemical course of the hydride migration can be determined.

Chapter Three describes the $\text{BF}_3\cdot\text{OEt}_2$ and LiClO_4 catalysed rearrangement of deuterated analogues of optically active *p*-methylstyrene oxide. It is shown that the rearrangement reaction must proceed at least in part *via* a carbocation intermediate. The results are analysed by the method of Fujimoto and show that for both the $\text{BF}_3\cdot\text{OEt}_2$ and LiClO_4 catalysed reactions, the majority of the reaction occurs by epoxide opening with rotation of

the Lewis acid coordinated oxygen towards the aromatic group (66% : 34% and 57% : 43% respectively). This is in contrast to previous studies where it was assumed that this reaction pathway would not occur. In the LiClO_4 catalysed reaction, where epoxide opening occurs with rotation of the oxygen away from the aromatic group, hydride/deuteride migration occurs almost exclusively with inversion of configuration; while in the other reactions hydride migrates to an equal extent with inversion or retention of configuration.

In *Chapter Four*, deuterated fluorohydrin is synthesised from deuterated *p*-methylstyrene oxide and converted to aldehyde with an excess of $\text{BF}_3 \cdot \text{OEt}_2$ in order to determine whether fluorohydrin is an undetected intermediate in the $\text{BF}_3 \cdot \text{OEt}_2$ catalysed rearrangement of *p*-methylstyrene oxide. It is shown the conversion of fluorohydrin to aldehyde occurs by a nearly concerted mechanism, in contrast to the rearrangement of *p*-methylstyrene oxide to aldehyde which occurs via a carbocation. The rates of the two reactions are also not compatible and fluorohydrin is shown not to be an intermediate in the reaction.

Chapter Five describes the LiClO_4 and $\text{BF}_3 \cdot \text{OEt}_2$ catalysed rearrangement of deuterated optically active *m*-methoxystyrene oxide. The selectivity for hydride migration observed is consistent with the mechanism developed for the rearrangement of *p*-methylstyrene oxide in chapter 3. More of the reaction goes by epoxide opening with rotation towards the aryl group for the destabilised *m*-methoxy compared to the *p*-methyl substituted epoxide.

Chapter Six describes a computational investigation into the BF_3 and Li^+ catalysed rearrangement of various styrene oxide derivatives. Stationary points are calculated on the potential energy surfaces for the reactions and the stationary points are characterised by vibrational frequency calculations. Two conformations of carbocation are found on the Li^+ catalysed reaction surface. One structure has the C-O bond eclipsed with the adjacent C-aryl bond and both terminal hydrogens equally aligned for migration. The other cation minimum shows one terminal hydrogen already in hyperconjugation with the carbocation *p*-orbital, making it more likely to migrate. It is also shown that rotation of the oxygen

towards and away from the aryl group can be considered separately when analysing the reaction.

Chapter Seven describes a computational study into the BF_3 catalysed rearrangement of 2,3,3-trimethyl-1-butene oxide. The results are combined with a previous computational and experimental studies and it is shown that the reaction fits with the mechanism developed to explain the results of the rearrangement of styrene oxide derivatives. The synthesis of chiral deuterated, 1-octene oxide and 2,3,3-trimethyl-1-butene oxide and the attempted synthesis of *p*-methoxystyrene oxide is described in *Chapter Eight*. *Chapter Nine* describes an investigation into acetate participation in epoxide rearrangement reactions. In this study epoxide rearranged to ketone and no participation of acetate in a cyclisation reaction was observed. The final chapter details the experimental procedures used in the preceding chapters.

ACKNOWLEDGEMENTS

Thank you to Professor Jim Coxon for your guidance and support over the years and for giving me the opportunity to complete this degree.

Thanks too to Professor Michael Hartshorn for acting as an unofficial associate supervisor over the last part of my thesis. Without your help and encouragement this thesis would never have reached its current state.

Also Dr Jonathan Morris, who provided a lot of help with ideas and techniques for the synthetic part of this project and thank you to the Morris group who put up with me crashing their group meetings.

Thanks also to the technical staff in the department for their help. Particularly Rewi Thompson for help with NMR, Bruce Clark for running mass specs and Rob McGregor for your glassblowing expertise.

Thank you to everyone who I've shared a lab with over the years, from the old days on the 6th floor with the 'Men of Steel' to the nice new 838, which has slowly been taken over by the Abell group. I'd also like to thank all the other students and post docs who make this department a fun and stimulating place to work.

Thanks to all my family and friends outside of chemistry, particularly my mother, Susan for her love and support and semi-weekly home cooked meals.

Chapter One

Introduction

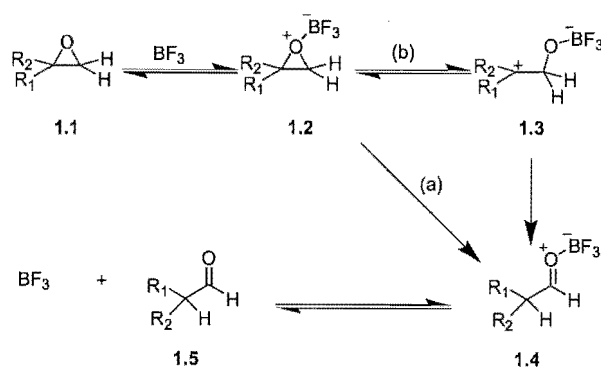
1.1 EPOXIDE STRUCTURE

The reactivity of the strained three membered epoxide ring makes the moiety ideal as an intermediate in organic synthesis and it is therefore not surprising to find epoxides important in biology. The epoxide moiety is present in many natural products and as an intermediate in many metabolic pathways.

The fast rate of epoxide opening reactions has traditionally been attributed to the relief of ring strain. However, recent work has shown that the rate acceleration is greater than can be attributed to relief of ring strain. Explanations include a stabilising interaction at the transition state from the symmetry of through bond orbitals¹ and stabilisation of the positive charge at the reaction centre by the oxygen leaving group.²

1.2 REARRANGEMENT OF EPOXIDES

Epoxide opening reactions can be facilitated by protic or Lewis acids and can be accompanied by either attack by an external nucleophile, or rearrangement involving migration of a substituent from one carbon of the epoxide ring to the other. Work in this thesis will concentrate on the Lewis acid catalysed rearrangement of α -substituted and α,α -disubstituted epoxides.³ A general mechanism of the rearrangement catalysed by BF_3 is shown in Scheme 1.1.

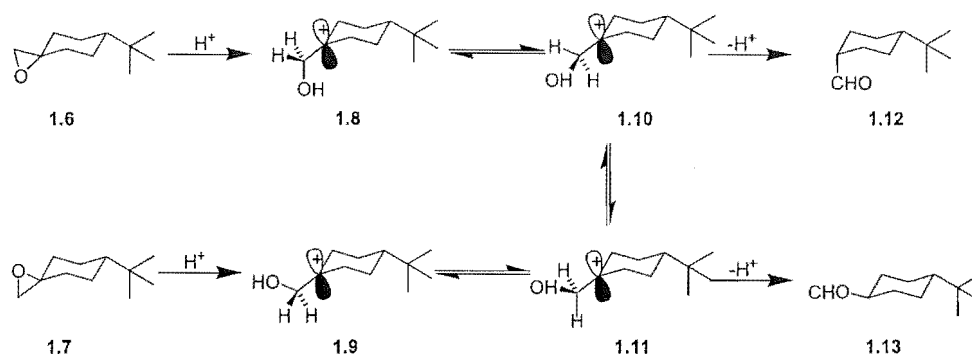


Scheme 1.1. Rearrangement of an epoxide with BF_3 .

Co-ordination of the BF_3 to either of the electron lone pairs of the epoxide provides electrophilic assistance for opening of the epoxide ring. Breaking of the epoxide C-O bond can occur either (a) with participation of the migrating hydrogen in a concerted process, or (b) without participation of the migrating group to give a short lived carbocation intermediate, where either of the two terminal hydrogens can migrate to give aldehyde.

Analysis of the selectivity for hydride migration can provide information about which of the two pathways is occurring. Rearrangement via pathway (a), where the bond making of the hydrogen to the migration terminus is involved in the breaking of the epoxide C-O bond, should result only in hydride migration with inversion of configuration at the migration terminus. Hydride migration with retention of configuration will only occur in the two step process (b), where free rotation about the C1-C2 bond of the carbocation positions a hydrogen to migrate with retention of configuration.

For many years, epoxide rearrangements were considered to be concerted. However, rearrangement of exocyclic epoxide gave epimeric mixtures of aldehydes, which can only occur when the reaction proceeds via a carbocation intermediate.⁴



Scheme 1.2. Schematic representation of epoxide rearrangement, where configuration of the ring is defined by a 4-*tert*-Bu group.

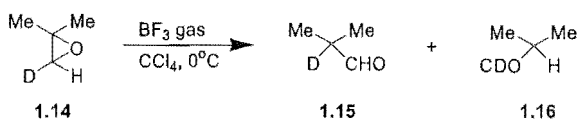
For rearrangement of each of the epoxides 1.6 and 1.7, an epimeric mixture of aldehydes 1.12 and 1.13 was obtained. In each case there was a marginal preference for aldehyde

formed from hydride migration with inversion of configuration, i.e. **1.12** from **1.6** and **1.13** from **1.7**. In a concerted process, the product of inversion would be formed exclusively. The observation that some aldehyde is formed from hydride migration with retention of configuration, is consistent with the reaction proceeding at least in part via a carbocation intermediate, especially when the concerted product would be the more thermodynamically stable equatorial aldehyde.

The marginal preference for aldehyde formation from hydride migration with inversion of configuration is explained by epoxide **1.6** initially opening to carbocation conformer **1.8**. A 60° rotation about the C1-C2 bond will give conformer **1.10**, where a hydrogen is aligned with the carbocation p orbital and can migrate with inversion of configuration. A further 60° rotation gives conformer **1.11**, where the other hydrogen is aligned to migrate with retention of configuration. If the rate of rotation were fast relative to the rate of migration, an identical ratio of epimeric aldehydes would be observed. The observed preference for the product formed from hydride migration with inversion of configuration results from the rate of rotation of the cation being comparable to the rate of hydride migration.

1.3 REARRANGEMENT OF SYMMETRICALLY 1,1-DISUBSTITUTED EPOXIDE

In order to obtain an estimate for the deuterium isotope effect for a 1,2 hydrogen migration, Blackett and co-workers⁵ rearranged the symmetrical epoxide 1,2-epoxy methylpropane **1.14** with BF_3 in CCl_4 (Scheme 1.3).

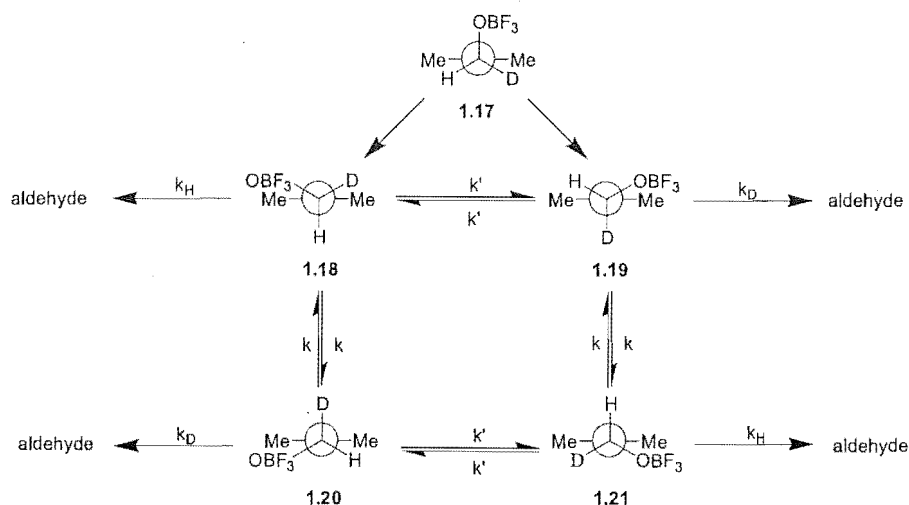


Scheme 1.3. BF_3 catalysed rearrangement of 1,2-epoxy methylpropane-1- d_1 .

The aldehyde reacted further with epoxide to give dioxolane and a small correction was necessary to account for an isotope effect in this process. The ratio of hydrogen to

deuterium migration (M_H/M_D) was 1.92. The primary isotope effect for the hydride shift can be obtained by adjusting the value of M_H/M_D by the small secondary deuterium isotope effect. It was assumed that the secondary isotope effect was in the range of 1.0-1.2 and the true primary isotope effect, $k_H/k_D = \text{ca. } 2$.

The rearrangement was considered to occur by the following mechanism:



Scheme 1.4. Migration of hydrogen and deuterium in the rearrangement of 1,2-epoxy methylpropane-1- d_1 .

It was assumed that there were six minimum energy conformations of cation that need to be considered. Four have a hydrogen or deuterium aligned for migration with the carbocation p orbital (**1.18**, **1.19**, **1.20** and **1.21**). The other two structures (**1.17** and its mirror image) have the OBF_3 group at 90 degrees to the cation plane. Recent gas phase calculations have however shown¹⁵ that none of these structures are minimum energy conformations at the B3LYP/6-31G* level of theory and that the only cation minimum has the C-O bond eclipsing the adjacent C-C bond.

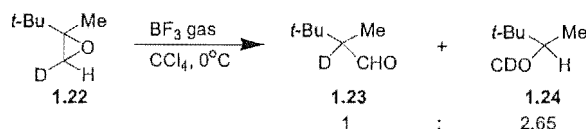
k_H (k_D) is the rate constant for the 1,2 migration of hydrogen (deuterium) from a carbon bearing a deuterium (hydrogen). The ratio k_H^D/k_D^H is the ratio of the rate of hydride

migration from a carbon carrying a deuterium / the rate of deuteride migration from a carbon carrying a hydrogen and hence the ratio contains both primary and secondary isotope effects. Calculations have been carried out by Aaron Thorpe¹⁵ to separate these effects.

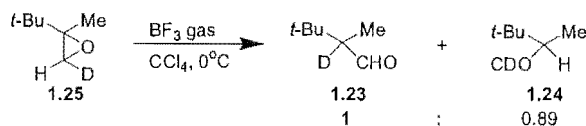
1.4 BF₃ CATALYSED REARRANGEMENT OF 2,3,3-TRIMETHYL-1-BUTENE OXIDE

Blackett et al.⁶ further investigated the selectivity for hydride migration in the rearrangement of α,α -disubstituted epoxide by rearrangement of the two deuterio isomers of 2,3,3-trimethyl-1-butene oxide **1.22** and **1.25**. In this system the symmetry present in the methylpropene oxide system is destroyed and more information can be obtained.

The reaction was again complicated by the aldehyde products reacting with epoxide to form dioxolane. Small corrections were therefore made to compensate for the secondary deuterium isotope effect for this reaction. The final, corrected ratios of deuterium labelled aldehydes are shown in Schemes 1.5 and 1.6.



Scheme 1.5. Rearrangement of **1.22**.

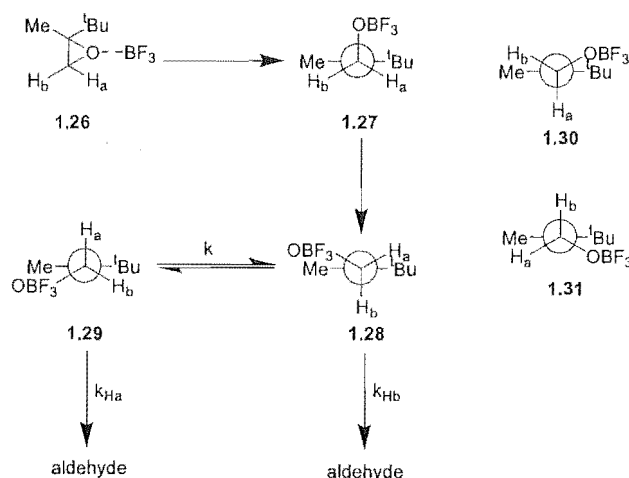


Scheme 1.6. Rearrangement of **1.25**.

More deuterium relative to hydride migration is observed in the rearrangement of epoxide **1.25** than in the rearrangement of epoxide **1.22**. Assuming that the deuterium isotope effect is the same or similar in both reactions, migration of the hydrogen *trans* to the bulky

tertiary butyl group will be preferred in the rearrangement of non deuterium labelled material.

Blackett's results were interpreted using the following mechanistic scheme:



Scheme 1.7. Blackett's mechanistic scheme for the rearrangement of 2,3,3-trimethylbut-1-ene oxide.

Co-ordination of BF_3 to epoxide facilitates ring opening to give cation conformer **1.27**. It was assumed that the OBF_3 group rotates in the direction to relieve the steric interaction between the bulky tertiary butyl group and the OBF_3 . A 60° rotation about the C1-C2 bond will give conformer **1.28**, where H_b is aligned with the cation p -orbital and can migrate. A further 60° rotation would give conformer **1.29**, where H_a is aligned with the adjacent p -orbital and can migrate. It was assumed that there is a barrier to rotation between the two essentially mirror image conformers, caused by the eclipsing of the methyl and OBF_3 groups.

Conformations **1.30** and **1.31** were assumed by Blackett to be too high in energy due to the steric interaction between the gauche arrangement of the OBF_3 and tertiary butyl groups. Blackett used racemic epoxides and so in his experiment aldehyde formed from conformer

1.28 is indistinguishable from aldehyde from conformer **1.31**. Likewise, it was not possible to determine the contribution of conformer **1.29** relative to **1.30**.

The studies reported in this thesis use optically active epoxide so that measurement of the full stereochemical course of hydride (deuteride) migration can be made.

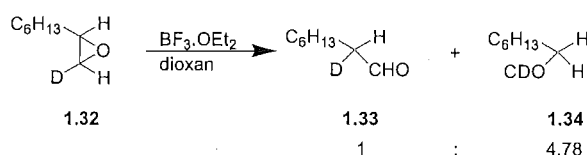
The relative values for the rate constants for deuteride ($k_D = 1.0$) compared to hydride ($k_H = 1.71$) migration and the rate constant for interconversion of conformers **1.28** and **1.29** ($k = 1.84$) can be evaluated using the expressions:⁶

$$x/x = 1/0.89 = (k_D / k_H)[1 + (k_H / k)]$$

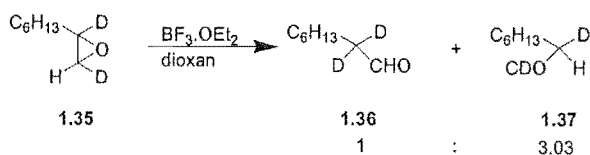
$$x/x = 2.65 = (k_H / k_D)[1 + (k_D / k)]$$

1.5 BF₃.OEt₂ CATALYSED REARRANGEMENT OF 1-OCTENE OXIDE

Lim et al.⁷ investigated the rearrangement of 1-deuterated and 1,2-dideuterated 1,2-epoxyoctane (**1.32** and **1.35**, Schemes 1.8 and 1.9), where a secondary carbocation intermediate could be formed in contrast to the tertiary cation in the system investigated by Blackett. Experiments also showed that an ether solvent (dioxane) was required to effect clean rearrangement of the less substituted epoxide. This was rationalised in terms of the extra stabilisation required for cleavage of a secondary as opposed to tertiary carbon-oxygen bond.



Scheme 1.8. Rearrangement of octene oxide.



Scheme 1.9. Rearrangement of octene oxide.

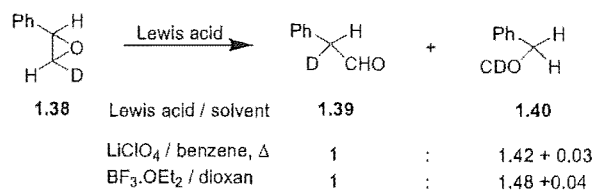
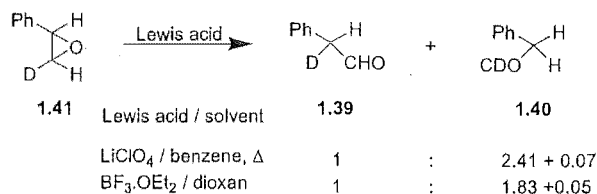
The results are consistent with the Blackett model, more deuterium migrates on rearrangement of **1.35** than **1.32**, showing that migration of the hydrogen *trans* to the bulky substituent is preferred over migration of the *cis* hydrogen.

The larger deuterium isotope effect calculated for the rearrangement of octene oxide ($k_{\text{H}}/k_{\text{D}} = 4.3$) than for the rearrangement of 2,3,3-trimethyl-1-butene oxide ($k_{\text{H}}/k_{\text{D}} = 1.7$) is consistent with the migrating hydrogen being more symmetrically bonded between C1 and C2 in the transition state for the rearrangement of octene oxide.

1.6 LiClO₄ AND BF₃·OEt₂ CATALYSED REARRANGEMENT OF STYRENE OXIDE

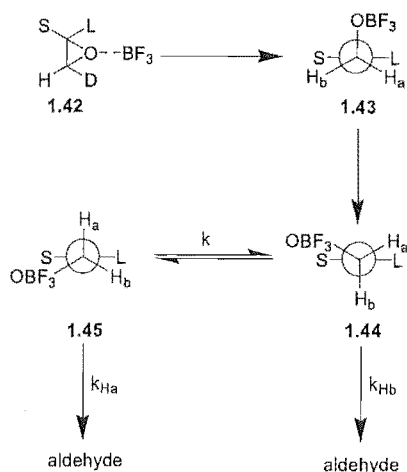
McDonald et al.⁸ investigated the rearrangement of racemic deuterated styrene oxide with LiClO₄ in refluxing benzene and with BF₃·OEt₂ in dioxan at room temperature (Schemes 1.10 and 1.11).^{*} It was expected that the aromatic substituent would stabilise a carbocation intermediate more than in the rearrangement of alkyl substituted epoxide, making it less likely that the reaction will occur via a concerted process.

^{*} A further investigation into the rearrangement of optically active styrene oxide by Shayne Nam has found that the results of McDonald may be compromised by traces of acid present in the samples of epoxide starting material.

Scheme 1.10. McDonald's rearrangement of styrene oxide-β-*d*₁.Scheme 1.11. McDonald's rearrangement of styrene oxide-β-*d*₁.

For the rearrangement of styrene oxide with both LiClO₄ and BF₃·OEt₂, more deuterium migration is observed from rearrangement of *trans*, rather than *cis* deuterated epoxide. This is similar to the selectivity observed from rearrangement of 2,3,3-trimethylbut-1-ene oxide and 1-octene oxide.

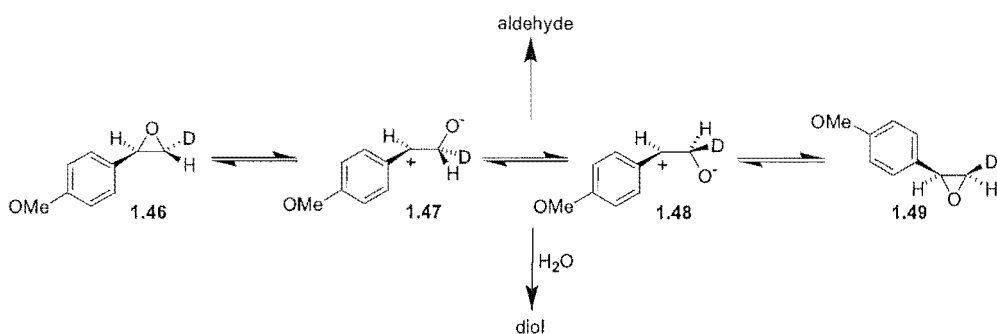
The results from all three of the above studies have been explained by the Blackett model (Scheme 1.12) where rotation of the cation intermediate occurs in the direction to relieve the 1,4 steric interaction between the bulky substituent and the O⁺BF₃ group. Conformation **1.44** is formed first, allowing hydrogen H_b to migrate with inversion of configuration, before rotation to form conformer **1.45**, where H_a can migrate with retention of configuration at the migration terminus. These two experiments used non-optically active epoxide and so the assumption that migration would occur from only these two conformations could not be tested.



Scheme 1.12. General mechanism of α,α -disubstituted epoxide rearrangement.

1.7 REARRANGEMENT OF *p*-METHOXYSTYRENE OXIDE

Whalen et al.⁹ examined the rearrangement of *p*-methoxystyrene oxide in an aqueous solution of 0.1 M NaClO₄ (Scheme 1.13). The ratio of hydrogen migration to deuterium migration was determined to be ca. 3:1. This ratio is similar to the kinetic isotope effect observed previously for a 1,2-hydride migration¹⁰ and it was therefore suggested that the cation intermediate is long lived and that both terminal hydrogens have equal migratory aptitudes.



Scheme 1.13. Reaction of *p*-methoxystyrene oxide in acidic solution.

Examination of unreacted epoxide starting material after one half-life of the reaction revealed that scrambling of the deuterium label between the *cis* and *trans* positions had occurred. This was attributed to epoxide opening to the stabilised carbocation, which has a long enough lifetime so that bond rotation and ring closure to the enantiomeric epoxide can occur before hydride migrates to form aldehyde (Scheme 1.13). Opening of the epoxide under these acidic conditions is therefore reversible.

Coxon et al.¹¹ later challenged Whalen's conclusions. Since isomerisation of the epoxide is not complete after one half-life of the reaction, the rate of hydride migration is comparable, with the rate of rotation for conversion between the cation conformers. Based on the observed preference for migration of the H_R terminal, prochiral proton (*trans* to the bulky substituent) in the rearrangement of 1-octene oxide and 2,3,3-trimethyl-1-butene oxide, it was argued that a similar bias for migration in the rearrangement of *p*-methoxystyrene oxide should exist when the rate of hydride migration is similar or greater than the rate of rotation of the carbocation.

A solution to this issue required that the rate constants for conversion of epoxide isomers vs. hydride migration be determined. Whalen et al.¹² showed that the two prochiral hydrogens did indeed migrate to an equal extent. The rate of conversion of **1.46** in an equilibrium mixture of **1.46** and **1.49** in 1 : 9 dioxane(*d*₈)-water (pH 9.1) was determined by ¹H NMR spectroscopy to be $2.4 \pm 0.1 \times 10^{-3} \text{ s}^{-1}$. The rate constant for epoxide conversion to aldehyde in the same solvent system was determined to be $7.1 \times 10^{-4} \text{ s}^{-1}$. The rate of equilibration of epoxide deuterioisomers therefore exceeds the rate of epoxide conversion to aldehyde by a factor of 3.4.

Whalen also measured the amount of hydrogen compared to deuterium migration that had occurred during aldehyde formation at various stages during the reaction. It was determined that the ratio of hydride/deuteride migration during aldehyde formation remained constant as the ratio of epoxides **1.46** : **1.49** changed. This showed that *cis* and *trans* deuterium have equal migratory aptitudes, within the experimental error. Further

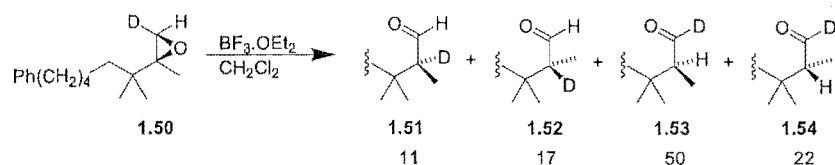
evidence for the equal migratory aptitudes of the *cis* and *trans* hydrogen (deuterium) comes from rate data, which shows that the rate adheres strictly to first order kinetics.

There were two important results from Whalen's study on the reaction of *p*-methoxystyrene oxide: (1) Epoxide opening to cation is reversible. (2) There is no stereoselection and both methylene hydrogens appear to have equal migratory aptitudes.

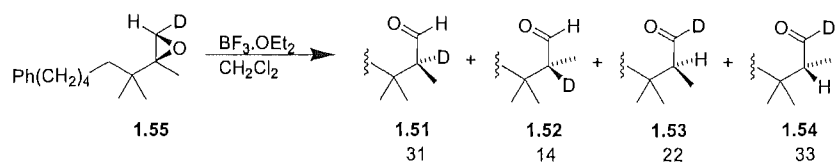
1.8 BF₃.OEt₂ CATALYSED REARRANGEMENT OF OPTICALLY ACTIVE 1,1-DISUBSTITUTED EPOXIDE

Fujimoto recently published an important paper,¹³ investigating the stereoselectivity of hydride migration in the rearrangement of optically active epoxides **1.50** and **1.55** (Schemes 1.14 and 1.15). The two α substituents on this epoxide have a similar steric requirement to the epoxide system studied by Blackett and so should have similar stereoselectivity for hydride migration.

The two deuterio isomers were synthesised enantioselectively using the Sharpless asymmetric dihydroxylation and epoxidation. The epoxides were rearranged with BF₃.OEt₂ in CH₂Cl₂ to give aldehyde, but in low yield (21%). The ratio of aldehydes **1.51-1.54** produced was analysed by reduction with LiAlH₄ or LiAlD₄ and reaction of the resulting alcohol with (*S*)-MPTACl to give the (*R*)-MPTA ester. The signals for the *S* and *R* protons at C2 of the aldehyde were separated in their ¹H NMR spectrum, allowing integration and determination of the relative aldehyde populations. The results are shown in Schemes 1.14 and 1.15.

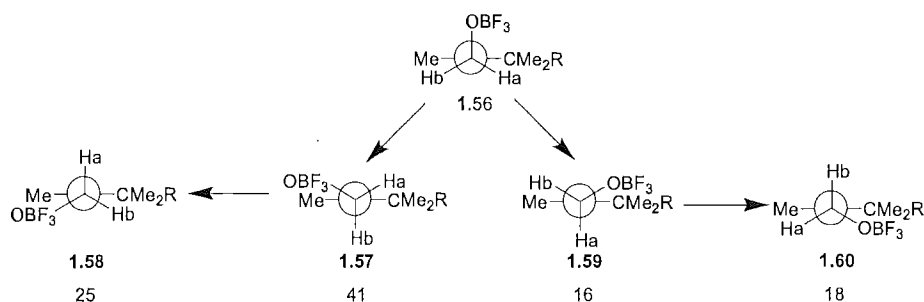


Scheme 1.14. Fujimoto's rearrangement of **1.50**.



Scheme 1.15. Fujimoto's rearrangement of **1.55**.

A deuterium isotope parameter z , was determined from the equation $31z : 14z : 22 : 33 = 50 : 22 : 11z : 17z$ to be 1.77. This is the amount deuterium migration is retarded relative to hydrogen migration. The value of z was used to estimate the relative amounts of aldehydes **1.51-1.54** that would be formed from undeuterated epoxide (41:18:16:25). This is the ratio of the four transition conformers for hydride migration shown in Scheme 1.16.



Scheme 1.16. Transition conformers in the rearrangement of undeuterated epoxide.

Fujimoto determined that in undeuterated epoxide, the hydrogen *trans* to the bulky substituent is 1.44 fold more likely to migrate than the *cis* hydrogen. This is similar to the result of Blackett et al., who determined that the *trans* hydrogen prefers to migrate by a ratio of ca. 1.9 : 1.

Blackett et al. only considered that conformers **1.57** and **1.58** were present in the rearrangement process because the system studied did not give sufficient experimental information to include in the analysis the possibility that on opening of the epoxide rotation might occur in both directions. The results from the rearrangement of optically active epoxide show that a significant amount (ca. 34%) of the reaction goes through

conformations **1.59** and **1.60**, where the bulky substituent and OBF_3^- groups are in a gauche orientation. The results also confirm that ‘the hydrogen *anti* to the bulky substituent prefers to migrate with inversion of configuration at the migrating terminus, whereas the hydrogen *syn* to the bulky substituent prefers to migrate with retention of configuration.’

1.8.1 Comparing the Fujimoto study to the Blackett Mechanism

The mathematics developed by Blackett to calculate rate constants for conversion between cation conformers relative to hydride (deuteride) migration can be applied to each side of the Fujimoto Scheme. A sensible answer can be obtained for the left hand side, but the right hand side, migration from conformer **1.60** is favoured over migration from conformer **1.59**. This does not make sense in terms of the Blackett model for conversion between cation minima structures. Calculations presented in this thesis on the rearrangement of 2,3,3-trimethyl-1-butene oxide go some way to explaining this result.

1.9 AB INITIO MOLECULAR ORBITAL CALCULATIONS

1.9.1 Rearrangement of protonated propene oxide

Calculations at the MP2/6-31G**//MP2/6-31G* level show that there is a concerted reaction pathway connecting protonated propene oxide to protonated propanal.¹⁴ Closer investigation of the reaction pathway reveals that hydride migration does not commence until breaking of the C-O bond is complete, giving a concerted asynchronous pathway.

Protonation can occur on either face of epoxide. Protonation of the face anti to the methyl group is favoured by 0.2 kcal/mol over protonation to the other face. The barrier for interconversion between the two invertomers is calculated at 16.9 kcal/mol (Figure 1.1) and conversion between 1.61 and 1.63 is most likely to occur by dissociation/reformation of the O-H bond.

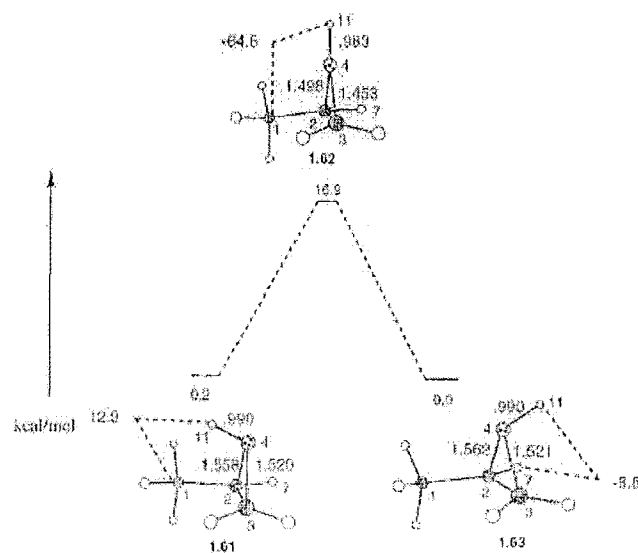


Figure 1.1. Conversion between invertomers of protonated propene oxide.

Transition states were found for epoxide opening with rotation of the OH^+ either towards or away from the methyl group. The lowest energy pathway connects **1.63** to **1.65**, via transition structure **1.64** (Figure 1.2). At the transition state for this reaction, opening of the epoxide ring is nearly complete while migration of the hydrogen has not begun to any significant extent.

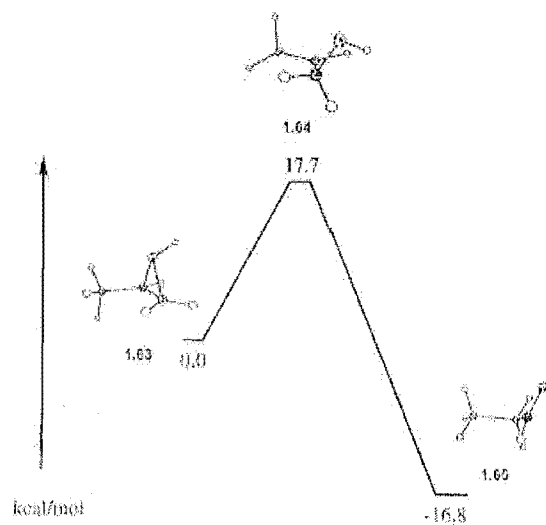


Figure 1.2. Concerted pathway for rearrangement of protonated propene oxide to protonated propanal.

Two carbocation minima were found. The planar structure **1.67**, where the C-O bond is in an eclipsed conformation with respect to the C2-methyl bond and structure **1.70**, where the C-O bond is eclipsing the adjacent C-H bond. IRC calculations showed that these cation structures were not intermediates for the rearrangement of epoxide to aldehyde.

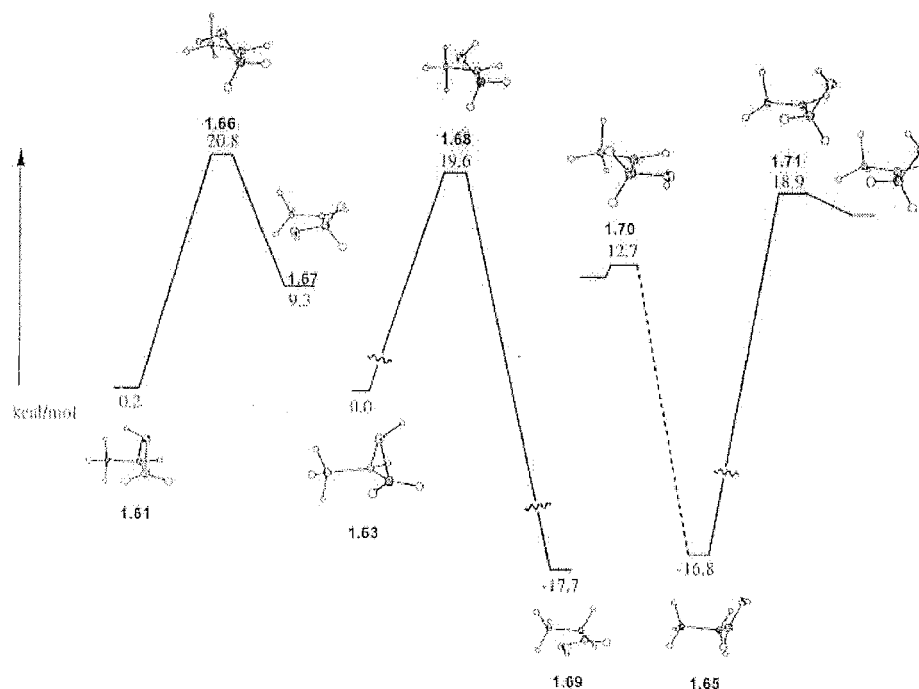


Figure 1.3. Reaction surface for the rearrangement of protonated propene oxide.

Structure **1.67**, where the C-O bond is eclipsing the adjacent C-C bond is 3.4 kcal lower in energy than **1.70**. The lowest energy pathway for concerted rearrangement involves ring opening of the epoxide with rotation in the direction towards the less stable carbocation.

1.9.2 Proton and BF_3 catalysed rearrangement of methylpropene oxide

The proton acid and BF_3 catalysed rearrangement of the symmetrically 1,1-disubstituted epoxide methylpropene oxide was investigated by computational methods.¹⁵

The potential energy surface for the H^+ catalysed rearrangement of methylpropene oxide to methylpropanal is shown in Figure 1.4. Protonated epoxide opens to the symmetrical carbocation **1.75**, where the C-O bond is eclipsed relative to the adjacent C-C bond. Hydride migration from **1.75**, via transition structure **1.76**, gives aldehyde. The primary and secondary deuterium isotope effects, calculated for the hydride migration step were 2.401 and 0.859 respectively. In contrast to the rearrangement of protonated propene oxide,

no concerted pathway was found connecting protonated methylpropene oxide and protonated methylpropanal.

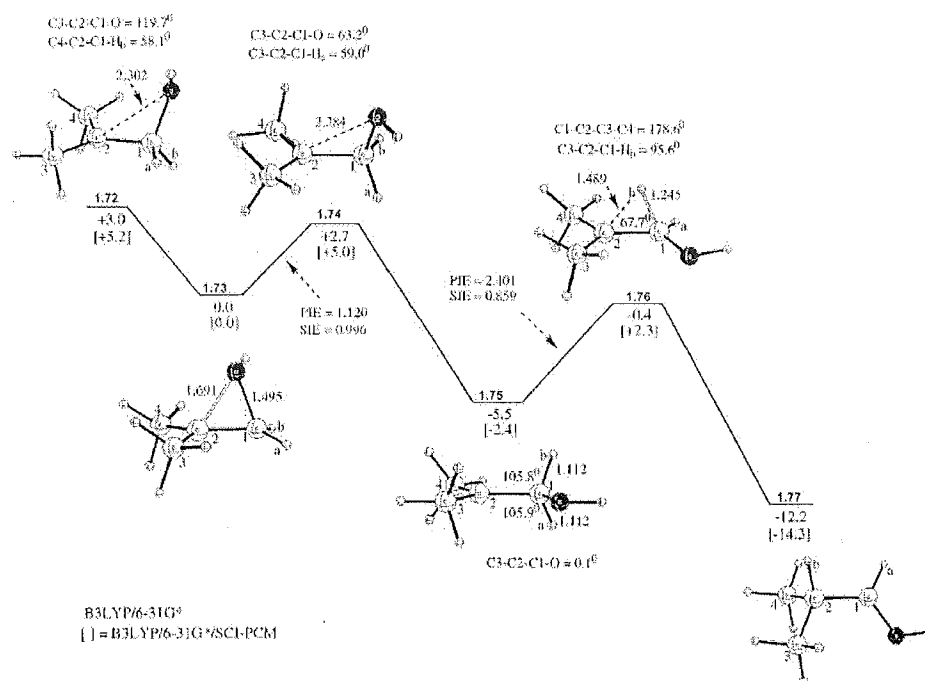


Figure 1.4. H^+ catalysed rearrangement of methylpropene oxide.

The potential energy surface calculated for the BF_3 catalysed rearrangement is shown in Figure 1.5. Similar to the H^+ catalysed reaction, epoxide opens to a discrete carbocation minimum before hydride migration occurs to give aldehyde.

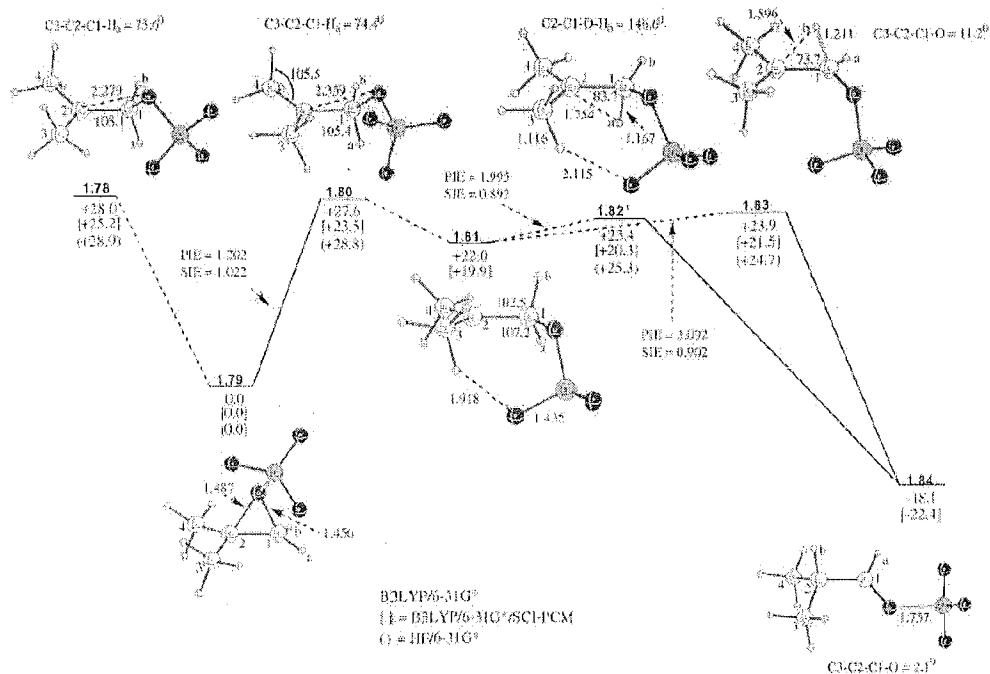


Figure 1.5. BF_3 catalysed rearrangement of methylpropene oxide.

The structure of the carbocation intermediate **1.81** has a fluorine from the BF_3 hydrogen bonded to a hydrogen from the adjacent methyl group. The transition state for interconversion between **1.81** and **1.81a** is shown in Figure 1.6. The symmetrical transition state **1.85** is 3.2 kcal/mol higher in energy than the minimum energy structures, but becomes 0.8 kcal/mol lower in energy than **1.81** and **1.81a** when a SCI-PCM single point solvent energy calculation is carried out on each of the structures.

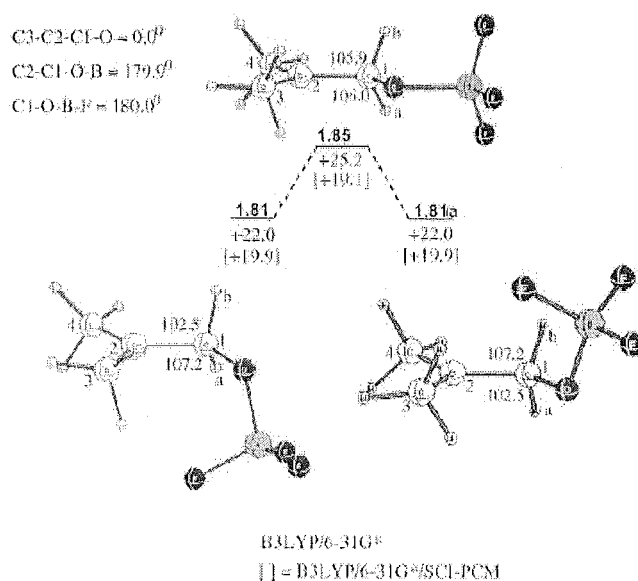


Figure 1.6. Conversion between cation minima.

The non-symmetrical geometry of the BF_3 group results in there being two transition states for hydride migration. Transition structure **1.82**, where the migrating hydrogen is on the same face as the BF_3 group, is 0.5 kcal/mol lower in energy than **1.83**. However, when an SCI-PCM single point solvent energy calculation is carried out on each of the structures, structure **1.83** becomes 0.6 kcal/mol lower in energy than **1.82**.

Primary and secondary deuterium isotope effects (PIE and SIE) were calculated for the hydride migration and these can be compared to the experimentally determined preference for migration, $M_H/M_D = 1.92$ (see section 1.3). The inverse SIE was $k_H/k_D = 0.811$ (an isotope effect of < 1 is considered an inverse isotope effect while $k_H/k_D > 1$ is considered a normal isotope effect). This could be applied to the experimentally determined value of M_H/M_D to obtain the corrected PIE of $k_H/k_D = 1.557$, which is close to the calculated value of $k_H/k_D = 1.677$. The small PIE reflects the fact that hydride migration is not very advanced in the transition state.

In contrast to the mechanistic scheme developed by Blackett to explain his experimental results, only one minimum conformation of carbocation was obtained, **1.81**, where the C-O

bond is eclipsing the adjacent C-C bond. Variations in cation were only due to the positioning of the BF_3 in and out of the plane of the carbocation. Migration of both methylene hydrogens should occur to an equal extent from the symmetrical carbocation.

1.9.3 BF_3 catalysed rearrangement of 2,3,3-trimethyl-1,2-epoxybutane

The BF_3 catalysed rearrangement of 2,3,3-trimethyl-1,2-epoxybutane was investigated by density functional theory B3LYP/6-31G* level calculations.¹⁶ Blackett had rearranged the epoxide with BF_3 gas in CCl_4 at 0°C and assumed that epoxide would open to a carbocation where the oxygen would always rotate away from the bulky tertiary butyl group.

The calculations included single point energy calculations with (SCRF) SCI-PCM solvation sphere with a dielectric constant of 2.23 (CCl_4). Consistent with the mechanism put forward by Blackett et al., only ring opening of epoxide with rotation away from the tertiary butyl group was considered. More recently Fujimoto et al. have shown that a significant amount of the reaction occurs by rotation of the OBF_3 group towards the bulkier tertiary butyl group. Further calculations are presented in this thesis that better explain the results from the experimental study.

Attack of a fluorine from BF_3 was determined to be a facile process (Figure 1.7). Fluorohydrin formation has been noted in several epoxide rearrangements, most notably by Fujimoto et al. in their rearrangement of **1.50** and **1.55**.

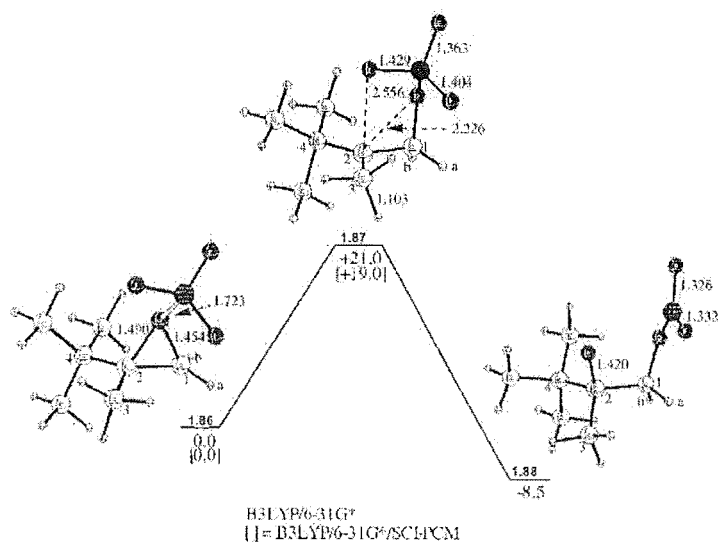


Figure 1.7. Attack of fluorine from BF_3 .

The potential energy surface calculated for the rearrangement is shown in Figure 1.8. Structure **1.90** has the C-O bond eclipsing the adjacent C^+ -methyl bond and structure **1.92** has a hydrogen hyperconjugating to the unfilled cation p-orbital. The two structures have identical energies when an SCI-PCM solvent calculation is carried out on each. Two transition states for hydrogen migration are calculated, like the potential energy surface for the BF_3 catalysed rearrangement of methylpropene oxide. The two transition states differ by whether the hydrogen is migrating on the same face as the BF_3 group (structure **1.94**) or the opposite face as in structure **1.93**.

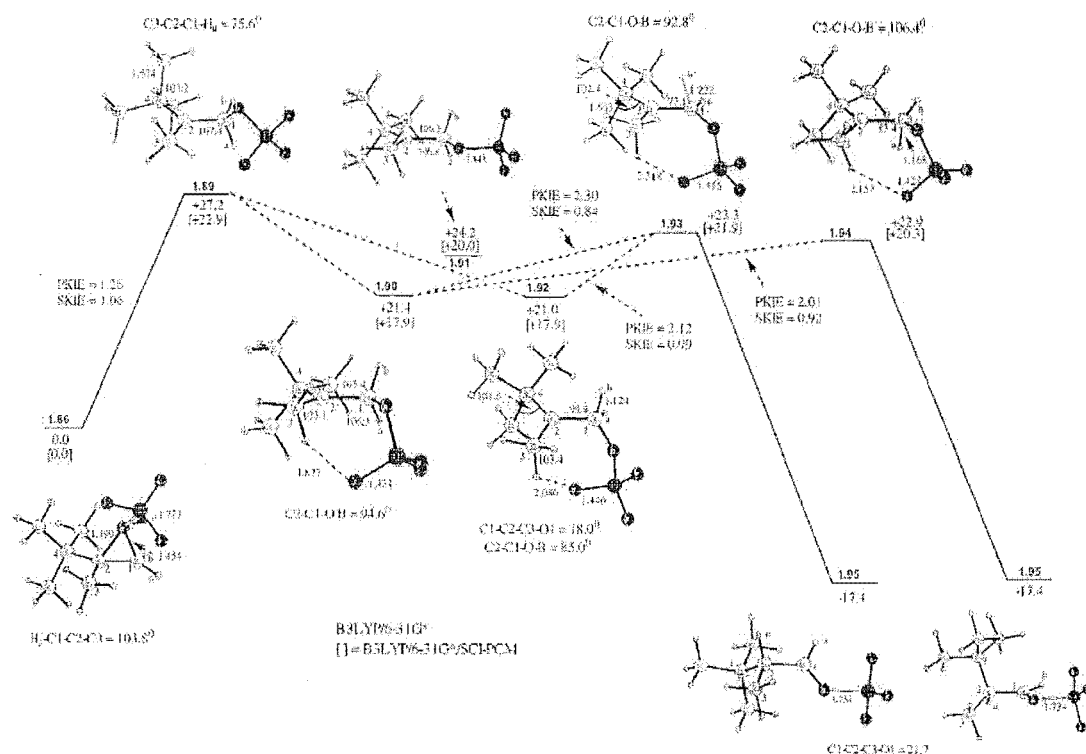


Figure 1.8. Potential energy surface for the BF_3 catalysed rearrangement of 2,3,3-trimethyl-1,2-epoxybutane.

1.10 FLUOROHYDRIN IN BF_3 CATALYSED EPOXIDE REARRANGEMENTS

The low yield obtained in the rearrangement of epoxide by Fujimoto et al. was due mainly to the efficacy with which epoxide gave fluorohydrin when the reaction was carried out at low temperatures or with a reduced amount of $\text{BF}_3 \cdot \text{OEt}_2$. Other examples exist in the literature¹⁷ where an attempted epoxide rearrangement with $\text{BF}_3 \cdot \text{OEt}_2$ has resulted in fluorohydrin formation and in one case¹⁸ more vigorous reaction conditions completed the transformation to epoxide.

Calculations on the BF_3 catalysed rearrangement of 2,3,3-trimethylbut-1-ene showed that the barrier to fluorohydrin formation was lower than the barrier to rearrangement in the gas phase. However fluorohydrin formation is not observed in the solution phase experiment of Blackett et al. It is expected that the cation will be solvated in the solution phase and this

will modify the electrophilicity of the cation centre and possibly block the approach of the fluorine to the cation.

1.11 THE HAMMETT EQUATION

In this thesis the effect of substituents on the aromatic ring of styrene oxide is investigated. The substituents are expected to either stabilise or destabilise the charged intermediates and transition states in the rearrangement process. The electron withdrawing or donating ability of a substituent can be measured by its σ value in the Hammett equation:

$$\log(k/k_0) = \sigma\rho$$

where k and k_0 are the rate constants for the reaction of the substituted and unsubstituted compound, σ is the substituent constant and ρ is the reaction constant.

The reaction of *m*-methoxystyrene oxide, styrene oxide, *p*-methylstyrene oxide and *p*-methoxystyrene oxide are discussed in this thesis. The *m*-methoxy group is electron withdrawing, having a positive σ_m with respect to hydrogen and the *p*-methyl and *p*-methoxy substituents are both electron donating relative to hydrogen and have a negative σ_p . Their σ values are shown in Table 1.1:¹⁹

Group	σ_p	σ_m
<i>meta</i> methoxy		+0.10
hydrogen	0	0
<i>para</i> methyl	-0.14	
<i>para</i> methoxy	-0.28	

Table 1.1. Hammett σ values.

A short lived carbocation intermediate has been impossible to study spectroscopically to date, except under super acid conditions, due to its transitory lifetime and therefore

molecular orbital calculations are used to determine barriers to rotation and minimum energy conformers of the cation intermediate.

Previous studies have investigated the structure of benzylic cations. The aromatic ring adopts a planar structure with respect to the empty p-orbital of the benzylic cation. The planar geometry allows overlap of the empty p-orbital with the filled π orbital of the aromatic ring (Figure 1.9). Computational studies at the HF/STO-3G level show that the structure of the benzyl cation is best represented by resonance structure **1.98**, where the most of the positive charge lies on the para carbon of the ring.²⁰

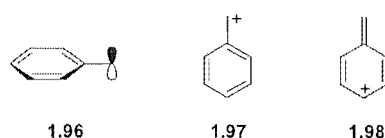


Figure 1.9. Structure of the benzylic cation.

The barrier to rotation about the phenyl-carbenium bond in a series of carbenium ions with different substituents was calculated by complete line shape analysis of the NMR spectrum or by spin saturation transfer.²¹ ΔG values ranged from 36 to 78 kJ mol^{-1} .

1.12 LEWIS ACID CATALYSTS FOR EPOXIDE REARRANGEMENTS

Many types of catalyst exist for promoting epoxide opening reactions. Protic acids have been used, but the conjugate base of a protic acid is often nucleophilic enough to prevent rearrangement of an opened epoxide. More usually, Lewis acids are used, where co-ordination of the Lewis acid to either of the epoxide lone pairs provides the electrophilic assistance necessary for epoxide opening.

Thorpe et al.¹⁵ have investigated the co-ordination of BF_3 and H^+ to epoxide. Co-ordination to the least hindered face is marginally preferred. Co-ordination of a proton to the less hindered face of propene oxide was calculated to be favoured by 0.2 kcal/mol over protonation to the more hindered face. The barrier for concerted conversion between the

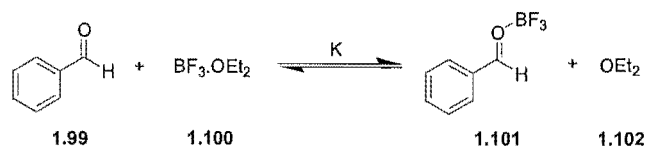
two protonated structures was calculated to be 16.9 kcal/mol at the MP2/6-31G**/MP2/6-31G* level of theory however interconversion is thought to be more likely by equilibrium between the coordinated forms and uncoordinated epoxide.

Studies investigating the structure of BF_3 ²² and other Lewis acids²³ co-ordinated to carbonyl compounds show that BF_3 co-ordinates to the lone pairs of the oxygen, while the interaction of a lithium ion is electrostatic. Examples also exist where both lone pairs on the oxygen are co-ordinated to a Lewis acid.²⁴

1.12.1 BF_3 as a catalyst

There are no experimental studies in the literature investigating the co-ordination of BF_3 to epoxides, however there should be similarities between BF_3 co-ordination to the lone pairs on carbonyl compounds and co-ordination to the lone pairs on epoxide. The electronic structures of BF_3 co-ordinated to carbonyl compounds has been extensively studied by *ab initio* molecular orbital calculations²⁵ and recently an x-ray crystal structure of BF_3 co-ordinated to benzaldehyde has been published.²⁶ The crystal structure shows that the BF_3 co-ordinates to the oxygen in a *trans* conformation.

A study has also been completed investigating the equilibrium constants between $\text{BF}_3 \cdot \text{OEt}_2$ and carbonyl compounds.²⁷ It was found that for the equilibrium:



Scheme 1.17. Equilibrium between $\text{BF}_3 \cdot \text{OEt}_2$ and BF_3 co-ordinated benzaldehyde.

the equilibrium constant, $K = 0.208$ in CH_2Cl_2 .

1.12.2 LiClO₄

Recent reports in the literature suggest that highly concentrated solutions of LiClO₄ in diethyl ether can induce highly selective transformations. In contrast to the Lewis acid BF₃, where co-ordination is expected to the lone pairs of an ether oxygen, LiClO₄ has been shown to interact in an electrostatic fashion with oxygen containing substrates.

1.12.3 MABR

Recently, a bulky Lewis acid methylaluminium bis(4-bromo-2,6-di-*tert*-butylphenoxide) (MABR) has been used to rearrange α,α -disubstituted epoxides with a high degree of control over the diastereoselectivity for hydride migration.²⁸ MABR has been used to rearrange a variety of epoxides to carbonyl compounds in high yield, with a high degree of regio- and stereoselectivity.

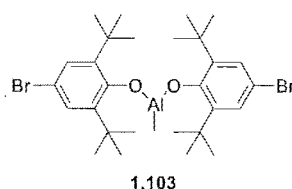
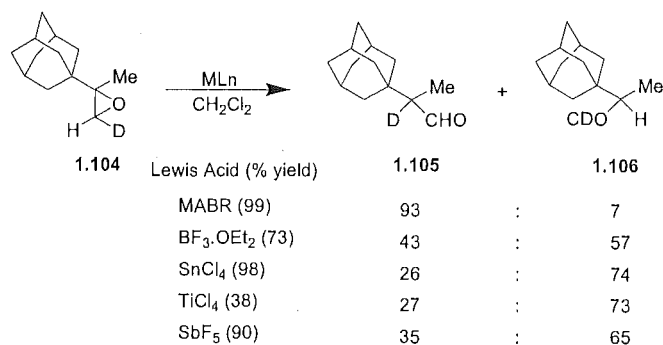
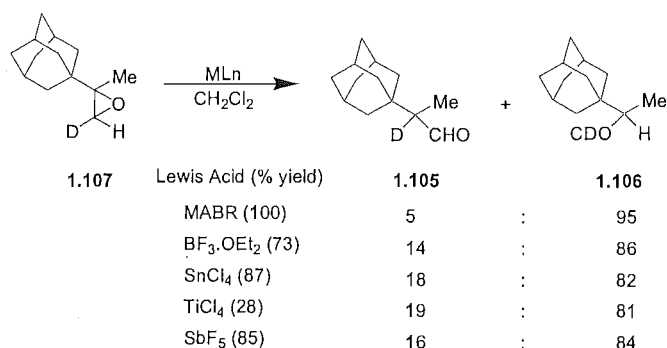


Figure 1.9. MABR.

The high degree of selectivity has been shown by the comparison of the ratio of aldehydes produced on rearrangement of *cis* and *trans* terminally deuterated epoxides. Various Lewis acids were used to effect the rearrangement of epoxides **1.104** and **1.107** (Schemes 1.18 and 1.19).²⁹ Each rearrangement reaction used 2 equivalents of Lewis acid in CH₂Cl₂:

Scheme 1.18. Lewis acid promoted rearrangement of **1.104**.Scheme 1.19. Lewis acid promoted rearrangement of **1.107**.

For each Lewis acid catalyst, more deuterium migration is observed for the rearrangement of **1.104** than **1.107**. This is consistent with the previously observed preference for migration of the hydrogen trans to the bulky substituent compared to migration of the *cis* hydrogen.⁶ The bulkiness of the MABR reagent explains the greater selectivity for rearrangement of the epoxides with MABR than for rearrangement with any other Lewis acid.

The steric interaction between the bulky adamantyl group and the bulky MABR Lewis acid will ensure that rotation of the oxygen co-ordinated Lewis acid will be in the direction to relieve the steric interaction. Rotation in the direction to relieve the steric interaction will

be much more favoured in the case of the bulkier Lewis acid. The selectivity observed is in all cases in agreement with the Blackett mechanism for epoxide rearrangement.

1.13 DEUTERIUM ISOTOPE EFFECTS

Isotope effects are a measure of the change in reaction rate as a result of isotopic substitution and reflect a change in structure of the reactant and transition structure of a chemical reaction. Isotope effects are divided into primary and secondary isotope effects and are considered “normal” when $k_H/k_D > 1$ and “inverse” when $k_H/k_D < 1$.

Primary isotope effects arise when the bond to an isotope is broken during the course of a chemical reaction; secondary isotope effects result when the isotope is at the reaction centre, but the bond is not broken during the reaction.

Isotope effects result from the change in the vibrational frequency in the reactant and transition state structure resulting from the different atomic mass of the isotopes. The deuterium isotope effect will be at a maximum when the hydrogen is symmetrically bonded in the transition state.³⁰

1.14 WORK CARRIED OUT IN THIS THESIS

The objective of work in this thesis is to further investigate the mechanism of epoxide rearrangement. Specifically, whether the rearrangement proceeds via a concerted or carbocation pathway and what factors influence the selectivity in the rearrangement process.

Of the mechanistic studies described above only that of Fujimoto et al. used optically active epoxide, other studies used racemic epoxide and assumptions were made about the stereoselectivity of the rearrangement process. In this investigation optically active epoxide is used and these assumptions can be tested. The use of epoxide substituents with differing electronic demand can further probe the fundamental mechanism for rearrangement by either stabilising, or destabilising any intermediates formed in the course of the reaction.

Chapter 2 deals with finding a method to analyse the products from the deuterium labelled epoxide rearrangement reaction. Using a combination of chiral derivatising agents and chiral shift reagents an NMR method is developed that distinguishes between aldehydes that are chiral by virtue of isotopic substitution.

The synthesis and rearrangement of regioselectively deuterated epoxides is described in chapters 3 and 5. Chapter 4 investigates whether fluorohydrin is formed as an intermediate in the $\text{BF}_3 \cdot \text{OEt}_2$ catalysed rearrangement of *p*-methylstyrene oxide and is responsible for the unexpected selectivity for hydride (deuteride) migration observed in this reaction.

Ab initio molecular orbital calculations are also used in order to obtain the structures and energies of different structures along the potential energy hypersurface of the reaction. Of particular interest is the investigation of the structure and conformation of any high energy intermediates formed, something that is impossible to determine by normal spectroscopic means due to the transitory lifetime of the intermediate.

¹ Sawicka, D.; Wilsey, S.; Houk, K. N. *J. Am. Chem. Soc.* **1999**, *121*, 864-865.

² Banks, H. D. *J. Org. Chem.* **2003**, *68*, 2639-2644.

³ Blackett, B. N.; Coxon, J. M.; Hartshorn, M. P.; Richards, K. E. *Aust. J. Chem.* **1970**, *23*, 2077-2084.

⁴ Blackett, B. N.; Coxon, J. M.; Hartshorn, M. P.; Jackson, B. L. J.; Muir, C. N. *Tetrahedron* **1969**, *25*, 1479.

⁵ Blackett, B. N.; Coxon, J. M.; Hartshorn, M. P.; Richards, K. E. *Aust. J. Chem.* **1970**, *23*, 839-840.

⁶ Blackett, B. N.; Coxon, J. M.; Hartshorn, M. P.; Richards, K. E. *J. Am. Chem. Soc.* **1970**, *92*, 2574-2575.

⁷ Coxon, J. M.; Lim, C. *Aust. J. Chem.* **1977**, *30*, 1137-1143.

⁸ Coxon, J. M.; McDonald, D. Q. *Tetrahedron Lett.* **1988**, *29*, 2575-2576.

⁹ Ukachukwa, V. C.; Blumenstein, J. J.; Whalen, D. L. *J. Am. Chem. Soc.* **1986**, *108*, 5039-5040.

¹⁰ (a) Collins, C. J.; Rainey, W. T.; Smith, W. B.; Kaye, I. A. *J. Am. Chem. Soc.* **1959**, *81*, 460. (b) Winstein, S.; Takahashi, J. *Tetrahedron* **1958**, *2*, 316.

¹¹ Coxon, J. M.; Hartshorn, M. P. *Tetrahedron Lett.* **1987**, *28*, 1333-1336.

¹² Ukachukwu, V. C.; Whalen, D. L. *Tetrahedron Lett.* **1988**, *29*, 293-296.

¹³ Hara, N.; Mochizuki, A.; Tatara, A.; Fujimoto, Y. *Tetrahedron Asymm.* **2000**, *11*, 1859-1868.

¹⁴ Coxon, J. M.; MacLagan, R. G. A. R.; Rauk, A.; Thorpe, A. J.; Whalen, D. *J. Am. Chem. Soc.* **1997**, *119*, 4712-4718.

¹⁵ Coxon, J. M.; Thorpe, A. J.; Smith, W. B. *J. Org. Chem.* **1999**, *64*, 9575-9586.

¹⁶ Coxon, J. M.; Thorpe, A. J. *J. Org. Chem.* **2000**, *65*, 8421-8429.

¹⁷ Marouka, K.; Murase, N.; Bureau, R.; Ooi, T.; Yamamoto, H. *Tetrahedron*, **1994**, *50*, 3663-3672.

¹⁸ Butke, G. P.; Jimenez, F.; Michalik, J.; Gorski, R. A. *J. Org. Chem.*, **1978**, *43*, 955-960.

¹⁹ March, J. *Advanced Organic Chemistry 3rd ed.* John Wiley and Sons **1985**.

²⁰ Kirmse, W.; Kund, K.; Ritzer, E. *J. Am. Chem. Soc.* **1986**, *108*, 6045-6046.

²¹ Jost, R.; Sommer, J. *J. Chem. Soc., Perkin Trans. 2* **1983**, 927-932.

²² Gung, B. W.; Wolf, M. A. *J. Org. Chem.* **1992**, *57*, 1370-1375.

²³ Wiberg, K. B.; Marquez, M.; Castejon, H. *J. Org. Chem.* **1994**, *59*, 6817-6822.

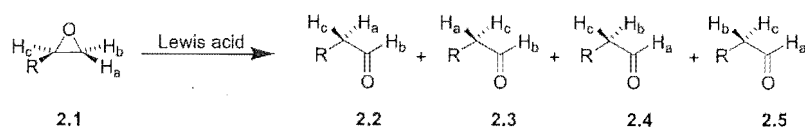
-
- ²⁴ Lewinski, J.; Zachara, J.; Horeglad, P.; Glinka, D.; Lipkowski, J.; Justyniak, I. *Inorg. Chem.* **2001**, *40*, 6086-6087.
- ²⁵ Gung, B. W.; Wolf, M. A. *J. Org. Chem.* **1992**, *57*, 1370-1375.
- ²⁶ Reetz, M. T.; Hullmann, M.; Massa, W.; Berger, S.; Rademacher, P.; Heymanns, P. *J. Am. Chem. Soc.* **1986**, *108*, 2405-2408.
- ²⁷ Gajewski, J. J.; Ngernmeersri, P. *Org. Lett.* **2000**, *2*, 2813-2815.
- ²⁸ Marouka, K.; Nagahara, S.; Ooi, T.; Yamamoto, H. *Tetrahedron Lett.* **1989**, *30*, 5607-5610.
- ²⁹ Maruoka, K.; Ooi, T.; Yamamoto, H. *Tetrahedron* **1992**, *48*, 3303-3312.
- ³⁰ O'Farral, R. A. M. *J. Chem. Soc. (B)* **1970**, 785-790.

Chapter Two

NMR Determination of Prochiral Deuterium and Hydrogen Populations

2.1 INTRODUCTION

Rearrangement of monosubstituted oxirane to aldehyde involves a 1,2 hydrogen shift (Scheme 2.1). The terminal epoxide hydrogens can migrate with retention or inversion of configuration to give four aldehydes. We require a method to determine the ratio of aldehydes **2.2-2.5** when any of the hydrogens Ha, Hb or Hc are replaced with deuterium.



Scheme 2.1. Rearrangement of monosubstituted epoxide.

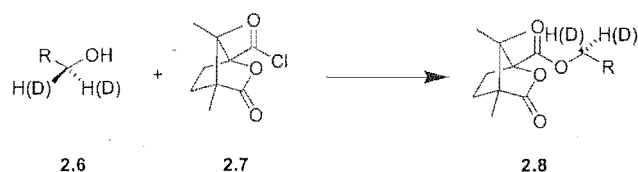
When either Ha or Hb are labelled as deuterium, the relative amount of hydrogen vs deuterium migration can be measured by a combination of ^1H and ^2H NMR. For example, in a deuterium NMR the integral for the signal of the deuterium at C1 relative to the C2 deuterium integral gives a direct measure of the relative amounts of aldehydes **2.2** and **2.3** vs **2.4** and **2.5**.

In order to measure the facial selectivity for hydride (deuteride) migration (ie the amount of aldehyde **2.2** vs the amount of **2.3** and the amount of **2.4** vs **2.5**), a method is required to measure the hydrogen and deuterium in each of the prochiral positions at C2 of the aldehyde. Since the C2 hydrogens are prochiral and indistinguishable in a normal NMR spectrum, asymmetry must be induced to make the prochiral protons magnetically non-equivalent and hence resolvable in an NMR spectrum. Furthermore the signals must be able to be fully resolved for accurate integration.

2.1.1 Chiral derivatising agents

Chiral derivatizing agents, chiral shift reagents and chiral solvating agents have all been used to induce asymmetry in prochiral protons.¹ For example camphanic chloride has been used as a chiral auxiliary for NMR resolution of prochiral protons adjacent to an alcohol functionality.² Primary alcohols have been reacted with (1*S*)-(-)-camphanic chloride to

form a chiral ester.³ The ester on its own did not provide sufficient asymmetry to resolve the prochiral protons, so further resolution was obtained by the addition of a europium shift reagent (either $\text{Eu}(\text{dpm})_3$ or $\text{Eu}(\text{dcm})_3$ (Figure 2.1)) to the NMR solution, allowing resolution and integration of the prochiral protons α - to the ester oxygen.



Scheme 2.2. Resolution of prochiral hydrogens/deuteriums by reaction with a chiral derivatising reagent.

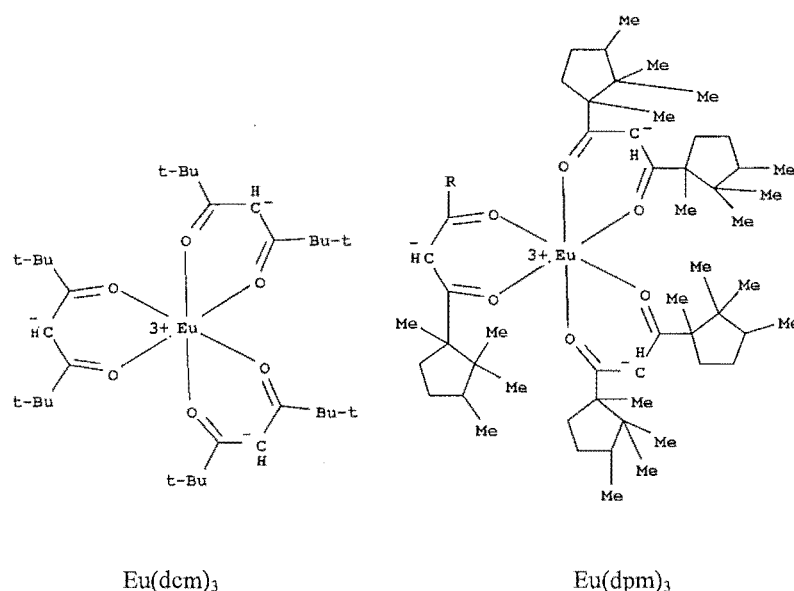


Figure 2.1. Structure of $\text{Eu}(\text{dpm})_3$ and $\text{Eu}(\text{dcm})_3$.

It was envisaged that a chiral acid chloride derivatising agent could be used to analyse the products from epoxide rearrangement if the aldehyde was first reduced to alcohol. In contrast to the previous work, where resolution of the prochiral protons α - to an ester

oxygen has been achieved, we require a system that will allow NMR separation of the protons β - to the ester oxygen.

2.1.2 Chiral shift reagents

When greater resolution is required in an NMR spectrum, a lanthanide shift reagent can be used. The lanthanide reagent is a hard Lewis acid that can be added to an NMR solution of a substrate. The metal co-ordinates to the hard Lewis basic groups of the substrate, creating a substrate-shift reagent complex that is in fast equilibrium with substrate and shift reagent.

A proton signal brought under the influence of a metal ion's paramagnetic field is deshielded and moves downfield in a ^1H NMR spectrum. The interaction between the paramagnetic metal and the NMR nucleus is known as a pseudocontact shift, a through space interaction and the magnitude of the downfield shift is inversely proportional to the cube of the average distance between the metal ion and the nucleus of interest.

Three factors influence the magnitude of a proton's downfield shift. As mentioned above, the distance of the proton nucleus from the metal centre is paramount, but also important is the equilibrium constant of the substrate-shift reagent complex. A third factor to influence the downfield shift is the geometry of the complex: the closer the proton is to the perpendicular pseudosymmetry axis of the shift reagent, the greater the shift.

A proton in close proximity to the paramagnetic field of the shift reagent is broadened due to the faster spin-lattice relaxation time of the proton from the influence of the paramagnetic field. For most metal ions, line broadening of the ^1H NMR signals is large rendering them ineffectual as shift reagents, however for lanthanides line broadening of the proton signals is small compared to the magnitude of the downfield shift.

Chiral ligands can be added to the lanthanide, creating a chiral shift reagent that can be used for the resolution of enantiomers in an NMR spectrum.⁴ The shift reagent used most extensively in our investigations is ytterbium tris[3-(heptafluoropropylhydroxymethylene)-(+)-camphorate ($\text{Yb}(\text{hfc})_3$) (Figure 2.2).

2.2 NMR SEPARATION OF THE PROCHIRAL PROTONS β - TO AN ESTER OXYGEN

We required that the prochiral protons be in a magnetically asymmetric environment so they would become magnetically non-equivalent and resolvable in a ^1H NMR spectrum. It was thought that a chiral derivatising agent may be able to be enhanced by the addition of a chiral shift reagent, resulting in a diastereomeric complex. This is similar to previous examples where camphanic acid chloride has been used as a chiral derivatising agent to introduce asymmetry to the environment and further resolution has been obtained by the use of (non-chiral) lanthanide shift reagents. In these previous examples, the protons α - to the ester linkage were resolved, however we require that the prochiral protons on the beta carbon also be resolved and this is considerably more demanding.

Reduction of the aldehyde product from rearrangement to an alcohol is required so that the chiral acid chloride derivatising agent can be added to give a chiral ester. Reduction of the aldehyde to an alcohol will also reduce the chance of enolisation of the aldehyde and loss of the deuterium label at C2. The alcohol formed from reduction of the rearrangement product of styrene oxide is 2-phenylethanol. Initial studies focused on the resolution of the prochiral protons in the 1 and 2 positions of this alcohol with the use of chiral derivatising agents and chiral shift reagents. Four chiral acid chlorides were investigated for use as chiral derivatising agents: (1*S*)-(-)-camphanic chloride **2.10**, *N*-(1-naphthalenesulfonyl)-*S*-phenylalanyl chloride **2.11**, *N*-(*p*-toluenesulfonyl)-*S*-phenylalanyl chloride **2.12** and *N*-(4-nitrophenylsulfonyl)-*S*-phenylalanyl chloride **2.13** (Figure 2.3).

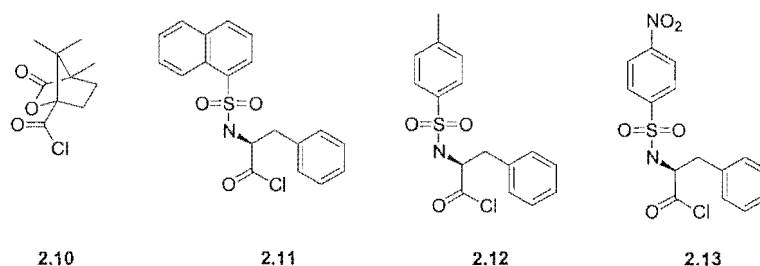
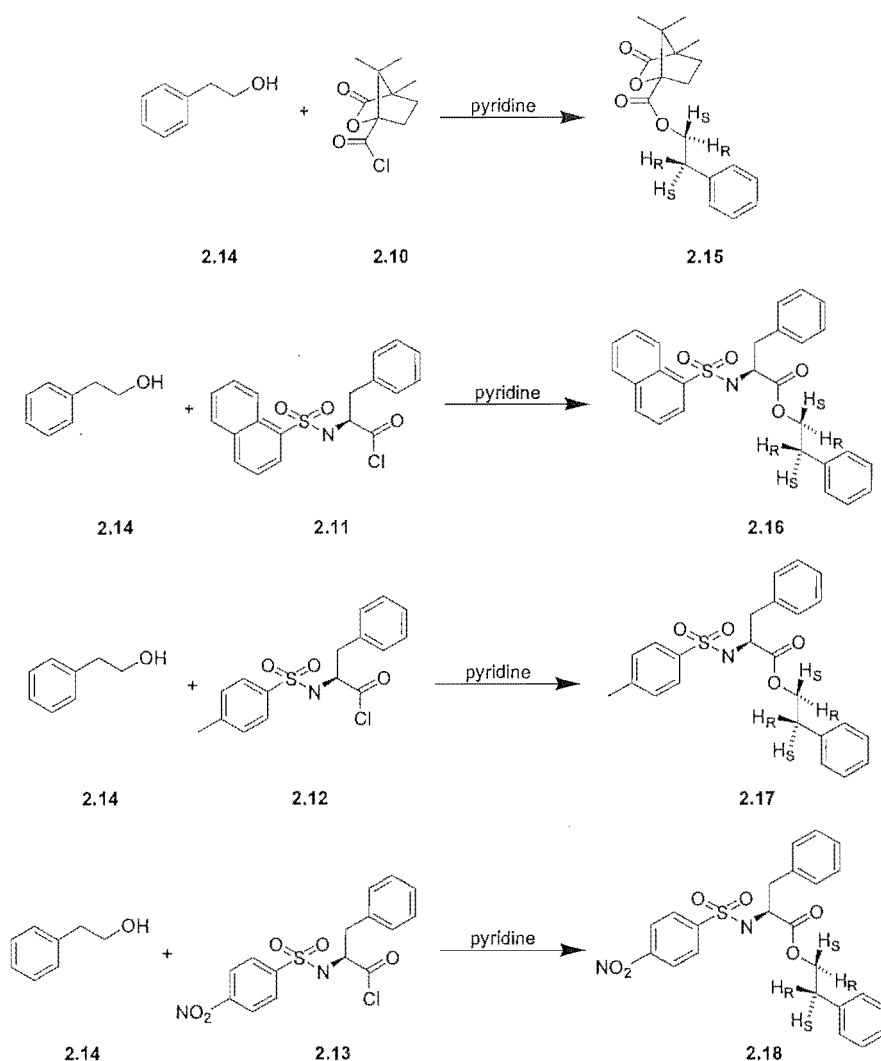


Figure 2.3. Chiral acid chlorides.

2.2.1 NMR resolution of esters derived from 2-phenylethanol

Each acid chloride **2.10-2.13** was reacted with 2-phenylethanol, to give a chiral ester. It was hoped that the chiral acid chloride might provide a sufficiently symmetric environment that the prochiral hydrogens both α - and β - to the ester oxygen would be resolved in a ^1H NMR spectrum (Scheme 2.3). Ester **2.17** was characterised by comparison of its ^1H NMR and IR spectra with those of esters **2.15**, **2.16** and **2.18**, no HRMS data was obtained for this compound.



Scheme 2.3. Esterification of 2-phenylethanol.

^1H NMR spectra were obtained for all four esters. All four chiral derivatising agents provided sufficient asymmetry to distinguish the prochiral protons α to the ester oxygen in a 500 MHz ^1H NMR spectrum, however resolution was not complete and full integration of the signals was not possible. A single signal was obtained for the protons β to the ester oxygen with a relative integral of 2, showing resolution of these protons was not possible.

Further asymmetry was added to the prochiral protons of each ester in the form of a lanthanide chiral shift reagent. Initially europium heptafluorobutyrylcamphorate ($\text{Eu}(\text{hfc})_3$) was used, the reagent was added incrementally to the NMR sample of ester in CDCl_3 , until a saturated solution was obtained. In all four cases the prochiral protons α to the ester oxygen were resolved into separate peaks. The ^1H NMR of esters **2.15**, **2.16** and **2.17** showed that it was not possible to resolve the prochiral protons β - to the ester oxygen in these esters. However when sufficient quantities of shift reagent were added to ester **2.18**, the signals for the β - prochiral protons were resolved into two separate peaks (Figure 2.4)

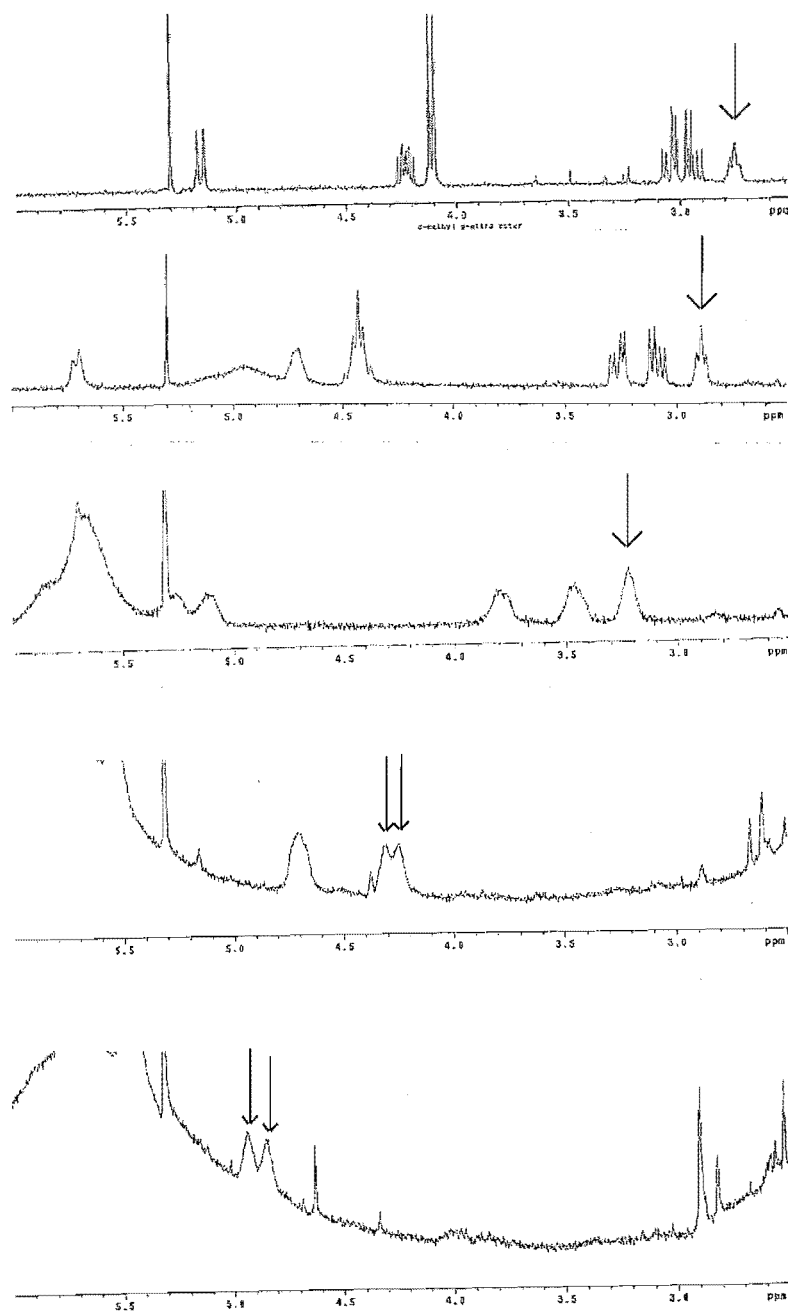


Figure 2.4. Incremental addition of $d\text{-Eu(hfc)}_3$ to **2.18**.

A large excess of shift reagent was added and gave large, broad peaks in the NMR spectrum, which interfere with the signals from the shift reagent complexed to shift

reagent. The $\text{Eu}(\text{hfc})_3$ shift reagent gave a broad peak in the region ($\sim 5\text{ppm}$) where the β -prochiral protons of 2-phenylethyl *N*-(4-nitrophenylsulfonyl)-(*S*)-2-amino-3-phenylpropanoate appeared when separated. The chiral shift reagent ytterbium *d*-3-heptafluorobutyrylcamphorate (*d*- $\text{Yb}(\text{hfc})_3$) gave similar NMR resolution of the prochiral protons, was less moisture sensitive and did not have a proton signal in the vital part of the NMR spectrum. For these reasons, further studies were conducted using *d*- $\text{Yb}(\text{hfc})_3$ as the chiral shift reagent.

Quantitative titrations were conducted by incremental addition of *d*- $\text{Yb}(\text{hfc})_3$ to 2-phenylethyl *N*-(4-nitrophenylsulfonyl)-(*S*)-2-amino-3-phenylpropanoate and 2-phenylethyl *N*-(4-methylphenylsulfonyl)-(*S*)-2-amino-3-phenylpropanoate. Graphs showing the downfield shifts of the proton signals from the esters on addition of *d*- $\text{Yb}(\text{hfc})_3$ are shown in Figures 2.6 and 2.7. It can be seen that the proton signals for H_3 and H_4 , α - to the ester linkage are separated by addition of sufficient $\text{Yb}(\text{hfc})_3$, however the signals for protons H_1 and H_2 remain indistinguishable. Similar separation is observed for the other two esters 2-phenylethyl (1*S*)-(-)-camphanate and 2-phenylethyl *N*-(1-naphthalenesulfonyl)-(*S*)-2-amino-3-phenylpropanoate.

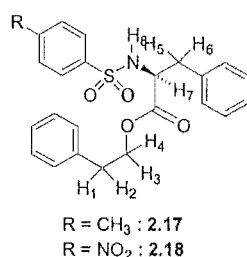


Figure 2.5. Protons of **2.17** and **2.18**.

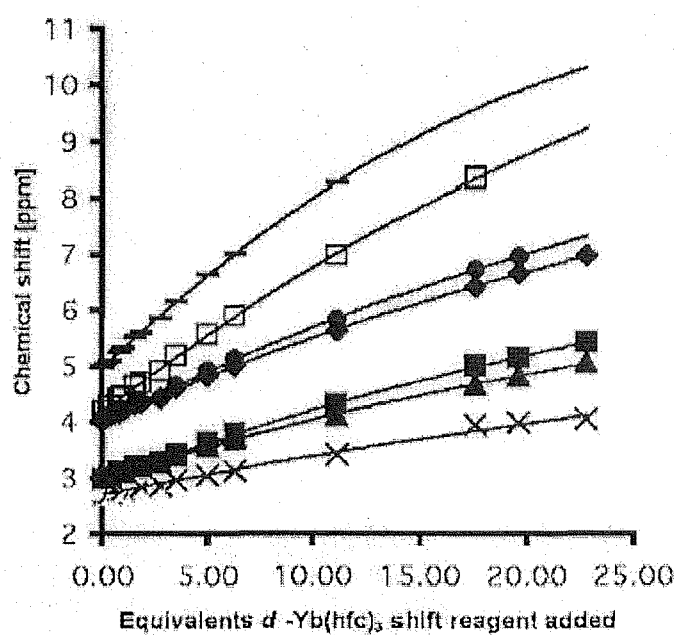


Figure 2.6. Graph showing the downfield shift of the proton resonances of **2.17** with added shift reagent. H₁ ×, H₂ ×, H₃ ◆, H₄ ■, H₅ ▲, H₆ ●, H₇ □, H₈ -. (Symbol × is used for both H₁ and H₂ in this particular graph as they are not differentiated).

Complexation of **2.18** with $d\text{-Yb(hfc)}_3$ results in complete resolution of both the α (H₃ and H₄) and β (H₁ and H₂) protons (Figure 2.7).

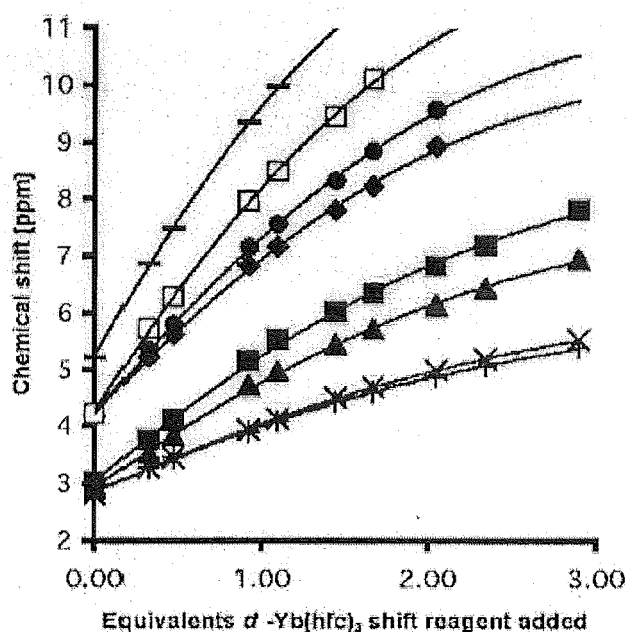


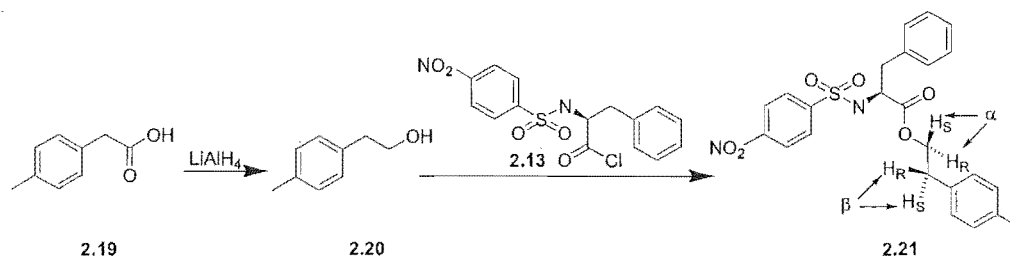
Figure 2.7. Graph showing the downfield shift of the proton resonances of **2.18** with added shift reagent. H₁ +, H₂ ×, H₃ ◆, H₄ ■, H₅ ▲, H₆ ●, H₇ □, H₈ -.

The extra asymmetry provided by the shift reagent to the ester **2.18** compared to the other similar esters **2.16** and **2.17** can be explained by noting that **2.18** contains the Lewis basic nitro group.

The *p*-nitro group in **2.18** is a hard Lewis base and so will co-ordinate to the lanthanide shift reagent. This is in contrast to **2.16** and **2.17**, where the naphthalene and tolyl groups will not co-ordinate to the shift reagent. Co-ordination of the *p*-nitro group will affect the equilibrium constant for formation of the ester-shift reagent complex and this could explain the greater downfield shift per equivalent of shift reagent for all proton resonances in **2.18** compared to **2.16** and **2.17**. The geometry of the shift reagent-ester complex will also be affected by the presence of the Lewis basic nitro group.

2.2.2 NMR resolution of esters derived from 2-(4-methylphenyl)ethanol

1-(4-Methyl)phenylethanol was made by the LiAlH_4 reduction of 4-methylphenyl acetic acid in 93% yield. Reaction of 1-(4-methyl)phenylethanol with *p*-nitro acid chloride gave ester.

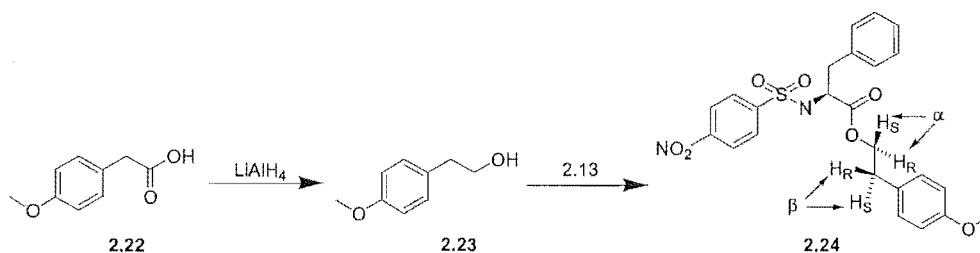


Scheme 2.4. Synthesis of 2-(4-methyl)phenylethyl *N*-(4-nitrophenylsulfonyl)-(*S*)-2-amino-3-phenylpropanoate.

Addition of $d\text{-Yb}(\text{hfc})_3$ chiral shift reagent to an NMR solution of **2.21**, showed that it was possible to separate both the α - and β - prochiral protons in the ^1H NMR spectrum. The separation was similar to that observed for **2.18**.

2.2.3 NMR resolution of esters derived from 2-(4-methoxyphenyl)ethanol

1-(4-Methoxy)phenylethanol was made by the LiAlH_4 reduction of 4-methoxyphenyl acetic acid in 85% yield. Reaction of 1-(4-methoxy)phenylethanol with *p*-nitro acid chloride gave ester.

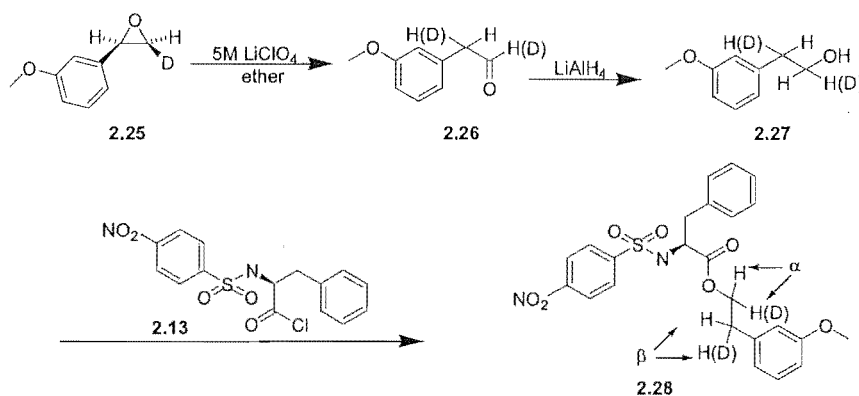


Scheme 2.5. Synthesis of 2-(4-methoxy)phenylethyl *N*-(4-nitrophenylsulfonyl)-(*S*)-2-amino-3-phenylpropanoate.

^1H NMR of **2.24** with $d\text{-Yb(hfc)}_3$ in a solution of CDCl_3 showed that the signals for the α - and β - prochiral protons were differentiated.

2.2.4 NMR resolution of esters derived from 2-(3-methoxyphenyl)ethanol

Deuterated 2-(3-methoxyphenyl)ethanol was made by rearrangement of *m*-methoxystyrene oxide, followed by reduction of the aldehyde. Esterification with **2.13** gave the ester, where it was possible to separate both the α - and β - prochiral protons by ^1H NMR spectroscopy by addition of $d\text{-Yb(hfc)}_3$.

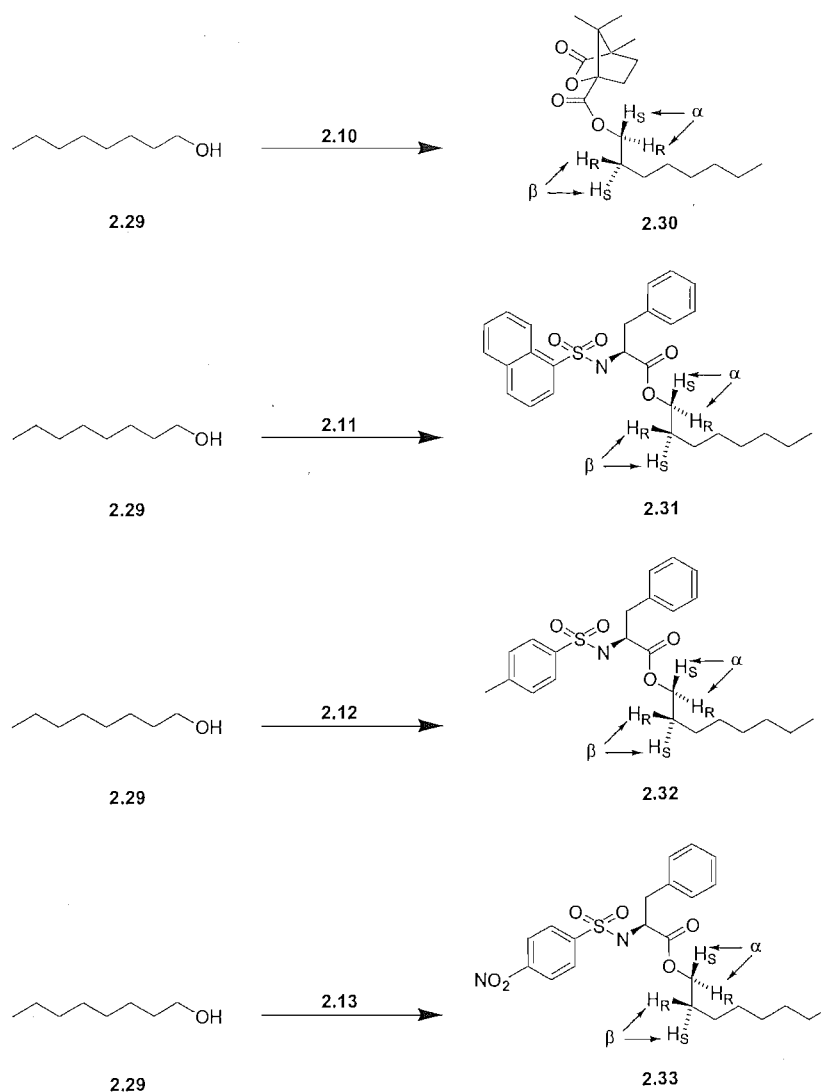


Scheme 2.6. Synthesis of **2.28**.

^1H NMR analysis with chiral shift reagents of 2-(3-methoxy)phenylethyl *N*-(4-nitrophenylsulfonyl)-(*S*)-2-amino-3-phenylpropanoate showed that separation of the β - prochiral protons was possible at a much lower concentration of chiral shift reagent, when the signals had not moved as far downfield and were not as broad as with the other reagents. This can be explained by noting the close proximity of the prochiral protons to the *meta* methoxy group which is Lewis basic. The chiral shift reagent is likely to coordinate to the methoxy group and hence bring the anisotropic magnetic field closer to the prochiral protons and provide greater differentiation at a lower concentration of shift reagent than was observed for the other aromatic substituted esters.

2.2.5 Attempted NMR resolution of esters derived from 1-octanol

Chiral esters were made from reaction of 1-octanol with each of the four chiral acid chlorides in Scheme 2.7. In each case the prochiral hydrogens α - to the ester linkage were partially separated in the NMR spectrum. Titration of each ester with d -Yb(hfc)₃ or d -Eu(hfc)₃ showed that complete separation and integration of the prochiral hydrogens α - to the ester linkage was possible, but no resolution of the β - proton signal was observed.



Scheme 2.7. Esters of 1-octanol.

2.2.5 Attempted NMR resolution of esters derived from 2,3,3-trimethylbutan-1-ol

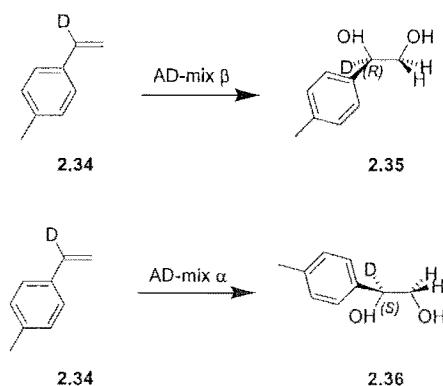
Four esters were made from reaction of each of the acid chloride in Figure 2.3 with 2,3,3-trimethylbutan-1-ol. No differentiation of the diastereomers was observed when the esters were analysed by NMR in the presence of $\text{Eu}(\text{hfc})_3$ chiral shift reagent. The esters produced by this series of reactions were characterised by ^1H NMR, no HRMS or elemental analysis data were obtained for these compounds.

2.3 ASSIGNING THE PROCHIRAL PROTONS β - TO THE ESTER OXYGEN IN A ^1H NMR SPECTRUM

Having resolved the signals for the two prochiral protons β - to the ester oxygen, it was necessary to assign each signal as H_S or H_R . In order to do this, esters were made from derivatives of 2-phenylethanol, synthesised stereoselectively deuterated in the 2 position. If the two deuterated epimers are present in unequal, known amounts, the two signals obtained for the β prochiral protons can be assigned as arising from *R* or *S* deuterated ester, based on their relative integral.

2.3.1 Assigning the prochiral protons β - to the ester oxygen in the ^1H NMR of ester derived from 2-(4-methylphenyl)ethanol

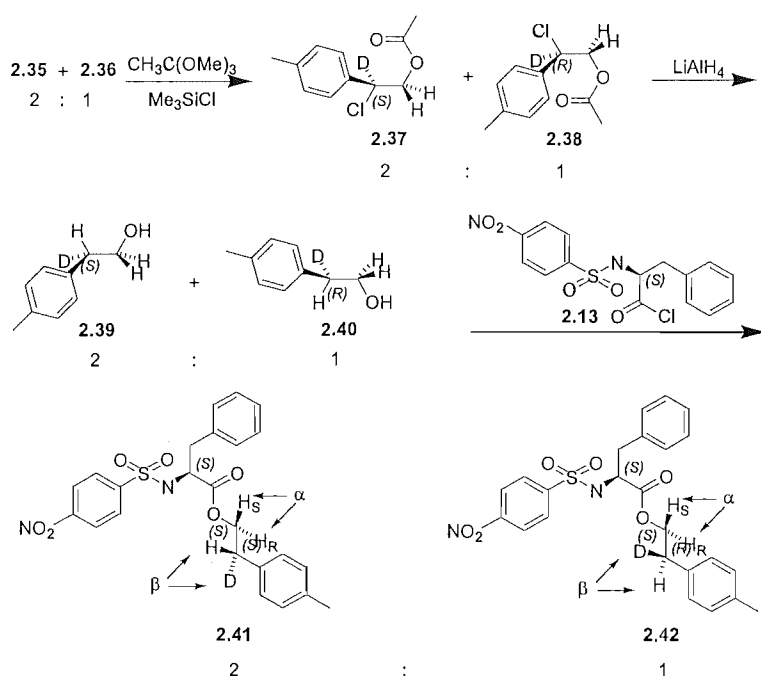
The synthesis started with the Sharpless asymmetric dihydroxylation of *p*-methylstyrene- α - d_1 with AD-mix β and AD-mix α to give (1*R*)-1-(4-methylphenyl)-1,2-ethanediol-1- d_1 and (1*S*)-1-(4-methylphenyl)-1,2-ethanediol-1- d_1 respectively (Scheme 2.8).



Scheme 2.8. Synthesis of (1*S*)- and (1*R*)-1-(4-methylphenyl)-1,2-ethanediol-1-*d*₁.

A 2:1 mixture of the *R* and *S* diols was subjected to the reaction sequence outlined in Scheme 2.9. Addition of trimethyl orthoacetate and chlorotrimethylsilane gave chloroacetates **2.37** and **2.38** (Scheme 2.9). Reduction with LiAlH₄ gave a 2:1 mixture of (2*S*)- and (2*R*)-*p*-methylphenylethan-1-ol-2-*d*₁. It has been shown previously⁶ for the reduction of the phenyl substituted compound that hydride displaces the chlorine in an S_N2 reaction, with inversion of configuration at the reaction centre.

Previously, Mosher⁶ has completed the same series of reactions to give selectively deuterated 2-phenylethanol. For this phenyl substituted compound, a 96:4 mixture of the secondary and primary chloro compounds were formed. Mosher et al.⁷ showed that reduction of this mixture with LiAlD₄ afforded the same ratio of primary to secondary alcohol, implying that styrene oxide is not an intermediate in the reaction. This is in accord with the results of Eliel.⁸

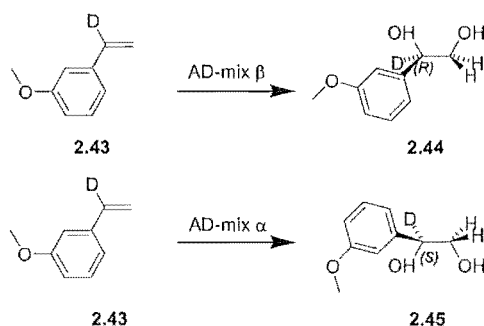
Scheme 2.9. Assigning the NMR spectra of the prochiral β protons of **2.21**.

Esterification of the 2:1 mixture of alcohols was achieved by the method outlined earlier and a 2:1 mixture of *S* and *R* esters deuterium labelled β to the ester oxygen was obtained (Scheme 2.10). The esters were analysed by ^1H NMR. When sufficient $d\text{-Yb(hfc)}_3$ was added to the ester mixture in CDCl_3 , the signal for the protons β - to the ester oxygen resolved into two separate signals, where the downfield peak was half the size of the upfield peak. This showed that the downfield peak is from the *R* ester; the upfield peak is from the *S* ester.

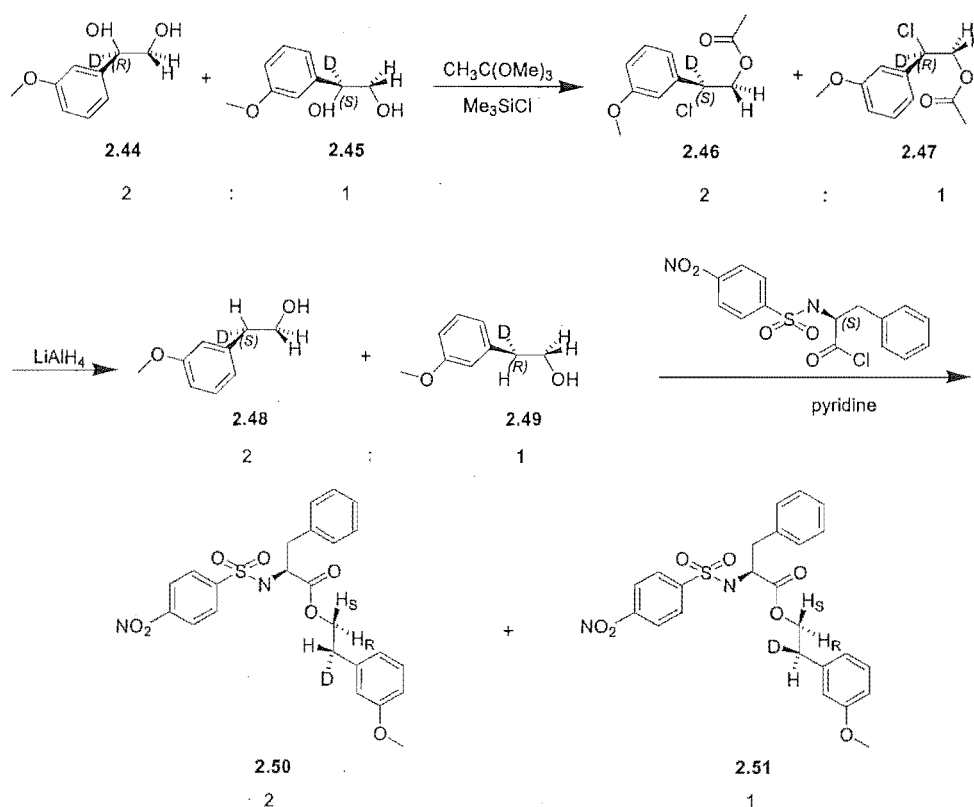
In undeuterated ester the H_S prochiral hydrogen β to the ester oxygen will resonate downfield from the H_R prochiral hydrogen. The pro-*S* hydrogen resonates downfield in other examples where the prochiral hydrogens α - to an ester oxygen have been resolved with the use of chiral derivatising agents and lanthanide shift reagents.^{2(d)}

2.3.2 Assigning the prochiral protons β - to the ester oxygen in the ^1H NMR of ester derived from 2-(3-methoxyphenyl)ethanol

The same reaction scheme was used to make a 2:1 mixture of deuterated 2-(3-methoxy)phenylethyl *N*-(4-nitrophenylsulfonyl)-(*S*)-2-amino-3-phenylpropanoate *S* and *R* at the position β - to the ester oxygen.



Scheme 2.10. Synthesis of (1*S*)- and (1*R*)-1-(3-methoxyphenyl)-1,2-ethanediol-1- d_1 .



Scheme 2.11. Synthesis of stereoselectively deuterated esters.

^1H NMR of the 2:1 mixture of stereoselectively deuterated esters in the presence of $d\text{-Yb}(\text{hfc})_3$ again gave a downfield peak that was half the size of the upfield peak. This shows that in undeuterated material, the pro-*S* prochiral hydrogen β - to the ester oxygen will resonate downfield from the pro-*R* hydrogen in the chiral shifted ^1H NMR spectrum of the ester.

2.4 RELATIONSHIP BETWEEN THE RELATIVE INTEGRALS OF THE PROCHIRAL PROTONS AND THE DELAY BETWEEN PULSES IN THE ^1H NMR

The downfield (H_S) signal of the separated β - prochiral protons is a broader peak in the ^1H NMR spectrum of the ester-shift reagent complex than the upfield peak, indicating a faster relaxation time due to its closer proximity to the paramagnetic field of the Yb shift reagent.

An experiment was conducted to determine whether the difference in relaxation time would affect the relative integrals of the two proton signals by varying the delay time between pulses when running the NMR spectrum.

d-Yb(hfc)₃ was added to undeuterated 2-phenethyl (*N*-4-nitrophenylsulfonyl)-(*S*)-2-amino-3-phenylpropanoate in CDCl₃ in an NMR tube. Sufficient *d*-Yb(hfc)₃ was added that the prochiral protons β to the ester linkage were resolved in the NMR spectrum. Five spectra were recorded over a period of time where the value of d1, the delay between pulses was varied between 0.5 and ten seconds. If the differing relaxation times of the two prochiral hydrogens did alter their relative integrals, the integral would systematically vary with changing d1.

d1 (s)	Downfield : Upfield proton integral
0.5	1.0051 : 1
0.5	1.0184 : 1
1	1.0469 : 1
5	1.0223 : 1
10	1.0074 : 1

Table 2.1. Integral of the prochiral protons β- to oxygen in **2.21**, with varying delay between NMR pulses.

It can be seen that in all cases the downfield peak is slightly larger than the upfield peak. This is due to a small overlapping peak from an impurity that was present in the sample. The exact position of the impurity peak changed in each spectrum as the equilibrium with the chiral shift reagent changed slightly over time and this could be responsible for the slight variation in the relative integral for the two prochiral proton peaks in the different NMR spectra.

There is no trend of the integral for one proton increasing relative to the other, with increasing d1. If a difference in relaxation time was responsible for a consistent under or

over estimation of the integral there would be a consistent trend as the delay between NMR pulses was increased, allowing both proton nuclei to relax before the next pulse is applied. If the two protons in the ester-shift reagent complex do have different relaxation times, it does not significantly affect the relative integrals of the two signals.

In the NMR analyses in this thesis all integrals are taken from NMR spectra with a delay between pulses of one second. Consistent with what has been noted previously for the integration of proton NMR signals in the presence of chiral shift reagent, a variation of approximately 5% was observed in the relative integrals from spectra taken at different concentrations of shift reagent.

2.5 INTEGRATION OF THE ^1H NMR SPECTRUM USING MATLAB

The signals of the prochiral proton signals β - to the oxygen of ester **2.18** were not fully resolved and accurate measurement of the relative integral of the two peaks was not therefore possible. Deconvolution of the peaks into two separate, overlapping lorentzian curves was achieved using a script for the mathematical modelling package MATLAB. The area under each of the separate lorentzian curves could then be calculated.

The MATLAB script iteratively found the least squares fit to the lorentzian distribution peaks and calculated the area of each peak, even when two peaks were overlapping. When two peaks were overlapping, the program calculated where each peak would occur in order to give the additive effect of the observed line. It was also necessary to take into account the sloping baseline for some of the spectra.

An example of the separation of overlapping peaks is shown in Figure 2.8.

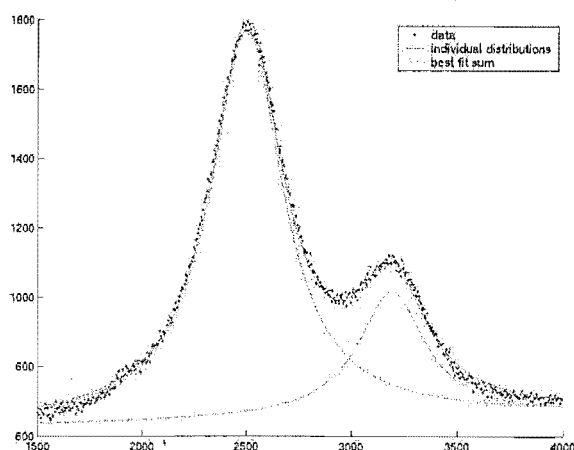


Figure 2.8. Integration of overlapping peaks in MATLAB. The relative integral of the peaks is 7.371 : 2.198.

Integration of the NMR spectra of the *m*-methoxy substituted ester **2.28** was also conducted using the MATLAB integration script, although complete separation of the β -prochiral proton signals was possible for this series of esters. The presence of the Lewis basic methoxy group in the *meta* position is probably responsible for the more complete resolution of the proton signals. The methoxy group will co-ordinate to the Lewis acidic shift reagent and change the geometry of the ester-shift reagent complex and enhance the resolution either by bringing the β -prochiral protons closer to the paramagnetic field of the Yb shift reagent or constraining the geometry of the ester.

¹ Parker, D. *Chem. Rev.* **1991**, *91*, 1441-1457.

² (a) Schwab, J. M. *J. Am. Chem. Soc.* **1981**, *103*, 1876-1878. (b) Schwab, J. M.; Li, W.; Thomas, L. P. *J. Am. Chem. Soc.* **1983**, *105*, 4800-4808. (c) Shapiro, S.; Arunachalam, T.; Caspi, E. *J. Am. Chem. Soc.* **1983**, *105*, 1642-1646. (d) Schwab, J. M.; Ray, T.; Ho C. *J. Am. Chem. Soc.* **1989**, *111*, 1057-1063.

³ Gerlach, H.; Zagalak, B. *J. Chem. Soc., Chem. Commun.* **1973**, 274-275.

⁴ McReary, M. D.; Lewis, D. W.; Wernick, D. L.; Whitesides, G. M. *J. Am. Chem. Soc.* **1974**, *96*, 1038-1054.

⁵ Meddour, A.; Canlet, C.; Blanco, L.; Courtieu, J. *Angew. Chem. Int. Ed.* **1999**, *38*, 2391-2393.

⁶ Elsenbaumer, R. L.; Mosher, H. S. *J. Org. Chem.* **1979**, *44*, 600-603.

⁷ Elsenbaumer, R. L.; Mosher, H. S. *J. Org. Chem.* **1979**, *44*, 600-603.

⁸ Eliel, E. L.; Delmonte, D. W. *J. Am. Chem. Soc.* **1958**, *80*, 1744; Eliel, E. L.; Rerick, M. H. *ibid.* **1960**, *82*, 1362.

Chapter Three

Synthesis and Lewis Acid Catalysed Rearrangement of *p*-Methylstyrene Oxide

3.1 INTRODUCTION

The Lewis acid catalysed rearrangement of mono-substituted epoxide involves a hydride 1,2 shift to give aldehyde. We wished to establish the stereochemical course of this reaction in detail. The stereochemical course of the hydride migration can be determined by the rearrangement of specifically deuterium labelled epoxides that are optically active. In particular we wish to analyse the regio- and stereochemical distribution of the deuterium label in the aldehyde products by the methods outlined in the previous chapter.

The investigation extends the previous studies of the rearrangement of mono-substituted and 1,1-disubstituted epoxide by using optically active labelled epoxide. Previous studies measured only the relative migratory aptitudes of the two terminal epoxide hydrogens by rearrangement of the racemic analogues of **3.1** and **3.2**. Rearrangement of optically active epoxides allows the full stereochemical course of the hydride or deuteride migration to be measured.

Four regioselectively deuterated, optically active isomers of *p*-methylstyrene oxide were synthesised (Figure 3.1).

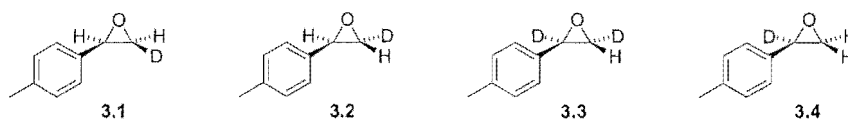


Figure 3.1. Deuterioisomers of *p*-methylstyrene oxide.

In addition to the *cis* and *trans* β-mono-deuterated epoxides **3.1** and **3.2**, we report the rearrangement of *cis*-α,β-dideuterated epoxide **3.3**, where the facial selectivity of hydrogen migration is measured and rearrangement of the α-mono-deuterated epoxide **3.4**, where the overall facial selectivity for hydride migration is measured.

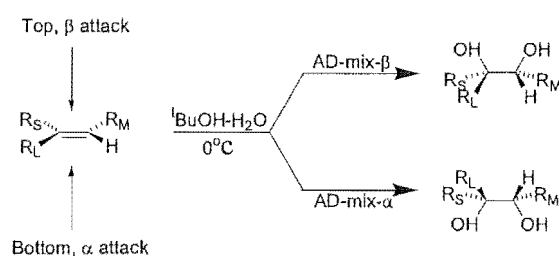
The synthesis of epoxides **3.1** - **3.3** results in an enriched mixture of epoxide deuterioisomers, the minor components of which have either no deuterium label, or have

the deuterium label non selectively positioned in the molecule. The ratio of the various epoxides in each mixture was determined and the results of each rearrangement were adjusted to establish the products from rearrangement of each epoxide. The error in each experiment was also estimated.

3.2 SYNTHESIS OF *P*-METHYLSTYRENE OXIDE

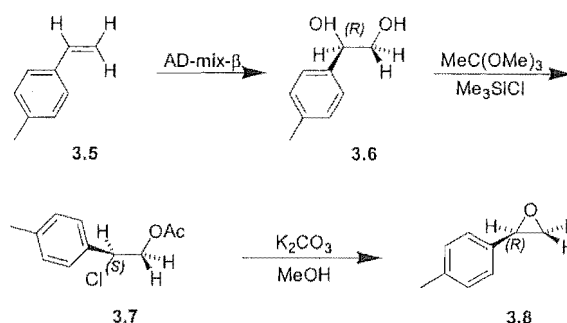
For the mechanistic studies, we required epoxides that were as enantiomerically pure as possible. Formation of epoxides directly from terminal alkenes, for example using Jacobson's epoxidation catalyst, does not give high enough ee values. Methods exist for conversion of 1,2-diols to epoxides with retention of the stereochemical integrity and the 1,2-diols can be made highly enantioselectively by the Sharpless asymmetric dihydroxylation procedure.

Two premixed Aldrich reagents are available for the asymmetric dihydroxylation reaction: AD-mix- α and AD-mix- β , which give opposite diol enantiomers (Scheme 3.1).

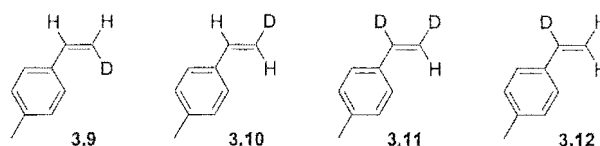


Scheme 3.1. Stereochemistry of the Sharpless dihydroxylation.

It has been shown that the Sharpless dihydroxylation reaction gives a 97% ee for the dihydroxylation of styrene¹ and a similar level of stereoselectivity was expected for the dihydroxylation of *p*-methylstyrene. Conversion of the diol to epoxide can be achieved by a number of methods, the most convenient is the one pot procedure of Kolb et al.² Diol is converted to a chlorohydrin ester and base mediated ester saponification gives epoxide. This method is known to give styrene oxide with an enantiomeric excess identical to the starting diol:

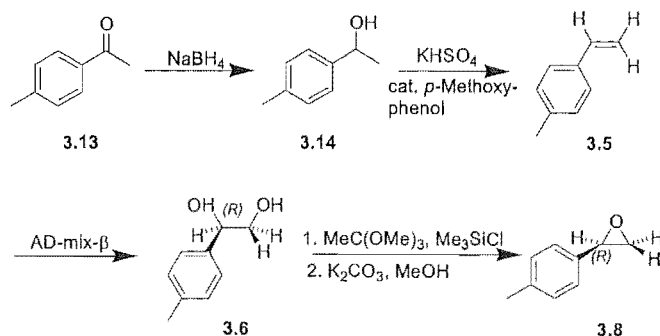
Scheme 3.2. Dihydroxylation and epoxidation of *p*-methylstyrene.

The four deuterated epoxides (**3.1** - **3.4**) can therefore be made from the corresponding alkene by Sharpless asymmetric dihydroxylation, followed by conversion of the diol to epoxide. The synthetic targets are the four deuterioisomers of *p*-methylstyrene shown in Figure 3.2:

Figure 3.2. Deutero isomers of *p*-methylstyrene.

3.2.1 Synthesis of undeuterated *p*-methylstyrene oxide

The Sharpless asymmetric dihydroxylation and epoxidation methodology was first tested on undeuterated material. 1-(4-Methylphenyl)ethanol **3.14** was made by reduction of 4-methylacetophenone with sodium borohydride. Dehydration of the alcohol by heating with potassium bisulfate with catalytic *p*-methoxyphenol gave *p*-methylstyrene. Sharpless asymmetric dihydroxylation then gave the diol and epoxide was formed using trimethyl orthoacetate and trimethylsilyl chloride, followed by ring closing saponification with K_2CO_3 in MeOH (Scheme 3.3).

Scheme 3.3. Synthesis of undeuterated *p*-methylstyrene.

Experiments showed that the effective yield of the Sharpless asymmetric dihydroxylation reaction could be increased by extraction of the diol with ethyl acetate. The literature procedure called for extraction of the diol from the aqueous layer with CH_2Cl_2 . Difficulties were encountered with emulsion formation and this was avoided by using ethyl acetate.

d-Yb(hfc)₃ chiral shift reagent was added incrementally to **3.8**. At a concentration of *d*-Yb(hfc)₃ sufficient to resolve the α protons of racemic **3.8**, only one peak was obtained for the α hydrogen in the ^1H NMR spectrum, showing that **3.8** was formed with a greater than 95% ee.

Further confirmation of the enantiomeric excess of the epoxide was obtained from comparing optical rotation measurements to literature values where the enantiomeric excess had been determined independently by chiral HPLC. $[\alpha]_D^{20} +26$ (*c* 1.2, PhH) [lit.³ $[\alpha]_D^{20} +27$ (*c* 0.98, PhH, ee 95%)].

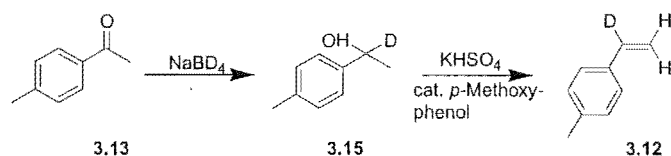
p-Methylstyrene oxide is more reactive than styrene oxide, especially in the presence of traces of acid and problems were encountered with the storage and purification of the *p*-methyl styrene epoxide. Purification by flash chromatography on silica gel was not possible, due to rearrangement of *p*-methylstyrene oxide catalysed by the acidic silica gel. Basic alumina also catalysed the decomposition of *p*-methylstyrene oxide on the column. Storage of *p*-methylstyrene oxide was only possible for a short time in the freezer. The

product from epoxidation was approximately 95% pure, as determined by ^1H NMR and this material was used in the Lewis acid catalysed rearrangement reactions without further purification.

The successful synthesis of *p*-methylstyrene oxide showed that the Sharpless asymmetric dihydroxylation and epoxidation via the ortho ester is a viable route to optically active epoxide. The synthesis of the deuterated *p*-methylstyrene oxides is reported below.

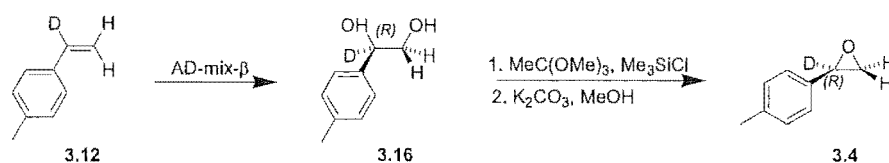
3.2.2 Synthesis of *p*-methylstyrene oxide- α - d_1

Deuterium was introduced by sodium borohydride reduction of *p*-methylacetophenone. Dehydration of the alcohol with potassium bisulfate gave the α -deuterated *p*-methylstyrene 3.12. ^1H NMR showed > 99% deuterium incorporation at the α carbon:



Scheme 3.4. Synthesis of *p*-methylstyrene- α - d_1 .

The epoxide was prepared using the methodology outlined above. The Sharpless asymmetric dihydroxylation with AD-mix- β gave (1*R*)-1-(4-methylphenyl)ethane-1,2-diol-1- d_1 3.16 which was converted to epoxide by reaction with trimethylorthoacetate and trimethylsilyl chloride to give chlorohydrin ester. Ring closure was effected by saponification with potassium carbonate in methanol. *p*-Methylstyrene oxide- α - d_1 3.4 was formed 99% regioselectively deuterated in the α - position.

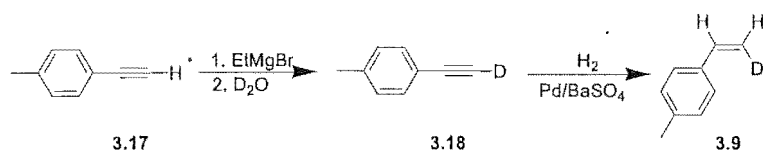


Scheme 3.5. Formation of (αR)-*p*-methylstyrene oxide- α - d_1 from *p*-methylstyrene- α - d_1 .

3.2.3 Synthesis of (αR),(βS)-*p*-methylstyrene oxide- β - d_1

p-Methylstyrene-*cis*- β - d_1 **3.9** was made by the method outlined in Scheme 3.6. A previous researcher in our group, Dr Luke Ueda-Sarson had made a sample of *p*-methylphenyl acetylene that was used as the starting material in the following investigation.

Deuterium incorporation was achieved by removal of the acidic terminal alkyne proton with ethyl magnesium bromide. The magnesium salt was quenched with D_2O to give *p*-methylphenyl acetylene-2- d_1 **3.18**. Ethyl magnesium bromide was used as the base in preference to butyl lithium because a higher level of deuterium incorporation was achieved when using the Grignard reagent in previous experiments on the deuteration of 1-octyne. Greater than 99% deuterium incorporation was achieved, as determined by 1H NMR spectroscopy.



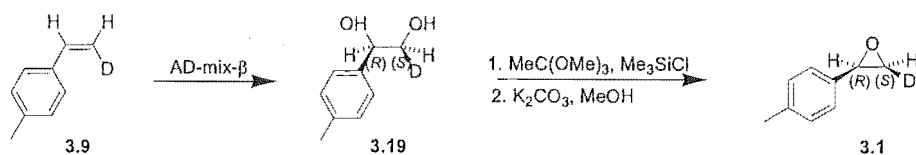
Scheme 3.6. Synthesis of *p*-methylstyrene-*cis*- β - d_1 .

The alkyne triple bond was reduced under a hydrogen atmosphere over a palladium catalyst. Quinoline is used to modify the reactivity of the palladium surface to allow alkyne co-ordination to the surface, while the less reactive alkene is blocked. A terminal alkene, conjugated to an aromatic group is very reactive and competes efficiently with quinoline for sites on the palladium catalyst. The palladium catalyst can then catalyse *cis-trans* isomerisation or hydrogen exchange reactions of the alkene.

Some scrambling of the deuterium label between the three vinylic positions was observed in the reduction of *p*-methylphenyl acetylene-2- d_1 **3.18** to *p*-methylstyrene-*cis*- β - d_1 **3.9**. The *cis-trans* isomerisation of the alkene could be minimised by stopping the reaction

short of full reduction. For a full discussion of the effect of reaction time on isomerisation of the alkene, see section 5.1.2.

Epoxide **3.1** was then made by the Sharpless asymmetric dihydroxylation with AD-mix- β and epoxidation with trimethylorthoacetate / trimethylsilyl chloride followed by K_2CO_3 / MeOH.



Scheme 3.7. Formation of $(\alpha R),(\beta S)$ -*p*-methylstyrene oxide- β - d_1 **3.1** from *p*-methylstyrene-*cis*- β - d_1 **3.9**.

3.2.3.1 Isomers of $(\alpha R),(\beta S)$ -*p*-methylstyrene oxide- β - d_1

The same ratio of epoxide deuterioisomers were present in the final epoxide mixture, as formed in the hydrogenation of deuterated alkyne described above. Table 3.1 shows the 1H and 2H NMR integrals of the α and β positions of $(\alpha R),(\beta S)$ -*p*-methylstyrene oxide- β - d_1 **3.1**.

	<i>trans</i> integral	<i>cis</i> integral	α integral
1H nmr	0.90	0.17	1.00
2H nmr	0.06	1.00	0.04

Table 3.1. 1H and 2H NMR integrals for the α and β hydrogen / deuterium signals of **3.1**.

The ratio of epoxides can then be calculated as shown below:

We introduce the parameters x and y , to multiply the integrals from the 1H and 2H NMR integral respectively and convert the integrals (in arbitrary units) into the fraction of total

hydrogen and deuterium in each position, where total hydrogen + deuterium in each position = 1:

$$0.90x + 0.06y = 1 \dots\dots(1)$$

$$0.17x + 1.00y = 1 \dots\dots(2)$$

$$1.00x + 0.04y = 1 \dots\dots(3)$$

Using equations 2 and 3 : $x = 0.967$, $y = 0.836$.

Each deuterioisomer gives rise to one signal in the deuterium NMR spectrum. The amount of each epoxide can therefore be obtained by multiplying each deuterium signal by y to get the fraction of the corresponding epoxide. The remainder is undeuterated epoxide **3.8**. The following ratio of epoxides is obtained:

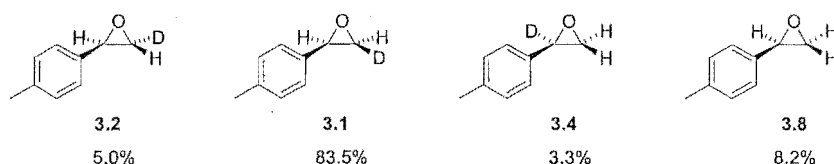
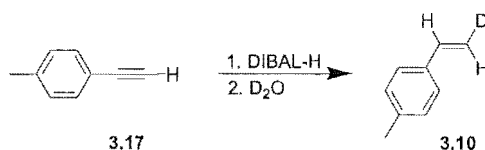


Figure 3.3. Isomers of $(\alpha R),(\beta S)$ -*p*-methylstyrene oxide- β - d_1 .

3.2.4 Synthesis of $(\alpha R),(\beta R)$ -*p*-methylstyrene oxide- β - d_1

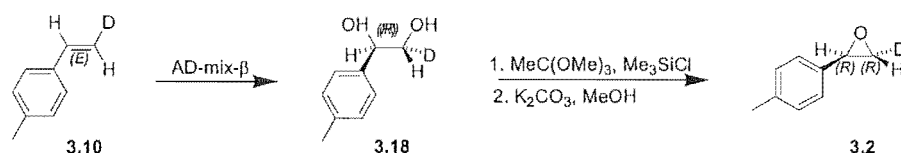
trans- β -Deutero-*p*-methylstyrene **3.10** was made by the diisobutyl aluminium hydride reduction of *p*-methylphenyl acetylene:



Scheme 3.8. Synthesis of *p*-methylstyrene-*trans*- β - d_1 .

The yield of this reaction was about 50%, with $80\pm 5\%$ deuterium incorporation in the *trans* β position. The remaining $20\pm 5\%$ of the material was predominantly undeuterated *p*-methylstyrene with approximately 5% each of the α -deuterated and *trans*- β -deuterated *p*-methylstyrene.

(αR),(βR)-*p*-Methylstyrene oxide- β - d_1 **3.2** was prepared by the method described above for undeuterated *p*-methylstyrene oxide **3.8**:



Scheme 3.9. Synthesis of (αR),(βR)-*p*-methylstyrene oxide- β - d_1 from *p*-methylstyrene-*trans*- β - d_1 .

3.2.4.1 Isomers of (αR),(βR)-*p*-methylstyrene oxide- β - d_1

The epoxide contained a mixture of deuterioisomers **3.1**, **3.4** and **3.8** and the method described above is used to calculate the ratio of these isomers. The ^1H and ^2H NMR integrals are shown in Table 3.2.

	<i>trans</i> integral	<i>cis</i> integral	α integral
^1H nmr	0.16	1.01	1.00
^2H nmr	1.00	0.06	0.02

Table 3.2. ^1H and ^2H NMR integrals for the α and β hydrogen / deuterium signals of **3.2** (batch 1).

The product enriched in **3.2** (85%) was shown to contain **3.1** (5%), **3.4** (2%) and **3.8** (8%). Synthesis of a second batch of *trans* deuterated epoxide, using the same conditions as the

first produced a slightly different ratio of deuterated epoxides (**3.1** (5%), **3.2** (77%), **3.4** (2%) and **3.8** (17%)).

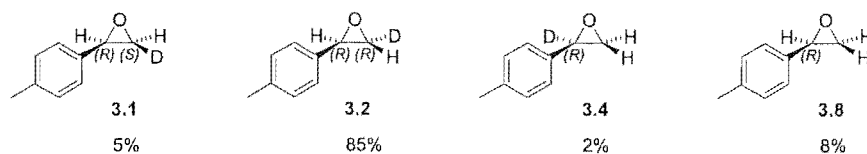


Figure 3.4. Isomers formed in the synthesis of (αR),(βR)-*p*-methylstyrene oxide- β - d_1 (batch 1).

	trans integral	cis integral	α integral
^1H nmr	0.22	0.92	1.00
^2H nmr	1.00	0.06	0.02

Table 3.3. ^1H and ^2H NMR integrals for the α and β hydrogen / deuterium signals of **3.2** (batch 2).

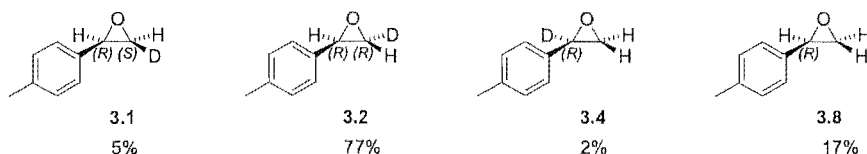
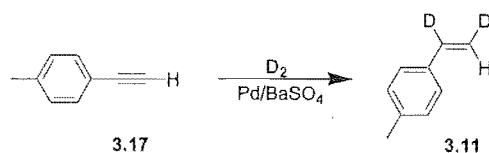


Figure 3.5. Isomers in the synthesis of (αR),(βR)-*p*-methylstyrene oxide- β - d_1 (batch 2).

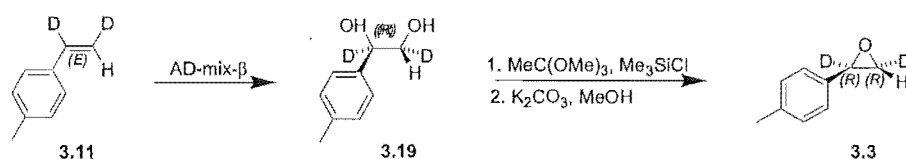
3.2.5 Synthesis of (αR),(βR)-*p*-methylstyrene oxide- α,β - d_2

cis- α,β -Dideuterated *p*-methylstyrene **3.3** was prepared by the Pd/BaSO₄ catalysed reduction of *p*-methylphenyl acetylene **3.17** under a deuterium atmosphere:

Scheme 3.10. Synthesis of *p*-methylstyrene-*cis*- α,β - d_2 .

The reaction produced approximately 85% dideuterium incorporation. The results were similar to those observed for the palladium catalysed hydrogen reduction of *p*-methylphenylacetylene-2- d_1 3.17. Some scrambling of deuterium was observed and to a similar extent as in the hydrogenation of deuterated alkyne.

The deuterated *p*-methylstyrene 3.11 was converted to deuterated *p*-methylstyrene oxide 3.3 following the same route as for the other deuterioisomers described above:

Scheme 3.11. Synthesis of (αR),(βR)-*p*-methylstyrene oxide- α,β - d_2 from *p*-methylstyrene-*cis*- α,β - d_2 .

3.2.5.1 Isomers of (αR),(βR)-*p*-methylstyrene oxide- α,β - d_2

The enriched (αR),(βR)-*p*-methylstyrene oxide- α,β -(d_0 , d_1 , d_2 , d_3) contained between zero and three deuterium labels, which made calculation of the ratio of deuterio isomers more complicated compared to the monodeuterated compounds.

Determination of the deuterium content of the epoxide by mass spectrometry was not possible, however high resolution mass spectrometry of the esters formed after rearrangement and reduction of the epoxide provided a measure of the relative amounts of undeuterated, monodeuterated, dideuterated and trideuterated material in the starting

mixture. This information, along with integrals obtained from ^1H and ^2H NMR spectra of the epoxide was used to calculate the relative amounts of each deuterated epoxide isomer. The NMR data and mass spectral data are shown below in Tables 3.4 and 3.5:

	<i>trans</i> integral	<i>cis</i> integral	α integral
^1H nmr	0.18	1.00	0.13
^2H nmr	5.85	1.00	6.0

Table 3.4. ^1H and ^2H NMR integrals for the α and β hydrogen / deuterium signals of 3.3.

Number of ^2H labels	% of total compound
0	2.0
1	10.8
2	80.2
3	6.0

Table 3.5. Measurement of the number of deuterium labels by mass spectrometry.

The sample produced is in fact a mixture of the following seven epoxides:

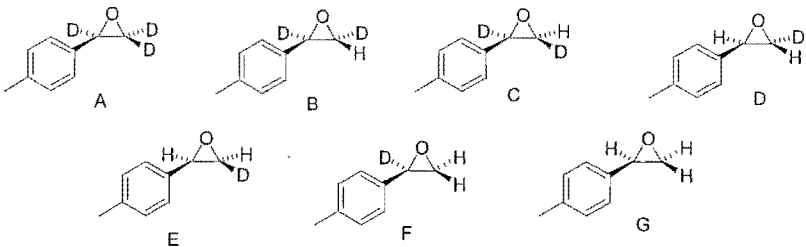


Figure 3.6. Isomers obtained from synthesis of dideuterated epoxide 3.3.

From mass spectrometry data:	From ^2H nmr :	From ^1H nmr :
$A = 6.0, G = 2.0,$	$C + F - D = 0.15x$	$B + D - (C + E) = 0.82y$
$D + E + F = 0.102$	$B + F - E = 5x$	$B + F - E = 0.87y$
$B + C = 0.802$	$B + D - (C + E) = 4.85x$	$C + F - D = 0.05y$

The values of x and y can be solved:

$$6.0x + 0.13y = 1 \dots\dots(1)$$

$$1x + 1y = 1 \dots\dots\dots(2)$$

$$5.85x + 0.18y = 1 \dots\dots(3)$$

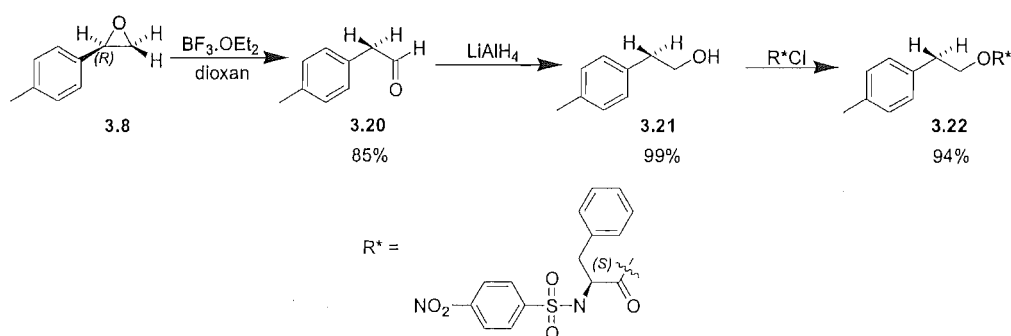
Using equations 2 and 3 : $x = 0.15, y = 0.85$.

The simultaneous equations are solved using the “solve function” in the mathematical modelling program Matlab. The amount of epoxide **E** was not able to be determined from the simultaneous equations, however since **E** is expected to be only a very minor component of the product mixture, it was assigned a value of 1%. This is an upper limit since the product could not be determined from the various spectra. The amount of **A** and **G** is obtained directly from the mass spectral data. The ratio of the other deuterio isomers is obtained from solving the various simultaneous equations, resulting in the calculated ratio **A** : **B** : **C** : **D** : **E** : **F** : **G** of: 6.0 : 71.6 : 8.6 : 8.1 : 1 : 1.7 : 2.0.

3.3 $\text{BF}_3 \cdot \text{OEt}_2$ CATALYSED REARRANGEMENT OF *P*-METHYLSTYRENE OXIDE

3.3.1 Rearrangement of undeuterated *p*-methylstyrene oxide with $\text{BF}_3 \cdot \text{OEt}_2$

The $\text{BF}_3 \cdot \text{OEt}_2$ catalysed rearrangement was initially carried out on undeuterated epoxide **3.8**. A dilute solution of *p*-methylstyrene oxide in dioxan was established as the appropriate conditions and resulted in little intermolecular reaction. Using a catalytic amount of $\text{BF}_3 \cdot \text{OEt}_2$ resulted in an 85% yield of aldehyde after 15 minutes stirring at room temperature. The reaction was carried out first on 100 mg scale, then on a smaller scale (15 mg) and a similar yield and ratio of products was obtained in both experiments.



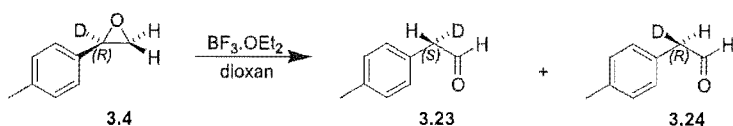
Scheme 3.12. Rearrangement, reduction and esterification of undeuterated (αR)-*p*-methylstyrene oxide.

The undeuterated product aldehyde was reduced with LiAlH_4 and the resulting alcohol was reacted with *N*-(4-nitrophenylsulfonyl)-*S*-phenylalanyl chloride, to give a chiral ester where the protons, originating from C2 of the aldehyde are distinguishable in the ^1H NMR spectra, on addition of $d\text{-Yb}(\text{hfc})_3$ chiral shift reagent (Scheme 3.12).

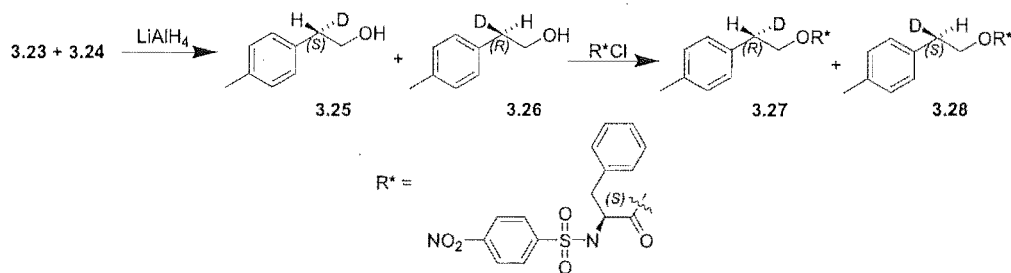
3.3.2 Rearrangement of α -deuterated epoxide

To determine the stereoselectivity for hydride migration (αR)-*m*-methylstyrene oxide- $\alpha\text{-}d_1$ **3.4** was first rearranged and the overall facial selectivity for hydride migration was determined. (αR)-*p*-Methylstyrene oxide- $\alpha\text{-}d_1$ was made with $> 95\%$ ee, and approximately 99% D incorporation at the α position.

Rearrangement of this optically active, α -deuterium labelled epoxide gives two aldehyde products **3.23** and **3.24**, which are enantiomers due to isotopic substitution at C2 (Scheme 3.13). Aldehyde **3.23** is formed from hydride migration with retention of configuration, while **3.24** results from hydride migration with inversion of configuration at the migration terminus.

Scheme 3.13. Rearrangement of (αR)-*m*-methylstyrene oxide- α - d_1 .

For analysis, the aldehyde products are reduced to alcohols **3.25** and **3.26** which are esterified with *N*-(4-nitrophenylsulfonyl)-*S*-phenylalanyl chloride to give the diastereomeric esters **3.27** and **3.28**, which are different due to the chirality at the carbon β -to the ester linkage. The relative integral of the β - H_S and H_R resonances in the chiral shifted 1H NMR of the ester were measured to get the ratio of **3.27** : **3.28**.

Scheme 3.14. Reduction and esterification of **3.23** and **3.24**.

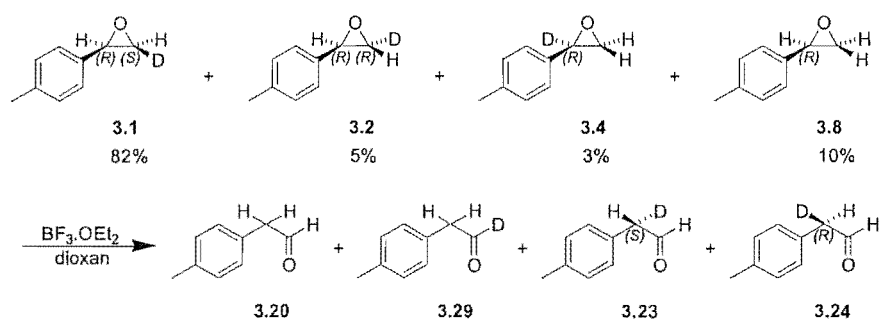
Three separate rearrangement reactions were conducted. In each case the aldehyde products were reduced with $LiAlH_4$ and esterified with *N*-(4-nitrophenylsulfonyl)-*S*-phenylalanyl chloride. The relative amounts of esters **3.27** and **3.28** were determined for each experiment by 1H NMR of the ester in the presence of $Yb(hfc)_3$ chiral shift reagent (Table 3.6). The ratio of esters **3.27** and **3.28** should be identical to the ratio of aldehydes **3.23** and **3.24**.

Reaction	H migration with retention of configuration 3.27 (and 3.23)	H migration with inversion of configuration 3.28 (and 3.24)
1	47%	53%
2	44%	56%
3	49%	51%
average	47±3%	53±3%

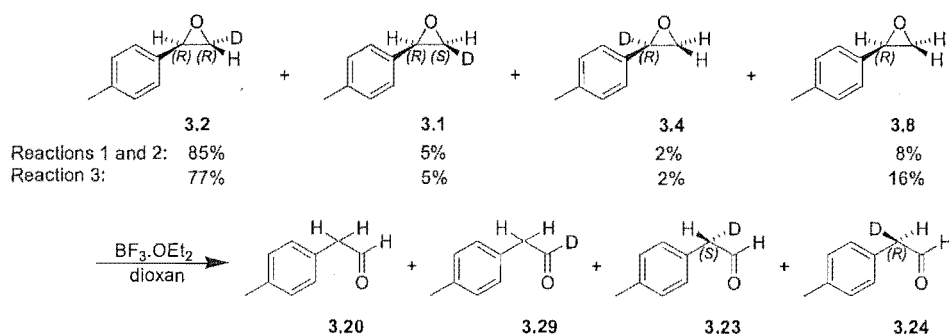
Table 3.6. Inversion / retention of configuration in the rearrangement of (αR)-*p*-methylstyrene oxide- α - d_1 .

3.3.3 Rearrangement of (αR),(βS)-*p*-methylstyrene oxide- β - d_1 and (αR),(βR)-*p*-methylstyrene oxide- β - d_1 with $\text{BF}_3 \cdot \text{OEt}_2$

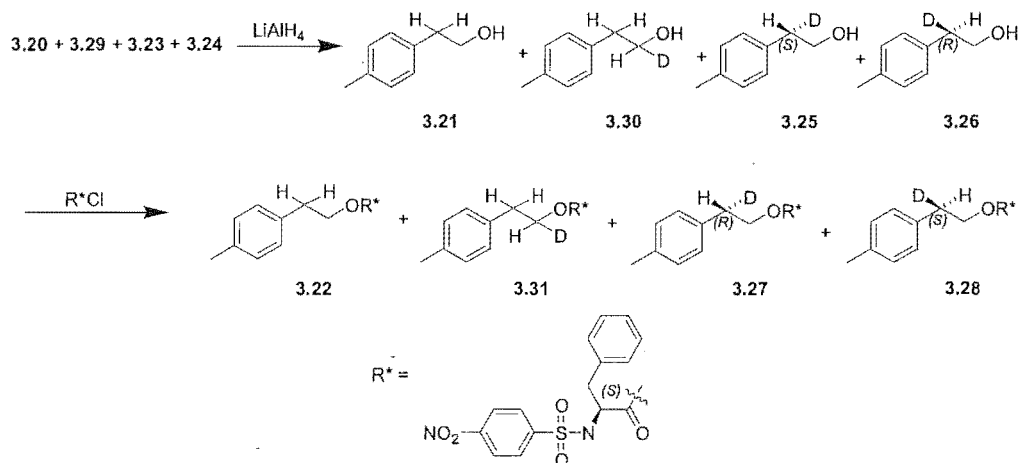
(αR),(βS)-*p*-Methylstyrene oxide- β - d_1 , **3.1** (enriched 82%, Scheme 3.15) and (αR),(βR)-*p*-methylstyrene oxide- β - d_1 , **3.2** (enriched 85% and 77% respectively, Scheme 3.16) were reacted as above. Each epoxide contained quantities of the other deuterio isomers **3.2** (**3.2**), **2.4** and **3.8**. Rearrangement of this mixture of epoxides gives four aldehydes (Schemes 3.15 and 3.16).



Scheme 3.15. Rearrangement of (αR),(βS)-*p*-methylstyrene oxide- β - d_1 .

Scheme 3.16. Rearrangement of (αR),(βR)-*p*-methylstyrene oxide- β - d_1 .

For each reaction the ratio of aldehydes is determined by reduction with LiAlH_4 and conversion of the resulting alcohol to ester with *N*-(4-nitrophenylsulfonyl)-*S*-phenylalanyl chloride:

Scheme 3.17. Reduction and esterification of aldehydes **3.20**, **3.29**, **3.23** and **3.24**.

Calculation of the deuterium isotope content of the esters **3.22**, **3.31**, **3.27** and **3.28** formed from rearrangement of **3.1**, shows that 8.04% of the product mixture contains no label, compared to 91.96% of the ester that has one deuterium label. This agrees, within experimental error with the ratio of deuterio isomers determined by analysis of the ^1H and ^2H NMR spectra of the starting epoxide and demonstrated that no deuterium label is lost in

the rearrangement and sequence of reaction involved in the analysis. The amount of undeuterated aldehyde **3.20** (and ester **3.22**) is therefore the same as the amount of undeuterated epoxide **3.8**.

Reaction	α ^2H NMR integral	β ^2H NMR integral	β H_S ^1H NMR integral	β H_R ^1H NMR integral
1	66.6	33.4	1	1.239
2	66.6	33.4	1	1.038
3	67.6	32.4	1	1.003
4	68.4	31.6	1	1.167

Table 3.7. ^2H and ^1H NMR integral of ester from rearrangement of **3.1**.

Reaction	α ^2H NMR integral	β ^2H NMR integral	β H_S ^1H NMR integral	β H_R ^1H NMR integral
1	67.8	32.2	1.057	1
2	71.1	28.9	1.031	1
3	71.3	28.7	1.164	1
4	71.7	28.3	1.160	1

Table 3.8. ^2H and ^1H NMR integral of ester from rearrangement of **3.2**.

Ester **3.31** is responsible for the ^2H NMR signal α to the ester oxygen, while **3.27** and **3.28** give rise to a ^2H NMR signal at the β position. The amount of **3.31** relative to **3.27** and **3.28** can therefore be obtained by comparison of the ^2H NMR integral for the α and β positions. This can be converted into the percentage of total ester, by multiplying by the fraction of deuterated ester, i.e. the amount of **3.31** as a percentage of total ester in reaction 1 for the rearrangement of **3.1**, is therefore $66.6 \times 0.9 = 60\%$.

Esters **3.22**, **3.31** and **3.28** give rise to the $H_S \beta$ 1H NMR signal, while **3.22**, **3.31** and **3.27** all contribute to the $H_R \beta$ proton signal. The known amount of signal arising from **3.22** and **3.31** can be subtracted from both the H_S and H_R 1H integral to give the amounts of **3.28** and **3.27**. The 1H NMR integral in arbitrary units must first be converted to a fraction of total ester by multiplying by x , calculated for each reaction below. See Appendix A for a discussion of the method of determination of x .

Rearrangement of **3.1**:

Reaction 1: $x = (2-0.30)/2.239 = 0.7593$

Reaction 2: $x = (2-0.30)/2.038 = 0.8342$

Reaction 3: $x = (2-0.29)/2.003 = 0.8537$

Reaction 4: $x = (2-0.28)/2.167 = 0.7937$

Reaction	3.20 (3.22)	3.29 (3.31)	3.23 (3.27)	3.24 (3.28)
1	10%	60%	24%	6%
2	10%	60%	17%	13%
3	10%	61%	15%	14%
4	10%	62%	21%	7%

Table 3.9. Ratio of aldehydes formed from rearrangement of impure **3.1**.

Rearrangement of **3.2**:

Reaction 1: $x = (2-0.30)/2.057 = 0.8264$

Reaction 2: $x = (2-0.27)/2.031 = 0.8518$

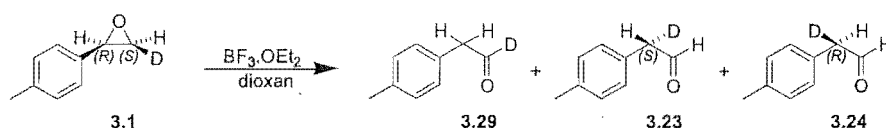
Reaction 3: $x = (2-0.24)/2.164 = 0.8133$

Reaction 4: $x = (2-0.24)/2.160 = 0.8148$

Reaction	3.20 (3.22)	3.29 (3.31)	3.23 (3.27)	3.24 (3.28)
1	8%	62%	13%	17%
2	8%	65%	12%	15%
3	16%	60%	5%	19%
4	16%	60%	5%	19%

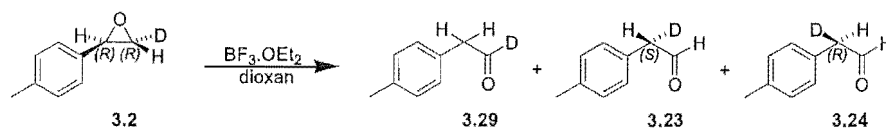
Table 3.10. Ratio of aldehydes formed from rearrangement of impure **3.2**.

The amount of aldehyde produced by rearrangement of the minor isomers **3.2** (**3.1**), **3.4** and **3.8** can be subtracted from the results in tables 3.9 and 3.10, to give the corrected ratio of aldehydes that would be produced on rearrangement of a sample of pure **3.1** (or **3.2**). For details of this procedure see Appendix B.

Scheme 3.18. Rearrangement of pure **3.1**.

Reaction	H migration (3.29)	D migration with inversion of configuration (3.23)	D migration with retention of configuration (3.24)
1	69%	25%	6%
2	69%	17%	14%
3	70%	15%	15%
4	71%	22%	7%
average	70±3%	20±4%	10±4%

Table 3.11. Distribution of aldehydes formed from rearrangement of pure **3.1**.

Scheme 3.19. Rearrangement of pure **3.2**.

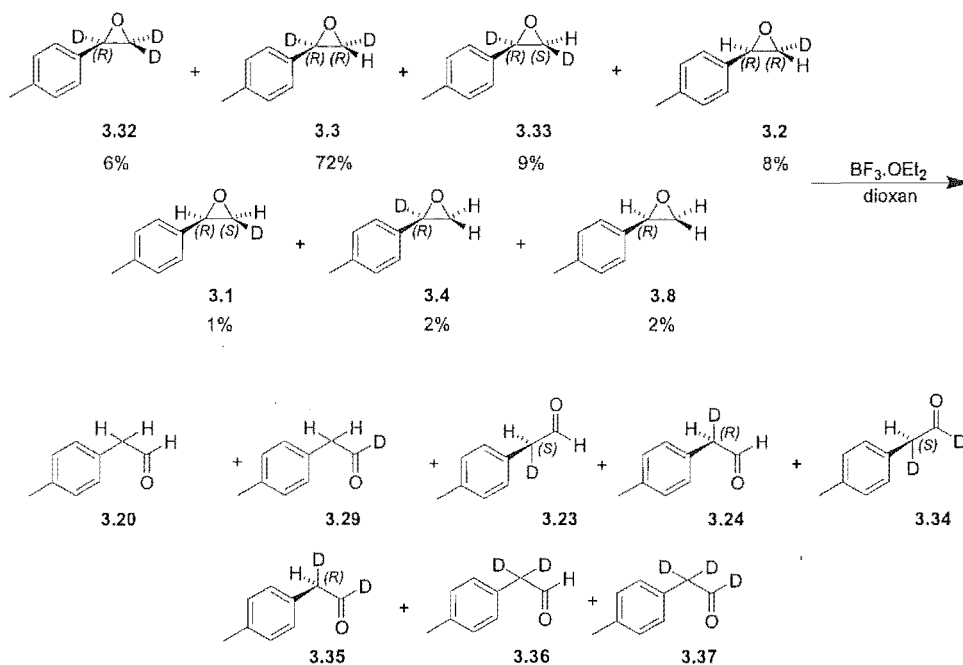
Reaction	H migration (3.29)	D migration with inversion of configuration (3.23)	D migration with retention of configuration (3.24)
1	69%	13%	18%
2	73%	6%	21%
3	73%	6%	21%
4	73%	6%	21%
average	73±3%	6±4%	21±4%

Table 3.12. Distribution of aldehydes formed from rearrangement of pure **3.2**.

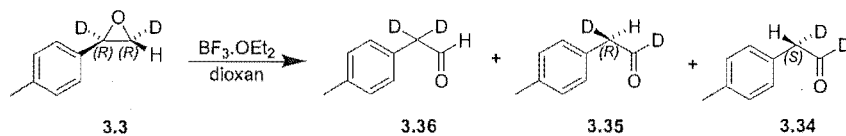
3.3.3 $\text{BF}_3\cdot\text{OEt}_2$ catalysed rearrangement of $(\alpha R),(\beta R)$ -*p*-methylstyrene oxide- α,β - d_2

Due to the number of minor deuterioisomers formed in the synthesis $(\alpha R),(\beta R)$ -*p*-methylstyrene oxide- α,β - d_2 , analysis of the results for the rearrangement of this epoxide were more complicated.

Using a combination of mass spectrometry, and ^1H and ^2H NMR, it was shown that the epoxide mixture contained the ratio of deuterioisomers shown in Scheme 3.20. Rearrangement of this ratio of epoxides with a Lewis acid will give a mixture of aldehydes **3.20-3.37**.

Scheme 3.20. Rearrangement of (αR),(βR)-*p*-methylstyrene oxide- α,β - d_2 .

The ratio of aldehydes produced on rearrangement of a sample of pure **3.3** can be obtained by the method outlined in Appendix C (Scheme 3.31, Table 3.13).

Scheme 3.21. Rearrangement of pure **3.3**.

Reaction	D migration (3.36)	H migration with inversion of configuration (3.35)	H migration with retention of configuration (3.34)
1	32%	61%	7%
2	35%	53%	12%
3	28%	61%	11%
average	32±4%	58±6%	10±3%

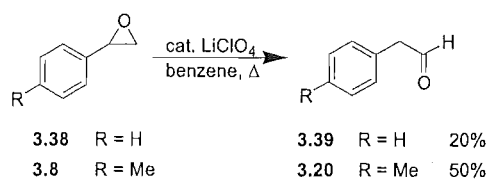
Table 3.13. Distribution of aldehydes formed from rearrangement of pure 3.3.

The results from the $\text{BF}_3\cdot\text{OEt}_2$ catalysed rearrangement of 3.3 show that racemisation of the aldehyde deuterioisomers is minimal under the reaction conditions and is ignored in the subsequent analysis.

3.4 LiClO_4 CATALYSED REARRANGEMENT OF *P*-METHYLSTYRENE OXIDE

Dr Quentin McDonald reported the rearrangement of styrene oxide to aldehyde in high yield with a catalytic amount of LiClO_4 in refluxing benzene.⁴ Attempts to reproduce his results with commercially available, racemic styrene oxide were unsuccessful. Even after reaction times of several days, only a 20% yield of aldehyde was obtained, the rest was unreacted starting material and polymerised aldehyde.

A higher yield of aldehyde was obtained for the rearrangement of *p*-methylstyrene oxide when 50% of the epoxide was converted to aldehyde after 24 hours at reflux. Longer reaction times produced more polymer.

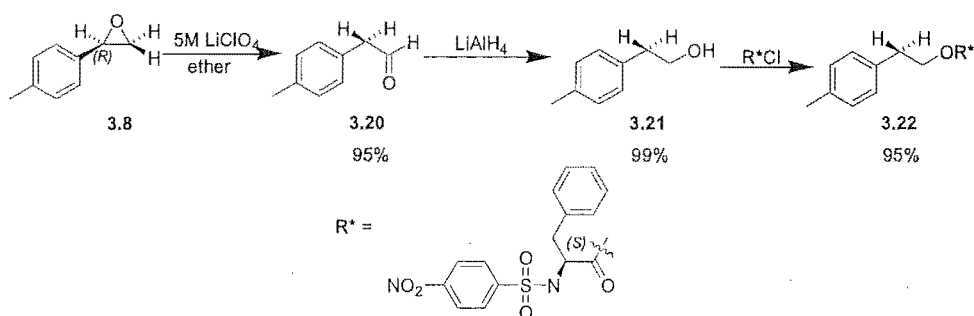


Scheme 3.22. Rearrangement of styrene oxide and *p*-methylstyrene oxide with LiClO₄ in refluxing benzene.

Recent reports in the literature indicate that the Lewis acidity of the lithium ion is modified in highly concentrated solutions of lithium perchlorate in diethylether resulting in more selective transformations than other, more traditional Lewis acids such as BF₃.⁵ *p*-Methylstyrene oxide was rearranged with 5M lithium perchlorate in ether, affording aldehyde in high yield. We discovered that the lithium perchlorate needed to have been freshly dried (150°C for 24 hours over P₂O₅ under vacuum).

3.4.1 LiClO₄ catalysed rearrangement of undeuterated *p*-methylstyrene oxide

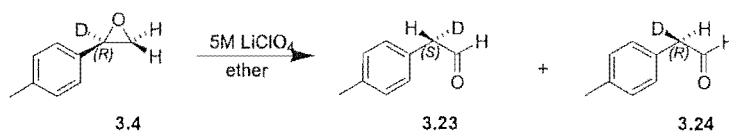
Undeuterated *p*-methylstyrene oxide was allowed to react with 5M LiClO₄ in diethylether to give aldehyde **3.20** in high yield. As for the BF₃·OEt₂ catalysed reactions above, the aldehyde produced was reduced with LiAlH₄ and the resulting alcohol was esterified with *N*-(4-nitrophenylsulfonyl)-*S*-phenylalanyl chloride. The protons β- to the oxygen of the ester were resolvable by NMR by the addition of *d*-Yb(hfc)₃ followed by integration of the relevant signals.



Scheme 3.23. Rearrangement and esterification of undeuterated *p*-methylstyrene oxide with 5M LiClO₄ in diethylether.

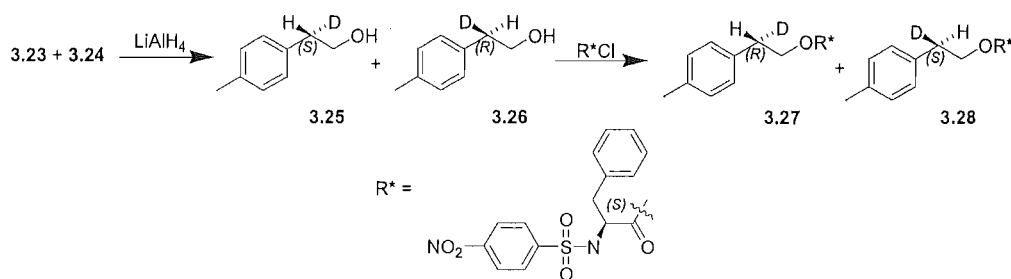
3.4.2 LiClO₄ catalysed rearrangement of (α R)-*p*-methylstyrene oxide- α -d₁

LiClO₄ catalysed rearrangement of (α R)-*p*-methylstyrene oxide- α -d₁ gives two aldehydes: **3.24**, from hydride migration with inversion of configuration and **3.23**, from hydride migration with retention of configuration.



Scheme 3.24. LiClO₄ promoted rearrangement of (α R)-*p*-methylstyrene oxide- α -d₁.

The reactions were analysed by reduction of the aldehyde to alcohol and esterification with *N*-(4-nitrophenylsulfonyl)-*S*-phenylalanyl chloride to give the *S* and *R* deuterio isomers **3.27** and **3.28**:

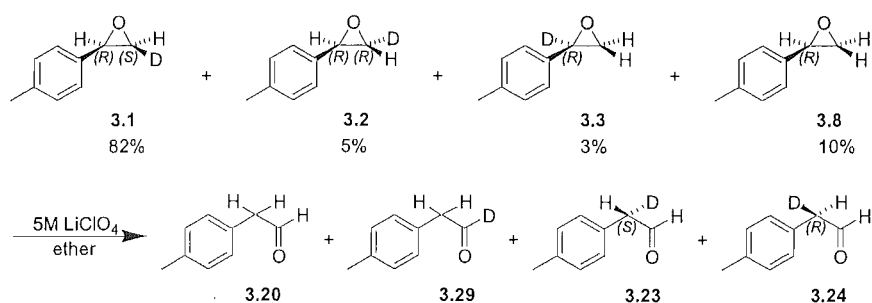
Scheme 3.25. Reduction and esterification of **3.23** and **3.24**.

The relative populations of esters **3.27** and **3.28** were determined by integration of the relative prochiral proton signals, separated by the addition of Yb(hfc)₃. The ratio of **3.27** : **3.28** is the same as the ratio of aldehydes **3.23** and **3.24**.

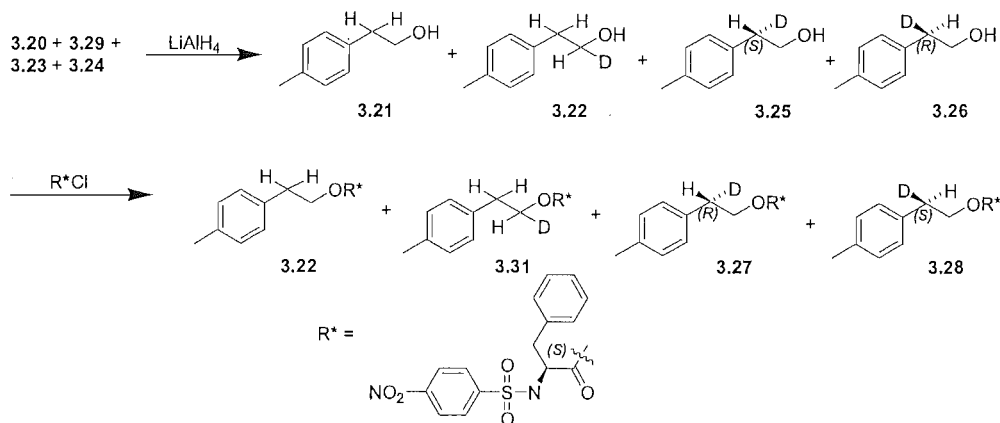
Reaction	H migration with retention of configuration 3.27 (and 3.23)	H migration with inversion of configuration 3.28 (and 3.24)
1	12%	88%
2	16%	84%
average	14±6%	86±13%

Table 3.14. Ratio of aldehydes produced by LiClO₄ promoted rearrangement of (*αR*)-*m*-methylstyrene oxide-*α*-d₁.

The results in Table 3.14 show that hydride migration with inversion of configuration is favoured over migration with retention of configuration by 6 : 1. This is in contrast to the BF₃ catalysed rearrangement of **3.4**, where there was little or no preference for hydride migration with inversion of configuration.

3.4.3 Rearrangement of (αR),(βS)-*p*-methylstyrene oxide- β - d_1 Scheme 3.26. LiClO_4 promoted rearrangement of (αR),(βS)-*p*-methylstyrene oxide- β - d_1 .

The ratio of aldehydes was again obtained by analysis of the ratio of esters from reduction and esterification of the aldehydes:

Scheme 3.27. Reduction and esterification of aldehydes from rearrangement of (αR),(βS)-*p*-methylstyrene oxide- β - d_1 .

The esters were analysed by ^2H NMR and ^1H NMR in the presence of $d\text{-Yb}(\text{hfc})_3$ chiral shift reagent:

Reaction	C1 ^2H NMR integral	C2 ^2H NMR integral	C2 H _S ^1H NMR integral	C2 H _R ^1H NMR integral
1	81	19	1	1.0806
2	76.5	23.5	1	1.2074
3	84	16	1	1.1043

Table 3.15. NMR data of the esters produced from rearrangement, reduction and esterification of (αR),(βS)-*p*-methylstyrene oxide- β - d_1 .

Reaction 1: $x = (2 - 0.17) / 2.0806 = 0.8796$

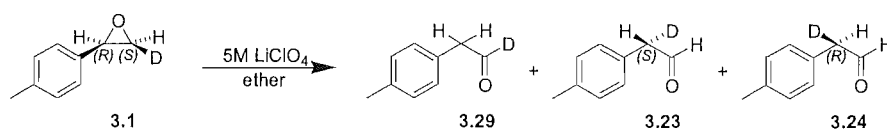
Reaction 2: $x = (2 - 0.21) / 2.2074 = 0.8109$

Reaction 3: $x = (2 - 0.15) / 2.1043 = 0.8792$

Reaction	3.20 (3.22)	3.29 (3.31)	3.23 (3.27)	3.24 (3.28)
1	10%	73%	12%	5%
2	10%	69%	19%	2%
3	10%	75%	12%	3%

Table 3.16. LiClO_4 promoted rearrangement of (αR),(βS)-*p*-methylstyrene oxide- β - d_1 .

Using the method outlined above, the aldehyde that would be produced from rearrangement of the minor isomers is established and incorporated into the analysis to give the ratio of aldehydes that would be produced on rearrangement of a sample of pure 3.1.



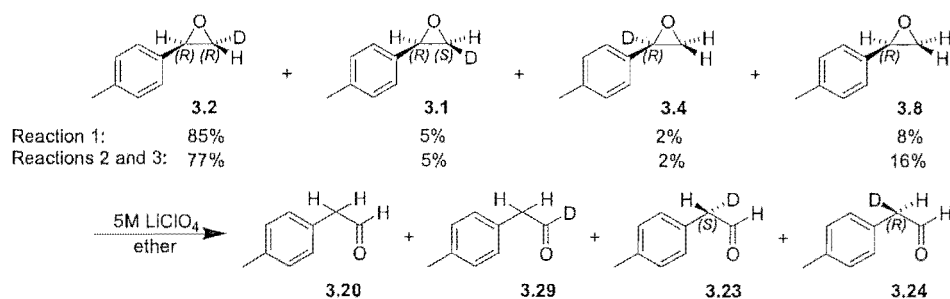
Scheme 3.28. LiClO_4 promoted rearrangement of pure (αR),(βS)-*p*-methylstyrene oxide- β - d_1 .

Reaction	H migration (3.29)	D migration with inversion of configuration (3.23)	D migration with retention of configuration (3.24)
1	85%	10%	4%
2	81%	18%	2%
3	89%	9%	2%
average	85±5%	12±4%	3±3%

Table 3.17. LiClO₄ promoted rearrangement of pure (αR),(βS)-*p*-methylstyrene oxide- β -*d*₁.

Again, like the BF₃ catalysed rearrangement of **3.1**, the *cis*, deuterium labelled hydrogen migrates almost exclusively with inversion of configuration. Only a very small amount of deuterium migration is observed.

3.4.4 Rearrangement of (αR),(βR)-*p*-methylstyrene oxide- β -*d*₁

Scheme 3.29. LiClO₄ promoted rearrangement of (αR),(βR)-*p*-methylstyrene oxide- β -*d*₁.

Reaction	C1 ² H NMR integral	C2 ² H NMR integral	C2 H _S ¹ H NMR integral	C2 H _R ¹ H NMR integral
1	61.4	38.6	1	1.080
2	60.9	39.1	1.015	1
3	59	41	1	1.063

Table 3.18. LiClO₄ promoted rearrangement of (αR),(βR)-*p*-methylstyrene oxide- β -*d*₁.

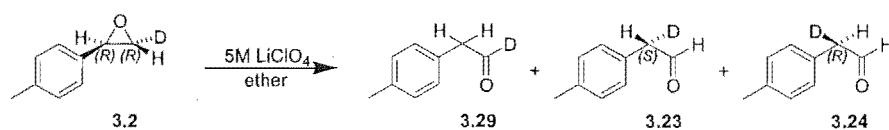
Reaction 1: $x = (2-0.36)/2.080 = 0.7885$

Reaction 2: $x = (2-0.33)/2.015 = 0.8288$

Reaction 3: $x = (2-0.34)/2.063 = 0.8047$

Reaction	3.20 (3.22)	3.29 (3.31)	3.23 (3.27)	3.24 (3.28)
1	8%	56%	21%	15%
2	16%	51%	16%	17%
3	16%	50%	20%	14%

Table 3.19. LiClO₄ promoted rearrangement of (αR),(βR)-*p*-methylstyrene oxide- β -*d*₁.



Scheme 3.30. Rearrangement of **3.2** with LiClO₄ in diethylether.

Reaction	H migration (3.29)	D migration with inversion of configuration (3.23)	D migration with retention of configuration (3.24)
1	61%	23%	16%
2	60%	19%	21%
3	59%	23%	18%
average	60±3%	22±4%	18±4%

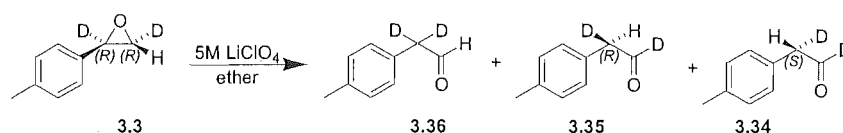
Table 3.20. LiClO₄ promoted rearrangement of pure (αR),(βR)-*p*-methylstyrene oxide- β -*d*₁.

LiClO₄ catalysed rearrangement of *trans* deuterated **3.2** results in more deuterium compared to hydrogen migration than for rearrangement of the *cis* deuterated **3.1**. The

deuterium in **3.2** migrates equally with inversion or retention of configuration, i.e. there is no facial selectivity for migration of the *trans* deuterium.

3.4.5 LiClO₄ catalysed rearrangement of (αR),(βR)-*p*-methylstyrene oxide- α,β -d₂

The ratio of aldehydes formed from rearrangement of the enriched mixture of **3.3** was corrected for the presence of minor isomers by the method outlined in Appendix C to give the ratio aldehydes that would be formed on rearrangement of a sample of pure **3.3**.



Scheme 3.31. LiClO₄ catalysed rearrangement of (αR),(βR)-*p*-methylstyrene oxide- α,β -d₂.

Reaction	D migration (3.36)	H migration with inversion of configuration (3.35)	H migration with retention of configuration (3.34)
1	39%	57%	4%
2	39%	61%	0%
3	49%	47%	4%
average	39±5%	59±5%	2±5%

Table 3.21. LiClO₄ catalysed rearrangement of (αR),(βR)-*p*-methylstyrene oxide- α,β -d₂.

The results for the LiClO₄ catalysed rearrangement of (αR),(βR)-*p*-methylstyrene oxide- α,β -d₂ are consistent with the ratio of aldehydes obtained from rearrangement of **3.1** and show that the aldehyde products are not racemising under the reaction conditions.

3.4.6 Racemisation of unreacted epoxide

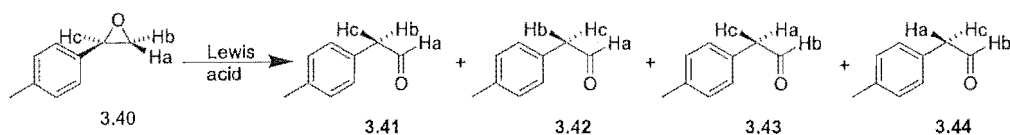
Whalen et al.⁶ has reported scrambling of the deuterium label in unreacted epoxide in the rearrangement of *p*-methoxystyrene oxide in aqueous solution after one half life of the

reaction. Whalen interpreted this result as the epoxide opening to a carbocation intermediate of sufficient lifetime that bond rotation could occur, before closure to the enantiomeric epoxide.

In order to check if *p*-methylstyrene oxide was opening to carbocation and closing to give the enantiomeric epoxide, an aliquot was taken from the reaction mixture after one half life of the LiClO₄ catalysed rearrangement of epoxide **3.1** and analysed by ¹H NMR. If enantioisomerism was occurring under the reaction conditions, the signal for the β-proton *cis* to the aromatic group would get larger relative to the *trans* β-proton signal. The ratio of the ¹H NMR integrals for the β-protons were identical to the starting epoxide, showing that no scrambling of the deuterium label was occurring in the reaction under the reaction conditions that we were interested in.

3.5 SUMMARY OF RESULTS

The results from all the Lewis acid catalysed rearrangements of *p*-methylstyrene oxide are summarised in Table 3.22:



Scheme 3.32. Rearrangement of deuterium labelled epoxide.

Lewis acid	Epoxide	3.41	3.42	3.43	3.44
BF ₃ .OEt ₂	3.4 (Ha=Hb=H, Hc=D)	53±3%*	47±3%*	*	*
	3.1 (Ha=D, Hb=Hc=H)	70±3%		20±4%	10±4%
	3.2 (Hb=D, Ha=Hc=H)	6±4%	21±4%	73±3%	
	3.3 (Ha=H, Hb=Hc=D)	32±4%		58±6%	10±3%
LiClO ₄	3.4 (Ha=Hb=H, Hc=D)	86±13%*	14±6%*	*	*
	3.1 (Ha=D, Hb=Hc=H)	85±5%		12±4%	3±3%
	3.2 (Hb=D, Ha=Hc=H)	22±4%	18±4%	60±3%	
	3.3 (Ha=H, Hb=Hc=D)	39±5%		59±5%	2±5%

Table 3.22. Summary of the Lewis acid catalysed rearrangement of *p*-methylstyrene oxide. For rearrangement of the deuterated epoxide, a maximum of three different aldehydes are produced.

* For these experiments, aldehydes 3.43 and 3.44 are identical to 3.41 and 3.42 respectively.

3.6 DISCUSSION OF ERRORS

The largest error in the above experiments is associated with the measurement of the relative amount of hydrogen and deuterium in each of the prochiral positions from the rearrangement of β -deuterated epoxide. Variations of between 5 and 10% were obtained in the relative ^1H NMR integral at different concentrations of chiral shift reagent.

Facial selectivity measurements of the products from rearrangement of epoxide deuterated in the α position are more accurate due to the fact that the measurements are obtained from a ^1H NMR spectrum. In the products from rearrangement of β -deuterated epoxide, only approximately 30% of the material contains a migrated deuterium label so a small difference in the ^1H NMR integral represents a much larger difference in the amount of deuterium in each prochiral position. The measurements are however accurate and reproducible enough to show the preference for migration with inversion or retention of configuration of the two terminal epoxide hydrogens.

In the $\text{BF}_3 \cdot \text{OEt}_2$ catalysed rearrangements the difference between the amount of deuterium relative to hydrogen migration from the rearrangement of *cis* deuterated epoxide **3.1** (70% H migration) and *trans* deuterated epoxide **3.2** (73% H migration) is probably not significant. Neither is the measured preference for hydrogen migration with inversion of configuration measured from the rearrangement of α -deuterated epoxide, which is really 50 : 50 within the experimental error.

More selectivity is observed in the rearrangement of epoxide with LiClO_4 and the experiments show good reproducibility. The error for each experimentally derived parameter is estimated and shown in the Tables above.

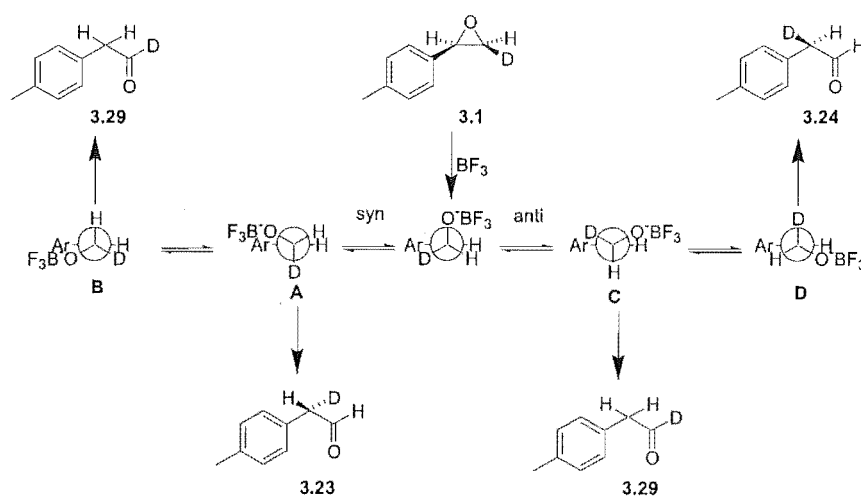
3.7 DISCUSSION

3.7.1 The rearrangement of *cis*- and *trans* epoxide (3.1 and 3.2)

The conformations for hydride migration leading to aldehyde for the rearrangements of $(\alpha R), (\beta S)$ -*p*-methylstyrene oxide- β - d_1 and $(\alpha R), (\beta R)$ -*p*-methylstyrene oxide- β - d_1 are shown in Schemes 3.34 and 3.35.

3.7.1.1 The rearrangement of *cis*- β -deuterated epoxide (3.1)

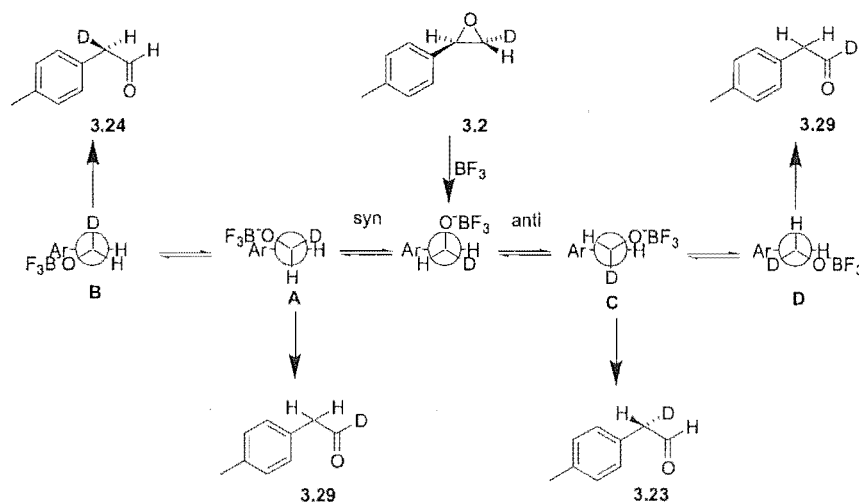
The rearrangement of (αR),(βS)-*p*-methylstyrene oxide- β - d_1 is shown in Scheme 3.34. Hydrogen migration from conformers **B** and **C** give aldehyde **3.29**, while deuterium migration with inversion of configuration from conformer **A**, gives aldehyde **3.23** and deuterium migration with retention of configuration from conformer **D**, gives aldehyde **3.24**. Conformations **A** and **B** have the OBF_3 and larger aromatic group in a gauche orientation and should therefore be disfavoured on steric grounds.



Scheme 3.34. Carbocation conformations in the rearrangement of **3.1**.

3.7.1.2 The rearrangement of *trans*- β -deuterated epoxide (3.2)

The four conformations of carbocation leading to hydride or deuteride migration for the rearrangement of **3.2** are shown in Scheme 3.35.

Scheme 3.35. Carbocation in the rearrangement of **3.2**.

3.7.2 Calculation of the facial selectivity for hydride migration in the $\text{BF}_3 \cdot \text{OEt}_2$ rearrangement of β -deuterated epoxide

The results from the $\text{BF}_3 \cdot \text{OEt}_2$ catalysed rearrangement of $(\alpha R, \beta S)$ -*p*-methylstyrene oxide- β - d_1 **3.1** ($\text{Ha}=\text{D}$) and $(\alpha R, \beta R)$ -*p*-methylstyrene oxide- β - d_1 **3.2** ($\text{Hb}=\text{D}$) are shown in Scheme 3.36. The four transition conformers for hydride (deuteride) migration are shown.

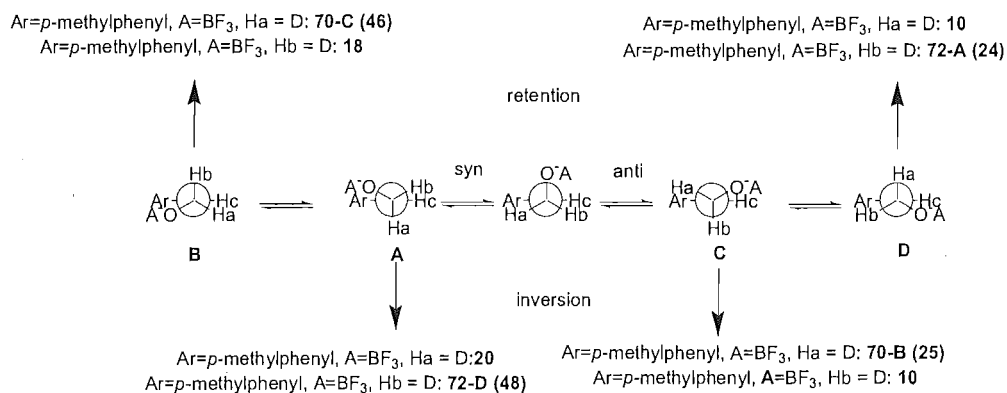
Each experiment gives the facial selectivity for deuterium migration, but not for hydrogen migration. The facial selectivity for migration of either Ha or Hb is the same regardless of whether Ha or Hb is hydrogen or labelled as deuterium. The facial selectivity for migration of Ha in epoxide where $\text{Ha}=\text{H}$ is therefore obtained from facial selectivity for migration of Ha in the experiment where $\text{Ha}=\text{D}$. The relative contributions of each of the four transition conformers can therefore be calculated:

From experiment 1 ($\text{Ha}=\text{D}$): $\text{B}+\text{C}=70$ (H migration) and $\text{A}/\text{D}=20/10$ (D migration).

From experiment 2 ($\text{Hb}=\text{D}$): $\text{A}+\text{D}=72$ (H migration) and $\text{B}/\text{C}=18/10$ (D migration).

Using the ratio of B/C in experiment 2, $\text{B}=46$ and $\text{C}=25$ in experiment 1.

Using the ratio of A/D in experiment 1, $\text{A}=48$ and $\text{D}=24$ in experiment 2.



Scheme 3.36. Experimental results for the BF₃.OEt₂ catalysed rearrangement of (α*R*),(β*S*)-*p*-methylstyrene oxide-β-*d*₁ and (α*R*),(β*R*)-*p*-methylstyrene oxide-β-*d*₁.

3.7.3 Fujimoto method to calculate the selectivity for hydride migration in undeuterated epoxide

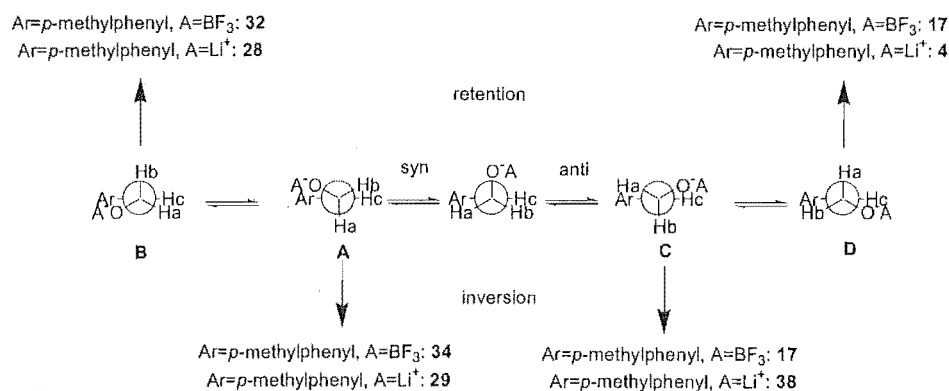
The method of Fujimoto⁷ can be used to estimate the relative contribution of each transition conformer when undeuterated epoxide is rearranged. It is assumed that deuterium migration is retarded to the same extent, relative to hydrogen migration in each of the four possible transition conformers for hydrogen / deuterium migration. A deuterium isotope parameter, *z* (the amount deuterium migration is retarded relative to hydrogen migration) can then be calculated to satisfy the relation: 46 : 20*z* : 25 : 10*z* = 18*z* : 48 : 10*z* : 24.

It is therefore determined that *z* = 2.5 and the relative contribution of each of the four transition conformers in undeuterated material can then be estimated. The ratio **B** : **A** : **C** : **D** is 46 : 50 : 25 : 25, or 32% : 34% : 17% : 17%.

3.7.4 Results for the Fujimoto analysis of LiClO₄ promoted rearrangement of β-deuterated epoxide.

The same calculation can be performed for the LiClO₄ promoted rearrangement of β-deuterated *p*-methylstyrene oxides **3.1** and **3.2** and the ratio of **B** : **A** : **C** : **D** is determined

to be 28% : 29% : 38% : 4%. The results calculated for both the $\text{BF}_3 \cdot \text{OEt}_2$ and LiClO_4 catalysed rearrangements of undeuterated *p*-methylstyrene oxide are shown schematically in Scheme 3.37.



Scheme 3.37. Estimation of the hydride migration for undeuterated *p*-methylstyrene oxide.

3.7.5 Comparison to the results from α - and α,β -dideuterated epoxide (3.4 and 3.3)

Scheme 3.37 above was derived using data only from the rearrangements of (αR),(βS)-*p*-methylstyrene oxide- β - d_1 3.1 and (αR),(βR)-*p*-methylstyrene oxide- β - d_1 3.2. The results in Scheme 3.37 can be compared to the measurements obtained from the $\text{BF}_3 \cdot \text{OEt}_2$ and LiClO_4 catalysed rearrangements of α -deuterated and α,β -dideuterated *p*-methylstyrene oxide 3.4 and 3.3.

3.7.6 Results for the rearrangement of α deuterated epoxide (3.4)

The rearrangement of α -deuterated epoxide gives a measure of the facial selectivity for hydride migration. The selectivity observed for the LiClO_4 and $\text{BF}_3 \cdot \text{OEt}_2$ catalysed rearrangements of (αR)-*p*-methylstyrene oxide- α - d_1 3.4 can be compared to the selectivity calculated above, based on the rearrangement of (αR),(βS)-*p*-methylstyrene oxide- β - d_1 3.1 and (αR),(βR)-*p*-methylstyrene oxide- β - d_1 3.2.

3.7.6.1 $\text{BF}_3 \cdot \text{OEt}_2$ catalysed rearrangement of (αR) -*p*-methylstyrene oxide- α - d_1

Hydrogen migration with inversion of configuration is marginally preferred over hydrogen migration with retention of configuration by a ratio of 53% : 47%. This ratio can be regarded as 1 : 1, within experimental error. In Scheme 3.37, it can be seen that hydride migration with inversion of configuration is calculated to be favoured by a ratio of 51 : 49, which is in good agreement with the experimental result.

3.7.6.2 LiClO_4 catalysed rearrangement of (αR) -*p*-methylstyrene oxide- α - d_1

The LiClO_4 catalysed rearrangement of α -deuterated epoxide shows that hydride migration with inversion of configuration is hugely favoured over hydride migration with retention of configuration, by a ratio of 84% : 16%. In Scheme 3.37 above hydride migration with inversion of configuration is also calculated to be favoured, but by a ratio of only 67% : 33%. The difference in the two ratios reflects the experimental error associated with all three experiments used to derive these ratios.

3.7.7 Results for the rearrangement of dideuterated epoxide (3.3)

Two parameters are measured in the rearrangement of $(\alpha R), (\beta R)$ -*p*-methylstyrene oxide- α, β - d_2 **3.3**. The facial selectivity of the hydrogen *cis* to the aromatic group is measured, along with the amount of hydrogen relative to deuterium migration.

3.7.7.1 $\text{BF}_3 \cdot \text{OEt}_2$ catalysed rearrangement of $(\alpha R), (\beta R)$ -*p*-methylstyrene oxide- α, β - d_2

The ratio of hydrogen to deuterium migration in the $\text{BF}_3 \cdot \text{OEt}_2$ rearrangement of $(\alpha R), (\beta R)$ -*p*-methylstyrene oxide- α, β - d_2 **3.3** is 68 : 32. This ratio can be compared to the measured selectivity for hydrogen relative to deuterium migration of the equivalent mono- β -deuterated epoxide, $(\alpha R), (\beta R)$ -*p*-methylstyrene oxide- β - d_1 **3.2**, where the ratio is 73 : 27. These two ratios are similar and the difference reflects the experimental error in the ratios for the dideuterated epoxide:

The experiment also measured the facial selectivity for migration of the hydrogen *cis* to the aromatic group. The ratio of hydrogen migration with inversion with respect to retention of

configuration was established as 58 : 10. This is significantly different from the results from the $\text{BF}_3 \cdot \text{OEt}_2$ catalysed rearrangement of $(\alpha R), (\beta R)$ -*p*-methylstyrene oxide- β - d_1 **3.2**, where a preference for migration of the deuterium *cis* to the aromatic group was found to be 20 : 10, in favour of migration with inversion of configuration. It is expected that these two ratios be the same. The difference represents a large experimental error in one of the experiments.

3.7.7.2 LiClO_4 catalysed rearrangement of $(\alpha R), (\beta R)$ -*p*-methylstyrene oxide- α, β - d_2

The LiClO_4 catalysed rearrangement of $(\alpha R), (\beta R)$ -*p*-methylstyrene oxide- α, β - d_2 **3.3** is consistent with the results from the LiClO_4 catalysed rearrangement of the two mono- β -deuterated epoxides.

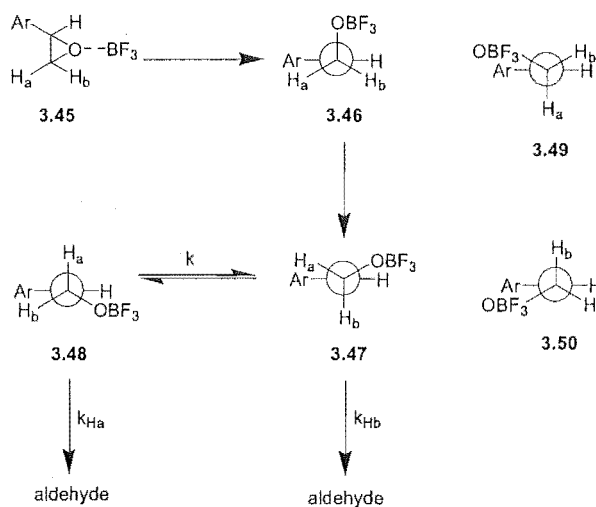
Migration of hydrogen is favoured over deuterium by a ratio of 61 : 39. This is close to the results observed for the LiClO_4 catalysed rearrangement of $(\alpha R), (\beta R)$ -*p*-methylstyrene oxide- β - d_1 **3.2**, where migration of hydrogen over deuterium is favoured by a ratio of 60 : 40.

The hydrogen (*cis* to the aromatic group) migrates almost exclusively with inversion of configuration, inversion is favoured by 59 : 2. This is similar to the rearrangement of $(\alpha R), (\beta S)$ -*p*-methylstyrene oxide- β - d_1 **3.1**, where migration of the deuterium *cis* to the aromatic group with inversion of configuration is favoured by a ratio of 12 : 3. These two results on their own indicate that the *cis* hydrogen or deuterium migrates almost exclusively with inversion of configuration, as seen in Scheme 3.37.

3.7.8 Comparison to the Blackett model

The results from previous studies into the rearrangement of non-optically active epoxide have been analysed using the mechanism first put forward by Blackett et al.⁸ The Blackett mechanism for the rearrangement of arene oxide is shown in Scheme 3.33 below. Epoxide opens to a carbocation, which rotates in only one direction, aligning H β with the cation p-orbital where migration can take place. A further 60° rotation about the C1-C2 bond of the

cation aligns H_a with the cation p-orbital and migration of H_a can occur. If the rate of rotation between the carbocation conformers, k , is slower or similar to the rate of hydride migration, k_{H_a} and k_{H_b} , migration of H_b will be preferred to migration of H_a .



Scheme 3.33. Blackett mechanism for the BF_3 catalysed rearrangement of arene oxide.

In an investigation into the Lewis acid catalysed rearrangement of racemic *cis*- and *trans*- β -deuterated styrene oxide, McDonald found that more deuterium migrated on rearrangement of the *trans* deuterated epoxide than the *cis* deuterated epoxide. He therefore concluded that migration of the hydrogen *trans* to the phenyl group would be preferred to migration of the *cis* hydrogen in undeuterated epoxide. Hydride migration is always preferred to deuteride migration, as expected from a normal deuterium isotope effect.

The results in Table 3.22 show that more deuterium migrates on rearrangement of *trans*- β -deuterated epoxide 3.2 than *cis*- β -deuterated epoxide 3.1 in the $LiClO_4$ in ether catalysed reaction, which is consistent with previous results of McDonald. However, in the $BF_3 \cdot OEt_2$ catalysed rearrangement reported above, slightly more deuterium relative to hydrogen migrates in the rearrangement of (αR),(βS)-*p*-methylstyrene oxide- β - d_1 3.1 (30% : 70%) than in the rearrangement of (αR),(βR)-*p*-methylstyrene oxide- β - d_1 3.2 (27% : 73%). i.e.

more deuterium migrates on rearrangement of the epoxide deuterated *cis* rather than *trans* to the aryl group. The difference in these two ratios is however just within the error for the experiment.

The two conformations for hydride migration where the OBF_3 and aryl groups are in a gauche orientation (**3.49** and **3.50**, Scheme 3.33) are thought not to occur in the Blackett mechanism, due to the gauche interaction between the bulky substituent and the OBF_3 , or O^-Li^+ . Therefore, in the Blackett mechanism, Hb is assumed to always migrate with inversion of configuration and Ha to always migrate with retention of configuration, even when either Ha or Hb are labelled as deuterium.

The results in Table 3.22 show migration of Hb with retention of configuration and Ha with inversion of configuration (migration from conformers **3.49** and **3.50** in Scheme 3.33) are significant parts of the reaction. This shows that the assumption made in the Blackett mechanism that the carbocation rotates in only one direction is not correct for the LiClO_4 or $\text{BF}_3\cdot\text{OEt}_2$ catalysed rearrangement of *p*-methylstyrene oxide. Hydride migration from all four possible hydride migration conformers must be considered.

3.7.9 Mechanistic implications

Calculations performed by Aaron Thorpe on the acid catalysed rearrangement of propene oxide have shown that in some cases hydride migration may be concerted with ring opening of the epoxide and a discrete carbocation intermediate is not formed during the reaction. Only hydride migration with inversion of configuration will occur in a concerted rearrangement. In both the LiClO_4 and $\text{BF}_3\cdot\text{OEt}_2$ catalysed rearrangements of *p*-methylstyrene oxide, a significant amount of hydride (deuteride) migration with retention of configuration is occurring, showing that most if not all of the reaction is proceeding via a carbocation pathway.

The reaction can be divided into rotation of the carbocation bringing the Lewis acid coordinated oxygen either *syn* to the aromatic group, giving conformers **A** and **B** and rotation of the oxygen *anti* to the aromatic group to give conformers **C** and **D** (Scheme 3.37).

For the $\text{BF}_3 \cdot \text{OEt}_2$ catalysed rearrangement, rotation *syn* to the aromatic group is preferred by a ratio of 66 : 34 (**A+B** : **C+D**, Scheme 3.37). In the LiClO_4 catalysed reaction the ratio is 58 : 42 in favour of *syn* rotation. In the previously published results for the rearrangement of styrene oxide, it was assumed that only *anti* cation rotation could occur. These experiments clearly show that not only is rotation of the cation in the *syn* direction occurring in the rearrangement of *p*-methylstyrene oxide, but it is the favoured pathway for reaction in both the $\text{BF}_3 \cdot \text{OEt}_2$ and LiClO_4 catalysed reactions.

The facial selectivity for hydride migration can be examined when the reaction is divided into rotation of the Lewis acid co-ordinated oxygen towards and away from the aromatic substituent, as in Scheme 3.37. In the $\text{BF}_3 \cdot \text{OEt}_2$ catalysed reaction both pathways result in an equal amount of hydride migration with inversion and retention of configuration. In the LiClO_4 reaction, rotation towards the aromatic substituent gives an equal amount of hydride migration with inversion and retention of configuration, but only hydride migration with inversion of configuration is observed from the *anti* carbocation.

¹ Sharpless, K. B.; Amberg, W.; Bennani, Y. L.; Crispino, G. A.; Hartung, J.; Jeong, K.; Kwong, H.; Morikawa, K.; Wang, Z.; Xu, D.; Zhang, X. *J. Org. Chem.* **1992**, *57*, 2768-2771.

² Kolb, H. C.; Sharpless, K. B. *Tetrahedron* **1992**, *48*(48), 10515-10530.

³ Moussou, P.; Archelas, A.; Baratti, J.; Furstoss, R. *J. Org. Chem.* **1998**, *63*, 3532-3537.

⁴ Coxon, J. M.; McDonald, D. Q. *Tetrahedron Lett.* **1988**, *29*, 2575-2576.

⁵ Sankararaman, S.; Nesakumar, J. E. *Eur. J. Org. Chem.* **2000**, 2003-2011.

⁶ Ukachukwa, V. C.; Blumenstein, J. J.; Whalen, D. L. *J. Am. Chem. Soc.* **1986**, *108*, 5039-5040.

⁷ Hara, N.; Mochizuki, A.; Tatara, A.; Fujimoto, Y. *Tetrahedron Asym.* **2000**, *11*, 1859-1868.

⁸ Blackett, B. N.; Coxon, J. M.; Hartshorn, M. P.; Richards, K. E. *J. Am. Chem. Soc.* **1970**, *92*, 2574-2575.

Chapter Four

The Role of Fluorohydrin in the Rearrangement of *p*-Methylstyrene Oxide

4.1 INTRODUCTION

The $\text{BF}_3 \cdot \text{OEt}_2$ catalysed rearrangement of *p*-methylstyrene oxide shows an unexpected selectivity for hydrogen migration. A greater proportion of deuterium relative to hydrogen migration is observed in the rearrangement *cis*- compared to *trans*- β -deuterated *p*-methylstyrene oxide (30% compared to 27%), showing that migration of the hydrogen *cis* to the aromatic group in *p*-methylstyrene oxide would be slightly preferred over migration of the *trans* hydrogen in undeuterated epoxide. This is in contrast to previous investigations into the selectivity for migration of terminal hydrogen/deuterium in the rearrangement of 1-substituted and 1,1-disubstituted epoxides, where migration of hydrogen *trans* to the bulky substituent occurs in preference to the *cis* hydrogen.¹

It was necessary to test whether the unusual selectivity is a result of fluorohydrin being an intermediate in the rearrangement process. Fluorohydrin has been previously isolated from $\text{BF}_3 \cdot \text{OEt}_2$ catalysed reactions of epoxides where a fluorine atom reacts at the carbocation centre.² In one case where fluorohydrin is formed in a reaction more vigorous reaction conditions converted the fluorohydrin to a carbonyl compound.³ Gas phase *ab initio* and density functional calculations on BF_3 co-ordinated 2,3,3-trimethyl-1-butene oxide⁴ show the barrier to fluorohydrin formation is comparable to that for rearrangement to aldehyde.

This chapter describes the synthesis of fluorohydrin from deuterated *p*-methylstyrene oxides and conversion of fluorohydrin to aldehyde with $\text{BF}_3 \cdot \text{OEt}_2$. The rate and selectivity of the reaction for conversion of fluorohydrin to aldehyde is analysed to determine whether this reaction is occurring in the rearrangement of *p*-methylstyrene oxide to *p*-methylphenylacetaldehyde.

4.2 SYNTHESIS OF FLUOROHYDRIN

Relatively few methods exist for the formation of fluorohydrins. One method that has gained widespread use in recent times is amine based HF reagents. A previous study has shown that fluorine addition to epoxide with HF-amine reagents occurs preferentially with inversion of configuration at the site of fluorine attack.⁵

(αS)-*p*-Methylstyrene oxide- α -*d* (**4.1**), (αR),(βS)-*p*-methylstyrene oxide- β -*d* (**4.2**), and (αR),(βR)-*p*-methylstyrene oxide- α,β -*d*₂ (**4.3**) (Figure 1), were synthesised using the Sharpless asymmetric dihydroxylation, and epoxidation by the method of Sharpless et al.,⁶ as described in Chapter 3.

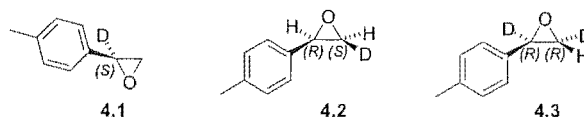
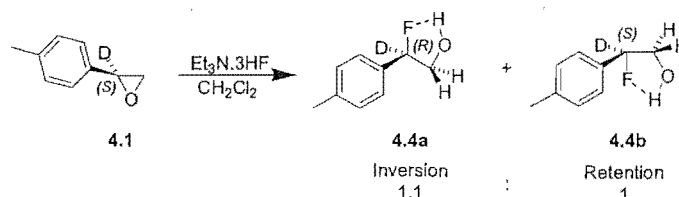


Figure 4.1. Isomers of *p*-methylstyrene oxide.

Epoxide **4.1** underwent reaction with triethylamine trihydrofluoride, to give fluorohydrin **4.4** in 75% yield (Scheme 1) and the enantiomeric excess of the fluoride addition was determined from ²H NMR in the presence of a chiral shift reagent.



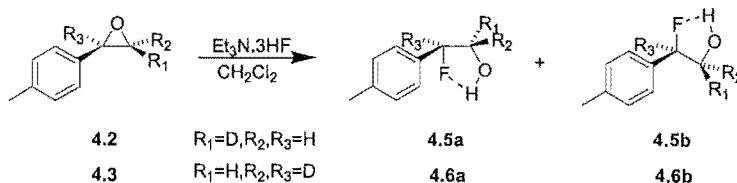
Scheme 4.1. Fluorine addition to (αS)-*p*-methylstyrene oxide- α -*d*₁.

²H NMR of **4.4a** and **4.4b** gives a doublet at 5.53ppm ($J_{D-F} = 7.64\text{Hz}$). Diastereomeric complexes were created by gradual addition of Ytterbium tris[3-(heptafluoropropylhydroxymethylene)-(+)-camphorate] (Yb(hfc)₃) chiral shift reagent. The deuterium peak moved downfield on each addition of Yb(hfc)₃ and split into two broad singlets. At high concentrations of shift reagent, the D-F coupling is not observed.

Integration of the two deuterium signals proved difficult due to line broadening at high concentrations of paramagnetic chiral shift reagent, decreasing the signal to noise ratio. Direct integration of the NMR spectrum gave a ratio of 1.2 : 1 for the downfield peak compared to the upfield peak.

We have previously written a script for the Matlab software package that uses least squares analysis to iteratively fit a curve to the Lorentzian line shapes produced in an NMR spectrum. This method is particularly useful for integration of signals that are overlapping. Integration using the Matlab script gave a ratio of 1.1 : 1 for the downfield : upfield peaks. The ratio of **4.4a** : **4.4b** is therefore 1.1 : 1 or the reverse namely 1 : 1.1.

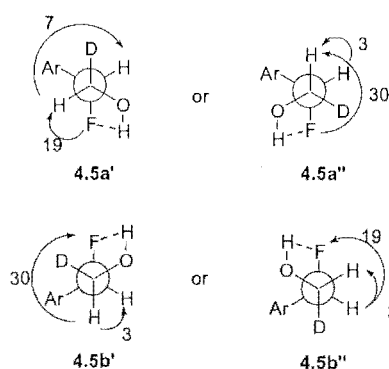
(1*S*)-2-Fluoro-2-(*p*-methylphenyl)ethanol-1-*d*₁ (**4.5**) was synthesised by reaction of (*αR*),(*βS*)-*p*-methylstyrene oxide-*β-d*₁ (**4.2**) with triethylamine trihydrofluoride (Scheme 4.2). It has previously been reported that fluorohydrins are conformationally restricted due to the hydrogen bonding between the fluorine and hydroxyl moieties⁷ and the terminal hydrogens of a fluorohydrin such as **4.5** will have different chemical shifts. The relative amounts of **4.5a** and **4.5b**, which are diastereomers due to isotopic substitution, can be determined from the relative integral of R₂ in **4.5a** compared to R₂ in **4.5b**.



Scheme 4.2. Fluorohydrin formation from *β*-deuterated epoxides **2** and **3**.

We can tentatively assign the proton signals for the mixture of **4.5a** and **4.5b** based on their H-H and H-F⁸ coupling constants. The coupling constants and likely conformations of fluorohydrins **4.5a** and **4.5b** are shown in Table 4.1 and Figure 4.2.

^1H NMR signal (δ)	$J_{\text{H-H}}$	$J_{\text{H-F}}$	relative integral
5.44	$^3J_{\text{H-H}} = 7.325$	$^2J_{\text{H-F}} = 48.343$	1
3.91	$^3J_{\text{H-H}} = 7.326$	$^3J_{\text{H-F}} = 18.555$	0.49
3.78	not observed*	$^3J_{\text{H-F}} = 30.276$	0.58

Table 4.1. ^1H NMR coupling constants and integrals for **4.5**.Figure 4.2. The most important conformations of **4.5** with coupling constants.

From Table 4.1, the proton signal at 3.91 ppm has an H-H coupling constant of 7 and an H-F coupling constant of 19. The proton signal at 3.78 has a small H-H coupling and an H-F coupling constant of 30. The coupling constants show that either of the conformations for **4.5a** in Figure 4.2 could be present, but neither proton signal has a small H-H coupling constant and an H-F coupling constant of close to 19, as predicted for **4.5b''**. **4.5b** must therefore exist primarily as conformer **4.5b'** which gives the proton signal at 3.78 ppm. The signal at 3.91 ppm is therefore for **4.5a** as conformer **4.5a'**.[†]

* The proton signals are broad because of faster relaxation due to the adjacent deuterium atom and so a small coupling constant would not be observed.

[†] Care must be taken in assigning coupling constants to specific conformers as the coupling constants are from the weighted average of all possible conformations.

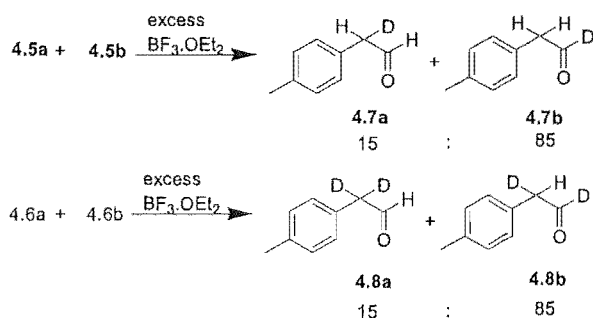
The presence of an NOE correlation between the signals at 3.78 and 5.44 is consistent with the signal at 3.78 arising from **4.5b** in conformation **4.5b'**. From the integrals in Table 4.1, **4.5a** and **4.5b** are formed in a ratio of 1 : 1.18 in the fluorine addition reaction. This indicates that there is a slight preference of fluorine attack with retention of configuration perhaps resulting from the appropriate ion pair of the epoxide and HF.

(1*R*)-2-Fluoro-2-(*p*-methylphenyl)ethanol-1,2-*d*₂ **4.6** was made from (α *R*),(β *R*)-*p*-methylstyrene oxide- α,β -*d*₂ **4.3**. Integration of the proton signals for the C1 proton showed **6a** and **6b** were formed in a ratio of 1:1.13. The ratio for the formation of **4.6** is the same, within experimental error as the diastereomeric excess for formation of **4.5**, showing that the secondary deuterium isotope effect has little or no effect on the stereochemical outcome of the fluorine addition reaction.

4.3 CONVERSION OF FLUOROHYDRIN TO ALDEHYDE WITH BF₃·OEt₂

In order to determine whether fluorohydrin could be converted to aldehyde and at what rate, the fluorohydrin was subjected to the same reaction conditions used to effect rearrangement of the epoxide to aldehyde. *p*-Methylstyrene oxide has been rearranged directly to aldehyde in high yield with catalytic amounts BF₃·OEt₂ in dioxan and it should be noted that the reaction is complete within 15 minutes. When fluorohydrin **4.5** was subjected to these reaction conditions, no aldehyde was observed and starting material was recovered unchanged.

Conversion of fluorohydrins **4.5a** and **4.5b** to aldehydes **4.7a** and **4.7b**, formed from migration of deuterium and hydrogen respectively can however be accomplished with an excess of BF₃·OEt₂ (Scheme 4.3) and increased reaction time. Reaction of (1*S*)-2-fluoro-2-(*p*-methylphenyl)ethanol-1-*d* **4.5** with excess BF₃·OEt₂ in dioxan for 15 minutes resulted in partial conversion to aldehyde, after 4 hours a trace of fluorohydrin still remained and a 40% yield of aldehyde was obtained. The relative amount of **4.7a** and **4.7b** was measured from the ²H NMR spectrum to be 15% to 85%.



Scheme 4.3. Conversion of fluorohydrin to aldehyde.

Reaction of fluorohydrin **4.6a** and **4.6b** with excess $\text{BF}_3 \cdot \text{OEt}_2$ for 4 hours again gave a ratio of aldehyde formed from migration of deuterium to hydrogen (**4.8a** and **4.8b**) of 15% : 85%.

The deuterium isotope effect for each reaction is large, >5.7 , compared to a value of 2.3 for the rearrangement of the styrene oxides. The larger isotope effect shows that the hydrogen is more symmetrically aligned in the transition state for the migration and that the reaction mechanism is more concerted, with hydrogen participating in the removal of fluorine, than in the BF_3 catalysed reaction of the epoxide where the reaction occurs by way of a carbocation intermediate.

4.4 CONCLUSION

The rate of conversion of 2-fluoro-2-(*p*-methylphenyl)ethanol to aldehyde (reaction incomplete after 4 hours) is much slower than rearrangement of *p*-methylstyrene oxide to aldehyde (reaction complete within 5 minutes). This establishes that the aldehyde produced in the rearrangement does not arise via the fluorohydrin. Also, the deuterium isotope effect is larger in the formation of aldehyde from fluorohydrin than in the $\text{BF}_3 \cdot \text{OEt}_2$ catalysed rearrangement of β -deuterated styrene oxide to aldehyde, indicating that the two reactions occur by different mechanisms. The fluorohydrin gives aldehyde in a concerted process with a relatively symmetrical positioning of the migrating hydrogen between the two carbons at the transition state, while rearrangement of the epoxide occurs by way of a cation and hydrogen transfer is far from symmetrical at the transition state for the reaction.

These two factors rule out fluorohydrin being an undetected intermediate in the $\text{BF}_3 \cdot \text{OEt}_2$ catalysed rearrangement of *p*-methylstyrene oxide to *p*-methylphenyl acetaldehyde.

¹ Blackett, B. N.; Coxon, J. M.; Hartshorn, M. P.; Richards, K. E. *J. Am. Chem. Soc.* **1970**, *92*, 2574-2575.

² Maruoka, K.; Murase, N.; Bureau, R.; Ooi, T.; Yamamoto, H. *Tetrahedron* **1994**, *50*, 3663. Coxon, J. M.; Hartshorn, M. P.; Lawrey, M. G. *Chem. and Ind.* **1969**, 1558.

³ Butke, G. P.; Jimenez M, F.; Michalik, J.; Gorski, R. A.; Rossi, N. F.; Wemple, J. *J. Org. Chem.* **1978**, *43*, 954.

⁴ Coxon, J. M.; Thorpe, A. J. *J. Org. Chem.* **2000**, *65*, 8421-8429.

⁵ Umezawa, J.; Takahashi, O.; Furuhashi, K.; Nohira, H. *Tetrahedron: Asymmetry* **1993**, *4*, 2053.

⁶ Kolb, H. C.; Sharpless, K. B. *Tetrahedron* **1992**, *48*, 10515.

⁷ Coxon, J. M.; Hartshorn, M. P.; Lewis, A. J.; Richards, K. E.; Swallow, W. H. *Tetrahedron* **1969**, *25*, 4445.

⁸ Thibaudeau, C.; Plavec, J.; Chattopadhyaya, J. *J. Org. Chem.* **1998**, *63*, 4967-4984.

Chapter Five

Synthesis and Lewis Acid Catalysed Rearrangement of *m*-Methoxystyrene Oxide

5.1 SYNTHESIS OF *M*-METHOXYSTYRENE OXIDE

In order to analyse the Lewis acid catalysed rearrangement of *m*-methoxystyrene oxide, four deuterated analogues (Figure 5.1) were synthesised and their $\text{BF}_3 \cdot \text{OEt}_2$ and LiClO_4 catalysed rearrangement products were analysed by the method described in Chapter 2.

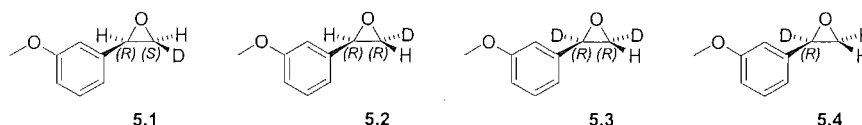


Figure 5.1. Deuterioisomers of *m*-methoxystyrene oxide.

The synthetic method is similar to that used in the synthesis of the deuterated isomers of *p*-methylstyrene oxide. Sharpless dihydroxylation gives optically active diol, which can be converted to epoxide with retention of the stereochemical integrity. Again, four deuterio isomers of *m*-methoxystyrene oxide are required for this study (Figure 5.2).

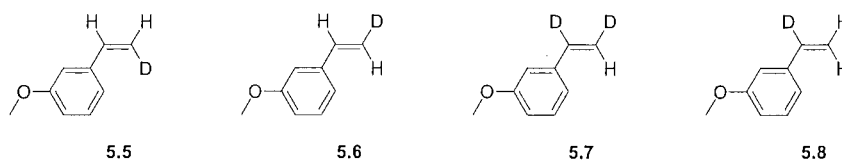
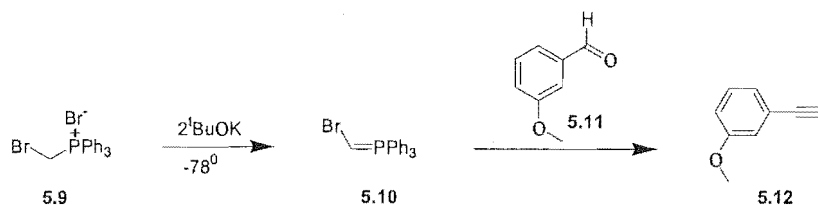


Figure 5.2. Deuterioisomers of *m*-methoxystyrene.

5.1.1 Synthesis of *m*-methoxyphenyl acetylene

Initially, *m*-methoxyphenylacetylene **5.12** was synthesised as described below, it later became commercially available and later reactions used the commercially available material.

Substituted phenylacetylenes have been synthesised by reaction of the phosphorus ylide **5.10** with a benzylic aldehyde (Scheme 5.3). Bromo phosphorane **5.9** was made by a literature procedure.¹ The phosphorus ylide was made by treatment of **5.9** with $t\text{BuOK}$ at -78° . Reaction of the ylide with **5.11** gave acetylene **5.12** in low yield (ca 25%).



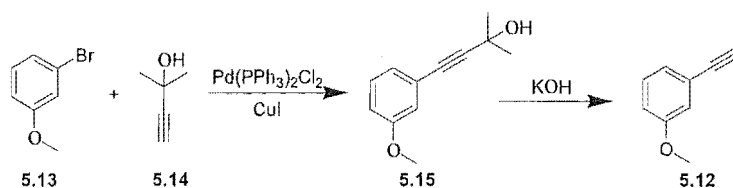
Scheme 5.3. Formation of *m*-methoxyphenyl acetylene (method 1).

It was hoped that a higher yield of **5.12** could be obtained from the Sonogashira coupling reaction, which has gained widespread use in recent years due to its efficiency and selectivity. The reaction uses palladium and copper iodide to catalyse the coupling of an aromatic bromide or iodide with a terminal alkyne. Acetylene itself is not a suitable substrate for this reaction, but an alkynol such as **5.14** can be used, and base catalysed removal of acetone will give the desired, terminal alkyne.

The coupling of *m*-bromoanisole with **5.14** was attempted using Et_3N as the solvent. At room temperature there was no reaction after 14 hours. The reaction under reflux gave a 10% yield of alkynol **5.15** after 14 hours and none of the starting material **5.14** was left.

m-Bromoanisole was used as the starting material for this reaction because some was readily available in the laboratory. It would be expected that the iodo compound would be more reactive than the bromo and give a higher yield for the reaction. The reaction was initially carried out at room temperature and no reaction occurred. The reaction was repeated, this time heating the reaction mixture at reflux and a 10% yield of **5.15** was obtained.

Reports in the literature indicate that higher yields can be obtained for hindered, or unreactive aromatic iodides or bromides when pyrrolidine is used as the solvent.² The Sonogashira reaction was repeated in refluxing pyrrolidine. A 90% yield of **5.15** was obtained:

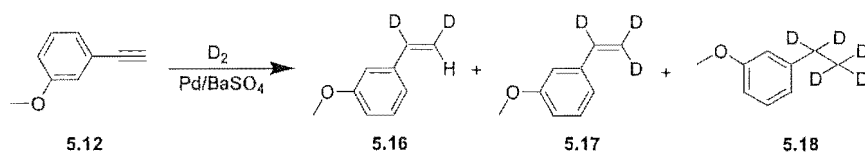


Scheme 5.4. Formation of *m*-methoxyphenyl acetylene by the Sonogashira coupling reaction.

Several attempts to effect KOH-catalysed removal of acetone from alkynol **5.15** to give alkyne **5.12** were made. Initially, following a literature procedure, dry solvents were used under an inert atmosphere and care was taken to grind KOH under an inert atmosphere to avoid it absorbing water from the atmosphere. On one occasion slightly less care was taken to stop the ground KOH becoming wet and a higher yield of alkyne was obtained! It was discovered that in order for the reaction to proceed in high yield, damp KOH must be used.

5.1.2 Synthesis of *m*-methoxystyrene-*cis*- α,β - d_1

Initial attempts to reduce *m*-methoxyphenyl acetylene with D_2 gas, using the same procedure as used for reduction of *p*-methylphenyl acetylene gave α,β,β -trideuterated-*m*-methoxystyrene **5.17** instead of the expected α,β -*cis*-dideuterated compound **5.16**:



Scheme 5.5. Reduction of *m*-methoxyphenyl acetylene.

It is possible for the palladium to catalyse *cis-trans* isomerisation or hydrogen exchange reactions. Quinoline is added to the reaction in order to compete with the alkene product for co-ordination sites on the palladium surface and thereby minimise over-reduction and isomerisation. When a terminal reactive alkene is the product from a hydrogenation, the alkene can compete with the quinoline for co-ordination to the palladium catalyst, allowing

the palladium to catalyse *cis-trans* isomerisation and hydrogen exchange reactions of the alkene.

Alkyne co-ordinates far more readily to palladium than alkene. Hydrogen exchange should therefore be minimised by stopping the reaction before it reaches completion. Several experiments were conducted where the reaction was stopped after varying amounts of reduction or over reduction had occurred:

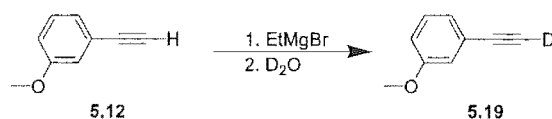
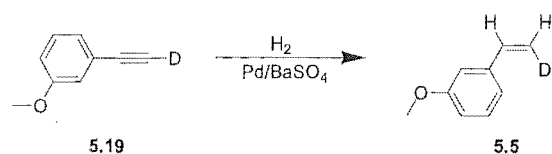
alkyne : alkene : alkane (5.12 : 5.16 + 5.17 : 5.18)	dideuterated : trideuterated alkene (5.16 : 5.17)
0 : 44 : 56	14 : 86
0 : 45 : 55	27 : 73
0 : 85 : 15	70 : 30
0 : 97 : 3	75 : 25
50 : 50 : 0	95 : 5

Table 5.1. Hydrogenation of *m*-methoxyphenyl acetylene.

The results show that the reaction must be stopped well short of full reduction in order to obtain the best yield of the desired dideuterated product. The reaction mixture was subjected to the Sharpless asymmetric dihydroxylation and unreacted alkyne was easily separated from the optically active diol by column chromatography.

5.1.3 Synthesis of *m*-methoxystyrene-*cis*- β - d_1

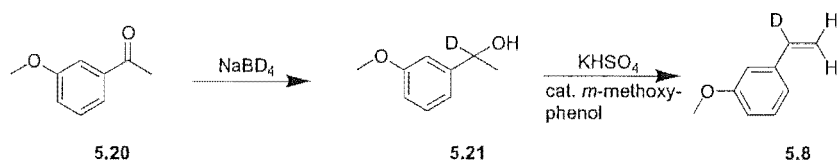
m-Methoxystyrene-*cis*- β - d_1 **5.5** was made by the palladium on barium sulphate catalysed hydrogenation of *m*-methoxyphenyl acetylene-2- d_1 **5.19** (made from deuteration of *m*-methoxyphenyl acetylene, Scheme 5.6). The same reaction conditions were used as for the deuterium reduction of *m*-methoxyphenyl acetylene above (Scheme 5.7).

Scheme 5.6. Deuteration of *m*-methoxyphenyl acetylene.Scheme 5.7. Hydrogenation of *m*-methoxyphenyl acetylene-2-*d*₁.

A similar ratio of *cis* and *trans* deuterated alkene as for the deuterogenation reaction was obtained.

5.1.4 Synthesis of *m*-methoxystyrene- α -*d*₁

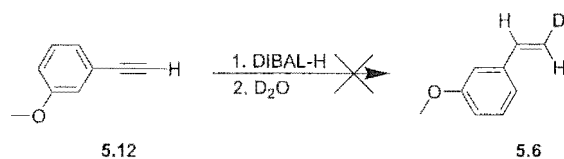
m-Methoxystyrene- α -*d*₁ **5.8** was made by the same procedure used for the formation of the *p*-methyl analogue (Scheme 5.8).

Scheme 5.8. Synthesis of *m*-methoxystyrene- α -*d*₁.

5.1.5 Attempted synthesis of *m*-methoxystyrene-*trans*- β -*d*₁

The diisobutylaluminium hydride reduction of alkynes and work up with D₂O gives the *trans* deuterated alkene. Reaction of *m*-methoxyphenyl acetylene **5.12** with diisobutylaluminium hydride for 2 days gave no alkene and a complex mixture of products. Reports in the literature indicate that diisobutylaluminium hydride can be used to reduce aromatic methoxy groups.³ This reaction is usually slow at room temperature, but has been

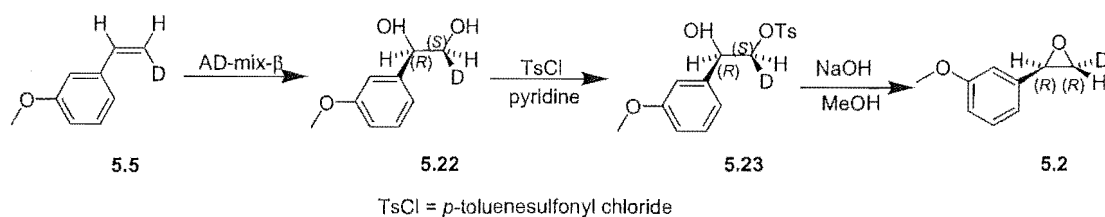
used in synthesis at elevated temperatures. It is likely that this unselective reaction is faster than reduction of the alkyne.



Scheme 5.9. Attempted synthesis of *m*-methoxystyrene-*trans*- β - d_1 .

5.1.6 Synthesis of (αR),(βR)-*m*-methoxystyrene oxide- β - d_1

(αR),(βR)-*m*-Methoxystyrene oxide- β - d_1 **5.2** was made by epoxidation of (1*R*), (2*S*)-1-(3-methoxyphenyl)ethane-1,2-diol **5.22** via a primary tosylate, with inversion of configuration at the terminal carbon (Scheme 5.10).

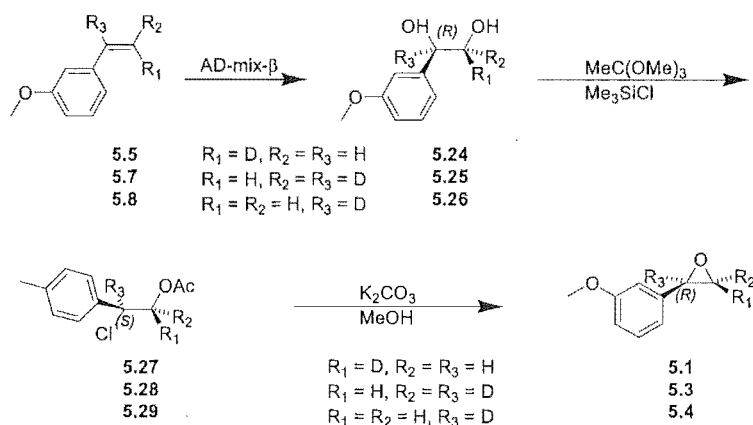


Scheme 5.10. Synthesis of (αR),(βR)-*m*-methoxystyrene oxide- β - d_1 .

Optical rotation measurements showed that the enantiomeric excess of epoxide made by this method is the same as that made by the chlorohydrin ester method.

5.1.7 Sharpless asymmetric dihydroxylation and epoxidation of *m*-methoxystyrenes

(αR),(βS)-*m*-Methoxystyrene oxide- β - d_1 **5.1**, (αR),(βR)-*m*-methoxystyrene oxide- α , β - d_2 **5.2** and (αR)-*m*-methoxystyrene oxide- α - d_1 **5.4** were made by Sharpless asymmetric dihydroxylation of deuterioisomers of *m*-methoxystyrene **5.5**, **5.7** and **5.8** and epoxidation by formation of the chlorohydrin ester followed by base catalysed saponification:

Scheme 5.11. Synthesis of *m*-methoxystyrene oxide *via* chlorohydrin ester.

m-Methoxystyrene oxide is less sensitive to air, moisture and acid than *p*-methylstyrene oxide so purification by column chromatography on silica gel was possible. Also samples of epoxide could be stored at room temperature, in a laboratory atmosphere for several days with no noticeable loss of epoxide.

5.1.8 Calculation of isomers

The same method was used to analyse the isomeric purity of *m*-methoxystyrene oxides as was used in the synthesis of *p*-methylstyrene oxide. The isomeric purity of (αR),(βS)-*m*-methoxystyrene oxide- β - d_1 **5.1** and (αR),(βR)-*m*-methoxystyrene oxide- β - d_1 **5.2** was analysed by the same method as (αR),(βS)-*p*-methylstyrene oxide- β - d_1 **3.1** and (αR),(βR)-*p*-methylstyrene oxide- β - d_1 **3.2**. The proton and deuterium NMR spectra were analysed as shown below.

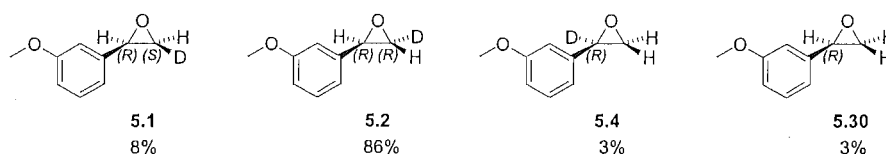
5.1.8.1 Isomers of (αR),(βS)-*m*-methoxystyrene oxide- β - d_1

The integrals of the α and β signals of the ^1H and ^2H NMR spectra of (αR),(βS)-*m*-methoxystyrene oxide- β - d_1 **5.1** are shown in Table 5.2.

	<i>trans</i> integral	<i>cis</i> integral	α integral
^1H nmr	1	0.15	1.11
^2H nmr	0.09	1	0.03

Table 5.2. ^1H and ^2H NMR integrals of (αR),(βS)-*m*-methoxystyrene oxide- β - d_1 .

The same method of analysis is used as for the derivatives of *p*-methylstyrene oxide (see chapter 3 for details on the calculation). These NMR data give the following ratio of epoxides:

Figure 5.3. Deutero isomers of *m*-methoxystyrene oxide.

5.1.8.2 Isomers of (αR),(βR)-*m*-methoxystyrene oxide- β - d_1

The ^1H and ^2H NMR integrals for (αR),(βR)-*m*-methoxystyrene oxide- β - d_1 **5.2** are shown in Table 5.3.

	<i>trans</i> integral	<i>cis</i> integral	α integral
^1H nmr	0.14	0.9	1
^2H nmr	100	10.13	2.7

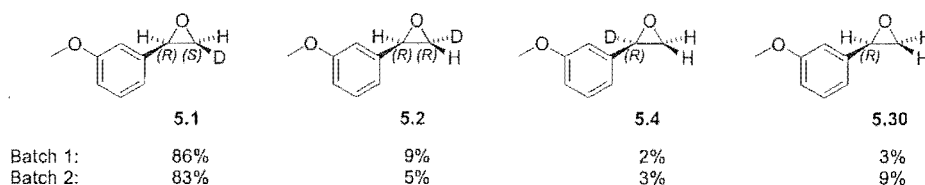
Table 5.3. ^1H and ^2H NMR integrals of (αR),(βR)-*m*-methoxystyrene oxide- β - d_1 (batch 1).

A second batch of (αR),(βR)-*m*-methoxystyrene oxide- β - d_1 was made, the ^1H and ^2H NMR integrals are shown in Table 5.4.

	<i>trans</i> integral	<i>cis</i> integral	α integral
^1H nmr	0.15	0.85	0.94
^2H nmr	100	5.85	3.16

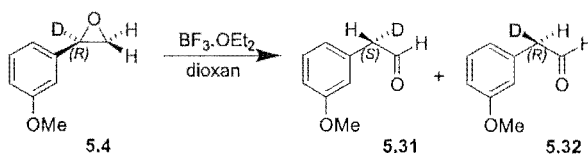
Table 5.4. ^1H and ^2H NMR integrals of (αR),(βR)-*m*-methoxystyrene oxide- β - d_1 (batch 2).

These two sets of NMR data give the following ratio of epoxide deuterium isomers:

Figure 5.4. Deutero isomers of *m*-methoxystyrene oxide.

5.2 $\text{BF}_3 \cdot \text{OEt}_2$ CATALYSED REARRANGEMENT OF *M*-METHOXYSTYRENE OXIDE

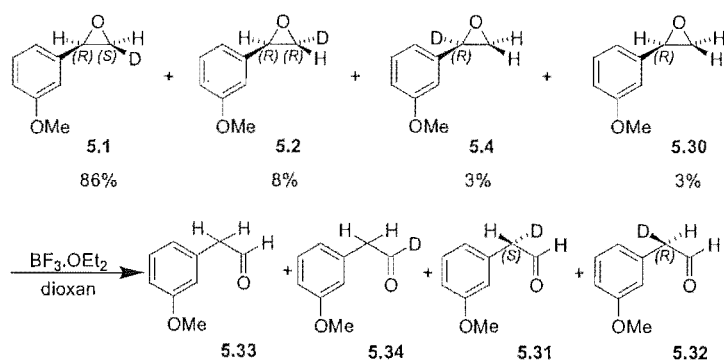
5.2.1 $\text{BF}_3 \cdot \text{OEt}_2$ catalysed rearrangement of (αR)-*m*-methoxystyrene oxide- α - d_1

Scheme 5.12. $\text{BF}_3 \cdot \text{OEt}_2$ catalysed rearrangement of (αR)-*m*-methoxystyrene oxide- α - d_1 .

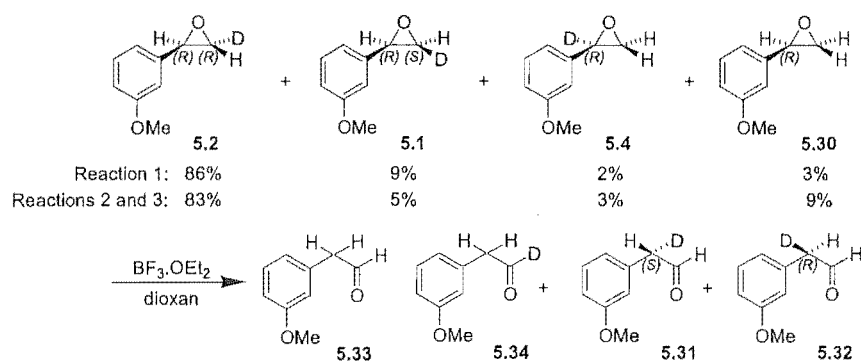
Reaction	H migration with retention of configuration (5.31)	H migration with inversion of configuration (5.32)
1	50%	50%
2	48%	52%
3	50%	50%
average	50±3%	50±3%

Table 5.5. Ratio of aldehydes formed from rearrangement of (αR)-*m*-methoxystyrene oxide- α - d_1 .

5.2.2 $\text{BF}_3 \cdot \text{OEt}_2$ catalysed rearrangement of (αR),(βS)-*m*-methoxystyrene oxide- β - d_1 and (αR),(βR)-*m*-methoxystyrene oxide- β - d_1



Scheme 5.13. $\text{BF}_3 \cdot \text{OEt}_2$ catalysed rearrangement of enriched (αR),(βS)-*m*-methoxystyrene oxide- β - d_1 .



Scheme 5.14. $\text{BF}_3 \cdot \text{OEt}_2$ catalysed rearrangement of enriched $(\alpha R), (\beta R)$ -*m*-methoxystyrene oxide- β - d_1 .

Reaction	C1 ^2H NMR integral	C2 ^2H NMR integral	C2 H _S ^1H NMR integral	C2 H _R ^1H NMR integral
1	69	31	1	1.15
2	68	32	1	1.24
3	68	32	1	1.04

Table 5.6. ^1H and ^2H NMR data of the esters formed from rearrangement of $(\alpha R), (\beta S)$ -*m*-methoxystyrene oxide- β - d_1 .

Reaction	C1 ^2H NMR integral	C2 ^2H NMR integral	C2 H _S ^1H NMR integral	C2 H _R ^1H NMR integral
1	65	35	1.140	1
2	68	32	1.090	1
3	68	32	1.275	1

Table 5.7. $\text{BF}_3 \cdot \text{OEt}_2$ catalysed rearrangement of $(\alpha R), (\beta R)$ -*m*-methoxystyrene oxide- β - d_1 .

The ratio of aldehydes can then be determined by the method outlined in chapter 3:

$$\text{Reaction 1: } x = (2 - 0.30) / 2.15 = 0.7907$$

Reaction 2: $x = (2-0.31)/2.24 = 0.7545$

Reaction 3: $x = (2-0.31)/2.04 = 0.8284$

Reaction	5.33	5.34	5.31	5.32
1	3%	67%	21%	9%
2	3%	66%	25%	6%
3	3%	66%	17%	14%

Table 5.8. Ratio of aldehydes formed from rearrangement of (αR),(βS)-*m*-methoxystyrene oxide- β - d_1 .

And likewise the ratio can be calculated from the NMR data of (αR),(βR)-*m*-methoxystyrene oxide- β - d_1 :

Reaction 1: $x = (2-0.34)/2.14 = 0.7757$

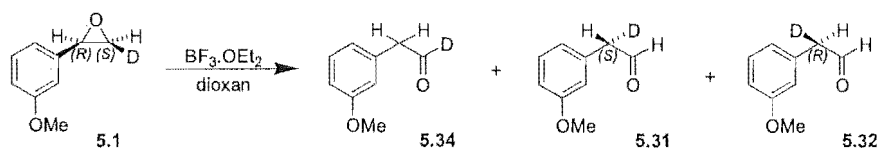
Reaction 2: $x = (2-0.29)/2.09 = 0.8182$

Reaction 3: $x = (2-0.29)/2.275 = 0.7516$

Reaction	5.33	5.34	5.31	5.32
1	3%	63%	12%	22%
2	9%	62%	11%	18%
3	9%	62%	4%	25%

Table 5.9. $\text{BF}_3 \cdot \text{OEt}_2$ catalysed rearrangement of (αR),(βR)-*m*-methoxystyrene oxide- β - d_1 .

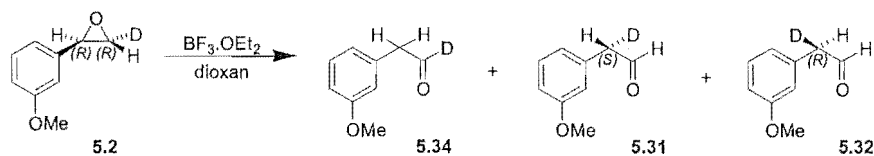
The ratio of aldehydes that would be produced on rearrangement of a sample of pure **5.1** (Scheme 5.15, Table 5.10) or **5.2** (Scheme 5.16, Table 5.11) can be obtained by subtracting the expected ratio of aldehydes produced from rearrangement of the contaminating deuterioisomers of *m*-methoxystyrene oxide. See Appendix A for details.



Scheme 5.15. $\text{BF}_3 \cdot \text{OEt}_2$ catalysed rearrangement of $(\alpha R), (\beta S)$ -*m*-methoxystyrene oxide- β - d_1 .

Reaction	H migration (5.34)	D migration with inversion of configuration (5.31)	D migration with retention of configuration (5.32)
1	71%	20%	9%
2	70%	24%	6%
3	70%	17%	13%
average	$70 \pm 3\%$	$20 \pm 4\%$	$10 \pm 4\%$

Table 5.10. $\text{BF}_3 \cdot \text{OEt}_2$ catalysed rearrangement of $(\alpha R), (\beta S)$ -*m*-methoxystyrene oxide- β - d_1 .



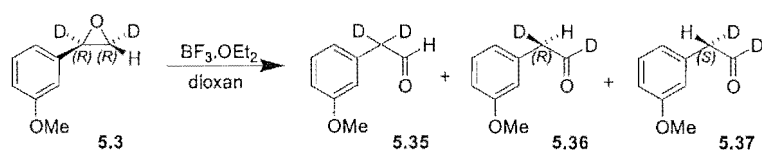
Scheme 5.16. $\text{BF}_3 \cdot \text{OEt}_2$ catalysed rearrangement of $(\alpha R), (\beta R)$ -*m*-methoxystyrene oxide- β - d_1 .

Reaction	H migration (5.34)	D migration with inversion of configuration (5.31)	D migration with retention of configuration (5.32)
1	66%	7%	27%
2	70%	9%	21%
3	70%	11%	19%
average	69±3%	9±3%	22±4%

Table 5.11. BF₃.OEt₂ catalysed rearrangement of (α*R*),(β*R*)-*m*-methoxystyrene oxide-β-*d*₁.

5.2.3 BF₃.OEt₂ catalysed rearrangement of (α*R*),(β*R*)-*m*-methoxystyrene oxide-α,β-*d*₂

Dideuterated epoxide **5.3** was rearranged with BF₃.OEt₂ in dioxan. Epoxide **5.3** was synthesised containing quantities of other deuterioisomers of *m*-methoxystyrene oxide. It was estimated from ¹H and ²H NMR that the epoxide was 80% enriched as the dideuterated epoxide **5.3**. No accurate determination was made of the exact composition of the epoxide mixture and so the results below have not been corrected for the presence of other isomers of *m*-methoxystyrene oxide. The ratio of aldehydes was analysed as above.

Scheme 5.17. BF₃.OEt₂ catalysed rearrangement of (α*R*),(β*R*)-*m*-methoxystyrene oxide-α,β-*d*₂.

Reaction	D migration (5.35)	H migration with inversion of configuration (5.36)	H migration with retention of configuration (5.37)
1	36%	41%	23%
2	38%	39%	23%
3	35%	42%	23%
average	36±4%	41±5%	23±5%

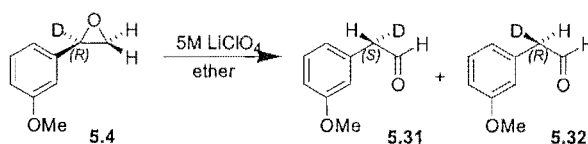
Table 5.12. $\text{BF}_3 \cdot \text{OEt}_2$ catalysed rearrangement of $(\alpha R), (\beta R)$ -*m*-methoxystyrene oxide- α, β - d_2 .

The ratio of aldehydes produced in this reaction shows that racemisation of deuterated *m*-methoxyphenyl acetaldehyde under the reaction conditions can not be occurring to any significant extent.

5.3 LiClO_4 CATALYSED REARRANGEMENT OF *M*-METHOXYSTYRENE OXIDE

5.3.1 LiClO_4 catalysed rearrangement of (αR) -*m*-methoxystyrene oxide- α - d_1

Isomers of *m*-methoxystyrene oxide were rearranged under the same conditions used for the rearrangement of *p*-methylstyrene oxide. The epoxide was stirred at room temperature for 18 hours in a 5M solution of LiClO_4 in diethyl ether, giving a 95% yield of aldehyde.



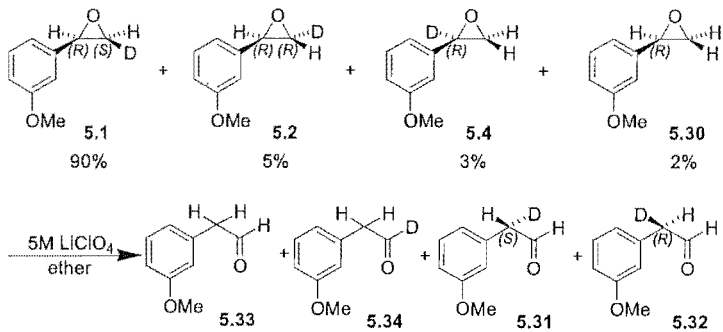
Scheme 5.18. LiClO_4 promoted rearrangement of (αR) -*m*-methoxystyrene oxide- α - d_1 .

Reaction	H migration with retention of configuration (5.31)	H migration with inversion of configuration (5.32)
1	50%	50%
2	48%	52%
3	53%	47%
average	50±5%	50±5%

Table 5.13. LiClO₄ promoted rearrangement of (α*R*)-*m*-methoxystyrene oxide-α-*d*₁.

5.3.2 LiClO₄ catalysed rearrangement of (α*R*),(β*S*)-*m*-methoxystyrene oxide-β-*d*₁

The same reaction conditions were used for the rearrangement of enriched *cis* deuterated epoxide 5.1 (Scheme 5.19, Table 5.14).



Scheme 5.19. LiClO₄ promoted rearrangement of (α*R*),(β*S*)-*m*-methoxystyrene oxide-β-*d*₁.

Reaction	C1 ² H NMR integral	C2 ² H NMR integral	C2 H _S ¹ H NMR integral	C2 H _R ¹ H NMR integral
1	71	29	1	1.35
2	70	30	1	1.43

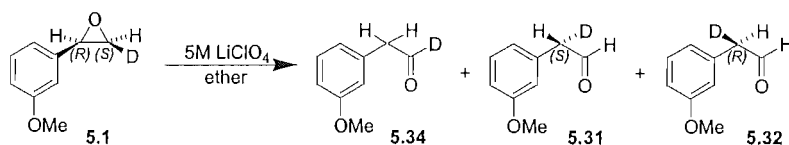
Table 5.14. LiClO₄ promoted rearrangement of (α*R*),(β*S*)-*m*-methoxystyrene oxide-β-*d*₁.

From the data shown in the table above, the ratio of aldehydes **5.33**, **5.34**, **5.31** and **5.32** is calculated. The percentage of undeuterated aldehyde **5.33** is the same as the percentage of undeuterated epoxide **5.30**, i.e. 2%. The amount of C1 deuterated aldehyde **5.34** is $0.71 \times 0.98 = 70\%$. The amount of aldehydes **5.31** and **5.32** can be obtained from subtracting the contribution to the ^1H NMR signal from **5.33** and **5.34**. See Appendix A for details.

Reaction	5.33	5.34	5.31	5.32
1	2%	70%	27%	1%
2	2%	69%	29%	0%

Table 5.15. LiClO_4 promoted rearrangement of $(\alpha R), (\beta S)$ -*m*-methoxystyrene oxide- β - d_1 .

The aldehyde formed from rearrangement of **5.2**, **5.4** and **5.30** can be subtracted from the above results to get the ratio of aldehydes that would be produced from rearrangement of a sample of pure **5.1**. See Appendix B for details.



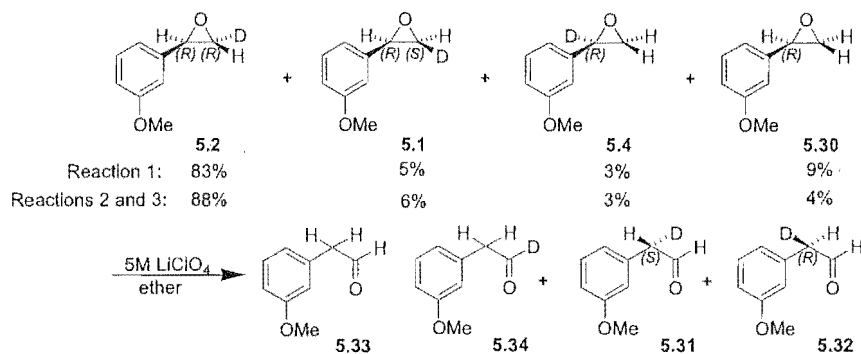
Scheme 5.20. LiClO_4 promoted rearrangement of $(\alpha R), (\beta S)$ -*m*-methoxystyrene oxide- β - d_1 .

Reaction	H migration (5.34)	D migration with inversion of configuration (5.31)	D migration with retention of configuration (5.32)
1	73%	26%	1%
2	72%	28%	0%
average	$73 \pm 3\%$	$27 \pm 4\%$	$0 \pm 3\%$

Table 5.16. LiClO_4 promoted rearrangement of $(\alpha R), (\beta S)$ -*m*-methoxystyrene oxide- β - d_1 .

5.3.3 LiClO₄ catalysed rearrangement of (αR),(βR)-*m*-methoxystyrene oxide- β -*d*₁

The rearrangement of the enriched *trans* deuterated *m*-methoxystyrene oxide **5.2** is shown in Scheme 5.21.



Scheme 5.21. LiClO₄ promoted rearrangement of (αR),(βR)-*m*-methoxystyrene oxide- β -*d*₁.

Reaction	C1 ² H NMR integral	C2 ² H NMR integral	C2 H _S ¹ H NMR integral	C2 H _R ¹ H NMR integral
1	68	32	1.23	1
2	65	35	1.29	1
3	67	33	1.32	1

Table 5.17. LiClO₄ promoted rearrangement of (αR),(βR)-*m*-methoxystyrene oxide- β -*d*₁.

From these data, the following ratio of aldehydes is obtained:

For rxn 1: $x = (2-0.2912)/2.23 = 0.7663$

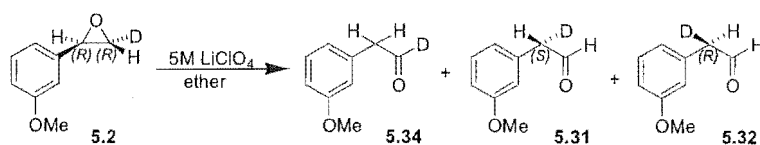
For rxn 2: $x = (2-0.336)/2.29 = 0.7266$

For rxn 3: $x = (2-0.3168)/2.32 = 0.7255$

Reaction	5.33	5.34	5.31	5.32
1	9%	62%	6%	23%
2	4%	63%	7%	28%
3	4%	64%	5%	28%

Table 5.18. LiClO₄ promoted rearrangement of (α*R*), (β*R*)-*m*-methoxystyrene oxide-β-*d*₁.

Aldehyde produced by rearrangement of epoxide isomers **5.1**, **5.4** and **5.30** is subtracted from the results above, giving the ratio of aldehydes that would be obtained from rearrangement of pure epoxide **5.2**.

Scheme 5.22. LiClO₄ promoted rearrangement of (α*R*), (β*R*)-*m*-methoxystyrene oxide-β-*d*₁.

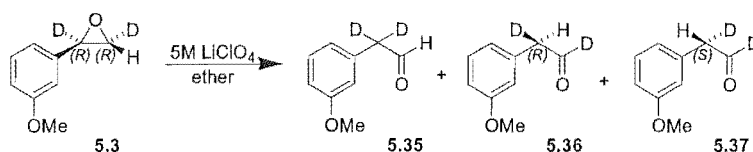
Reaction	H migration (5.34)	D migration with inversion of configuration (5.31)	D migration with retention of configuration (5.32)
1	70%	5%	25%
2	67%	3%	28%
3	69%	3%	27%
average	69%	4%	27%

Table 5.19. LiClO₄ promoted rearrangement of (α*R*), (β*R*)-*m*-methoxystyrene oxide-β-*d*₁.

5.3.4 LiClO₄ catalysed rearrangement of (α*R*), (β*R*)-*m*-methoxystyrene oxide-α,β-*d*₂

As for the BF₃·OEt₂ catalysed rearrangement of **5.3**, the exact ratio of deuterioisomers present in the mixture of enriched **5.3** was not determined and the ratio of aldehydes

produced in the rearrangement process were not corrected for the presence of other deuterioisomers. It was estimated from the ^1H and ^2H NMR integrals that the mixture was 80% enriched with **5.3**. The ratio of aldehydes was analysed as above.



Scheme 5.23. LiClO_4 promoted rearrangement of $(\alpha R),(\beta R)$ -*m*-methoxystyrene oxide- α,β - d_2 .

Reaction	D migration (5.35)	H migration with inversion of configuration (5.36)	H migration with retention of configuration (5.37)
1	34%	53%	13%
2	32%	58%	10%
3	35%	53%	12%
average	$34\pm 3\%$	$55\pm 4\%$	$12\pm 3\%$

Table 5.20. LiClO_4 promoted rearrangement of $(\alpha R),(\beta R)$ -*m*-methoxystyrene oxide- α,β - d_2 .

The epoxide starting material contains approximately 15% hydrogen in the α position, so the measured ratio of 55% : 12% represents close to 100% hydrogen migration with inversion of configuration, consistent with the rearrangement of **3.2**. Importantly the reaction also shows that once formed, the deuterated *m*-methoxyphenyl acetaldehydes are not racemising under the reaction conditions.

5.4 DISCUSSION

5.4.1 Fujimoto analysis of results

The results for the rearrangement of *m*-methoxystyrene oxide can be analysed in the same way as the results for the rearrangement of *p*-methylstyrene oxide in Chapter Three. The results from the rearrangement of (αR),(βS)-*m*-methoxystyrene oxide- β - d_1 **5.1** and (αR),(βR)-*m*-methoxystyrene oxide- β - d_1 **5.2** are used in the analysis and the results from the rearrangement of (αR)-*m*-methoxystyrene oxide- α - d_1 **5.4** and (αR),(βR)-*m*-methoxystyrene oxide- α , β - d_2 **5.3** are used for comparison.

5.4.1.1 Calculation of the facial selectivity for hydride migration in the $\text{BF}_3\cdot\text{OEt}_2$ catalysed rearrangement of β -deuterated epoxide

The results from the $\text{BF}_3\cdot\text{OEt}_2$ catalysed rearrangements of (αR),(βS)-*m*-methoxystyrene oxide- β - d_1 **5.1** (Ha=D) and (αR),(βR)-*m*-methoxystyrene oxide- β - d_1 **5.2** (Hb=D) are shown in Scheme 5.24. The four transition conformers for hydride (deuteride) migration are shown.

Each experiment gives the facial selectivity for deuterium migration, but not for hydrogen migration. It is assumed that the facial selectivity for migration of either Ha or Hb is the same regardless of whether Ha or Hb is hydrogen or labelled as deuterium. The facial selectivity for migration of Ha in epoxide where Ha=H is therefore obtained from facial selectivity for migration of Ha in the experiment where Ha=D. The relative contributions of each of the four transition conformers can therefore be calculated:

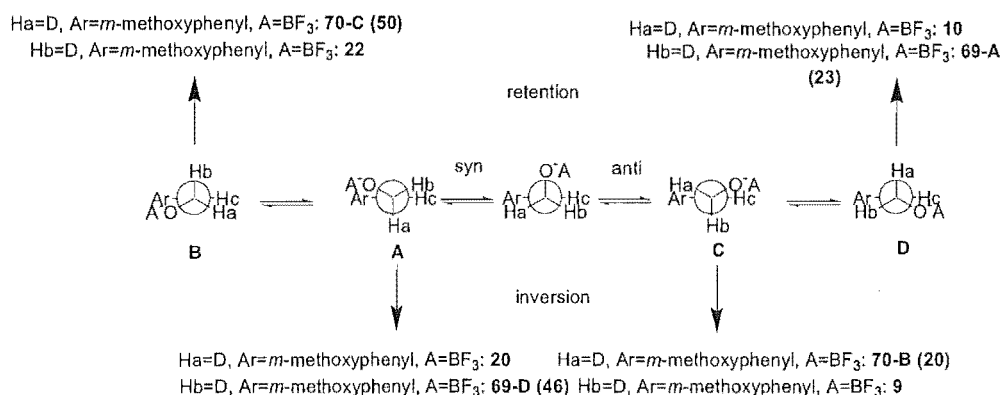
From experiment 1 (Ha=D): B+C=70 (H migration) and A/D=20/10 (D migration).

From experiment 2 (Hb=D): A+D=69 (H migration) and B/C=22/9 (D migration).

Using the ratio of B/C from experiment 2, in experiment 1: B=50 and C=20.

Using the ratio of A/D from experiment 1, in experiment 2: A=46 and D=23.

The experimental results of the $\text{BF}_3\cdot\text{OEt}_2$ catalysed rearrangements of **5.1** and **5.2** are shown in Scheme 5.24:



Scheme 5.24. Experimental results for the BF₃.OEt₂ catalysed rearrangement of (αR),(βS)-*m*-methoxystyrene oxide- β -d₁ **5.1** and (αR),(βR)-*m*-methoxystyrene oxide- β -d₁ **5.2**.

The results can be analysed by the same method used for *p*-methylstyrene oxide used in Chapter three. The deuterium isotope parameter, *z* is calculated to satisfy the relation: 50 : 20*z* : 20 : 10*z* = 22*z* : 46 : 9*z* : 23. *z* = 2.3 and the ratio **B** : **A** : **C** : **D** = 50 : 46 : 21 : 23 or 36% : 33% : 15% : 16%.

5.4.1.2 Calculation of the facial selectivity for hydride migration in the LiClO₄ catalysed rearrangement of β -deuterated epoxide

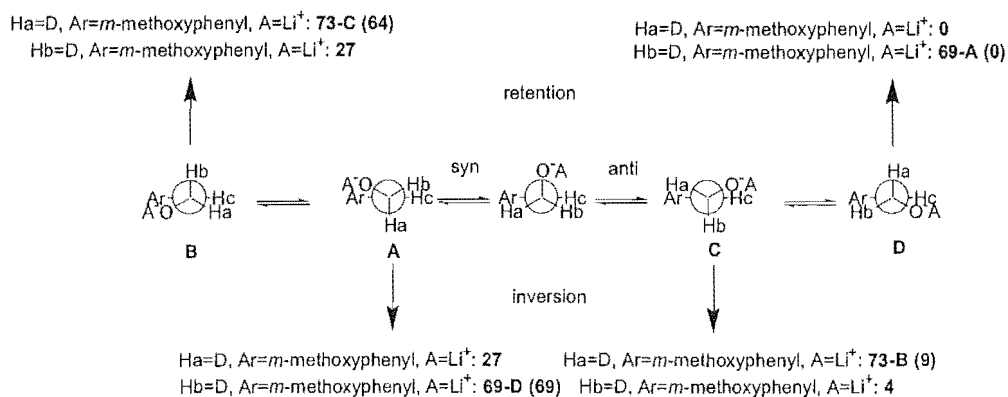
The same method can be used to analyse the results for the LiClO₄ catalysed rearrangement of *m*-methoxystyrene oxide:

From experiment 1 (Ha=D): B+C=73 (H migration) and A/D=27/0 (D migration).

From experiment 2 (Hb=D): A+D=69 (H migration) and B/C=27/4 (D migration).

Using the ratio of B/C from experiment 2, in experiment 1: B=64 and C=9.

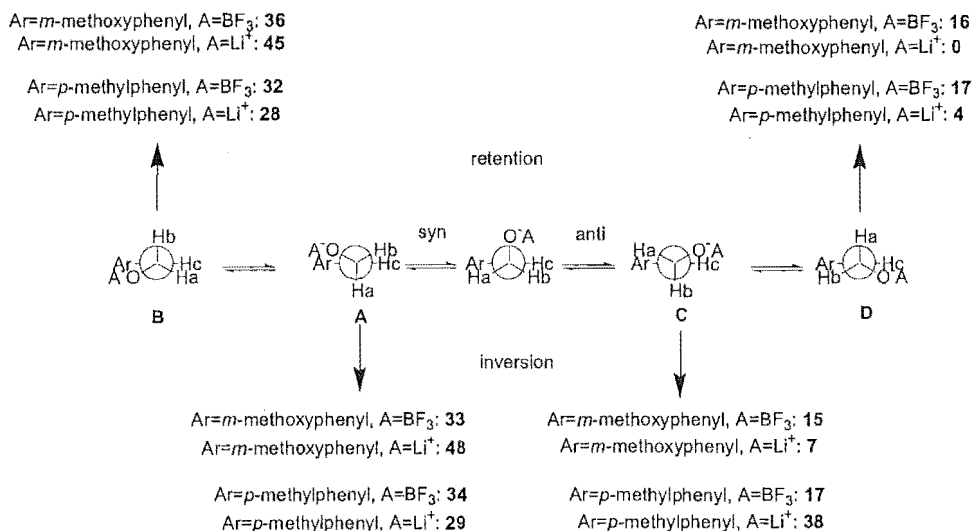
Using the ratio of A/D from experiment 1, in experiment 2: A=69 and D=0.



Scheme 5.25. Experimental results for the LiClO₄ catalysed rearrangement of (*αR*),(*βS*)-*m*-methoxystyrene oxide-β-*d*₁ and (*αR*),(*βR*)-*m*-methoxystyrene oxide-β-*d*₁.

The deuterium isotope parameter, *z* is calculated for the LiClO₄ catalysed rearrangement to satisfy the relation: 64 : 27*z* : 9 : 0*z* = 27*z* : 69 : 4*z* : 0. In this case *z* = 2.5 and the ratio of conformers **B** : **A** : **C** : **D** is 64 : 68 : 9 : 0, or 45% : 48% : 7% : 0% (Scheme 5.26).

The results from the BF₃·OEt₂ and LiClO₄ catalysed rearrangements of both *m*-methoxy and *p*-methylstyrene oxide are summarised in Scheme 5.26.



Scheme 5.26. Estimation of the hydride migration for undeuterated *p*-methyl- and *m*-methoxy- styrene oxide.

5.4.2 Comparison with the results from rearrangement of α -deuterated and α,β -dideuterated epoxide

The results shown in Scheme 5.26, derived from the results of the rearrangement of the *cis* and *trans* β -deuterated epoxides **5.1** and **5.2**, can be compared to the results from the rearrangement of α -deuterated and α,β -dideuterated epoxides **5.4** and **5.3**.

5.4.2.1 Results for the rearrangement of α -deuterated epoxide

Rearrangement of α -deuterated epoxide **5.4**, gives a measure of the facial selectivity for rearrangement of undeuterated epoxide.

5.4.2.1.1 BF₃.OEt₂ catalysed rearrangement of (αR)-*m*-methoxystyrene oxide- α -*d*₁

The results in Scheme 5.26 predict that the facial selectivity for hydride migration in the rearrangement of undeuterated styrene should be (33 + 15) : (36 + 16) = 48 : 52 inversion / retention of configuration. The rearrangement of **5.4** gives a ratio for inversion : retention of hydride migration of 50 : 50. It is difficult to envisage a mechanism that would give

more hydride migration with retention than inversion of configuration and both results are 50 / 50 within experimental error.

5.4.2.1.2 LiClO₄ catalysed rearrangement of (αR)-*m*-methoxystyrene oxide- α -*d*₁

The results for the LiClO₄ catalysed rearrangement of **5.4** show that an equal amount of hydride migrates with inversion or retention of configuration. This result is consistent within experimental error with the results in Scheme 5.26 which show that hydride migration with inversion of configuration should be favoured by a ratio of 55 : 45.

5.4.2.2 Results for the rearrangement of dideuterated epoxide

The results for the BF₃.OEt₂ and LiClO₄ catalysed rearrangement of 85% enriched **5.3**, shown in Tables 5.12 and 5.20 have not been corrected for the presence of other deuterioisomers of *m*-methoxystyrene oxide. The rearrangement results can still be compared qualitatively with the results shown in Scheme 5.26.

5.4.2.2.1 BF₃.OEt₂ catalysed rearrangement of (αR),(βR)-*m*-methoxystyrene oxide- α,β -*d*₂

Results in Table 5.12 show that migration of the hydrogen *cis* to the *m*-methoxyphenyl group proceeds preferentially with inversion of configuration by a ratio of 41 : 23. This is consistent with the results in Scheme 5.26 which shows that the ratio should be 33 : 16.

5.4.2.2.2 LiClO₄ catalysed rearrangement of (αR),(βR)-*m*-methoxystyrene oxide- α,β -*d*₂

The results for the LiClO₄ catalysed rearrangement of **5.3** in Table 5.20 show that migration of the hydrogen *cis* to the aromatic group (Ha in Scheme 5.26) should proceed preferentially with inversion of configuration by a ratio of at least 55 : 12. The results calculated in Scheme 5.26 show that this ratio should be 22 : 0, which is close to the uncorrected ratio from Table 5.20.

5.5 IMPLICATIONS AND MAJOR RESULTS OF THIS STUDY. THE MECHANISM OF EPOXIDE REARRANGEMENT WITH BF_3OEt_2 AND LiClO_4

In all four of the systems investigated in this thesis (LiClO_4 and BF_3OEt_2 catalysed rearrangement of both *m*-methoxy- and *p*-methyl- styrene oxide), opening of epoxide with rotation of the Lewis acid co-ordinated oxygen towards the aromatic group is preferred to epoxide opening with rotation away from the aromatic group (Table 5.21).

Examination of Table 5.21 shows that epoxide opening with rotation towards the aromatic group is more favoured for the electron withdrawing *m*-methoxy substituted styrene oxide compared to styrene oxide with the electron donating *p*-methyl substituent. The cation formed in the rearrangement of *m*-methoxystyrene oxide is likely to be less stabilised and so stabilisation from adopting the eclipsed conformation is likely to be more important in this system.

Epoxide	Lewis Acid	Rotation towards aryl : away from aryl
<i>p</i> -methylstyrene oxide	BF_3OEt_2	66 : 34
<i>p</i> -methylstyrene oxide	LiClO_4	57 : 42
<i>m</i> -methoxystyrene oxide	BF_3OEt_2	69 : 31
<i>m</i> -methoxystyrene oxide	LiClO_4	93 : 7

Table 5.21. Epoxide opening with rotation towards and away from the aromatic group.

In the LiClO_4 catalysed rearrangements, hydride migration from opened epoxide where rotation away from the aromatic group has occurred is accompanied by hydride migration (almost) exclusively with inversion of configuration. In all other cases (BF_3 catalysed rearrangements and LiClO_4 catalysed rearrangement with rotation toward the aromatic group), there is little or no selectivity for hydride (deuteride) migration with inversion of configuration (Table 5.22).

Epoxide	Lewis Acid	Rotation towards aryl (inversion : retention)	Rotation away from aryl (inversion : retention)
<i>p</i> -methylstyrene oxide	BF ₃ .OEt ₂	34 : 32	17 : 17
<i>p</i> -methylstyrene oxide	LiClO ₄	29 : 28	38 : 4
<i>m</i> -methoxystyrene oxide	BF ₃ .OEt ₂	33 : 36	15 : 16
<i>m</i> -methoxystyrene oxide	LiClO ₄	48 : 45	7 : 0

Table 5.22. Facial selectivity for hydride migration.

The results show that the rearrangement reactions must proceed via a carbocation intermediate, except for the case of the LiClO₄ catalysed rearrangement where opening of the epoxide occurs with rotation away from the aromatic group, where a concerted reaction mechanism is possible.

¹ Wolinsky, J.; Erickson, K. L. *J. Org. Chem.* **1965**, 2208-2211.

² Alami, M.; Ferri, F.; Linstrumelle, G. *Tetrahedron Lett.* **1993**, 34, 6403.

³ Winterfeldt, E. *Synthesis* **1975**, 617-630.

Chapter Six

Computational Study into the Li^+ and BF_3 Catalysed Rearrangement of Styrene Oxides

6.1 INTRODUCTION

The results for the $\text{BF}_3\cdot\text{OEt}_2$ and LiClO_4 catalysed rearrangements of *p*-methyl- and *m*-methoxy- styrene oxide were presented in Chapters 3 and 5. We have modelled these systems using *ab initio* molecular orbital and density functional theory calculations with the Gaussian '94¹ and Gaussian '03² suites of computational chemistry programs. Further calculations were carried out on other substituted styrene oxide systems to determine the effect of electron withdrawing or electron donating substituents on the rearrangement reaction.

The LiClO_4 catalysed reaction is modelled by calculating the geometry of the stationary points on the reaction surface when a Li^+ ion is co-ordinated to the epoxide oxygen, transition states and products. The calculations are performed in the gas phase, where no account is taken of solvent present and the ClO_4^- ion is not included in the model.

The $\text{BF}_3\cdot\text{OEt}_2$ catalysed reaction is modelled by calculating the energy and geometry of stationary points on the reaction surface where a BF_3 is co-ordinated to a lone pair of the oxygen in the epoxide, transition states and products. Again no effort is made to include the effects of solvent on the reaction. While it might be expected that the BF_3 catalysed reaction surface would be a better model for the experimental reaction than the Li^+ reaction surface, optimisations with BF_3 often converge to a structure where fluorine attacks the carbocation centre, forming fluorohydrin. In the solution phase reaction, fluorohydrin is not formed as easily due to the cation centre being solvated which blocks approach of the fluorine. There are however reactions where fluorohydrin is a product.³

6.2 Li^+ CATALYSED REARRANGEMENT OF STYRENE OXIDES

Initial calculations were performed on the Li^+ co-ordinated styrene oxide system. The B3LYP/6-31+G* optimised structure for Li^+ co-ordinated to styrene oxide is shown in Figure 6.1. The Li^+ co-ordinates to one of the lone pairs on the epoxide oxygen and also interacts with the aromatic ring. No stationary point was found where the Li^+ was co-ordinated to the oxygen's other lone pair.

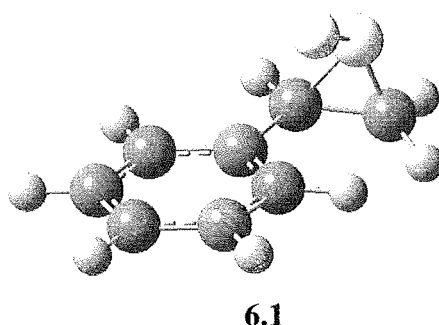


Figure 6.1. Li^+ co-ordinated to styrene oxide.

Two transition states were calculated for opening of the epoxide to carbocation (Figure 6.1). The phenyl- C^+ -C-O dihedral angle is significantly distorted from a 90° dihedral angle of the epoxide in both transition states, showing that rotation about the C1-C2 bond occurs at the same time as opening of the epoxide ring. Transition state **6.2**, where the C-O bond is rotating towards the aromatic ring is calculated to be higher in energy than **6.3**, by 4 kcal.

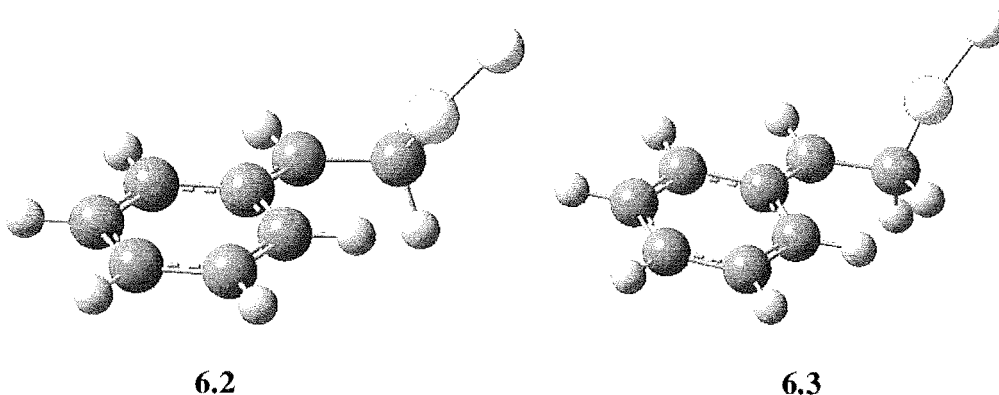


Figure 6.2. Transition states for epoxide opening.

Two minimum energy conformations of carbocation were found (Figure 6.3). Structure **6.4** has the C-O bond eclipsed with the adjacent C-phenyl bond and is 3.3 kcal lower in energy than **6.5**. Structure **6.5**, where the oxygen is anti to the aromatic group has a hydrogen in conjugation with the carbocation p-orbital. There will also exist a conformation which is

the mirror image of **6.5**, where the other hydrogen is in hyperconjugation with the carbocation.

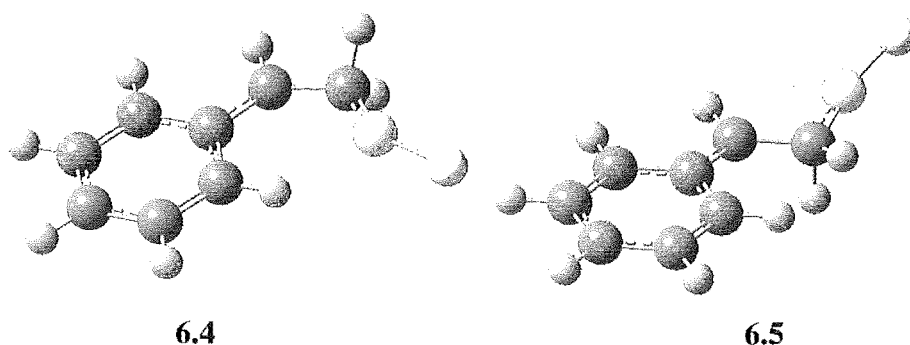


Figure 6.3. Conformations of carbocation.

It is expected that both the terminal hydrogens of the symmetrical carbocation **6.4** will migrate with equal propensity, while hydride migration from conformer **6.5**, where a hydrogen is already exhibiting hyperconjugation, will result in the preferential migration of that hydrogen.

Transition state structures for hydride migration from each of the carbocation conformers were calculated (Figure 6.4).

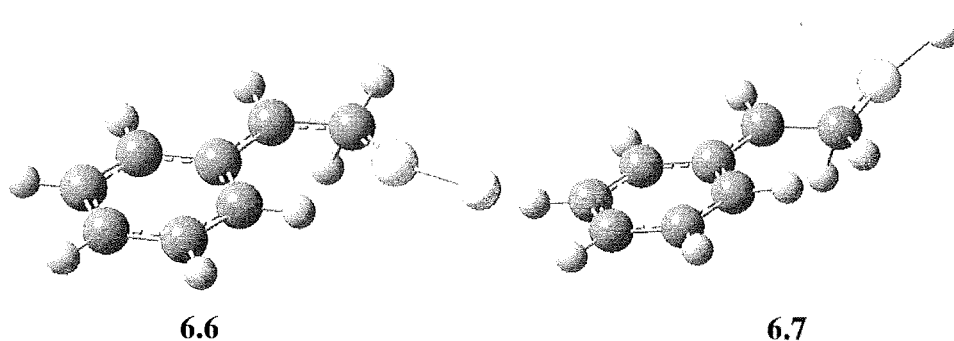


Figure 6.4. Transition states for hydride migration.

The eclipsed transition state for hydride migration, **6.6** is calculated to be 1.6 kcal lower in energy than **6.7**. Both transition states will have mirror images where the other terminal hydrogen migrates. Transition state **6.6** has the C-O bond close to being eclipsed with the C-phenyl bond.

The energy of the structures can be shown on a reaction surface (Figure 6.5). It is of note that the transition state for opening of epoxide with rotation toward the aromatic ring, **6.2** is calculated to be higher in energy than the transition state for epoxide opening with rotation away, **6.3**, while the cation minima where the oxygen has rotated toward the aromatic ring, **6.4**, is lower in energy than the anti cation **6.5**.

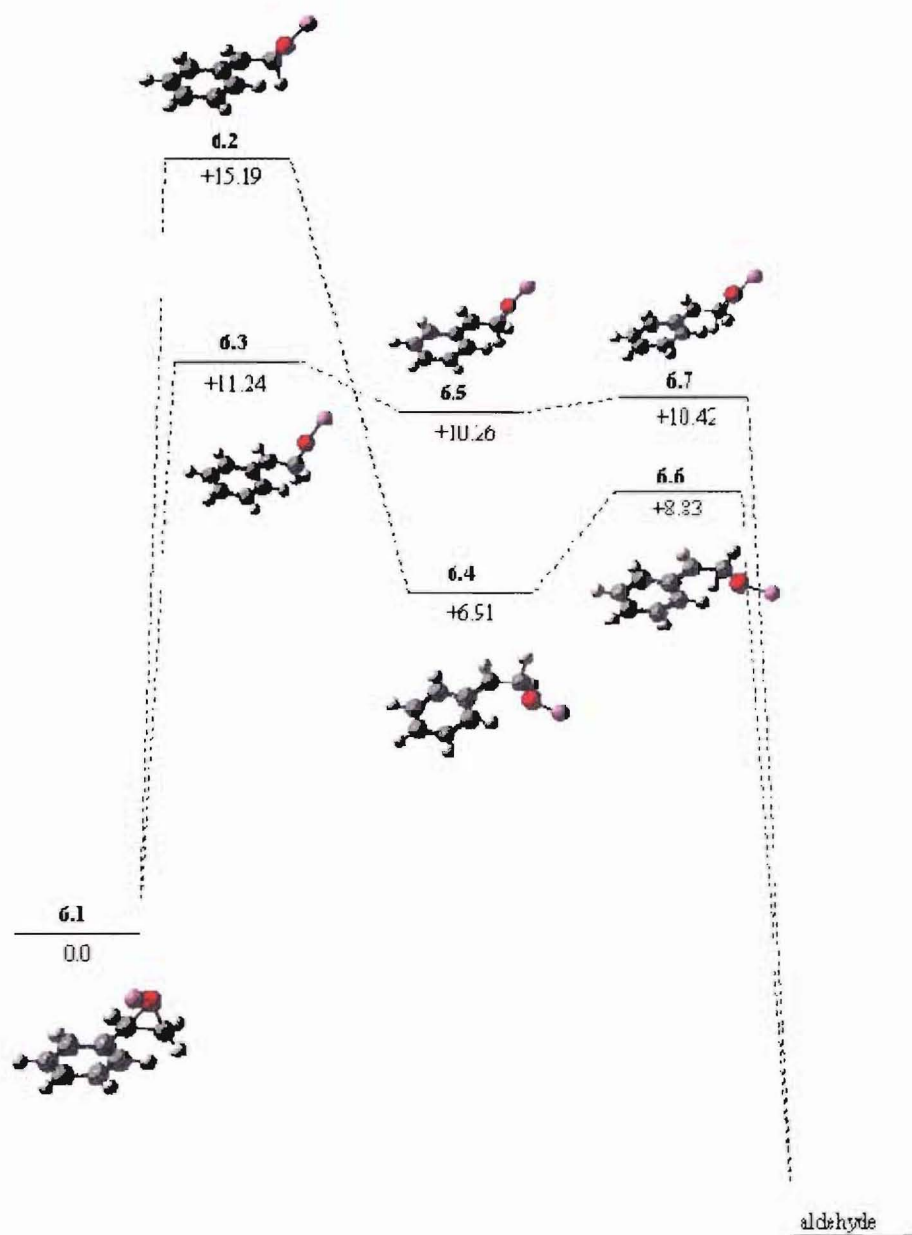


Figure 6.5. Reaction surface for the Li^+ catalysed rearrangement of styrene oxide. Structures are optimised at the B3LYP/6-31G* level of theory. Relative energies are in kcal and are corrected for the zero point vibrational energy.

Stationary points were also calculated for the Li^+ catalysed rearrangement of *m*-methoxystyrene oxide (Figure 6.6), *p*-methylstyrene oxide (Figure 6.7) and *p*-methoxystyrene oxide (Figure 6.8). All structures were optimised at the B3LYP/6-

31+G**/B3LYP/6-31+G* level of theory and the zero point vibrational energy has been added. The energy of Li^+ co-ordinated aldehyde was only calculated for the *p*-methoxystyrene oxide reaction surface.

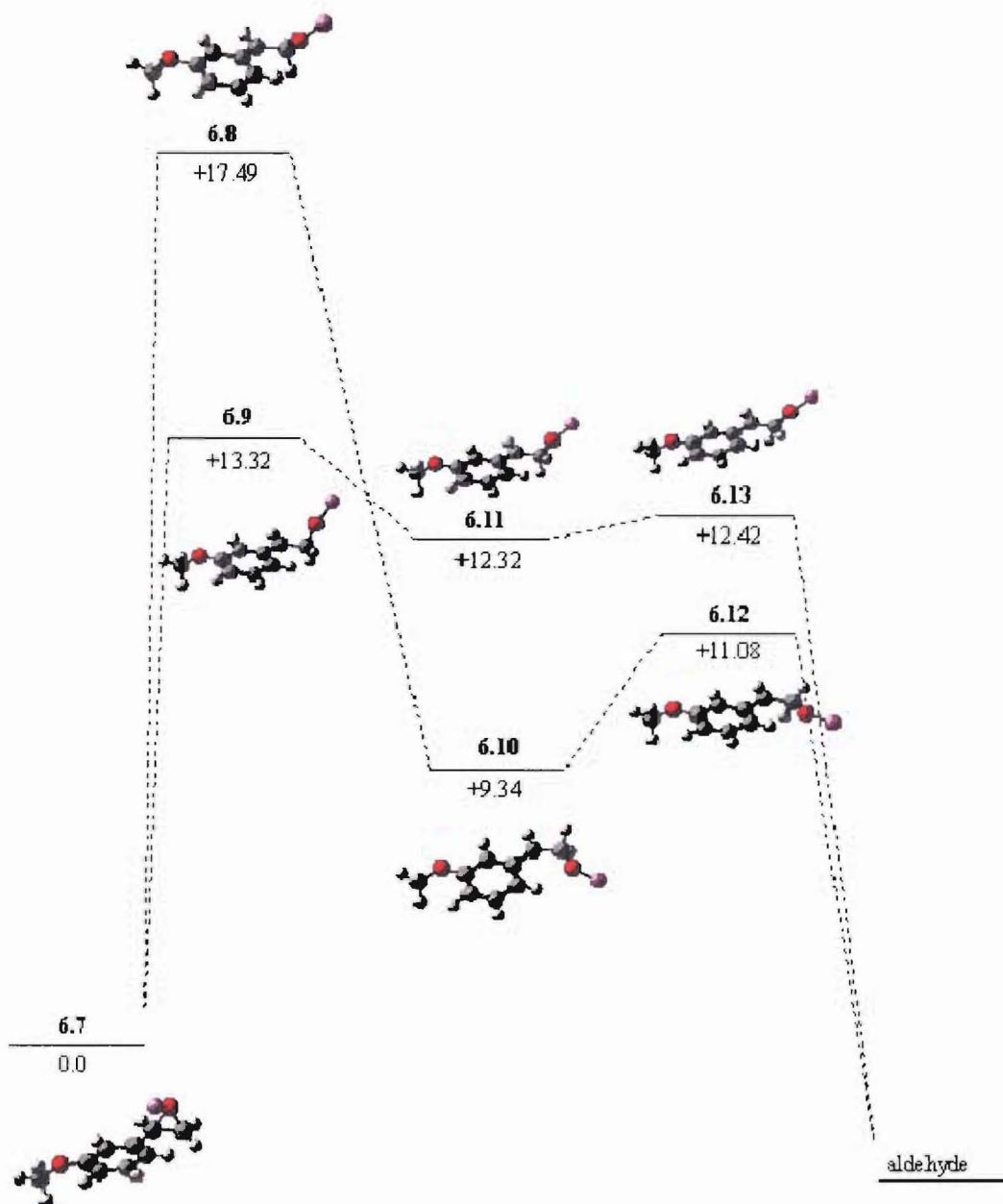


Figure 6.6. Reaction surface for the Li^+ catalysed rearrangement of *m*-methoxystyrene oxide. Structures are optimised at the B3LYP/6-31G* level of theory. Relative energies are in kcal and are corrected for the zero point vibrational energy.

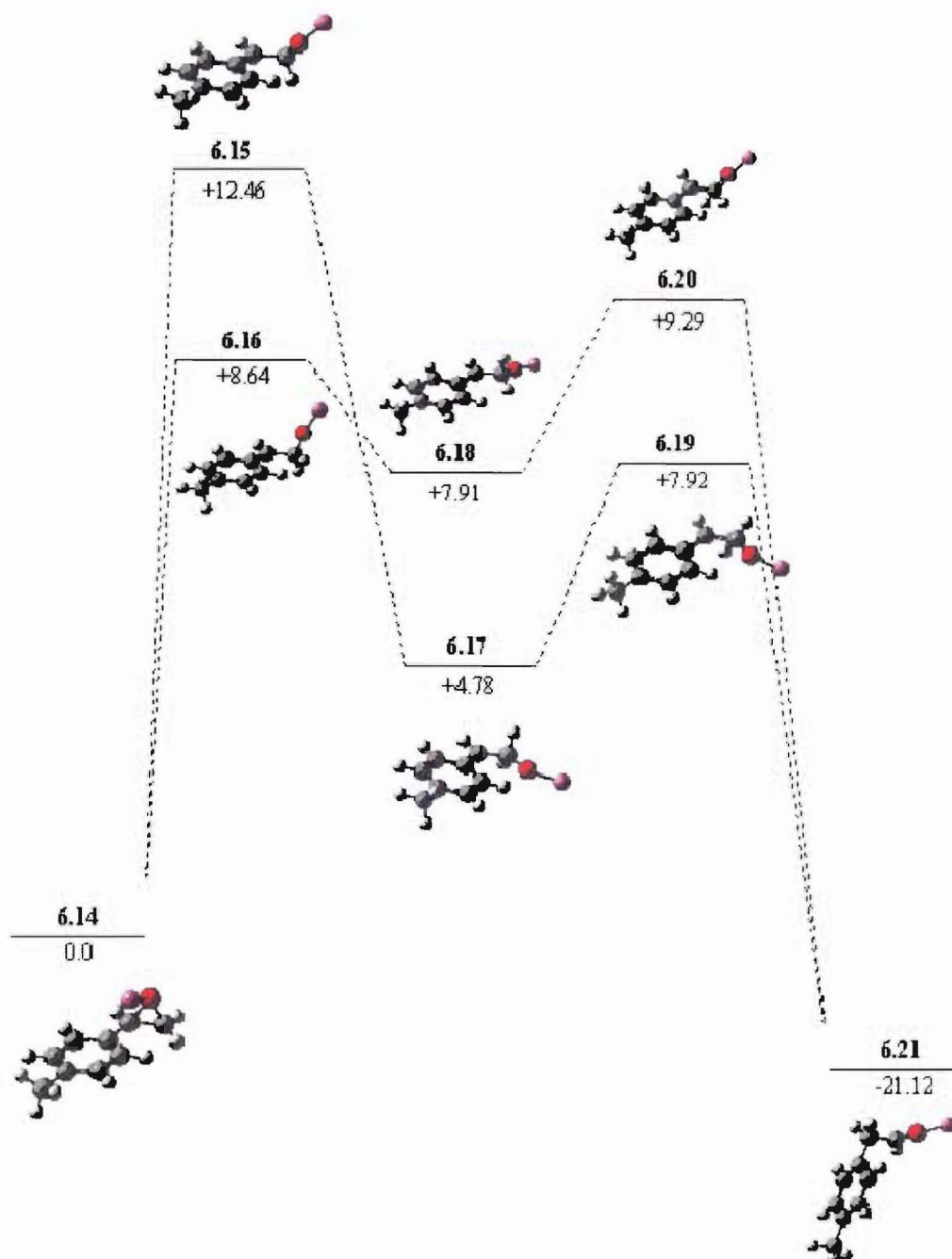


Figure 6.7. Reaction surface for the Li^+ catalysed rearrangement of *p*-methylstyrene oxide. Structures are optimised at the B3LYP/6-31G* level of theory. Relative energies are in kcal and are corrected for the zero point vibrational energy.

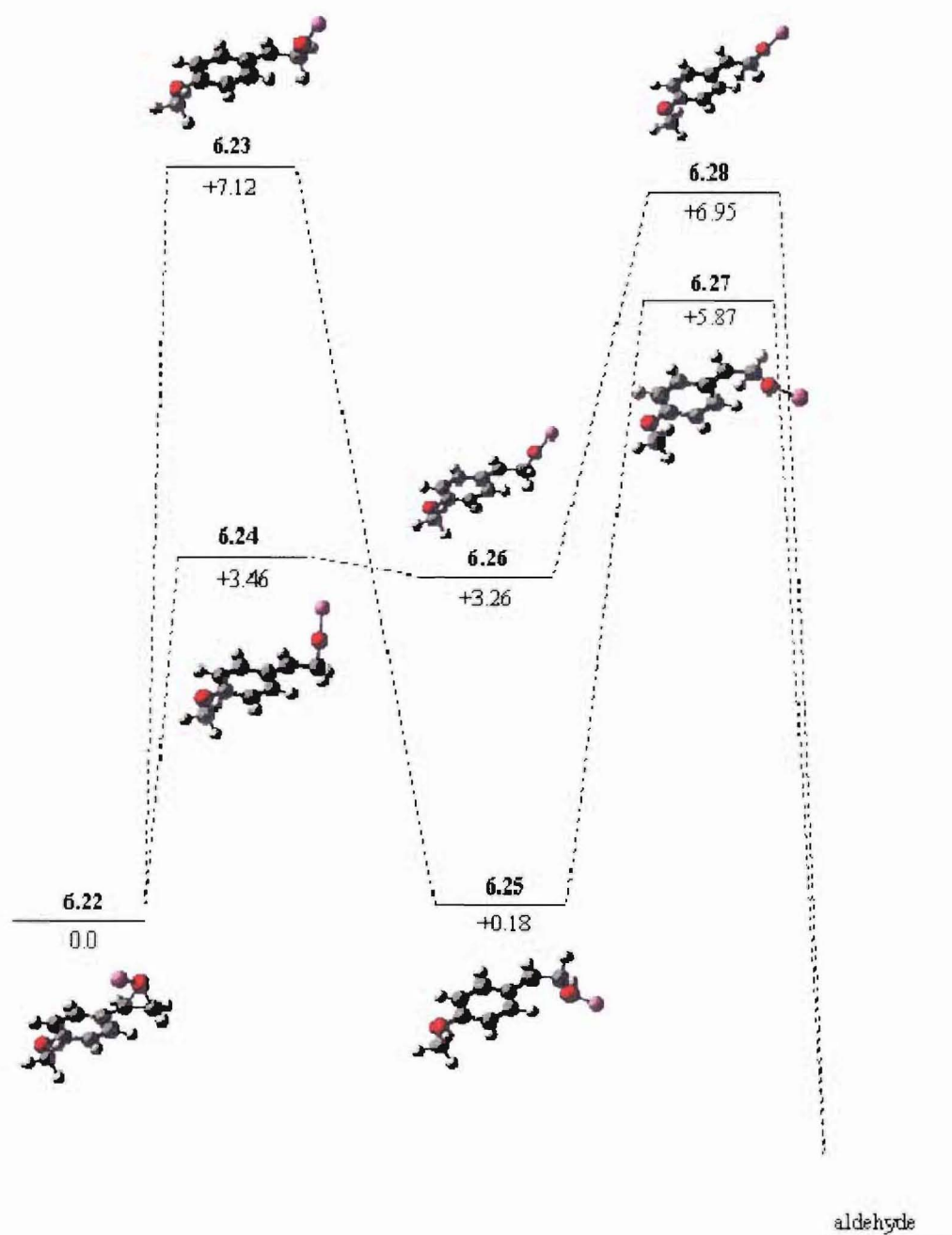
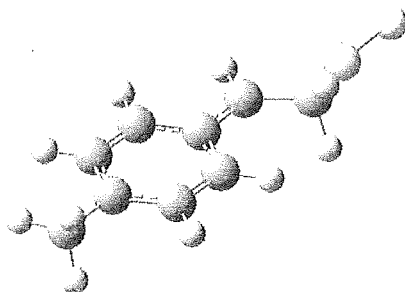


Figure 6.8. Reaction surface for the Li^+ catalysed rearrangement of *p*-methoxystyrene oxide. Structures are optimised at the B3LYP/6-31G* level of theory. Relative energies are in kcal and are corrected for the zero point vibrational energy.

It can be seen that the energy of the transition states and intermediates on the reaction surface get comparatively lower in energy relative to starting epoxide as the electron donating nature of the substituent increases in the series *m*-methoxy, hydrogen, *p*-methyl, *p*-methoxy.

6.2.1 Conversion between anti cations

It is expected that the cations where the oxygen is *anti* to the aryl group (**6.5**, **6.11**, **6.18** and **6.26**) might convert to their enantiomers. Transition state **6.29** was found on the *p*-methyl styrene oxide potential energy surface, where the C-O bond is eclipsed with the adjacent C-H bond. Animation of the imaginary frequency in Gaussview showed that **6.29** was the transition state for conversion between **6.18** and its enantiomer.



6.29

Figure 6.5. Transition state for conversion of **6.18** to its mirror image.

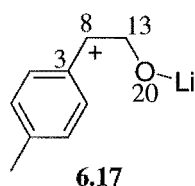
The energy of this transition state **6.29** is only 0.2 kcal/mol higher in energy than the cation minima **6.18** without correcting for the zero point vibrational energy and actually becomes lower in energy when the zero point energy correction is applied to both structures. This compares to the energy of the transition state for hydride migration **6.20** which is calculated to be 1.4 kcal higher in energy than **6.18**, showing that rotation of the cation should be fast relative to hydride migration. In the solution phase rearrangement of *p*-methyl- and *m*-methoxystyrene oxide with LiClO₄ however, no conversion of **6.18** to its enantiomer is observed.

6.3 GEOMETRY OF EPOXIDE OPENING

In order to determine the importance of rotation of the oxygen in the ring opening of epoxide, two potential energy surface scans were carried out. The energy of structures obtained from rotating the C(3)-C(8)-C(13)-O(20) dihedral angle in structure **6.17** are shown in Figure 6.6. The highest energy structures have the C-O bond at 90° to the plane of the carbocation.

The energy on rotation about the C1-C2 bond of the *p*-methylstyrene carbocation **6.17** was obtained by rotating the dihedral angle in 30° increments (Figure 6.7), a single point energy calculation performed on each structure without optimisation. The surface scan will therefore overestimate the energy of all structures relative to the starting structure **6.17**.

The calculation shows the energy of the structure with a dihedral angle of 180° (**6.33**, Figure 6.7) is lower in energy than when the dihedral angle is 150° and 210° structures **6.32** and **6.34** where the carbon-hydrogen bond can stabilise the cation centre by hyperconjugation. When these structures are fully optimised the C2-C1-H angle becomes smaller and the energy of structures **6.32** and **6.34** become lower in energy than structure **6.33** where stabilisation by hyperconjugation is not possible.



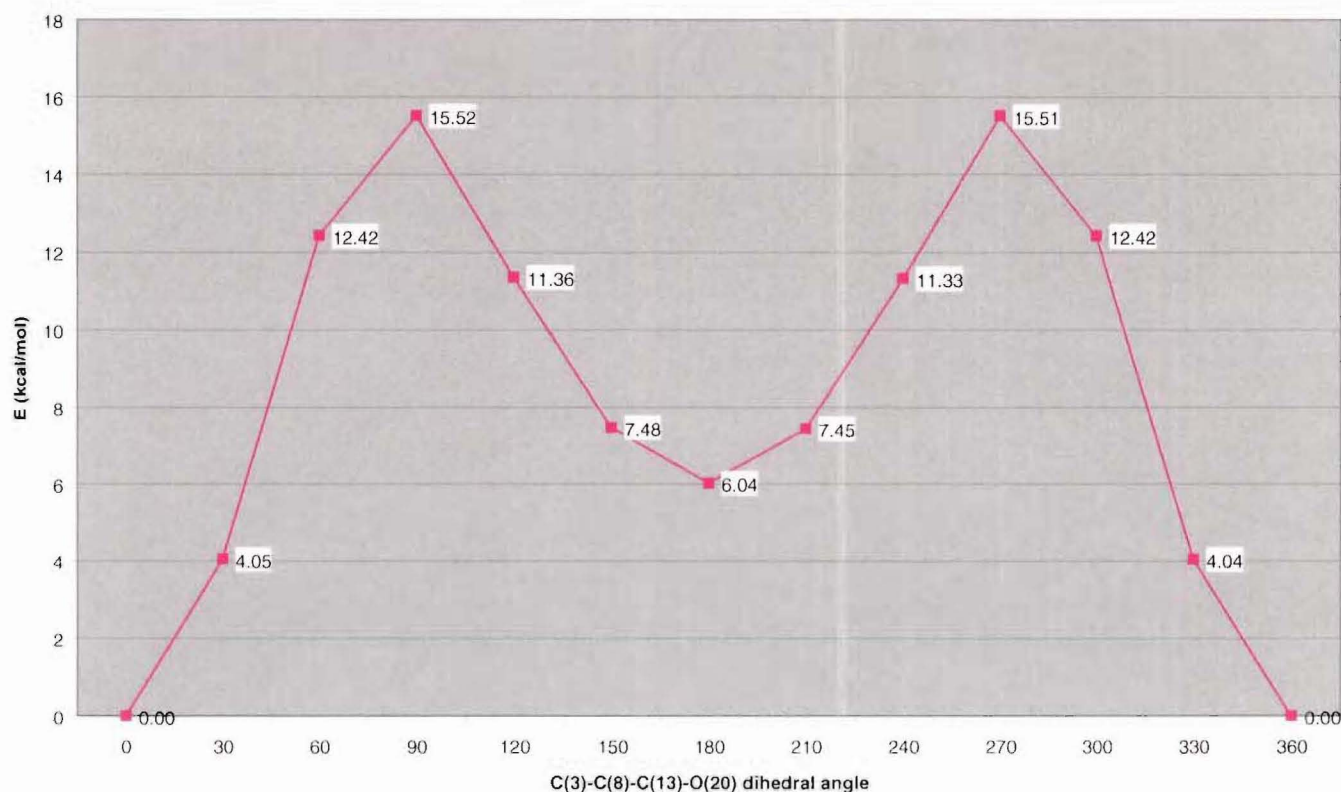


Figure 6.6. Potential energy surface obtained by single point calculations varying the dihedral angle about the C1-C2 bond of cation intermediate **6.17**.

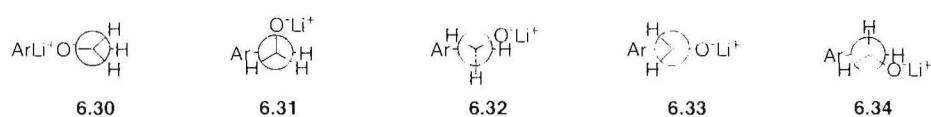


Figure 6.7. Conformations on the potential energy surface.

The potential energy surface shows that structure **6.31**, where the C-O bond is at 90° to the plane of the carbocation is the highest energy conformer. This contrasts to the mechanisms put forward by Blackett and Fujimoto, where it was thought that epoxide initially opens to this carbocation conformer and then rotates to allow hydride migration.

Calculations presented above indicate that ring opening of the epoxide always occurs with rotation of the oxygen either towards (*syn* cation) or away (*anti* cation) from the aromatic ring. The high energy of the 90° cation **6.31** in the potential energy surface above indicates that once epoxide has opened to either the *syn* or *anti* cation, conversion between the two via structure **6.31** is unlikely.

In order to further investigate the likely contribution of conformer **6.31** and the importance of concerted ring opening and bond rotation to the rearrangement reaction, a further potential energy surface scan was examined. The energy of the molecule was calculated as the $\text{C}\alpha\text{-C}\beta\text{-O}$ angle of the epoxide was increased (Figure 6.8).

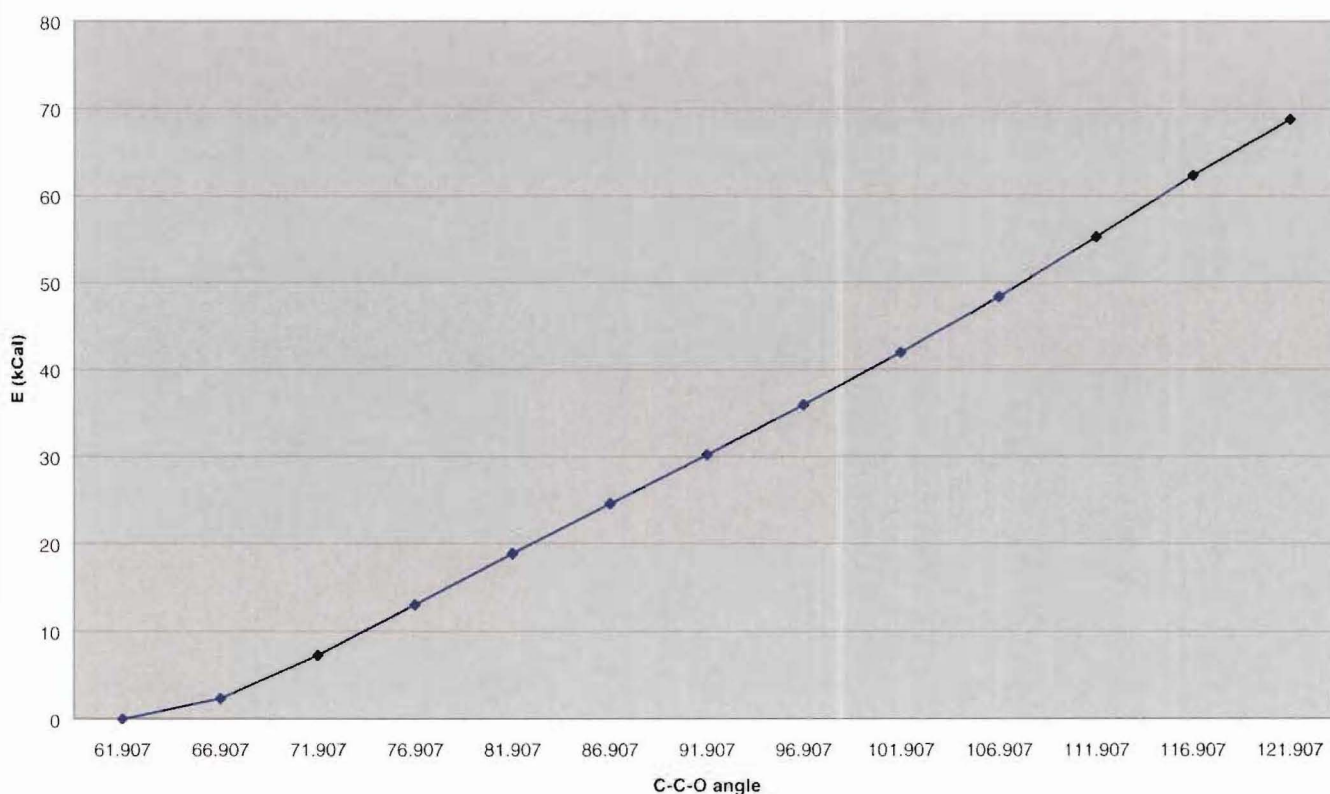


Figure 6.8. The B3LYP/6-31G* energy of Li^+ co-ordinated *p*-methylstyrene oxide with increasing $\text{C}\alpha\text{-C}\beta\text{-O}$ angle.

It can be seen that the energy of the molecule increases in an almost linear manner as the epoxide opens. There is no barrier that would indicate cation conformer **6.31** is a minimum on the potential energy surface. Ring closure back to epoxide would therefore be expected to be spontaneous from conformer **6.31**.

6.4 BF_3 CATALYSED REARRANGEMENT OF STYRENE OXIDES

Attempts were made to calculate the potential energy surface for the BF_3 catalysed reaction. Stationary points for BF_3 co-ordinated to epoxide and aldehyde were found at the HF/6-31G* level of theory. Transition states for hydride migration were also found at this level of theory. The calculations show that BF_3 can co-ordinate to either face of the epoxide. Co-ordination *anti* to the aromatic group is calculated to be lower in energy at the HF/STO-3G level of theory.

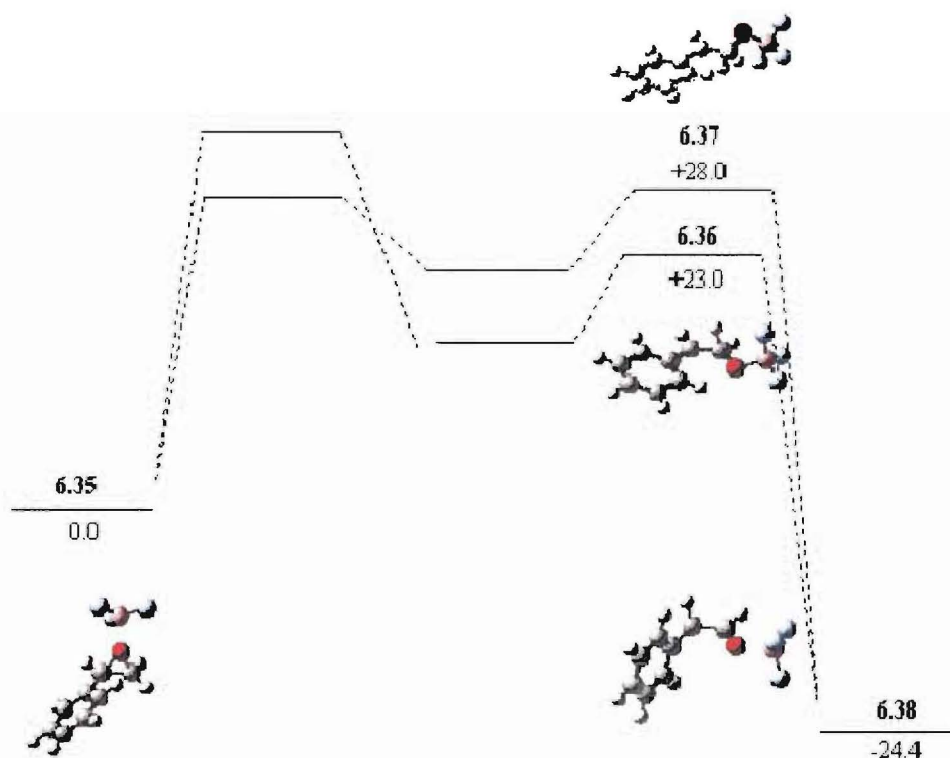
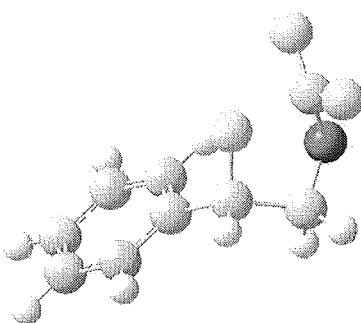


Figure 6.9. BF_3 catalysed rearrangement of styrene oxide. Stationary points are optimised at the HF/6-31G* level of theory and energies are in kcal/mol.

Attempts to find stationary points for the transition states for epoxide opening to cation and for cation minima were unsuccessful. Geometry optimisations for these structures resulted in structures where a fluorine from the BF_3 attacked the cation, giving a fluorohydrin (Figure 6.10).



6.39

Figure 6.10. Intramolecular reaction of fluorine.

6.5 COMPARISON TO EXPERIMENT

The calculations presented above for the rearrangement of *m*-methoxy- and *p*-methylstyrene oxide (Figure 6.6 and 6.7 respectively) can be used to explain the results of the rearrangements of and *m*-methoxy- *p*-methylstyrene oxide in chapters 3 and 5. The calculations show that epoxide opens to cation and hydride migration from the cation produces aldehyde. There is no evidence of a concerted rearrangement process for these aromatic substituted epoxides. The calculations also show that the rearrangement reaction can be divided into two separate reaction pathways: rotation of the Lewis acid co-ordinated oxygen towards and away from the aromatic group.

Transition states for opening of epoxide with rotation both towards and away from the aromatic group are shown in Figures 6.6 and 6.7. These transition states are the rate limiting steps for both rearrangement processes. In both cases the transition state for epoxide opening with rotation away from the aromatic ring is calculated to be 4.2 and 3.8 kcal lower in energy than the transition state for rotation towards the aromatic ring. This is

contrast to the experimental results which show that epoxide opening with rotation towards the aromatic ring is always favoured. The difference between the calculations and the experiment shows that the gas phase model does not give reliable energies for comparison to experiment.

6.5.1 Qualitative explanation for the selectivity for hydride migration in the rearrangement of *m*-methoxy- and *p*-methylstyrene oxide

The calculations can be used to qualitatively explain the selectivity for hydride migration observed in the experimental results for the LiClO₄ and BF₃.OEt₂ catalysed rearrangement of *p*-methyl- and *m*-methoxy styrene oxide when the reaction is divided into epoxide opening with rotation towards and away from the aromatic ring.

Epoxide opens with rotation towards the aromatic ring to give carbocation **6.10** (**6.17**), where the C-O bond is eclipsed with the C⁺-Ar bond. Both hydrogens are symmetrically positioned with respect to the cation p-orbital and will migrate to an equal extent via transition state **6.12** (**6.19**) and its mirror image. In this reaction pathway the terminal epoxide hydrogen *cis* to the aromatic group will migrate with inversion of configuration and the epoxide hydrogen *trans* to the aromatic group will migrate with retention of configuration.

Epoxide opening with rotation away from the aromatic group gives carbocation **6.11** (**6.18**), where the *trans* terminal epoxide hydrogen exhibits hyperconjugation to the cation p-orbital and is positioned to migrate with inversion of configuration. In the LiClO₄ catalysed rearrangement of *p*-methyl and *m*-methoxystyrene oxide migration of the *trans* terminal epoxide hydrogen with inversion of configuration is observed exclusively (within experimental error) on this reaction pathway.

Rearrangement of *m*-methoxy- and *p*-methylstyrene oxide with BF₃.OEt₂ gives an equal amount of hydride migration with inversion and retention of configuration from rotation away from the aromatic ring. This could be explained by epoxide opening to a carbocation similar to **6.11** (**6.18**), but rotation of this cation to its mirror image is fast relative to the

rate of hydride migration, resulting in an equal amount of hydride migration with inversion and retention of configuration.

¹ Gaussian 94, Revision E.1, M. J. Frisch, G. W. Trucks, H. B. Schlegel, P. M. W. Gill, B. G. Johnson, M. A. Robb, J. R. Cheeseman, T. Keith, G. A. Petersson, J. A. Montgomery, K. Raghavachari, M. A. Al-Laham, V. G. Zakrzewski, J. V. Ortiz, J. B. Foresman, J. Cioslowski, B. B. Stefanov, A. Nanayakkara, M. Challacombe, C. Y. Peng, P. Y. Ayala, W. Chen, M. W. Wong, J. L. Andres, E. S. Replogle, R. Gomperts, R. L. Martin, D. J. Fox, J. S. Binkley, D. J. Defrees, J. Baker, J. P. Stewart, M. Head-Gordon, C. Gonzalez, and J. A. Pople, Gaussian, Inc., Pittsburgh PA, 1995.

² Gaussian 03, Revision B.04, M. J. Frisch, G. W. Trucks, H. B. Schlegel, G. E. Scuseria, M. A. Robb, J. R. Cheeseman, J. A. Montgomery, Jr., T. Vreven, K. N. Kudin, J. C. Burant, J. M. Millam, S. S. Iyengar, J. Tomasi, V. Barone, B. Mennucci, M. Cossi, G. Scalmani, N. Rega, G. A. Petersson, H. Nakatsuji, M. Hada, M. Ehara, K. Toyota, R. Fukuda, J. Hasegawa, M. Ishida, T. Nakajima, Y. Honda, O. Kitao, H. Nakai, M. Klene, X. Li, J. E. Knox, H. P. Hratchian, J. B. Cross, C. Adamo, J. Jaramillo, R. Gomperts, R. E. Stratmann, O. Yazyev, A. J. Austin, R. Cammi, C. Pomelli, J. W. Ochterski, P. Y. Ayala, K. Morokuma, G. A. Voth, P. Salvador, J. J. Dannenberg, V. G. Zakrzewski, S. Dapprich, A. D. Daniels, M. C. Strain, O. Farkas, D. K. Malick, A. D. Rabuck, K. Raghavachari, J. B. Foresman, J. V. Ortiz, Q. Cui, A. G. Baboul, S. Clifford, J. Cioslowski, B. B. Stefanov, G. Liu, A. Liashenko, P. Piskorz, I. Komaromi, R. L. Martin, D. J. Fox, T. Keith, M. A. Al-Laham, C. Y. Peng, A. Nanayakkara, M. Challacombe, P. M. W. Gill, B. Johnson, W. Chen, M. W. Wong, C. Gonzalez, and J. A. Pople, Gaussian, Inc., Pittsburgh PA, 2003.

³ Maruoka, K.; Murase, N.; Bureau, R.; Ooi, T.; Yamamoto, H. *Tetrahedron* **1994**, *50*, 3663. Coxon, J. M.; Hartshorn, M. P.; Lawrey, M. G. *Chem. and Ind.* **1969**, 1558.

Chapter Seven

BF₃ Catalysed Rearrangement of 2,3,3-Trimethyl-1,2-epoxybutane

7.1 MECHANISM OF THE BF₃ CATALYSED REARRANGEMENT OF 1,1-DISUBSTITUTED EPOXIDE

The BF₃ catalysed rearrangement of 2,3,3-trimethyl-1-butene oxide has been investigated both experimentally¹ and computationally². The experimental study of Blackett et al. used non-optimally active epoxide and he developed a mechanistic scheme that has been used to explain the selectivity for hydride and deuteride migration in other 1-substituted and 1,1-disubstituted epoxides^{3,4}. More recently Fujimoto et al.⁵ have published the results of the BF₃.OEt₂ catalysed rearrangement of optically active epoxides, where the two substituents on the epoxide have similar steric requirements as the methyl and tertiary butyl groups of 2,3,3-trimethyl-1-butene oxide.

The Fujimoto results challenge the assumption made by Blackett that rotation of a carbocation intermediate will only occur in the direction to minimise the steric interaction between the tertiary butyl group and the Lewis acid co-ordinated oxygen. Fujimoto has shown that in his system a significant amount of the hydride (deuteride) migration occurs from conformations where the oxygen and pseudo tertiary butyl groups are in a gauche conformation. The results of the Fujimoto study are shown in Schemes 1.14, 1.15 and 1.16 (Chapter One).

Thorpe et al. assumed the Blackett model and only investigated the potential energy surface for rotation *anti* to the tertiary butyl group (Figure 1.8, Chapter One). In the reaction surface calculated by Thorpe et al., two carbocation minima are found: one where a hydrogen is hyperconjugating with the cation p-orbital (**1.92**) and another where the C-O bond is eclipsed with the adjacent C-Me bond (**1.90**). Fujimoto found that when epoxide opens with rotation away from the pseudo tertiary butyl group, hydride migration with inversion of configuration is favoured by a ratio of 1.64 : 1.

The two studies can be reconciled as follows: epoxide will open first to a cation similar to **1.92**, where a hydrogen is aligned with the cation p-orbital for migration with inversion of configuration. At this point either the hydrogen can migrate, or the cation can rotate to the eclipsed structure **1.90**, where the facial selectivity for hydride migration is controlled by

the relative energies of the two transition states, **1.93** and **1.94**. If the rate of hydride migration from cation **1.92** is comparable to the rate of rotation between the two cation conformers, there will be a preference for hydride migration with inversion of configuration, as observed by Fujimoto for epoxide opening with rotation of the oxygen away from the pseudo tertiary butyl group.

The stereoselectivity for hydride migration from conformations where rotation has occurred towards the bulky group in the Fujimoto system is not easily rationalised in their paper. The calculations presented below can be used to explain this selectivity.

7.2 B3LYP/6-31G* DENSITY FUNCTIONAL CALCULATIONS

In this work calculations are performed investigating the BF₃ catalysed rearrangement of 2,3,3-trimethyl-1-butene oxide, where epoxide opening occurs with rotation of the OBF₃ group towards the tertiary butyl group. The calculations supplement the investigation of Thorpe et al.² where the assumption was made that only structures formed from rotation of the OBF₃ away from the tertiary butyl group needed to be considered. The stationary points optimised at the B3LYP/6-31G* level of theory are shown in Figure 7.1.

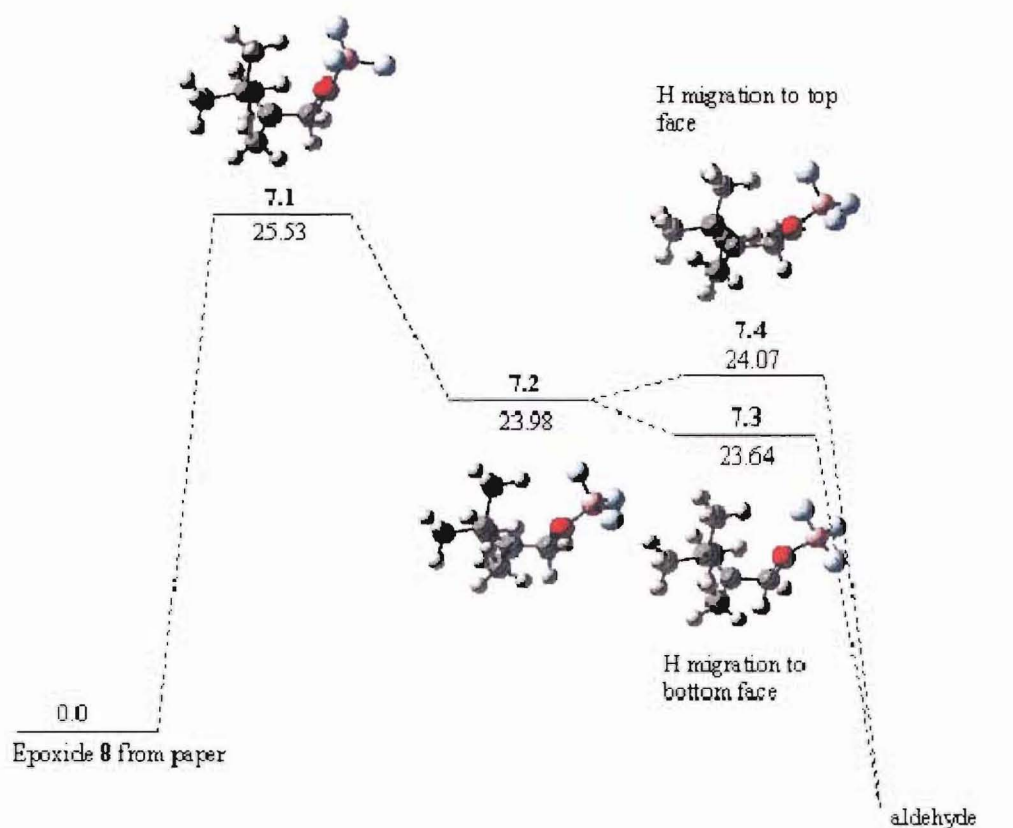


Figure 7.1. Stationary points for the BF_3 catalysed rearrangement of 2,3,3-trimethyl-1-butene oxide where rotation of the OBF_3 group occurs towards the tertiary butyl group.

Only one cation minimum, **7.2**, was found on this reaction pathway, in contrast to the two structures found by Thorpe for epoxide opening with rotation in the other direction. Epoxide will therefore open to the cation **7.2** via transition state **7.1** and the facial selectivity for hydride migration will be controlled by the small difference in the energies of the two transition states **7.3** and **7.4**.

This result is consistent with Fujimoto's experiment where hydride migration with inversion of configuration is favoured when the OBF_3 rotates away from the pseudo tertiary butyl group and there is minimal facial selectivity for rotation in the other direction.

Transition state **7.1** for opening to cation **7.2** is calculated to be 1.7 kcal/mol lower in energy than transition state **1.89** for opening to either of the cations where the OBF_3 group has rotated away from the tertiary butyl group (**1.90** and **1.92** Figure 1.8). This shows that the reaction pathway shown in Figure 7.1 is likely to be competing with epoxide opening with cation rotation in the other direction (Figure 1.8) as shown by the Fujimoto experiment.

Fujimoto found that hydride migration with retention of configuration was slightly favoured when rotation of the OBF_3 occurs towards the tertiary butyl group in his system. Two transition states for hydride migration are shown in Figure 7.1, **7.3** is calculated to be 0.4 kcal lower in energy than **7.4** and would give hydride migration with inversion of configuration. The two transition states calculated in the gas phase are so close in energy that their energies could be reversed in the solution phase reaction. This would explain the slight preference for hydride migration with retention of configuration observed by Fujimoto.

Transition state **7.3** is slightly lower in energy than the cation minima **7.2**. This is a result of the calculated zero point energy being greater for transition state **7.3**, lowering its energy relative to cation minima **7.2**. This effect has been observed by researchers previously.

7.3 REARRANGEMENT OF 2,3,3-TRIMETHYL-1-BUTENE OXIDE WITH BF_3 CO-ORDINATED TO THE MORE HINDERED FACE OF THE EPOXIDE

The structures shown in Figures 1.8 and 7.1 all have the OBF_3 group on the same face of the oxygen throughout the rearrangement process. Thorpe et al.² calculated a barrier of 3 kcal for movement of the BF_3 to the other face in both epoxide and cation. Optimised structures where the BF_3 group is co-ordinated to the other face of the oxygen are shown in Figure 7.2.

We were unable to locate the transition state for opening of the epoxide on this reaction pathway. Optimisations of the expected structure resulted in fluorine attack on the carbocation centre (fluorohydrin formation). In the transition state structure, hydrogen

bonding of the fluorine to the adjacent methyl, or tertiary butyl groups is not possible and so in the gas phase, the electronegative fluorine attacks the carbocation.

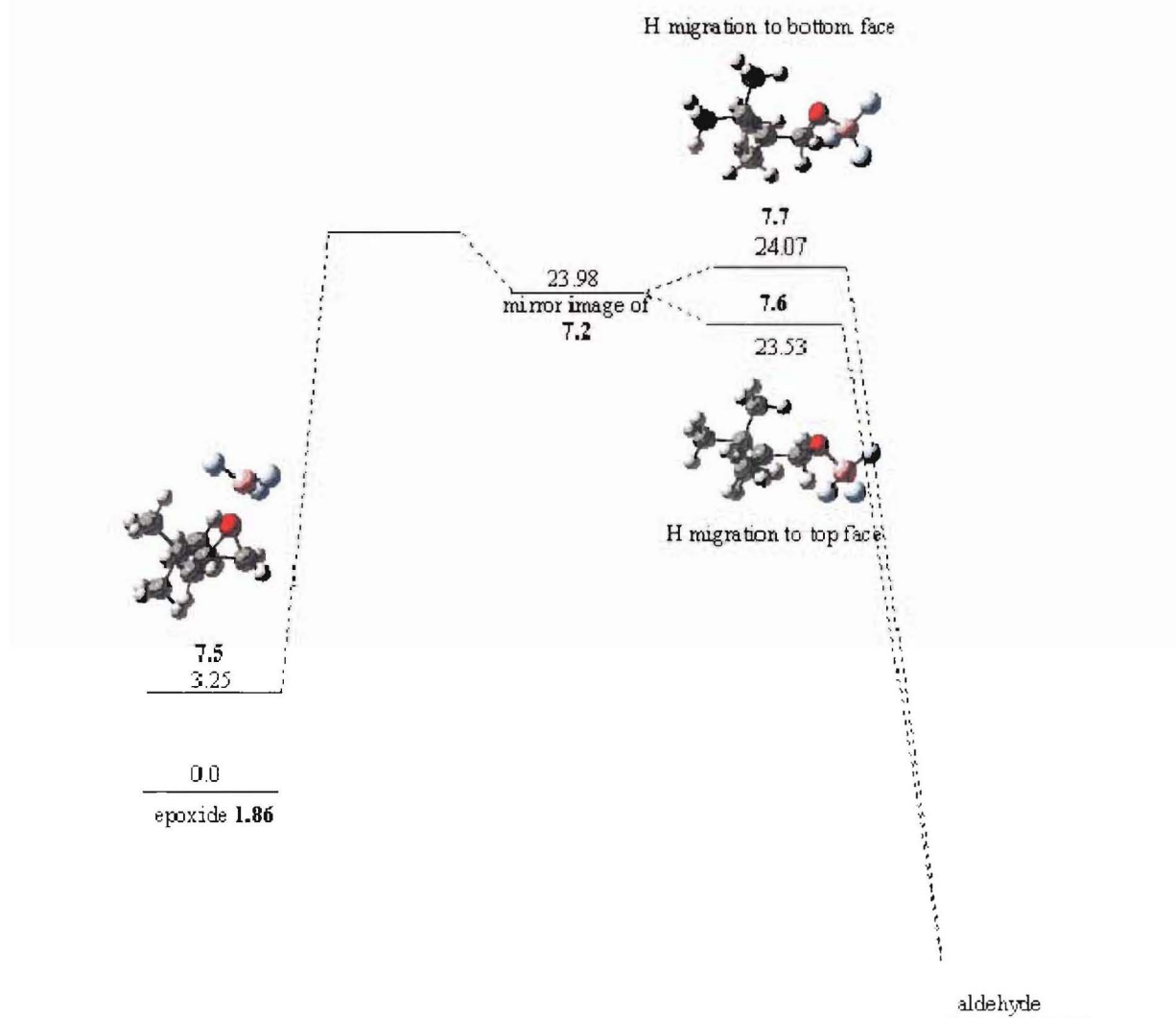


Figure 7.2. BF_3 co-ordination to the more hindered face of the epoxide.

Epoxide minima **7.5**, with BF_3 co-ordinated to the more hindered face is calculated to be 3.3 kcal higher in energy than **1.86**, so it is unlikely that much of the reaction would occur by this reaction pathway.

7.4 CONCLUSION

Structures on the potential energy surface for the rearrangement of 2,3,3-trimethyl-1-butene oxide where the OBF₃ group is in a *cis* conformation with respect to the bulky tertiary butyl group have been calculated. The reaction surface modifies that previously calculated by Thorpe et al. where only epoxide opening with rotation of the OBF₃ group away from the tertiary butyl group was considered. Rearrangement of epoxide with rotation of the OBF₃ group towards the tertiary butyl group is calculated to be comparable in energy to epoxide rearrangement with rotation away from the tertiary butyl group. The new reaction surface can be used to explain the selectivity for hydrogen and deuterium migration observed in the epoxide rearrangement of Fujimoto et al.

¹ Blackett, B. N.; Coxon, J. M.; Hartshorn, M. P.; Richards, K. E. *J. Am. Chem. Soc.* **1970**, *92*, 2574-2575.

² Coxon, J. M.; Thorpe, A. J. *J. Org. Chem.* **2000**, *65*, 8421-8429.

³ Coxon, J. M.; Lim, C. *Aust. J. Chem.* **1977**, *30*, 1137-1143.

⁴ Coxon, J. M.; McDonald, D. Q. *Tetrahedron Lett.* **1988**, *29*, 2575-2576.

⁵ Hara, N.; Mochizuki, A.; Tatara, A.; Fujimoto, Y. *Tetrahedron Asymm.* **2000**, *11*, 1859-1868.

Chapter Eight

Synthesis of 1-Substituted and 1,1-Disubstituted Epoxides

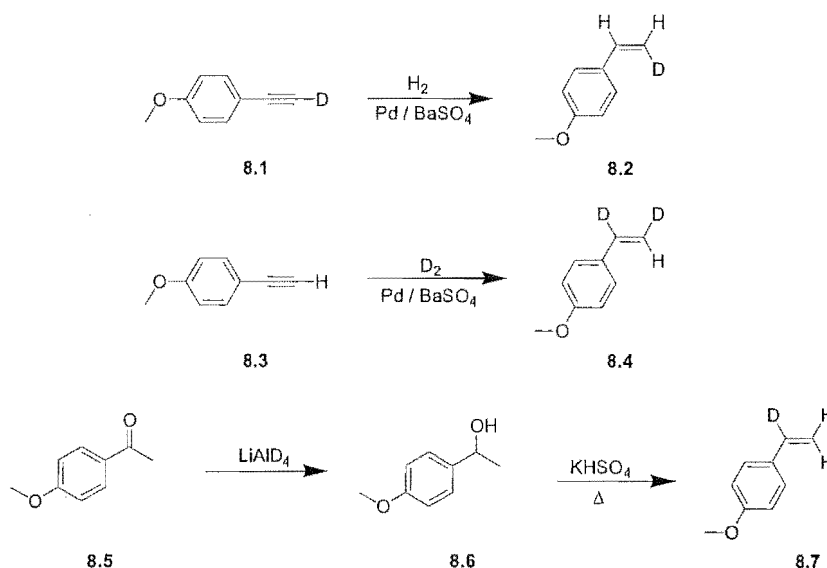
8.1 INTRODUCTION

We wanted to synthesise *p*-methoxystyrene oxide in order to determine what effect the strongly electron donating *p*-methoxy group would have on the selectivity for the Lewis acid catalysed rearrangement. A method had been developed to analyse the products from the rearrangement (see Chapter 2) and the results were to be compared to those of the rearrangement of *m*-methoxy- and *p*-methylstyrene oxide.

Attempts to synthesise *p*-methoxystyrene oxide regioselectively deuterated and optically active were however unsuccessful. The attempted synthesis is described below.

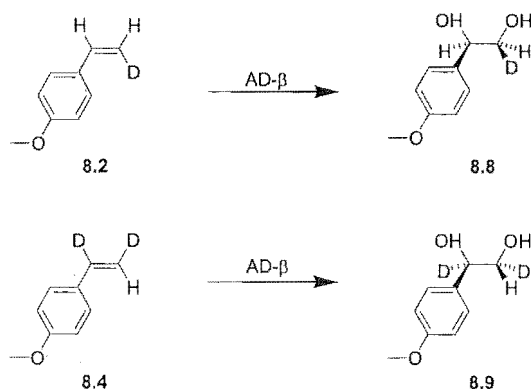
8.2 SYNTHESIS OF *P*-METHOXYSTYRENE OXIDE

The synthesis of *p*-methoxystyrene oxide used the same synthetic methodology used in the synthesis of *p*-methylstyrene oxide, described in Chapter 3. Three deuterated isomers of *p*-methoxystyrene were synthesised (Scheme 8.1):



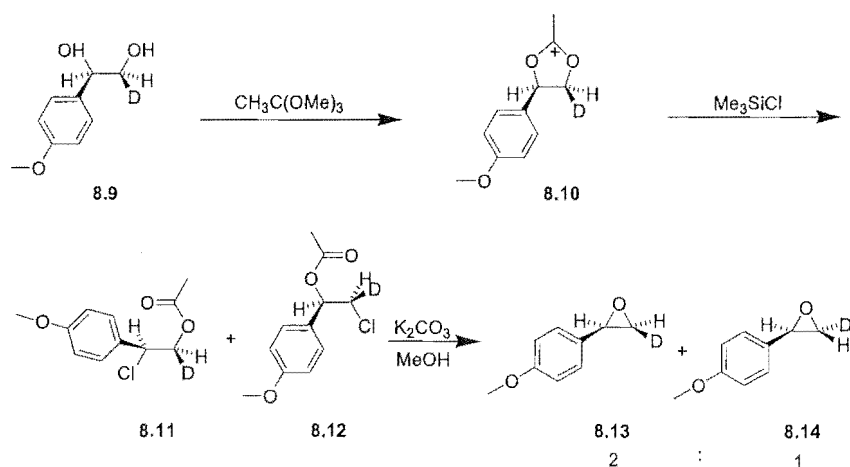
Scheme 8.1. Synthesis of isomers of *p*-methoxystyrene.

Alkenes 8.2 and 8.4 were converted to diol by the Sharpless asymmetric dihydroxylation procedure with retention of the regioselectivity of the deuterium label (Scheme 8.2):



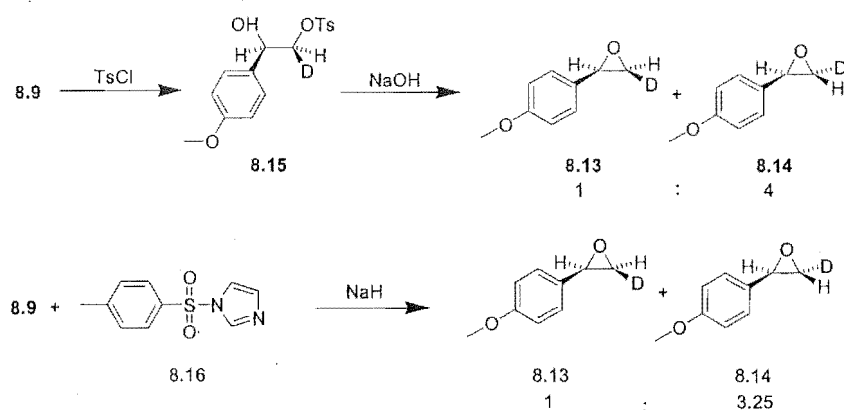
Scheme 8.2. Synthesis of (1*R*),(2*S*)-1-(4-methoxyphenyl)ethane-1,2-diol-2-*d*₁ and (1*R*),(2*R*)-1-(4-methoxyphenyl)ethane-1,2-diol-1,2-*d*₂.

Conversion of the diol to epoxide using the procedure of Kolb et al.¹ produced *cis* and *trans* deuterated *p*-methoxystyrene oxide in low yield (40%) in a 2 : 1 ratio. ¹H NMR showed that chlorohydrin esters **8.11** and **8.12** were formed in good yield, but problems occurred with the K₂CO₃ promoted ring closing saponification step. Attempts to improve the reaction by using shorter reaction times failed to improve the yield and selectivity for the reaction. Chlorohydrin esters **8.11** and **8.12** are novel compounds, but were not isolated and fully characterised.



Scheme 8.3. Synthesis of *p*-methoxystyrene oxide *via* the chlorohydrin ester.

Two other methods were attempted for converting diol to epoxide. Tosyl chloride can be used to react selectively with the primary alcohol and reaction of the primary tosylate with NaOH ² gives epoxide. A one step procedure where diol is reacted with *N*-(*p*-toluenesulfonyl)imidazole in the presence of NaH ³ was also used to give epoxide (Scheme 8.4). *N*-(*p*-Toluenesulfonyl)imidazole was made from *p*-toluenesulfonyl chloride and imidazole.⁴



Scheme 8.4. Conversion of (1*R*),(2*S*)-1-(4-methoxyphenyl)ethane-1,2-diol-2-*d*₁ to epoxide.

The two methods for epoxide formation shown in Scheme 8.4 gave better results. The method using tosyl chloride gave the best yield, but still only provided a 1:4 mixture of the deuterioisomers of *p*-methoxystyrene oxide.

A search of the literature showed one example where chiral 1-(4-methoxyphenyl)ethane-1,2-diol had been converted to epoxide, using a Mitsunobu cyclodehydration.⁵ Diol (97.5% ee) was reported to be converted to epoxide in 74% yield but with an ee of only 6%. The same method gave reasonable ee values for the formation of other substituted styrene oxides. No other examples for this reaction could be found.

We decided that a 4 : 1 mixture of deuterioisomers was inadequate to complete an investigation into the stereoselectivity of the Lewis acid catalysed rearrangement of *p*-methoxystyrene oxide.

The methods of *p*-methoxystyrene oxide formation are summarised in Table 8.1.

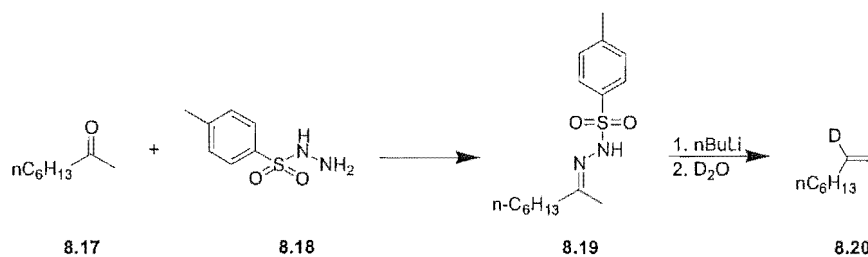
Method	Yield of epoxide	<i>cis</i> : <i>trans</i> deuterium
MeC(OMe) ₃ / Me ₃ SiCl	40%	2 : 1
TsCl / NaOH	85%	1 : 4
<i>N</i> -TsIm / NaH	70%	1 : 3.25

Table 8.1. Methods for formation of *p*-methoxystyrene oxide.

8.3 SYNTHESIS OF OCTENE OXIDE

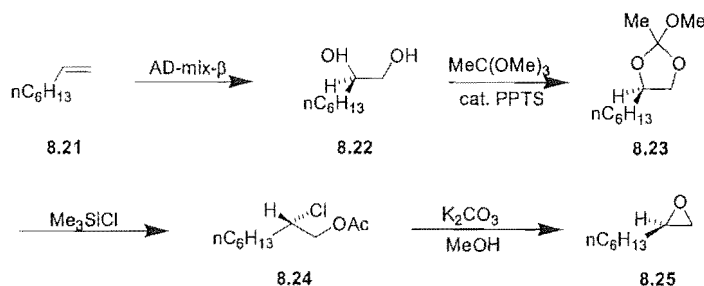
Deuterated 1-octene oxide was synthesised for a rearrangement study. No method was discovered that could analyse the stereoselectivity of the products from the rearrangement.

1-Octene oxide-2-*d*₁ was synthesised by the route shown below:



Scheme 8.5. Synthesis of 1-octene-2-*d*₁.

Alkene **8.20** was converted to diol by the Sharpless asymmetric dihydroxylation reaction. Epoxide was formed in good yield (Scheme 8.6).



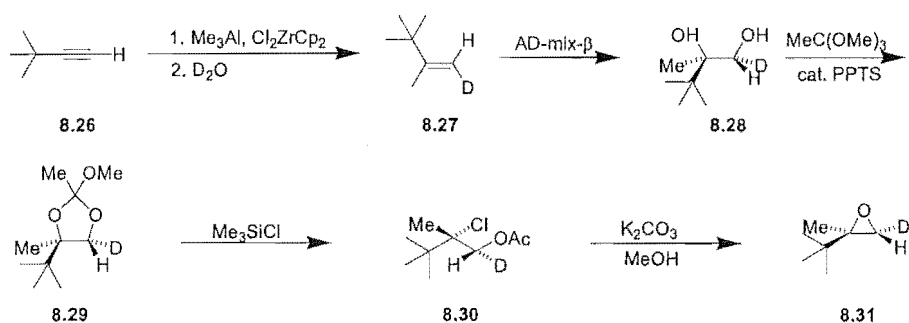
Scheme 8.6. Synthesis of octene oxide.

No attempt was made to determine the enantiomeric excess of the diol or epoxide.

8.4 SYNTHESIS OF 2,3,3-TRIMETHYL-1-BUTENE OXIDE

Deuterated 2,3,3-trimethyl-1-butene oxide was synthesised, but as for octene oxide, no method was able to be developed to analyse the stereoselectivity of the products from the Lewis acid catalysed rearrangement of the epoxide.

The method of synthesis is shown in Scheme 8.7. The synthesis begins with the zirconium catalysed carboalumination of alkyne **8.26**. Hexane from the trimethylaluminium solution and alkene **8.27** have similar boiling points and the yield of the reaction was reduced because of difficulties isolating the alkene. Dihydroxylation and epoxidation was achieved by the method used previously for the dihydroxylation and epoxidation of 1-octene.



Scheme 8.7. Synthesis of deuterated 2,3,3-trimethyl-1-butene.

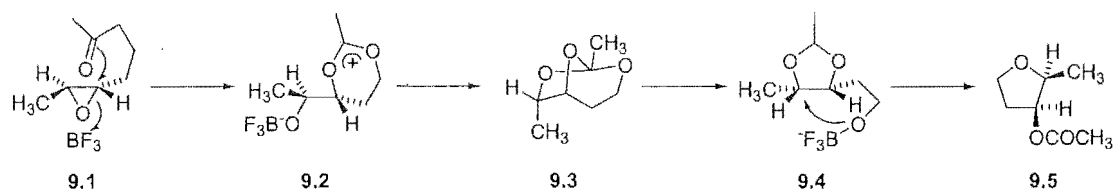
-
- ¹ Kolb, H. C.; Sharpless, K. B. *Tetrahedron* **1992**, *48*(48), 10515-10530.
² Wei, Z. L. et al. *Tetrahedron* **1998**, *54*, 13059-13072.
³ Cink, R. D.; Forsyth, C. J. *J. Org. Chem.* **1995**, *60*, 8122-8123.
⁴ Hicks, D. R.; Fraser-Reid, B. *Synthesis* **1974**, 203.
⁵ Weissman, S. A.; Rossen, K.; Reider, P. J. *Org. Lett.* **2001**, *3*(16), 2513-2515.

Chapter Nine

Intramolecular Acetate Attack on 1,2-Substituted Epoxide

9.1 INTRODUCTION

Mechanistic studies¹ into the BF_3 catalysed rearrangement of alkyl acetate substituted epoxides show that when acetate participates in the intramolecular epoxide cyclisation, a rearrangement occurs (Scheme 9.1). The reaction has been used in the synthesis of difficult compounds such as C-glycofuranosides² and a similar reaction occurs with carbamate substituted epoxides.³



Scheme 9.1. Intramolecular acetate participation in epoxide opening.

It has been shown that this type of rearrangement is sensitive to the electronic nature of the substituents. In order to test whether the rearrangement also occurs in aromatic systems, compounds of the type shown in Figure 9.1 were investigated. Each of the *cis* and *trans* epoxides were synthesised and reacted with the Lewis acids LiClO_4 and BF_3 .

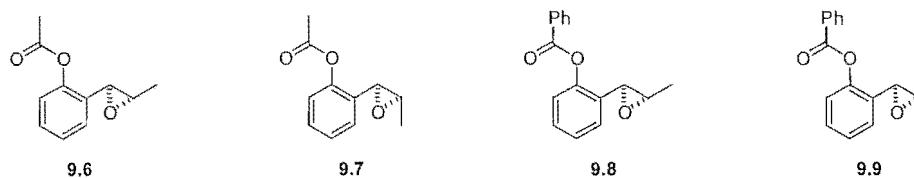
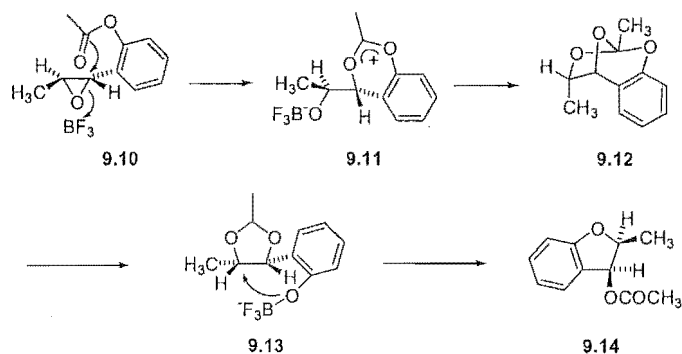


Figure 9.1. Epoxide cyclisation compounds.

The expected rearrangement reaction of epoxide **9.6** is shown in Scheme 9.2:



Scheme 9.2. Expected rearrangement of 1-(2-acetoxyphenyl)propene oxide with BF_3 .

9.2 MOLECULAR MODELLING

In an attempt to determine whether the acetate in compounds in Figure 9.1 would react intramolecularly, a molecular mechanics conformational search was performed on **9.6**. The lowest energy structure, which was calculated from a Boltzmann distribution to account for 40% of the conformations of **9.6** at room temperature is shown in Figure 9.2. It can be seen that the carbonyl oxygen is in close proximity to both the epoxide carbons and could react.

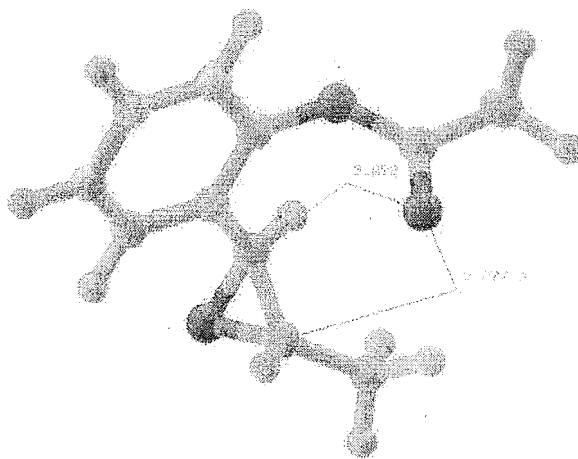
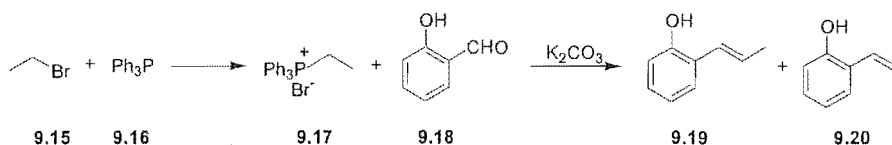


Figure 9.2. Lowest energy conformer of 1-(2-acetoxyphenyl)propene oxide from a molecular mechanics conformational search.

9.3 SYNTHESIS OF 1-(2-ACETOXYPHENYL)PROPENE OXIDE

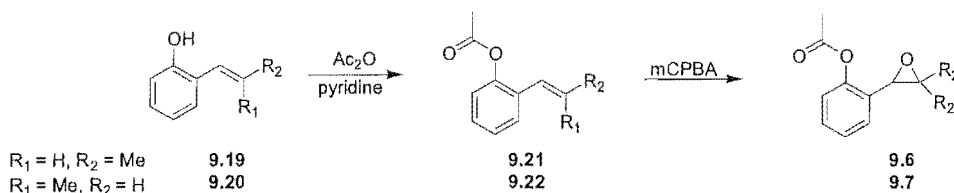
1-(2-Acetoxyphenyl)propene was synthesised by a modified phase transfer Wittig reaction⁴ (Scheme 9.3). The reaction gave a 4 : 1 or 3 : 1 mixture of the *E* and *Z* alkene, depending on the amount of water that was added to the reaction mixture.



Scheme 9.3. Synthesis of 1-(2-hydroxyphenyl)propene.

The *cis* and *trans* alkene isomers had very similar boiling points and so separation by distillation was not possible. The two alkene isomers also had the same R_F value on silica and alumina, however separation of the two alkenes was achieved by flash column chromatography using silver nitrate impregnated silica.⁵

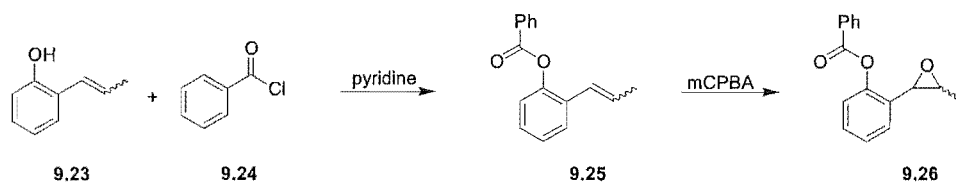
The acetate group was added to the alkene using acetic anhydride and pyridine. Epoxides **9.6** and **9.7** were made by epoxidation with mCPBA (Scheme 9.4).



Scheme 9.4. Synthesis of 1-(2-acetoxyphenyl)propene oxide.

9.4 SYNTHESIS OF 2-(3-METHYLOXIRANYL)-PHENYL BENZOATE

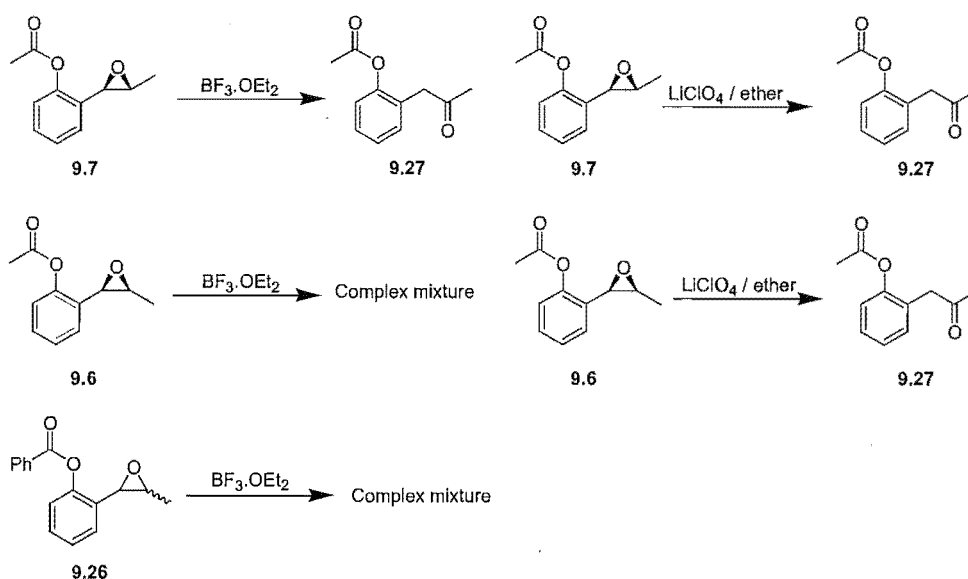
The benzoate analogue of **9.6** and **9.7** was made as a mixture of the *cis* and *trans* epoxides by reaction of a mixture of **9.19** and **9.20** with benzoyl chloride in pyridine and epoxidation with mCPBA (Scheme 9.5). Compounds **9.25** and **9.26** were characterised by ¹H NMR. No HRMS or analysis data were obtained for these new compounds.



Scheme 9.5. Synthesis of 2-(3-methyloxiranyl)-phenyl benzoate.

9.5 REARRANGEMENT OF EPOXIDES WITH LEWIS ACID

Each of the epoxides was rearranged with Lewis acid (either $\text{BF}_3 \cdot \text{OEt}_2$, or LiClO_4) in ether (Scheme 9.6). Every reaction gave either the rearranged ketone **9.27**, or a complex mixture of compounds. There was no evidence that acetate participates in the rearrangement process.



Scheme 9.6. Lewis acid catalysed rearrangement of epoxyacetates.

¹ Coxon, J. M.; Hartshorn, M. P.; Swallow, W. H. *J. Org. Chem.* **1974**, 39, 1142-1148.

² Chmielewski, M.; Guzik, P.; Hintze, B.; Daiewski, W. M. *Tetrahedron* **1985**, 41, 5929-5932.

³ Yamamoto, M.; Suzuki, M.; Kishikawa, K.; Kohmoto, S. *Synthesis* **1993**, 307.

⁴ le Bigot, Y.; Delmas, M.; Gaset, A. *Tetrahedron Lett.* **1983**, 24, 193-196.

⁵ Li, T.; Li, J.; Li, H. *J. Chromatography A* **1995**, 715, 372-375.

Summary and Future Work

Summary:

- Both the LiClO_4 and $\text{BF}_3 \cdot \text{OEt}_2$ catalysed rearrangement of styrene oxide derivatives proceed *via* a carbocation intermediate.
- The $\text{BF}_3 \cdot \text{OEt}_2$ catalysed rearrangement of *p*-methylstyrene oxide does not proceed *via* a fluorohydrin intermediate.
- The selectivity for hydride migration in the rearrangement is controlled by the relative energy of the carbocation intermediate conformers.
- Rotation of the oxygen is well advanced in the two transition states for opening of the epoxide ring. The two transition states lead to two separate rearrangement pathways.
- Factors other than just the steric bulk of the epoxide substituents determine the relative importance of each reaction pathway.
- In all epoxide systems studied experimentally, there is a preference for formation of a symmetrical carbocation intermediate, where the C-O bond is eclipsed relative to the adjacent C-C bond.

Future work:

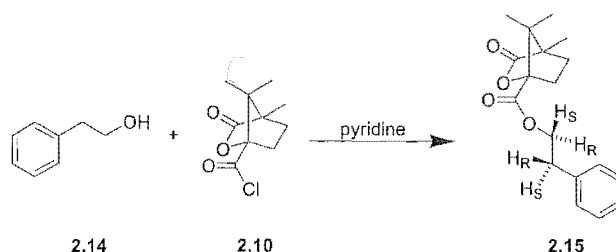
- A more accurate method could be developed to analyse the selectivity of hydride or deuteride migration in the rearrangement process.
- Other Lewis acids, such as the bulky Lewis acid MABR (see section 1.12.3, page 28) could be used to rearrange a series of chiral, deuterated epoxides.
- An NMR method could be developed to analyse the facial selectivity for hydride and deuteride migration in the rearrangement of alkyl substituted epoxides and the Lewis acid catalysed rearrangement of these epoxides could be studied experimentally.
- Calculations could be performed to further probe the stereoelectronic factors responsible for formation of symmetrical, as opposed to unsymmetrical carbocation intermediates.

Chapter Ten

Experimental

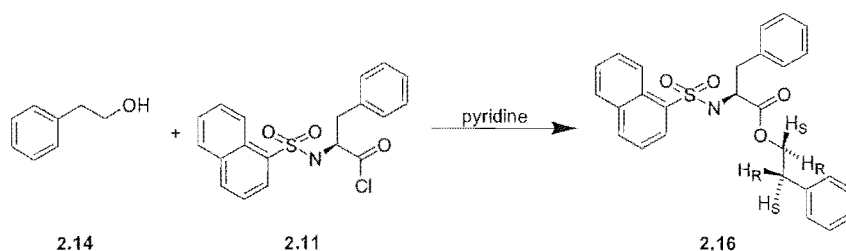
10.1 EXPERIMENTAL WORK DESCRIBED IN CHAPTER TWO

2-Phenylethyl (1*S*)-(-)-camphanate



2-Phenylethanol (0.055 mL, 0.46 mmol) and dry pyridine (0.056 mL, 0.69 mmol) were added to a solution of (1*S*)-(-)-camphanic chloride (100 mg, 0.46 mmol) in dry CH₂Cl₂ (5 mL) under N₂. After three hours the solution was washed with HCl (5 mL, 1M), saturated Na₂CO₃ (5 mL), dried over anhydrous Na₂SO₄ and the solvent removed on a rotary evaporator. The product was recrystallised from petroleum ether as needles (121 mg, 87%). mp 71 - 72°C. ¹H NMR (300 MHz, CDCl₃) δ 7.20- 7.35 (m, 5H), 4.46 (t, *J* = 7 Hz, 2H), 3.01 (t, *J* = 7 Hz, 2H), 1.6-2.4 (m, 4H), 1.09 (s, 3H), 0.95 (s, 3H), 0.84 (s, 3H). HRMS (ES) 303.1594 (MH⁺). C₁₈H₂₃O₄ requires 303.1596.

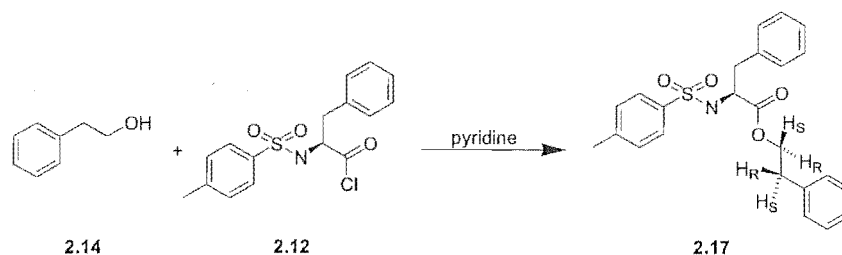
2-Phenylethyl (*N*-1-naphthalenesulfonyl)-(*S*)-2-amino-3-phenylpropanoate



2-Phenylethanol (0.097 mL, 0.82 mmol) and dry pyridine (0.100 mL, 1.29 mmol) were added to a solution of *N*-(1-naphthalenesulfonyl)-L-phenylalanyl chloride (306 mg, 0.82 mmol) in dry CH₂Cl₂ (5 mL) under N₂. After three hours the solution was washed with HCl (5 mL, 1M), saturated Na₂CO₃ (5 mL), dried over anhydrous Na₂SO₄ and the solvent removed on a rotary evaporator. The product was recrystallised from methanol-H₂O to

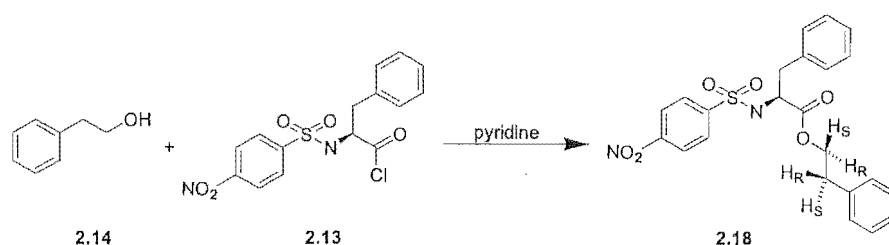
give a white solid (323 mg, 93%). mp 84 - 90°C. ^1H NMR (300 MHz, CDCl_3) δ 6.80-8.55 (m, 17H), 5.29 (d, J = 10 Hz, 1H), 4.16 (m, 1H), 3.84-3.96 (m, 2H), 2.87 (d, J = 6 Hz, 2H), 2.58 (t, J = 7 Hz, 2H). HRMS (ES) 460.1580 (MH^+). $\text{C}_{27}\text{H}_{26}\text{NO}_4\text{S}$ requires 460.1583.

2-Phenylethyl (*N*-4-methylphenylsulfonyl)-(*S*)-2-amino-3-phenylpropanoate



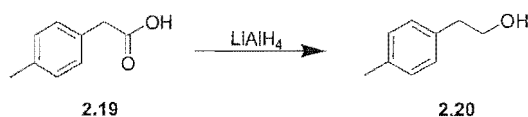
2-Phenylethanol (0.106 mL, 0.89 mmol) and dry pyridine (0.108 mL, 1.34 mmol) were added to a solution of *N*-(*p*-toluenesulfonyl)-L-phenylalanyl chloride (301 mg, 0.89 mmol) in dry CH_2Cl_2 (5 mL) under N_2 . After three hours the solution was washed with HCl (5 mL, 1M), saturated Na_2CO_3 (5 mL), dried over anhydrous Na_2SO_4 and the solvent removed on a rotary evaporator. 2-Phenylethyl (*N*-4-methylphenylsulfonyl)-(*S*)-2-amino-3-phenylpropanoate¹ was recrystallised from methanol as needles (360 mg, 88%). mp 134-135°C. IR (KBr, cm^{-1}) 3416, 3290, 1737, 1330, 1163, 1090. ^1H NMR (300 MHz, CDCl_3) δ 7.60-6.95 (m, 14H), 5.01 (d, J = 9 Hz, 1H), 4.17 (m, 1H), 4.03 (m, 2H), 2.97 (d, J = 6 Hz, 2H), 2.71 (t, J = 7 Hz, 2H), 2.38 (s, 3H).

2-Phenylethyl (*N*-4-nitrophenylsulfonyl)-(*S*)-2-amino-3-phenylpropanoate



2-Phenylethanol (0.103 mL, 0.84 mmol) and dry pyridine (0.103 mL, 1.33 mmol) were added to a solution of *N*-(4-nitrophenylsulfonyl)-L-phenylalanyl chloride (310 mg, 0.84 mmol) in dry CH_2Cl_2 (5 mL) under N_2 . After three hours the solution was washed with HCl (5 mL, 1M), saturated Na_2CO_3 (5 mL), dried over anhydrous Na_2SO_4 and the solvent removed on a rotary evaporator. The product was recrystallised from methanol as needles (366 mg, 96%). mp 100-102°C. IR (KBr, cm^{-1}) 3414, 3277, 1730, 1522, 1350, 1171, 1087. ^1H NMR (300 MHz, CDCl_3) δ 8.16-6.94 (m, 14H), 5.23 (d, $J = 10$ Hz, 1H), 4.22 (m, 1H), 4.15 (t, $J = 7$ Hz, 2H), 2.89-3.07 (m, 2H), 2.82(t, $J = 7$ Hz, 2H). HRMS (ES) 455.1276 (MH^+). $\text{C}_{23}\text{H}_{23}\text{N}_2\text{O}_6\text{S}$ requires 455.1277.

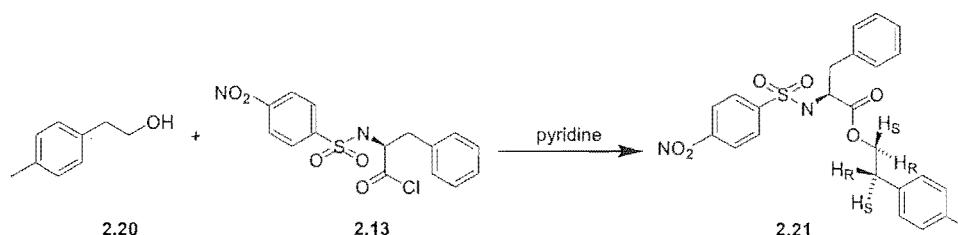
2-(4-Methyl)phenylethanol



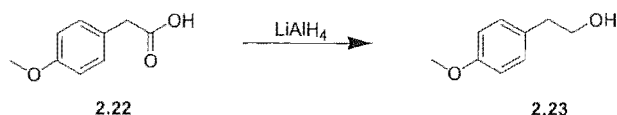
p-Tolyl acetic acid (215 mg, 1.43 mmol) in dry ether (5 mL) was added to a suspension of LiAlH_4 (81 mg, 2.15 mmol) in dry ether (5 mL) at 0°C. The reaction was stirred at room temperature for 4 days and ethyl acetate (1 mL) was added followed by 3N NaOH (1 mL). The organic layer was separated and the aqueous layer was extracted with ether. The combined organic extracts were dried with MgSO_4 , filtered and the solvent removed under reduced pressure to give 2-(4-methyl)phenylethanol² as a clear liquid (181 mg, 93%). ^1H

NMR (CDCl₃, 300 MHz) δ 7.12 (m, 4H), 3.84 (m, 2H), 2.83 (m, 2H), 2.34 (s, 3H), 1.65 (bs, 1H).

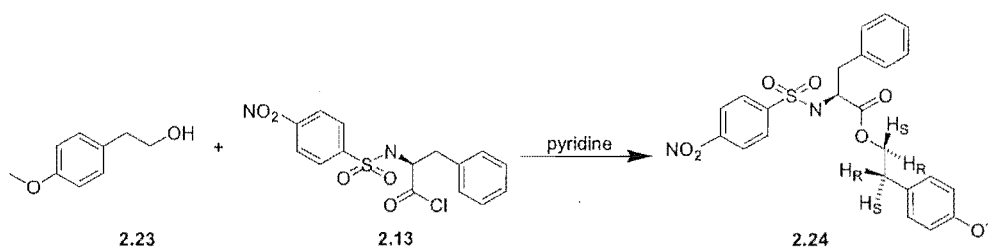
2-(4-Methyl)phenylethyl (*N*-4-nitrophenylsulfonyl)-(*S*)-2-amino-3-phenylpropanoate



2-(4-Methyl)phenyl-ethanol (0.1065 g, 0.782 mmol) and dry pyridine (0.076 mL, 1.17 mmol) were added to a solution of *N*-(4-nitrophenylsulfonyl)-L-phenylalanyl chloride (242 mg, 0.782 mmol) in dry CH₂Cl₂ (5 mL) under N₂. After three hours the solution was washed with HCl (5 mL, 1M), saturated Na₂CO₃ (5 mL), dried over anhydrous Na₂SO₄ and the solvent removed under reduced pressure. The product was recrystallised from methanol as needles (352 mg, 96%). mp 90 - 93 °C. ¹H NMR (500 MHz, CDCl₃) δ 8.14 (dd, *J* = 2.4, 6.8 Hz, 2H, Ar-H), 7.77 (dd, *J* = 2.0, 6.8 Hz, 2H, Ar-H), 7.22-7.19 (m, 3H, Ar-H), 7.13 (d, *J* = 7.8 Hz, 2H, Ar-H), 7.02 (d, *J* = 8.3 Hz, 2H, Ar-H), 6.96 (m, 2H, Ar-H), 5.25 (d, *J* = 9.8 Hz, 1H, N-H), 4.25-4.22 (m, 1H, NC-H), 4.12 (t, *J* = 6.8 Hz, 2H, CO₂CH₂), 3.04 (dd, *J* = 5.4, 13.7 Hz, 1H, NCHCH₂Ar), 2.93 (dd, *J* = 6.8, 13.7 Hz, 1H, NCHCH₂Ar), 2.77 (t, *J* = 6.8 Hz, 2H, CO₂CH₂CH₂Ar), 2.33 (s, 3H, Ar-CH₃). ¹³C NMR (75 MHz, CDCl₃) δ 170.4, 145.4, 136.5, 134.7, 134.0, 129.4, 129.3, 128.7, 128.7, 128.2, 127.4, 124.1, 66.6, 57.0, 39.2, 34.3, 21.0. HRMS (ES) 507.0988 (M⁺+K). C₂₄H₂₃N₂O₆SK requires 507.0947.

2-(4-Methoxy)phenylethanol

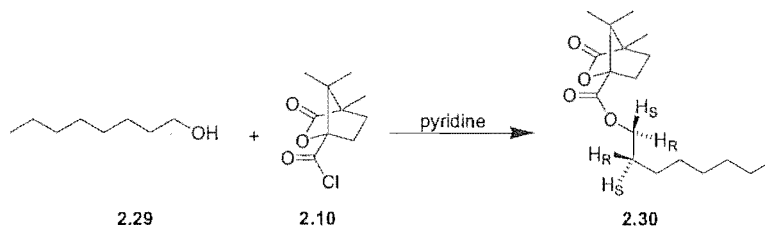
LiAlH₄ (0.425 g, 11.2 mmol) was added portionwise to a stirring solution of *p*-methoxyphenylacetic acid (1.8629 g, 11.2 mmol) in dry ether (25 mL) at 0°C. The solution was warmed to room temperature and stirred for 2 hours. Saturated NH₄Cl (2 mL) was added and the reaction mixture was left to stir for 48 hours at room temperature. Sufficient MgSO₄ was added to dry the solution. The solution was filtered and the solvent removed under reduced pressure to give 1-(4-methoxy)phenylethanol³ as a clear liquid (1.500 g, 88%). ¹H NMR (CDCl₃, 300 MHz) δ 7.15 (d, *J* = 8.3 Hz, 2H), 6.86 (d, *J* = 8.8 Hz, 2H), 3.82 (m, 2H), 3.79 (s, 3H), 2.81 (m, 2H), 1.71 (bs, 1H).

2-(4-Methoxy)phenylethyl
phenylpropanoate***N*-(4-nitrophenylsulfonyl)-(S)-2-amino-3-**

2-(4-Methyl)phenyl-ethanol (78.1 mg, 0.514 mmol) and dry pyridine (60 μL, 0.617 mmol) were added to a solution of *N*-(4-nitrophenylsulfonyl)-L-phenylalanyl chloride (171 mg, 0.514 mmol) in dry CH₂Cl₂ (5 mL) under N₂. After three hours the solution was washed with HCl (5 mL, 1M), saturated Na₂CO₃ (5 mL), dried over anhydrous Na₂SO₄ and the solvent removed under reduced pressure. The product was recrystallised from methanol as needles (244 mg, 98%). ¹H NMR (CDCl₃, 500 MHz) δ 8.15 (m, 2H), 7.78 (m, 2H), 7.26-

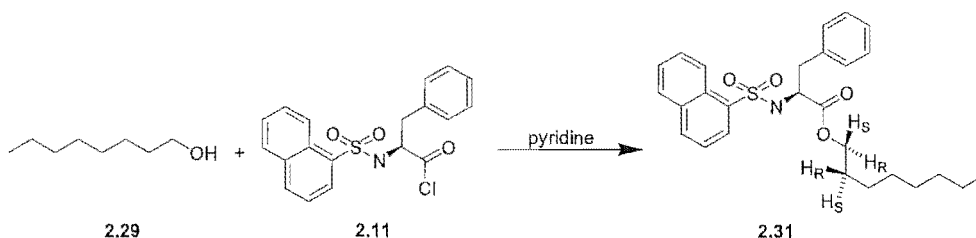
6.85 (m, 9H), 5.29 (m, 1H), 4.23 (m, 1H), 4.10 (m, 2H), 3.79 (s, 3H), 3.03 (m, 1H), 2.93 (m, 1H), 2.76 (m, 2H). HRMS (ES) 507.1203 (MNa^+). $\text{C}_{24}\text{H}_{24}\text{N}_2\text{O}_7\text{SNa}$ requires 507.1202.

Octyl (1*S*)-(-)-camphanate



1-Octanol (0.0695 mL, 0.438 mmol) was added to a stirring solution of (1*S*)-(-)-camphanyl chloride (0.095 g, 0.438 mmol) in dry CH_2Cl_2 under a nitrogen atmosphere. Pyridine (0.053 mL, 0.658 mmol) was added and the reaction mixture was stirred at room temperature for 8 hours. The reaction mixture was washed with 1 N HCl, saturated Na_2CO_3 and water. The organic extract was dried with MgSO_4 and the solvent removed under reduced pressure to give octyl (1*S*)-(-)-camphanate¹ as an oil (101 mg, 74%). ^1H NMR (300 MHz, CDCl_3) δ 4.23 (dd, $J = 6.3, 6.7$ Hz, 2H), 2.48-3.39 (m, 1H), 2.08-1.89 (m, 2H), 1.88-1.64 (m, 3H), 1.39-1.27 (m, 10H), 1.12 (s, 3H), 1.06 (s, 3H), 0.97 (s, 3H) 0.90-0.86 (m, 3H).

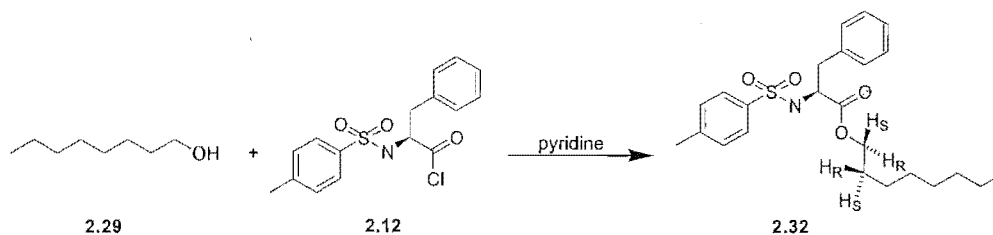
Octyl (*N*-1-naphthalenesulfonyl)-(*S*)-2-amino-3-phenylpropanoate



1-Octanol (0.0857 mL, 0.543 mmol) was added to a stirring solution of *N*-(1-naphthalenesulfonyl)-L-phenylalanyl chloride (0.203 g, 0.543 mmol) in dry CH_2Cl_2 under

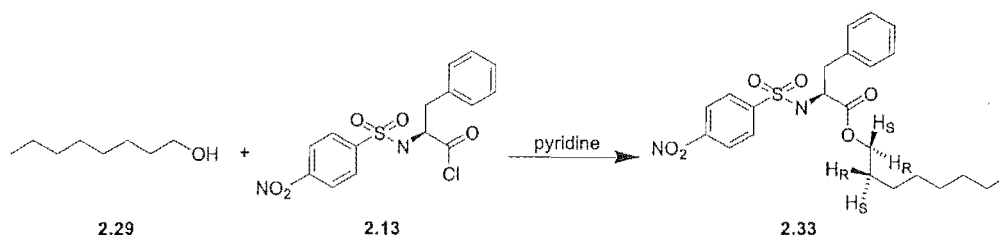
a nitrogen atmosphere. Pyridine (0.085 mL, 1.10 mmol) was added and the reaction mixture was stirred at room temperature for 8 hours. The reaction mixture was washed with 1 N HCl, saturated Na_2CO_3 and water. The organic extract was dried with MgSO_4 and the solvent removed under reduced pressure to give octyl (*N*-1-naphthalenesulfonyl)-(*S*)-2-amino-3-phenylpropanoate as an oil (226 mg, 89%). ^1H NMR (CDCl_3 , 300 MHz) δ 8.55 (d, $J = 8.8$ Hz, 1H), 8.19 (dd, $J = 7.3, 0.98$ Hz, 1H), 8.03 (d, $J = 7.8$ Hz, 1H), 7.90 (m, 1H), 7.62 (m, 2H), 7.49 (m, 1H), 7.10 (m, 3H), 6.94 (m, 2H), 5.29 (d, $J = 8.8$ Hz, 1H), 4.18 (m, 1H), 3.67 (m, 2H), 2.94 (d, $J = 6.3$ Hz, 2H), 1.59 (s, 2H), 1.24 (m, 8H), 0.89 (m, 3H). HRMS (ES) 468.2209 (MH^+). $\text{C}_{27}\text{H}_{34}\text{NO}_4\text{S}$ requires 468.2209.

Octyl (*N*-4-methylphenylsulfonyl)-(*S*)-2-amino-3-phenylpropanoate



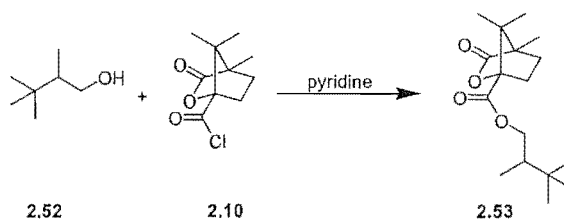
1-Octanol (0.0789 mL, 0.500 mmol) was added to a stirring solution of *N*-(*p*-toluenesulfonyl)-L-phenylalanyl chloride (0.169 g, 0.500 mmol) in dry CH_2Cl_2 under a nitrogen atmosphere. Pyridine (0.0607 mL, 0.750 mmol) was added and the reaction mixture was stirred at room temperature for 8 hours. The reaction mixture was washed with 1 N HCl, saturated Na_2CO_3 and water. The organic extract was dried with MgSO_4 and the solvent removed under reduced pressure to give octyl (*N*-4-methylphenylsulfonyl)-(*S*)-2-amino-3-phenylpropanoate as an oil (201 mg, 93%). ^1H NMR (CDCl_3 , 300 MHz) δ 7.65 (d, $J = 8.3$ Hz, 2H), 7.24 (m, 5H), 7.08 (m, 2H), 5.06 (d, $J = 9.3$ Hz, 1H), 4.19 (m, 1H), 3.81 (m, 2H), 3.03 (d, $J = 5.9$ Hz, 2H), 2.40 (s, 3H), 1.39 (m, 2H), 1.25 (m, 8H), 0.89 (m, 3H). HRMS (ES) 432.2209 (MH^+). $\text{C}_{24}\text{H}_{34}\text{NO}_4\text{S}$ requires 432.2209.

Octyl (*N*-4-nitrophenylsulfonyl)-(*S*)-2-amino-3-phenylpropanoate



1-Octanol (0.0826 mL, 0.523 mmol) was added to a stirring solution of *N*-(4-nitrophenylsulfonyl)-*L*-phenylalanyl chloride (0.193 g, 0.523 mmol) in dry CH_2Cl_2 under a nitrogen atmosphere. Pyridine (0.082 mL, 1.06 mmol) was added and the reaction mixture was stirred at room temperature for 8 hours. The reaction mixture was washed with 1 N HCl, saturated Na_2CO_3 and water. The organic extract was dried with MgSO_4 and the solvent removed under reduced pressure to give octyl (*N*-4-nitrophenylsulfonyl)-(*S*)-2-amino-3-phenylpropanoate as an oil (230 mg, 95%). ^1H NMR (CDCl_3 , 300 MHz) δ 8.21 (m, 2H), 7.84 (m, 2H), 7.22 (m, 3H), 7.05 (m, 2H), 5.28 (d, $J = 9.3$ Hz, 1H), 4.23 (m, 1H), 3.94 (t, $J = 6.8$ Hz, 2H), 3.04 (m, 2H), 1.48 (m, 2H), 1.23 (m, 8H), 0.88 (m, 3H). HRMS (ES) 463.1905 (MH^+). $\text{C}_{23}\text{H}_{31}\text{N}_2\text{O}_6\text{S}$ requires 463.1903.

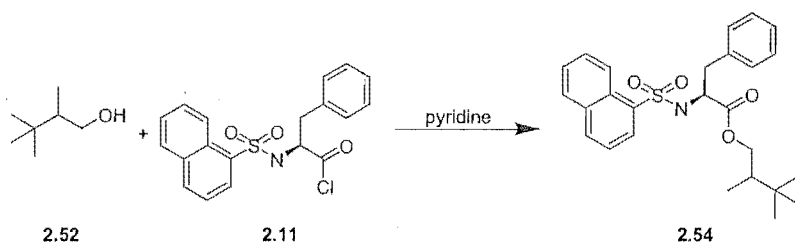
2,3,3-Trimethylbutyl (1*S*)-(-)-camphanate



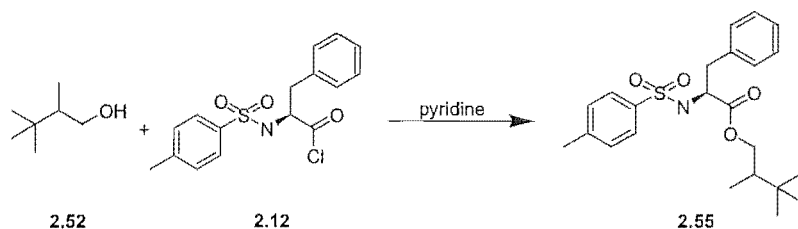
A solution of 2,3,3-trimethylbutanol (0.081 g, 0.70 mmol) and dry pyridine (0.069 mL, 0.89 mmol) was added to a solution of (1*S*)-(-)-camphanic chloride (0.151 g, 0.70 mmol) in dry CH_2Cl_2 (5 mL) under N_2 . After three hours the solution was washed with HCl (5 mL, 1M), saturated Na_2CO_3 (5 mL), dried over anhydrous Na_2SO_4 and the solvent was removed on a rotary evaporator to give an oil (162 mg, 78%). ^1H NMR (300 MHz, CDCl_3) δ 4.40

(m, 1H), 3.96 (m, 1H), 2.42 (m, 1H), 2.08-1.88 (m, 2H), 1.74-1.62 (m, 2H), 1.12 (s, 3H), 1.07 (s, 3H), 0.97 (s, 3H), 0.95 (d, $J = 7.0$ Hz, 3H), 0.93 (s, 9H). HRMS (ES) 297.2065 (MH^+). $C_{17}H_{29}O_6$ requires 297.2066.

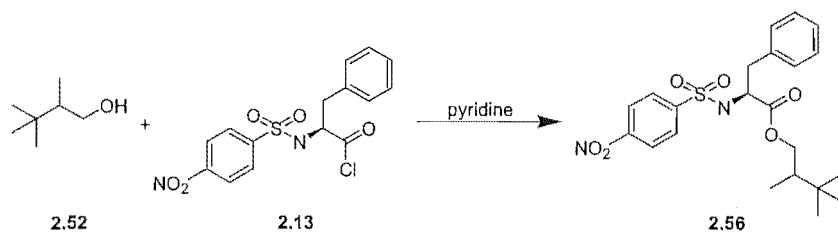
2,3,3-Trimethylbutyl (*N*-1-naphthalenesulfonyl)-(*S*)-2-amino-3-phenylpropanoate



A solution of 2,3,3-trimethylbutanol (0.085 g, 0.73 mmol) and dry pyridine (0.069 mL, 0.89 mmol) was added to a solution of *N*-(1-naphthalenesulfonyl)-*L*-phenylalanyl chloride (0.273 g, 0.73 mmol) in dry CH_2Cl_2 (5 mL) under N_2 . After three hours the solution was washed with HCl (5 mL, 1M), saturated Na_2CO_3 (5 mL), dried over anhydrous Na_2SO_4 and the solvent was removed on a rotary evaporator to give an oil (285 mg, 86%). 1H NMR (300 MHz, $CDCl_3$) δ 8.54 (d, $J = 8.3$ Hz, 1H), 8.13 (dd, $J = 1.5, 7.3$ Hz, 1H), 8.03 (d, $J = 8.3$ Hz, 1H), 7.91 (d, $J = 8.3$ Hz, 1H), 7.60 (m, 2H), 7.47 (t, $J = 7.8$ Hz, 1H), 7.06 (m, 3H), 6.94 (m, 2H), 4.12 (m, 1H), 3.36 (m, 1H), 2.92 (m, 2H), 1.15 (m, 1H), 0.77 (s, 9H), 0.62 (m, 3H).

2,3,3-Trimethylbutyl (*N*-4-methylphenylsulfonyl)-(*S*)-2-amino-3-phenylpropanoate


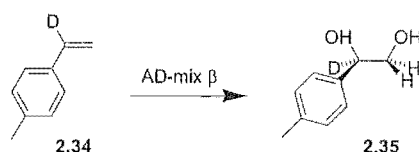
A solution of 2,3,3-trimethylbutanol (0.079 g, 0.68 mmol) and dry pyridine (0.069 mL, 0.89 mmol) was added to a solution of *N*-(4-methylphenylsulfonyl)-*L*-phenylalanyl chloride (0.297 g, 0.68 mmol) in dry CH_2Cl_2 (5 mL) under N_2 . After three hours the solution was washed with HCl (5 mL, 1M), saturated Na_2CO_3 (5 mL), dried over anhydrous Na_2SO_4 and the solvent was removed on a rotary evaporator to give an oil (261 mg, 92%). ^1H nmr (300 MHz, CDCl_3) δ 7.64 (d, J = 8.3 Hz, 2H), 7.24 (m, 5H), 7.09 (m, 2H), 5.03 (d, J = 9.3 Hz, 1H), 4.22-4.15 (m, 1H), 4.03-3.89 (m, 1H), 3.58-3.44 (m, 1H), 3.02 (d, J = 6.3 Hz, 1H), 2.38 (s, 3H), 1.28 (m, 1H), 0.80 (d, J = 2.0 Hz, 9H), 0.68 (d, J = 6.8 Hz, 3H).

2,3,3-Trimethylbutyl (*N*-4-nitrophenylsulfonyl)-(*S*)-2-amino-3-phenylpropanoate


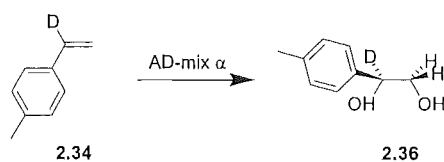
A solution of 2,3,3-trimethylbutanol (0.086 g, 0.74 mmol) and dry pyridine (0.069 mL, 0.89 mmol) was added to a solution of *N*-(4-nitrophenylsulfonyl)-*L*-phenylalanyl chloride (0.272 g, 0.74 mmol) in dry CH_2Cl_2 (5 mL) under N_2 . After three hours the solution was washed with HCl (5 mL, 1M), saturated Na_2CO_3 (5 mL), dried over anhydrous Na_2SO_4 and the solvent was removed on a rotary evaporator to give an oil (305 mg, 92%). ^1H nmr (300 MHz, CDCl_3) δ 8.23 (d, J = 8.8 Hz, 2H), 7.85 (d, J = 8.3 Hz, 2H), 7.23 (m, 3H), 7.06 (m,

2H), 7.25 (d, $J = 9.6$ Hz, 1H), 4.28-4.05 (m, 2H), 3.73-3.61 (m, 1H), 3.09-2.99 (m, 2H), 1.41 (m, 1H), 0.84 (s, 9H), 0.78 (dd, $J = 2.4, 6.8$ Hz, 3H). HRMS (ES) 449.1746 (MH^+). $\text{C}_{22}\text{H}_{29}\text{N}_2\text{O}_6\text{S}$ requires 449.1746.

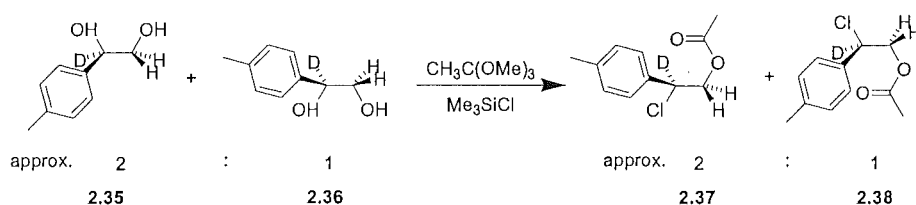
(1*R*)-1-(4-Methylphenyl)-1,2-ethanediol-1-*d*₁



p-Methylstyrene- α -*d*₁ (1.0 g, 8.4 mmol) was added to a vigorously stirring solution of AD-mix- β (11.76 g) in tertiary butyl alcohol (42 mL) and water (42 mL) at 0°C. The solution was stirred for 48 hours at 0°C. Sodium metabisulphite (12.6 g) was added and the reaction mixture was stirred for one hour, and allowed to warm to room temperature. The reaction mixture was diluted with CH_2Cl_2 , the organic layer separated and the aqueous layer extracted with ethyl acetate. The solvent was removed under reduced pressure and flash chromatography on silica gel (ethyl acetate / petroleum ether) gave (1*R*)-1-(4-methylphenyl)-1,2-ethanediol-1-*d*₁ as white crystals (0.92 g, 71 %). mp 72 - 74 °C. $[\alpha]_{\text{D}}^{20} -70$ (c 2.9, CHCl_3) [lit.⁴ $[\alpha]_{\text{D}}^{20} -67$ (c 0.90, CHCl_3 , ee > 97%) for undeuterated material]. ^1H NMR (500 MHz, CDCl_3) δ 7.24 (d, $J = 8.3$ Hz, 2H), 7.16 (d, $J = 7.8$ Hz, 2H), 3.71 (d, $J = 11.2$ Hz, 1H), 3.63 (d, $J = 11.7$ Hz, 1H), 2.34 (s, 3H). ^{13}C NMR (75 MHz, CDCl_3) δ 137.4, 129.0, 126.0, 74.0 (t, $J_{\text{CD}} = 21.3$ Hz), 67.8, 21.0.

(1*S*)-1-(4-Methylphenyl)-1,2-ethanediol-1-*d*₁

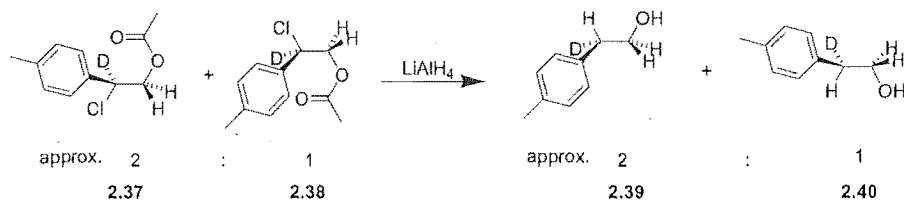
p-Methylstyrene- α -*d*₁ (0.50 g, 4.2 mmol) was added to a vigorously stirring solution of AD-mix- α (5.88 g) in tertiary butyl alcohol (21 mL) and water (21 mL) at 0°C. The solution was stirred for 48 hours at 0°C. Sodium metabisulphite (6.3 g) was added and the reaction mixture was stirred for one hour, warming to room temperature. The reaction mixture was diluted with CH₂Cl₂, the organic layer separated and the aqueous layer extracted with ethyl acetate. The solvent was removed under reduced pressure and flash chromatography on silica gel (ethyl acetate / petroleum ether) gave (1*S*)-1-(4-methylphenyl)-1,2-ethanediol-1-*d*₁⁴ as white crystals (0.43 g, 67 %). ¹H NMR (500 MHz, CDCl₃) δ 7.24 (d, *J* = 8.3 Hz, 2H), 7.16 (d, *J* = 7.8 Hz, 2H), 3.71 (d, *J* = 11.2 Hz, 1H), 3.63 (d, *J* = 11.7 Hz, 1H), 2.34 (s, 3H).

Mixture of (2*R*)- and (2*S*)-2-chloro-2-(4-methylphenyl)-ethyl acetate-2-*d*₁

(1*S*)-1-(4-Methylphenyl)-1,2-ethanediol-1-*d*₁ (0.116 g, 0.71 mmol) and (1*R*)-1-(4-methylphenyl)-1,2-ethanediol-1-*d*₁ (0.252 g, 1.64 mmol) were dissolved in dry CH₂Cl₂ (10 mL) and the solution cooled to 0°C. Trimethyl orthoacetate was added (359 μ l, 2.82 mmol), followed by trimethylsilyl chloride (364 μ l, 2.87 mmol). The solution was stirred for two hours, slowly warming to room temperature. The solvent was removed by evaporation under reduced pressure to give 2-chloro-2-(4-methylphenyl)-ethyl acetate-2-

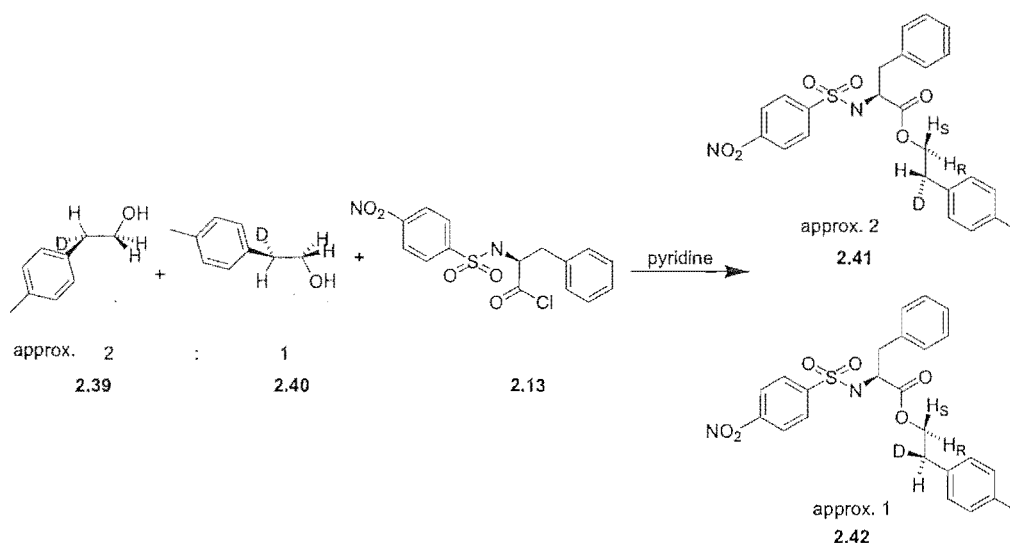
d_1 ⁵ as a colorless liquid (144 mg, 99%). ¹H NMR (500 MHz, CDCl₃) δ 7.22 (d, J = 7.8 Hz, 2H), 7.11 (d, J = 8.3 Hz, 1H), 4.43 (m, 2H), 2.28 (s, 3H), 1.99 (s, 3H).

Mixture of (2*R*)- and (2*S*)-2-(*p*-methylphenyl)ethanol-2- d_1



The mixture of (2*R*)- and (2*S*)-2-chloro-2-(4-methylphenyl)ethylacetate-2- d_1 (144 mg, 2.4 mmol) from above was dissolved in ether (10 mL) and LiAlH₄ was added (91 mg, 2.4 mmol). The solution was stirred at room temperature for two hours. Saturated NH₄Cl was added dropwise until the LiAlH₄ residues formed a paste on the bottom of the flask. The solution was dried by the addition of anhydrous MgSO₄, filtered and the solvent evaporated under reduced pressure to give a clear liquid.⁶ ¹H NMR (500 MHz, CDCl₃) δ 7.12 (m, 4H), 3.83 (d, J = 6.3 Hz, 2H), 2.81 (m, 1H), 2.33 (s, 3H), 1.65 (bs, 1H).

2-(4-Methyl)phenylethyl (*N*-4-nitrophenylsulfonyl)-(*S*)-2-amino-3-phenylpropanoate



A 2:1 mixture of (2*S*)- and (2*R*)-2-(4-methyl)phenyl-ethanol (0.1065 g, 0.782 mmol) and dry pyridine (0.076 mL, 1.17 mmol) were added to a solution of *N*-(4-nitrophenylsulfonyl)-L-phenylalanyl chloride (242 mg, 0.782 mmol) in dry CH₂Cl₂ (5 mL) under dry N₂. After three hours the solution was washed with HCl (5 mL, 1M), saturated Na₂CO₃ (5 mL), dried over anhydrous Na₂SO₄ and the solvent removed under reduced pressure. The product was purified by flash chromatography on silica gel (ethyl acetate / petroleum ether) and gave 2-(4-methyl)phenylethyl (*N*-4-nitrophenylsulfonyl)-(*S*)-2-amino-3-phenylpropanoate¹ as a white solid (322 mg, 88%). ¹H NMR (500 MHz, CDCl₃) δ 8.14 (dd, *J* = 2.4, 6.8 Hz, 2H), 7.77 (dd, *J* = 2.0, 6.8 Hz, 2H), 7.22-7.19 (m, 3H), 7.13 (d, *J* = 7.8 Hz, 2H), 7.02 (d, *J* = 8.3 Hz, 2H), 6.96 (m, 2H), 5.25 (d, *J* = 9.8 Hz, 1H), 4.25-4.22 (m, 1H), 4.12 (t, *J* = 6.8 Hz, 2H), 3.04 (dd, *J* = 5.4, 13.7 Hz, 1H), 2.93 (dd, *J* = 6.8, 13.7 Hz, 1H), 2.77 (t, *J* = 6.8 Hz, 2H), 2.33 (s, 3H).

NMR investigation of 2-(4-methyl)phenylethyl (*N*-4-nitrophenylsulfonyl)-(*S*)-2-amino-3-phenylpropanoate by the addition of Yb(hfc)₃ chiral shift reagent

Aliquots of *d*-Yb(hfc)₃ were added to a solution of 2-(4-methyl)phenylethyl (*N*-4-nitrophenylsulfonyl)-(*S*)-2-amino-3-phenylpropanoate in CDCl₃ in a 3 mL NMR tube until

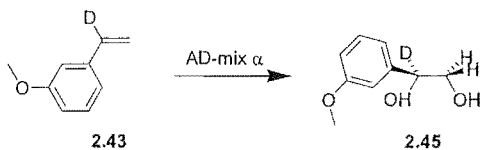
the prochiral protons β to the ester linkage were resolved in an NMR spectrum (approx. 10 eq. shift reagent added). The integral of the downfield peak was half the integral of the upfield peak. It was therefore concluded that in undeuterated material the downfield peak is H_S ; the upfield peak is H_R .

(1*R*)-1-(3-Methoxyphenyl)-1,2-ethanediol-1-*d*₁



m-Methoxystyrene- α -*d*₁ (0.3385 g, 2.507 mmol) was added to a vigorously stirring solution of AD-mix- β (3.51 g) in tertiary butyl alcohol (13 mL) and water (13 mL) at 0°C. The solution was stirred for 24 hours at 0°C. Sodium metabisulphite (3.8 g) was added and the reaction mixture was stirred for one hour and allowed to warm to room temperature. The reaction mixture was diluted with CH_2Cl_2 , the organic layer separated and the aqueous layer extracted with ethyl acetate. The solvent was removed under reduced pressure and flash chromatography on silica gel (ethyl acetate / petroleum ether) gave (1*R*)-1-(3-methoxyphenyl)-1,2-ethanediol-1-*d*₁⁴ as a colourless liquid (0.2403 g, 55%). $[\alpha]_D^{20} = -55.6$ (*c* 1.3, CHCl_3). ¹H NMR (500 MHz, CDCl_3) δ 7.27 (m, 1H), 6.93 (m, 2H), 6.83 (m, 1H), 3.80 (s, 3H), 3.73 (d, *J* = 11.2 Hz, 1H), 3.64 (d, *J* = 11.2 Hz, 1H), 2.54 (bs, 2H).

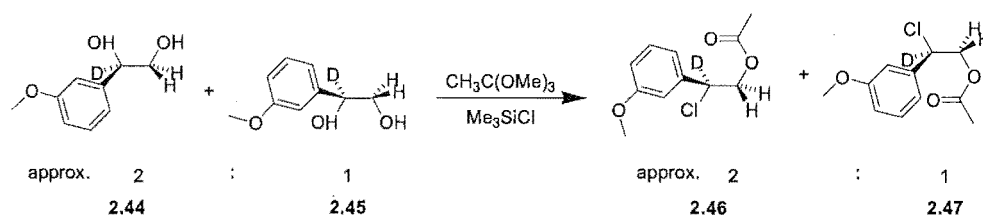
(1*S*)-1-(3-Methoxyphenyl)-1,2-ethanediol-1-*d*₁



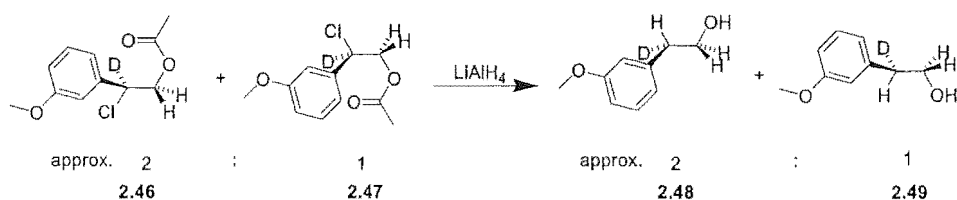
m-Methoxystyrene- α -*d*₁ (0.1824 g, 1.35 mmol) was added to a vigorously stirring solution of AD-mix- α (1.89 g) in tertiary butyl alcohol (7 mL) and water (7 mL) at 0°C. The

solution was stirred for 24 hours at 0°C. Sodium metabisulphite (2.0 g) was added and the reaction mixture was stirred for one hour and allowed to warm to room temperature. The reaction mixture was diluted with CH₂Cl₂, the organic layer separated and the aqueous layer further extracted with ethyl acetate. The solvent was removed under reduced pressure and flash chromatography on silica gel (ethyl acetate / petroleum ether) gave (1*S*)-1-(3-Methoxyphenyl)-1,2-ethanediol-1-*d*₁⁴ as a colourless liquid (149 mg, 65%). ¹H NMR (500 MHz, CDCl₃) δ 7.27 (m, 1H), 6.93 (m, 2H), 6.83 (m, 1H), 3.80 (s, 3H), 3.73 (d, *J* = 11.2 Hz, 1H), 3.64 (d, *J* = 11.2 Hz, 1H), 2.54 (bs, 2H).

Mixture of (2*R*)- and (2*S*)-2-chloro-2-(3-methoxyphenyl)-ethyl acetate-2-*d*₁



(1*S*)-1-(3-Methoxyphenyl)-1,2-ethanediol-1-*d*₁ (0.0520 g, 0.308 mmol) and (1*R*)-1-(3-methoxyphenyl)-1,2-ethanediol-1-*d*₁ (0.1063 g, 0.629 mmol) were dissolved in dry CH₂Cl₂ (5 mL) and the solution cooled to 0°C. Trimethyl orthoacetate was added (141 µl, 1.11 mmol), followed by trimethylsilyl chloride (143 µl, 1.13 mmol). The solution was stirred for two hours, slowly warming to room temperature. The solvent was removed under reduced pressure to give a yellowish oil.⁵ ¹H NMR (500 MHz, CDCl₃) δ 7.29 (t, *J* = 7.8 Hz, 1H), 6.98-6.88 (m, 3H), 4.43 (dd, *J* = 11.7, 21.0 Hz, 2H), 3.82 (s, 3H), 2.07 (s, 3H).

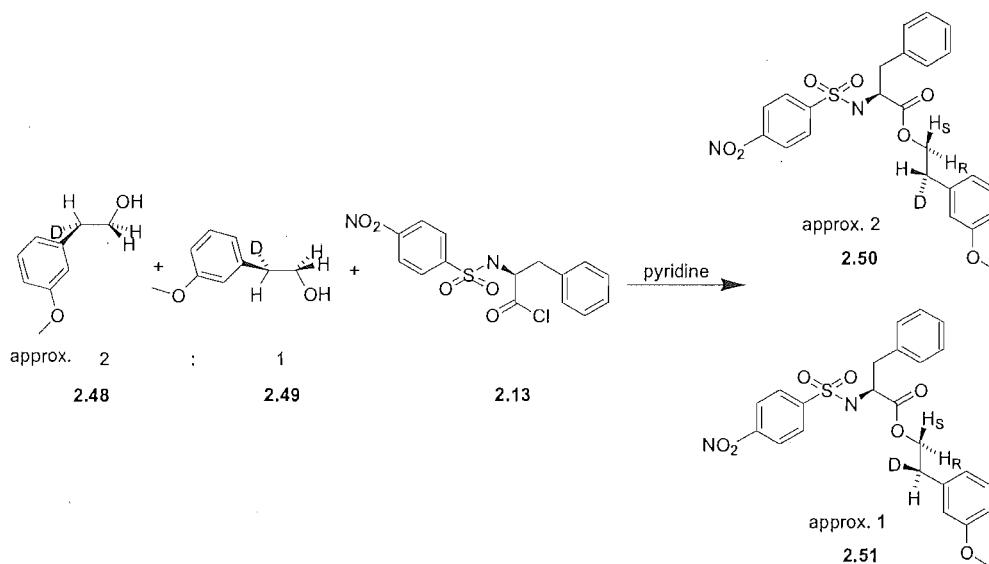
Mixture of (2*R*)- and (2*S*)-2-(3-methoxyphenyl)-ethanol-2-*d*₁


The 2:1 mixture of (2*S*)- and (2*R*)-2-chloro-2-(3-methoxyphenyl)-ethylacetate-2-*d*₁ (0.937 mmol) from above was dissolved in ether (10 mL) and LiAlH₄ was added (36 mg, 0.937 mmol). The solution was stirred at room temperature for 2.5 hours, before saturated NH₄Cl was added dropwise until the LiAlH₄ residues formed a paste on the bottom of the flask. The solution was dried (MgSO₄), filtered and the solvent evaporated under reduced pressure to give a yellowish oil⁷ (50% yield by ¹H NMR). ¹H NMR (500 MHz, CDCl₃) δ 7.31-6.78 (m, 4H), 3.92 (s, 2H), 3.80 (s, 3H), 2.83 (t, *J* = 2.0 Hz, 1H), 2.19 (bs, 1H).

**2-(3-Methoxy)phenylethyl
phenylpropanoate**

***N*-(4-nitrophenylsulfonyl)-(*S*)-2-amino-3-**

phenylpropanoate



The crude mixture of (*2R*)- and (*2S*)-2-(3-methoxyphenyl)-ethanol-2-*d*₁ (0.937 mmol) and dry pyridine (0.091 mL, 1.12 mmol) were added to a solution of *N*-(4-nitrophenylsulfonyl)-L-phenylalanyl chloride (346 mg, 0.938 mmol) in dry CH₂Cl₂ (5 mL) under N₂. After three hours the solution was washed with HCl (5 mL, 1M), saturated Na₂CO₃ (5 mL), dried over anhydrous Na₂SO₄ and the solvent removed under reduced pressure. The product was purified by flash column chromatography on silica gel (ethyl acetate / petroleum ether) to give a colourless oil (213 mg, 47% yield over 3 steps). ¹H NMR (500 MHz, CDCl₃) δ 8.16 (d, *J* = 8.8 Hz, 2H), 7.78 (d, *J* = 8.8 Hz, 2H), 7.26-7.18 (m, 4H), 6.96 (d, *J* = 6.3 Hz, 2H), 6.80 (dd, *J* = 2.0, 8.3 Hz, 1H), 6.72-6.68 (m, 2H), 5.14 (d, *J* = 9.3 Hz, 1H), 4.24-4.20 (m, 1H), 4.14 (dd, *J* = 2.9, 6.8 Hz, 2H), 3.80 (s, 3H), 3.04 (dd, *J* = 5.4, 13.7 Hz, 1H), 2.94 (dd, *J* = 6.8, 14.2 Hz, 1H), 2.78 (bs, 1H). HRMS (ES) 486.1447 (MH⁺). C₂₄H₂₄N₂O₇S²H requires 486.1445.

NMR study of 2-(3-methoxy)phenylethyl (*N*-4-nitrophenylsulfonyl)-(*S*)-2-amino-3-phenylpropanoate with the addition of Yb(hfc)₃ chiral shift reagent

Aliquots of *d*-Yb(hfc)₃ were added to a solution of 2-(3-methoxy)phenylethyl (*N*-4-nitrophenylsulfonyl)-(*S*)-2-amino-3-phenylpropanoate in CDCl₃ in a 3 mL nmr tube until the prochiral protons β to the ester linkage were resolved in an NMR spectrum. The integral of the downfield peak was half the integral of the upfield peak. It was therefore concluded that in undeuterated material the downfield peak is H_S; the upfield peak is H_R.

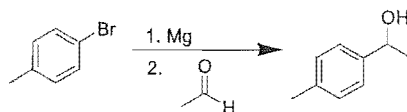
¹H NMR integral of 2-(3-methoxy)phenylethyl (*N*-4-nitrophenylsulfonyl)-(*S*)-2-amino-3-phenylpropanoate with varying d1

¹H NMR of 2-(3-methoxy)phenylethyl (*N*-4-nitrophenylsulfonyl)-(*S*)-2-amino-3-phenylpropanoate with sufficient Yb(hfc)₃ chiral shift reagent to separate the prochiral protons β- to the ester oxygen. The integral of the two signals was measured from NMR spectra taken with a varying the delay time between pulses.

d1 (s)	Downfield : Upfield proton integral
0.5	1.0051 : 1
0.5	1.0184 : 1
1	1.0469 : 1
5	1.0223 : 1
10	1.0074 : 1

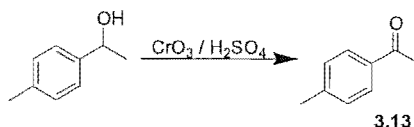
10.2 EXPERIMENTAL WORK DESCRIBED IN CHAPTER THREE

1-(4-Methylphenyl)ethanol

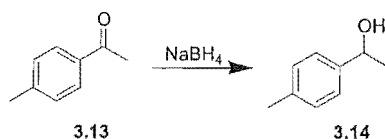


4-Bromotoluene (7.35 g, 42.9 mmol) in dry ether (40 mL) was added to magnesium turnings (1g, 41.5 mmol) in dry ether (30 mL), when no reaction occurred 1,2 dibromoethane (2 drops) was added. After stirring for one hour with no evidence of reaction, a small crystal of iodine was added. The reaction proceeded slowly. After stirring for one hour at room temperature, acetaldehyde (2.41 mL, 43.1 mmol) in dry ether (30 mL) was added dropwise. The solution was stirred for sixteen hour at room temperature. Water was added dropwise (30 mL) and the solution was filtered. The organic layer was separated and dried (Na₂SO₄). The product was purified by flash column chromatography on silica gel (pentane / ethyl acetate) to give 1-(*p*-methylphenyl)ethanol⁸ as a colourless liquid (4.11 g, 71%). ¹H NMR (300 MHz, CDCl₃) δ 7.22 (d, *J* = 8.3 Hz, 2H), 7.12 (d, *J* = 7.8 Hz, 2H), 4.79 (dd, *J* = 6.3, 12.7 Hz), 2.32 (s, 3H), 2.24 (s, 1H), 1.44 (s, 3H).

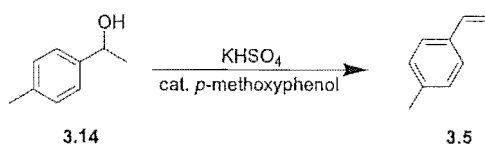
p-Methylacetophenone



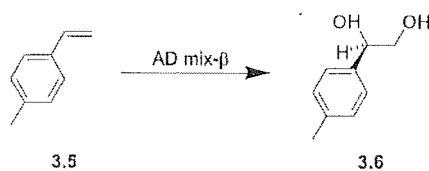
A solution of Jones' reagent (H₂SO₄ (0.9 mL) and CrO₃ (1.06 g) in H₂O (3 mL)) was added dropwise to 1-(*p*-methylphenyl)ethanol (1.0 g) in acetone (3 mL). When the colour of the solution changed from green to brown, sufficient sodium meta bisulphite was added to return the solution to a green colour. The aqueous solution was extracted with ether. The organic layer was dried (Na₂SO₄) and solvent was removed by rotary evaporation to give *p*-methylacetophenone⁹ as a yellowish liquid (0.65 g, 65%). ¹H NMR (CDCl₃) δ 7.86 (d, *J* = 7.8 Hz, 2H), 7.26 (d, *J* = 7.8 Hz, 2H), 2.57 (s, 3H), 2.41 (s, 3H).

1-(4-Methylphenyl)ethanol

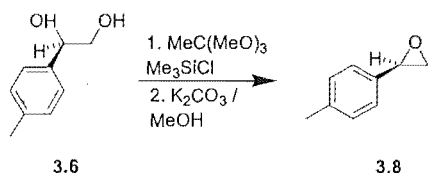
p-Methylacetophenone (9.55 g, 71 mmol) was added dropwise to a stirring solution of sodium borohydride (2.00 g, 52.9 mmol) in H₂O (15 mL) and ethanol (15 mL) at 0°C. After 2 hours stirring at room temperature the solution was saturated with NaCl, the organic layer was separated and the aqueous layer extracted with Et₂O. After drying over MgSO₄ the solvent was removed under reduced pressure to give 1-(*p*-methylphenyl)ethanol⁸ as a clear liquid (9.39 g, 97%). ¹H NMR (300 MHz, CDCl₃) δ 7.23 (d, *J* = 7.8 Hz, 2H), 7.13 (d, *J* = 7.8 Hz, 2H), 4.80 (m, 1H), 2.32 (s, 3H), 1.43 (s, 3H).

***p*-Methylstyrene**

1-(*p*-Methylphenyl)ethanol (8.85 g, 64.5 mmol), potassium bisulphate (1.13 g) and *p*-methoxyphenol (5 mg) were placed in a distillation apparatus. *p*-Methylstyrene and water were distilled into another flask. The organic layer was separated and dried (MgSO₄), giving *p*-methylstyrene¹⁰ as a colourless liquid (3.43 g, 45 %). ¹H NMR (300 MHz, CDCl₃) δ 7.30 - 7.08 (m, 4H), 6.62 (m, 1H), 5.68 (dd, *J* = 1.0, 17.6 Hz, 1H) 5.17 (dd, *J* = 1.0, 10.7 Hz, 1H), 2.32 (s, 3H).

(1*R*)-1-(4-Methylphenyl)-1,2-ethanediol

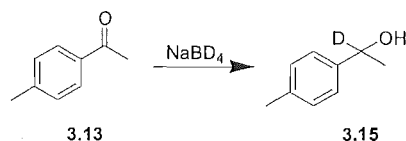
p-Methylstyrene (0.588 g, 5.0 mmol) was added to a vigorously stirring solution of AD mix- β (7.0 g) in tertiary butyl alcohol (25 mL) and water (25 mL) at 0°C. The solution was stirred for 48 hours at 0°C. The reaction mixture was diluted with CH₂Cl₂, the organic layer separated and the aqueous layer extracted with ethyl acetate. The solvent was removed under reduced pressure and flash chromatography on silica gel (ethyl acetate / petroleum ether) gave **3.6**⁴ as white crystals (0.58 g, 76 %). mp 72 – 74 °C. ¹H NMR (300 MHz, CDCl₃) δ 7.24 (d, J = 8.3 Hz, 2H), 7.16 (d, J = 7.8 Hz, 2H), 3.71 (d, J = 11.2 Hz, 1H), 3.63 (d, J = 11.7 Hz, 1H), 2.34 (s, 3H).

(α *R*)-*p*-Methylstyrene oxide

Trimethylsilyl chloride (0.289 mL, 2.29 mmol) was added to a stirring solution of trimethylorthoacetate (0.291 mL, 2.29 mmol) and (1*R*)-*p*-Methylphenylethan-1,2-diol (0.35 g, 2.29 mmol) in CH₂Cl₂ (10 mL) at 0°C. After 30 minutes, the solvent was removed under reduced pressure and the residue dissolved in methanol (10 mL). K₂CO₃ (0.6 g) was added, the mixture was stirred for 2 hours and the solvent was removed under reduced pressure. The residue was partitioned between H₂O and CH₂Cl₂. The organic layer was separated and dried over NaSO₄, filtered and the solvent evaporated under reduced pressure to give a clear liquid. The product was purified by distillation using a Kugelrohr apparatus. (0.256 g, 83%). $[\alpha]_{\text{D}}^{20}$ +26 (c 1.1, PhH) [lit.¹¹ $[\alpha]_{\text{D}}^{20}$ +27 (c 0.98, PhH, ee

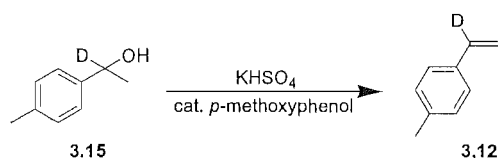
95%]. ^1H NMR (300 MHz, CDCl_3) δ 7.24-7.16 (m, 2H), 3.83 (dd, $J = 2.9, 3.9$ Hz, 1H), 3.14-3.11 (m, 1H), 2.81-2.78 (m, 1H), 2.34 (s, 3H).

1-(4-Methylphenyl)ethanol-1- d_1

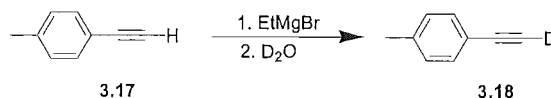


p-Methylacetophenone (5.003 g, 37 mmol) was added dropwise to a stirring solution of sodium borodeuteride (0.773 g, 18.5 mmol) in H_2O (10 mL) and ethanol (10 mL) at 0°C . After 2 hours stirring at room temperature the solution was saturated with NaCl, the organic layer was separated and the aqueous layer extracted with Et_2O . After drying over MgSO_4 the solvent was removed under reduced pressure to give 1-(*p*-methylphenyl)ethanol-1- d_1 ⁸ as a clear liquid, greater than 95% deuterated at C1 by ^1H NMR (4.85 g, 95%) ^1H NMR (300 MHz, CDCl_3) δ 7.26 (d, $J = 7.8$ Hz, 2H), 7.16 (d, $J = 7.8$ Hz, 2H), 2.34 (s, 3H), 1.83 (s, 1H), 1.47 (s, 3H).

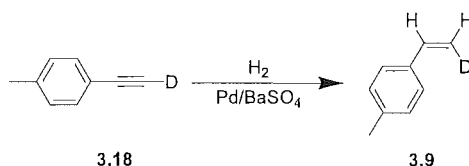
p-Methylstyrene- α - d_1



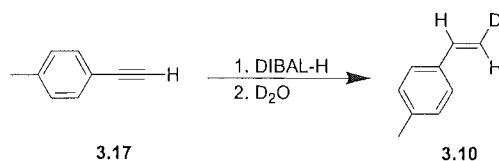
1-(*p*-Methylphenyl)ethanol-1- d_1 (1 g), potassium bisulphate (1.5 g) and *p*-methoxyphenyl (5 mg) were placed in a distillation apparatus. *p*-Methylstyrene- α - d_1 and water were distilled into another flask. The organic layer was separated and dried (MgSO_4), giving *p*-methylstyrene- α - d_1 ¹⁰ as a colorless liquid (0.52 g, 60 %). ^1H NMR (300 MHz, CDCl_3) δ 7.30 (d, $J = 8.3$ Hz, 2H), 7.14 (d, $J = 8.3$ Hz, 2H), 5.68 - 5.69 (m, 1H), 5.17 (d, $J = 1.5$ Hz, 1H), 2.33 (s, 3H). ^2H NMR (46 MHz, CHCl_3) δ 6.73 (s).

***p*-Methylphenylacetylene-1-*d*₁**

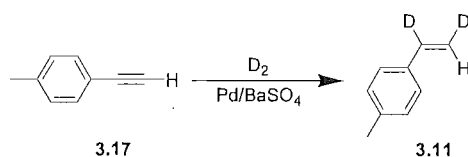
4-Methylphenylacetylene (6.13 g, 52.7 mmol) dissolved in dry Et₂O (15 mL) was added dropwise to a solution of excess EtMgBr in dry Et₂O (20 mL) and refluxed for 16 hours. D₂O (15 mL) was added and the reaction mixture refluxed for a further hour. After cooling to room temperature, the reaction mixture was filtered. The filtered solids were washed with pentane, and the filtrates were then combined and evaporated under reduced pressure to give a clear yellowish liquid¹² (6.2 g, 100%). The product showed greater than 99% deuterium incorporation by ¹H NMR. ¹H NMR (300 MHz, CDCl₃) δ 7.38 (d, *J* = 8 Hz, 2H), 7.12 (d, *J* = 8 Hz, 2H), 2.35 (s, 3H). ²H NMR (46 MHz, CHCl₃) δ 3.06 (s).

***p*-Methylstyrene-*cis*-β-*d*₁**

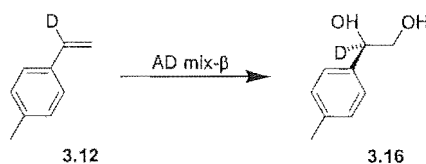
p-Methylphenylacetylene-1-*d*₁ (2.41 g, 20.6 mmol) was added to pentane (50 mL), quinoline (1 mL), and 10% Pd/BaSO₄ and stirred vigorously under an H₂ atmosphere for 2 hours, the solids were removed by filtration, and the filtrate washed successively with 1M HCl, 10% aq. Na₂CO₃, and H₂O, and dried with MgSO₄. The solvent was removed under reduced pressure to give a clear yellowish liquid¹⁰ (2.25 g, 92%). ¹H NMR (300 MHz, CDCl₃) δ 7.30 (d, *J* = 8.3, 2H), 7.13 (d, *J* = 8.3, 2H), 6.69 (d, *J* = 11 Hz, 1H), 5.16 (d, *J* = 11.2, 1H), 2.33 (s, 3H). ²H NMR (46 MHz, CHCl₃) δ 5.78 (s).

***p*-Methylstyrene-*trans*- β - d_1** 

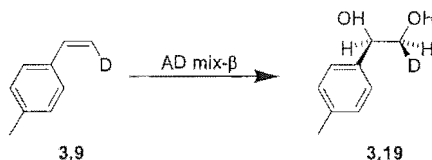
4-Methylphenylethyne (3.5 g, 30 mmol) was added slowly to a 1 M solution of diisobutylaluminium hydride in CH₂Cl₂ (50 mL) under N₂ at 0°C and stirred at room temperature for 24 hours. D₂O (1.8 mL) was slowly added and the mixture was stirred for an hour before extracting into pentane four times, filtering, and drying with MgSO₄. The solvent was removed under reduced pressure to give a clear yellow liquid¹⁰ (1.50 g, 42%). ¹H NMR (300 MHz, CDCl₃) δ 7.30 (d, J = 8 Hz, 2H), 7.12 (d, J = 8 Hz, 2H), 6.67 (d, J = 17 Hz, 1H), 5.67 (d, J = 17 Hz, 1H). ²H NMR (46 MHz, CHCl₃) δ 5.2 (s).

***p*-Methylstyrene-*cis*- α,β - d_2** 

4-Methylphenylethyne (1.72 g, 15 mmol) was added to pentane (50 mL), quinoline (1 mL) and 10% Pd/BaSO₄ (0.5 g) and stirred vigorously under a D₂ atmosphere. After 2 hours, the solids were removed by filtration, and the filtrate washed successively with 1 M HCl, 10% aq. Na₂CO₃, and H₂O, dried over MgSO₄, and the solvent removed under reduced pressure to give **3.11**¹⁰ as a clear yellowish liquid (1.21 g, 68%). ¹H NMR (300 MHz, CDCl₃) δ 7.29 (d, J = 8 Hz, 2H), 7.11 (d, J = 8 Hz, 2H), 5.66 (s, 1H), 2.32 (s, 3H). ²H NMR (46 MHz, CHCl₃) δ 7.46 (d, J = 24 Hz, 1D), 5.96 (d, J = 24 Hz, 1D).

(1*R*)-1-(4-Methylphenyl)-1,2-ethanediol-1-*d*₁

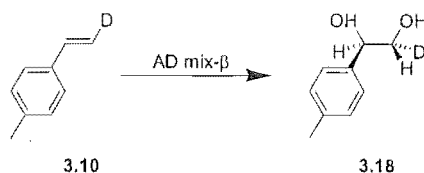
p-Methylstyrene- α -*d*₁ (1.0 g, 8.4 mmol) was added to a vigorously stirring solution of AD mix- β (11.76 g) in tertiary butyl alcohol (42 mL) and water (42 mL) at 0°C. The solution was stirred for 48 hours at 0°C. The reaction mixture was diluted with CH₂Cl₂, the organic layer separated and the aqueous layer extracted with ethyl acetate. The solvent was removed under reduced pressure and flash chromatography on silica gel (ethyl acetate / petroleum ether) gave **3.16**⁴ as white crystals (0.92 g, 71 %). mp 72 - 74 °C. $[\alpha]_D^{20}$ -70 (*c* 2.9, CHCl₃). ¹H NMR (500 MHz, CDCl₃) δ 7.24 (d, *J* = 8.3 Hz, 2H), 7.16 (d, *J* = 7.8 Hz, 2H), 3.71 (d, *J* = 11.2 Hz, 1H), 3.63 (d, *J* = 11.7 Hz, 1H), 2.34 (s, 3H). ¹³C NMR (75 MHz, CDCl₃) δ 137.4, 129.0, 126.0, 74.0 (t, *J*_{CD} = 21.3 Hz), 67.8, 21.0.

(1*R*),(2*S*)-1-(4-Methylphenyl)-1,2-ethanediol-2-*d*₁

p-Methylstyrene-*cis*- β -*d*₁ (0.770 g, 5.71 mmol) was added to a vigorously stirring solution of AD mix- β (7.98 g) in tertiary butyl alcohol (29 mL) and water (29 mL) at 0°C. The solution was stirred for 48 hours at 0°C. The reaction mixture was diluted with CH₂Cl₂, the organic layer separated and the aqueous layer extracted with ethyl acetate. The solvent was removed under reduced pressure and flash chromatography on silica gel (ethyl acetate / petroleum ether) gave **3.19**⁴ as white crystals (0.695 g, 79 %). mp 76 - 77 °C. $[\alpha]_D^{20}$ -68.5 (*c* 1.5, CHCl₃). ¹H NMR (300 MHz, CDCl₃) δ 7.20 (d, *J* = 8 Hz, 2H), 7.13 (d, *J* = 8 Hz, 2H), 4.72 (d, *J* = 3 Hz, 1H), 3.64 (d, *J* = 3 Hz, 1H), 3.23 (bs, 2H), 2.32 (s, 3H). ²H NMR

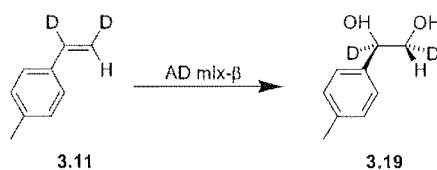
(CHCl₃) δ 3.59 (s). ¹³C NMR (75 MHz, CDCl₃) δ 137.3, 129.0, 126.0, 67.5 (t, J_{CD} = 21.3 Hz). MS: (M^+) 153.

(1*R*),(2*R*)-1-(4-Methylphenyl)-1,2-ethanediol-2-*d*₁



p-Methylstyrene-*trans*- β -*d*₁ (0.40 g, 3.36 mmol) was added to a vigorously stirring solution of AD mix- β (4.7 g) in tertiary butyl alcohol (17 mL) and water (17 mL) at 0°C. The solution was stirred for 48 hours at 0°C. The reaction mixture was diluted with CH₂Cl₂, the organic layer separated and the aqueous layer extracted with ethyl acetate. The solvent was removed under reduced pressure and flash chromatography on silica gel (ethyl acetate / petroleum ether) gave **3.18**⁴ as white crystals (0.4579 g, 89 % yield). mp 76 - 78 °C. $[\alpha]_D^{20}$ -70 (*c* 1.2, CHCl₃). ¹H NMR (300 MHz, CDCl₃) δ 7.25 (d, J = 8 Hz, 2H), 7.17 (d, J = 8 Hz, 2H), 4.79 (d, J = 8 Hz, 1H), 3.64 (d, J = 8 Hz, 1H), 2.35 (s, 3H), 2.20 (bs, 2H). ¹³C NMR (75 MHz, CDCl₃) δ 137.4, 129.1, 126.0, 74.5, 67.6 (t, J_{CD} = 21.3 Hz), 21.0. ²H NMR (CHCl₃) δ 3.73 (s).

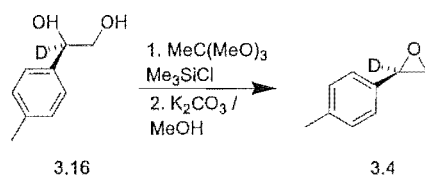
(1*R*),(2*R*)-1-(4-Methylphenyl)-1,2-ethanediol-1,2-*d*₂



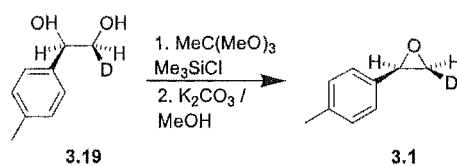
p-Methylstyrene-*cis*- α,β -*d*₂ (0.53 g, 4.42 mmol) was added to a vigorously stirring solution of AD mix- β (6.2 g) in tertiary butyl alcohol (10 mL) and water (10 mL) at 0°C. The solution was stirred for 48 hours at 0°C. The reaction mixture was diluted with CH₂Cl₂, the

organic layer separated and the aqueous layer extracted with ethyl acetate. The solvent was removed under reduced pressure and flash chromatography on silica gel (ethyl acetate / petroleum ether) gave **3.19**⁴ as white crystals (0.630 g, 92 %). mp 75 - 76 °C. $[\alpha]_D^{20}$ -64 (*c* 4.2, CHCl₃). ¹H NMR (300 MHz, CDCl₃) δ 7.25 (d, *J* = 8 Hz, 2H), 7.17 (d, *J* = 8 Hz, 2H), 3.63 (s, 1H), 2.64 (bs, 2H), 2.28 (s, 3H). ¹³C NMR (75 MHz, CDCl₃) δ 137.4, 129.0, 126.0, 74.0 (t, *J*_{CD} = 21.8 Hz), 67.5 (t, *J*_{CD} = 21.8 Hz), 21.0. ²H NMR (CHCl₃) δ 4.80 (s, 1D), 3.72 (s, 1D). MS: (*M*⁺) 154.

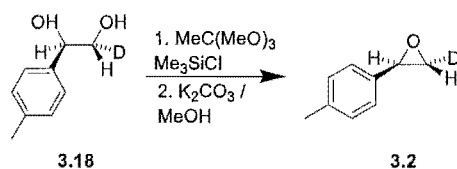
(*αR*)-*p*-Methylstyrene oxide-*α-d*₁



Trimethylsilyl chloride (0.41 mL, 3.2 mmol) was added to a stirring solution of trimethylorthoacetate (0.40 mL, 3.1 mmol) and (*1R*)-*p*-methylphenylethan-1,2-diol-1-*d*₁ (0.47 g, 3.0 mmol) in CH₂Cl₂ (20 mL) at 0°C. After 30 minutes, the solvent was removed under reduced pressure and the residue dissolved in methanol (20 mL). K₂CO₃ (1 g, 8 mmol) was added and the mixture was stirred for 2 hours before the solvent was removed under reduced pressure. The residue was partitioned between H₂O and CH₂Cl₂. The organic layer was separated and dried over NaSO₄, and the solvent evaporated under reduced pressure to give a clear liquid.¹¹ (0.38 g, 92%). $[\alpha]_D^{20}$ -2.8 (*c* 1.5, CHCl₃). $[\alpha]_D^{20}$ +26 (*c* 1.3, PhH) [lit.¹³ $[\alpha]_D^{20}$ +27 (*c* 0.98, PhH, ee 95%) for undeuterated epoxide]. IR (KBr) 1517.9, 1350.1, 923.8, 815.8, 758.0. ¹H NMR (500 MHz, CDCl₃) δ 7.19-7.14 (m, 4H), 3.12 (d, *J* = 5.4 Hz, 1H), 2.79 (d, *J* = 5.4 Hz, 1H), 2.34 (s, 3H).

(αR),(βS)-*p*-Methylstyrene oxide- β - d_1 

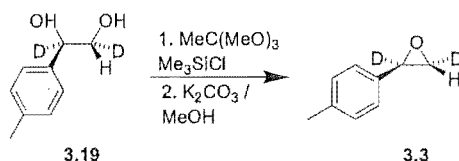
Trimethylsilyl chloride (0.41 mL, 3.2 mmol) was added to a stirring solution of trimethylorthoacetate (0.40 mL, 3.1 mmol) and (1*R*,2*S*)-*p*-methylphenylethane-1,2- d_1 (0.47 g, 3.0 mmol) in CH_2Cl_2 (20 mL) at 0°C. After 30 minutes, the solvent was removed under reduced pressure and the residue dissolved in methanol (20 mL). K_2CO_3 (1 g, 8 mmol) was added and the mixture was stirred for 2 hours before the solvent was removed under reduced pressure. The residue was partitioned between H_2O and CH_2Cl_2 . The organic layer was separated and dried over NaSO_4 , and the solvent evaporated under reduced pressure to give a clear liquid.¹¹ (0.38 g, 92%). ^1H NMR (300 MHz, CDCl_3) δ 7.16 (m, 4H), 3.82 (d, $J = 4$ Hz, 1H), 3.11 (d, $J = 4$ Hz), 2.34 (s, 3H). ^2H NMR (46 MHz, CHCl_3) δ 2.80 (s). MS: (M^+) 135.

(αR),(βR)-*p*-Methylstyrene oxide- β - d_1 

Trimethylsilyl chloride (0.41 mL, 3.2 mmol) was added to a stirring solution of trimethylorthoacetate (0.40 mL, 3.1 mmol) and (1*R*,2*R*)-*p*-methylphenylethane-1,2- d_1 (0.47 g, 3.0 mmol) in CH_2Cl_2 (20 mL) at 0°C. After 30 minutes, the solvent was removed under reduced pressure and the residue dissolved in methanol (20 mL). K_2CO_3 (1 g, 8 mmol) was added and the mixture was stirred for 2 hours before the solvent was removed under reduced pressure. The residue was partitioned between H_2O and CH_2Cl_2 . The organic layer was separated and dried over NaSO_4 , and the solvent evaporated under

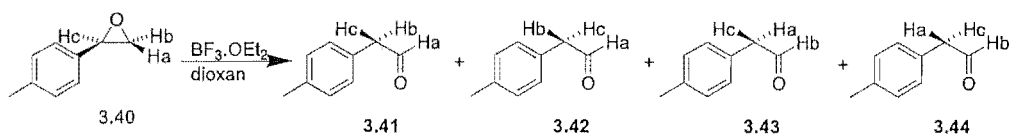
reduced pressure to give a clear liquid.¹¹ (0.38 g, 92%). ¹H NMR (300 MHz, CDCl₃) δ 7.15 (m, 4H), 3.81 (d, *J* = 3 Hz, 1H), 2.77 (d, *J* = 3 Hz, 1H), 2.34 (s, 3H). ²H NMR (46 MHz, CHCl₃) δ 3.13 (s).

(αR),(βR)-*p*-Methylstyrene oxide- α,β -*d*₂



Trimethylsilyl chloride (0.41 mL, 3.2 mmol) was added to a stirring solution of trimethylorthoacetate (0.40 mL, 3.1 mmol) and (1*R*,2*R*)-*p*-Methylphenylethan-1,2-diol-2-*d*₁ (0.47 g, 3.0 mmol) in CH₂Cl₂ (20 mL) at 0°C. After 30 minutes, the solvent was removed under reduced pressure and the residue dissolved in methanol (20 mL). K₂CO₃ (1 g, 8 mmol) was added and the mixture was stirred for 2 hours before the solvent was removed under reduced pressure. The residue was partitioned between H₂O and CH₂Cl₂. The organic layer was separated and dried over NaSO₄, and the solvent evaporated under reduced pressure to give a clear liquid.¹¹ (0.38 g, 92%). ¹H NMR (300 MHz, CDCl₃) δ 7.26 (d, *J* = 8 Hz, 2H), 7.15 (d, *J* = 8 Hz, 2H), 3.42 (s, 1H), 2.34 (s, 3H). ²H NMR (46 MHz, CHCl₃) δ 4.86 (s, 1D), 3.48 (s, 1D).

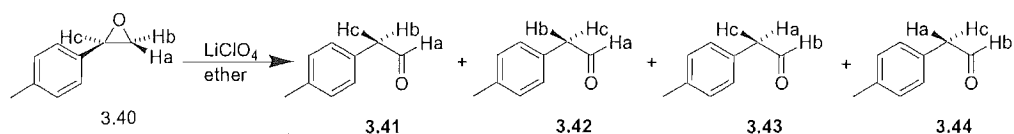
Rearrangement of epoxides with BF₃·OEt₂



BF₃·OEt₂ (5 μL) was added to a stirring solution of epoxide (15 μL) in 1,4 dioxan (5 mL) under an atmosphere of Ar. The reaction mixture was stirred at room temperature for 15 minutes, a saturated solution of K₂CO₃ (2 mL) was added and the solution was stirred for

30 minutes. Anhydrous K_2CO_3 was added and the solution was filtered and the solvent removed under reduced pressure.

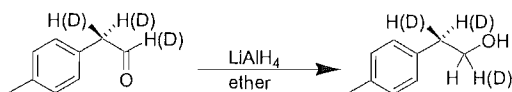
Rearrangement of epoxides with $LiClO_4$



$LiClO_4$ (1.55 g) was added to dry ether (3 mL, 5 M solution) at room temperature. Epoxide (15 μ L) was added and the solution left to stir for 18 hours at room temperature. The solution was washed with water, dried ($MgSO_4$) and the solvent was removed under reduced pressure. Formation of aldehyde was confirmed by 1H NMR.

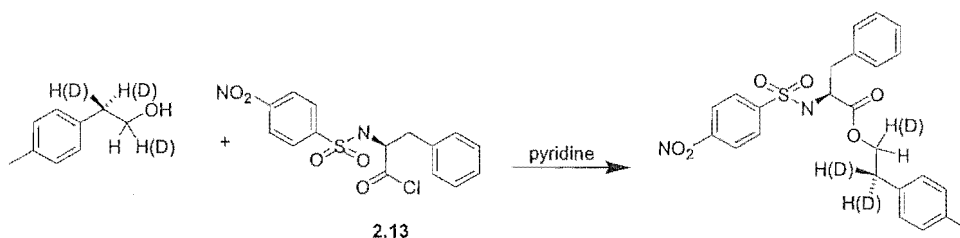
Analysis of rearrangement products

Reduction with $LiAlH_4$



The crude reaction product from the $BF_3 \cdot OEt_2$ catalysed rearrangement was dissolved in dry ether and $LiAlH_4$ (20 mg) was added. The suspension was stirred under Ar for 3 hours and sat. NH_4Cl was added dropwise until the $LiAlH_4$ residues formed a paste. The solution was dried ($MgSO_4$), filtered and the solvent was removed under reduced pressure.

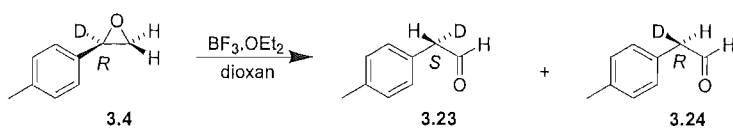
Esterification



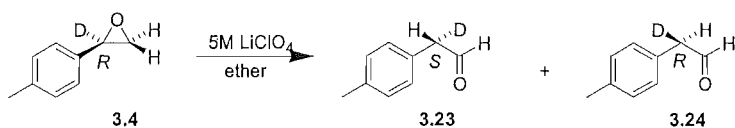
The crude reaction mixture from the LiAlH_4 reduction was dissolved in dry CH_2Cl_2 (5 mL), *N*-(4-nitrophenylsulfonyl)-L-phenylalanyl chloride (310 mg, 0.84 mmol) and dry pyridine (0.103 mL, 1.33 mmol) were added and the solution stirred at room temperature for 3 hours. The solution was washed with HCl (5 mL, 1M), saturated Na_2CO_3 (5 mL), dried over anhydrous Na_2SO_4 and the solvent removed on a rotary evaporator. The product was purified by flash column chromatography on silica gel (ethylacetate : petroleum ether).

NMR analysis with $\text{Yb}(\text{hfc})_3$ chiral shift reagent

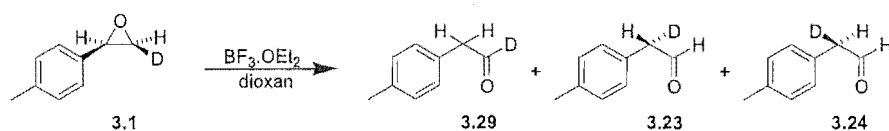
$\text{Yb}(\text{hfc})_3$ was added portionwise to an NMR sample of 2-Phenylethyl (*N*-4-nitrophenylsulfonyl)-(*S*)-2-amino-3-phenylpropanoate in CDCl_3 until the signals for the two protons β - to the ester oxygen become resolved. The relative integral of the two peaks was obtained using a curve-fitting algorithm in the mathematical modeling software package MATLAB.

BF₃.OEt₂ catalysed rearrangement of (α R)-*p*-Methylstyrene oxide- α -d₁

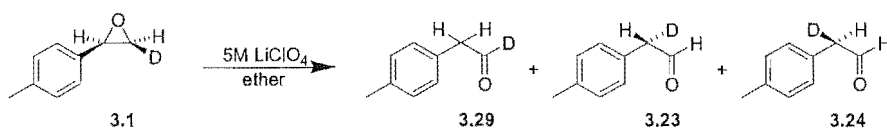
Reaction	H migration with retention of configuration 3.23	H migration with inversion of configuration 3.24
1	47%	53%
2	44%	56%
3	49%	51%

LiClO₄ catalysed rearrangement of (α R)-*p*-Methylstyrene oxide- α -d₁

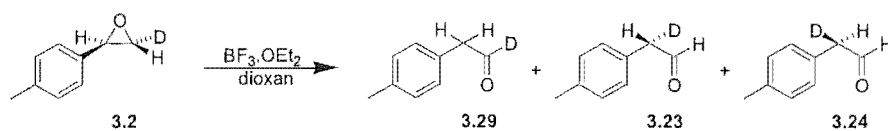
Reaction	H migration with retention of configuration 3.23	H migration with inversion of configuration 3.24
1	12%	88%
2	16%	84%

BF₃.OEt₂ catalysed rearrangement of (α*R*),(β*S*)-*p*-methylstyrene oxide-β-*d*₁


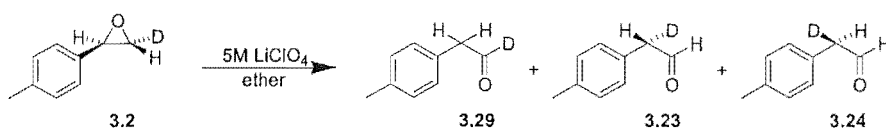
Reaction	H migration (3.29)	D migration with inversion of configuration (3.23)	D migration with retention of configuration (3.24)
1	69%	25%	6%
2	69%	17%	14%
3	70%	15%	15%
4	71%	22%	7%

LiClO₄ catalysed rearrangement of (α*R*),(β*S*)-*p*-methylstyrene oxide-β-*d*₁


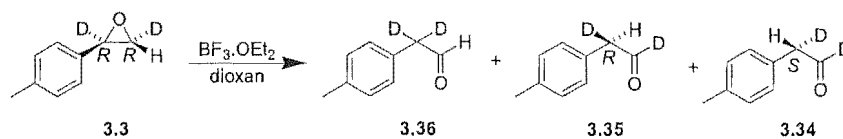
Reaction	H migration (3.29)	D migration with inversion of configuration (3.23)	D migration with retention of configuration (3.24)
1	85%	10%	4%
2	81%	18%	2%
3	89%	9%	2%

BF₃·OEt₂ catalysed rearrangement of (α*R*),(β*R*)-*p*-methylstyrene oxide-β-*d*₁


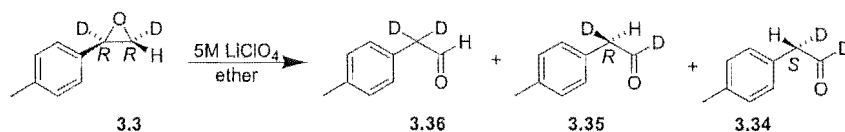
Reaction	H migration (3.29)	D migration with inversion of configuration (3.23)	D migration with retention of configuration (3.24)
1	69%	13%	18%
2	73%	6%	21%
3	73%	6%	21%
4	73%	6%	21%

LiClO₄ catalysed rearrangement of (α*R*),(β*R*)-*p*-methylstyrene oxide-β-*d*₁


Reaction	H migration (3.29)	D migration with inversion of configuration (3.23)	D migration with retention of configuration (3.24)
1	61%	23%	16%
2	60%	19%	21%
3	59%	23%	18%

BF₃.OEt₂ catalysed rearrangement of (α*R*),(β*R*)-*p*-methylstyrene oxide-α,β-*d*₂


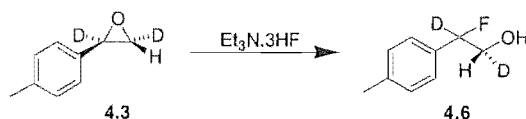
Reaction	D migration (3.36)	H migration with inversion of configuration (3.35)	H migration with retention of configuration (3.34)
1	32%	61%	7%
2	35%	53%	12%
3	28%	61%	11%

LiClO₄ catalysed rearrangement of (α*R*),(β*R*)-*p*-methylstyrene oxide-α,β-*d*₂


Reaction	D migration (3.36)	H migration with inversion of configuration (3.35)	H migration with retention of configuration (3.34)
1	39%	57%	4%
2	39%	61%	0%
3	49%	47%	4%

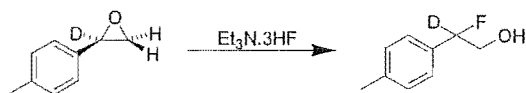
10.3 EXPERIMENTAL WORK DESCRIBED IN CHAPTER FOUR

2-Fluoro-2-*p*-tolyl-ethanol-1,2-*d*₂

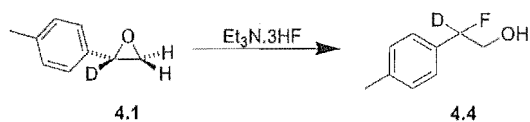


(αR),(βS)-*p*-Methylstyrene oxide- α,β -*d*₂ (19 mg, 0.14 mmol) was added to a stirring solution of Et₃N·3HF (150 mg, 0.93 mmol) in CH₂Cl₂ (3 mL) under an argon atmosphere. After 5 hours stirring at room temperature, the solution was washed with HCl (0.5 M) and H₂O. The organic extracts were dried with MgSO₄, filtered and the solvent was removed under reduced pressure to give 2-fluoro-2-*p*-tolyl-ethanol-1,2-*d*₂¹⁴ as a clear liquid (16 mg, 75%). ¹H NMR (500 MHz, CDCl₃) δ 7.29-7.17 (m, 4H), 3.87 (d, J = 18.0 Hz, 0.46 H), 3.76 (d, J = 31.3 Hz, 0.54 H), 2.36 (s, 3H). ²H NMR (46 MHz, CHCl₃) δ 5.53 (d, J_{DF} = 7.6 Hz, 1D), 3.89 (d, J_{DF} = 2.3 Hz, 1D).

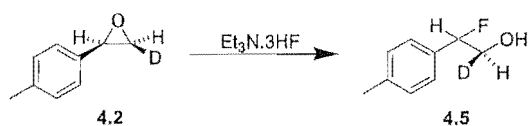
2-Fluoro-2-*p*-tolyl-ethanol-2-*d*₁ from (αR)-*p*-Methylstyrene oxide- α -*d*₁



(αR)-*p*-Methylstyrene oxide- α -*d*₁ (60 mg, 0.44 mmol) was added to a stirring solution of Et₃N·3HF (470 mg, 0.93 mmol) in CH₂Cl₂ (5 mL) under an argon atmosphere. After 5 hours stirring at room temperature, the solution was washed with HCl (0.5 M) and H₂O. The organic extracts were dried with MgSO₄, filtered and the solvent was removed under reduced pressure. The product was purified by column chromatography on alumina (ethyl acetate/petroleum ether 30 : 70) to give 2-fluoro-2-*p*-tolyl-ethanol-2-*d*₁¹⁴ as a clear liquid (42 mg, 61%). ¹H NMR (500 MHz, CDCl₃) δ 7.26-7.11 (m, 4H), 3.93 (dd, J = 12.7, 18.6 Hz, 1H), 3.80 (dd, J = 12.7, 29.8 Hz, 1H), 2.36 (s, 3H).

2-Fluoro-2-*p*-tolyl-ethanol-2-*d*₁ from (α *S*)-*p*-Methylstyrene oxide- α -*d*₁

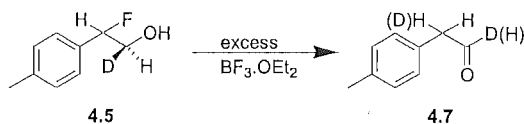
(α *S*)-*p*-Methylstyrene oxide- α -*d*₁ (134 mg, 0.99 mmol) was added to a stirring solution of Et₃N·3HF (1.011 g, 6.36 mmol) in CH₂Cl₂ (8 mL) under an argon atmosphere. After 5.5 hours stirring at room temperature, the solution was washed with HCl (0.5 M) and H₂O. The organic extracts were dried with MgSO₄, filtered and the solvent was removed under reduced pressure to give 2-fluoro-2-*p*-tolyl-ethanol-2-*d*₁¹⁴ as a clear liquid. The product was purified by flash column chromatography on silica gel (ethyl acetate/petroleum ether 40:60) (110 mg, 72%). [α]₂₀^D = -1.14 (*c* 1.1, CHCl₃) ¹H NMR (500 MHz, CDCl₃) δ 7.25-7.16 (m, 4H), 3.91 (dd, *J* = 12.7, 18.6 Hz, 1H), 3.78 (dd, *J* = 12.7, 30.3 Hz, 1H), 2.35 (s, 3H), 2.20 (bs, 1H). ²H NMR (46 MHz, CHCl₃) δ 5.53 (d, *J*_{DF} = 7.6 Hz).

(1*S*)-2-Fluoro-2-*p*-tolyl-ethanol-1-*d*₁

(α *R*),(β *S*)-*p*-Methylstyrene oxide- β -*d*₁ (37 mg, 0.27 mmol) was added to a stirring solution of Et₃N·3HF (309 mg, 1.92 mmol) in CH₂Cl₂ (5 mL) under an argon atmosphere. After 6 hours stirring at room temperature, the solution was washed with HCl (0.5 M) and H₂O. The organic extracts were dried with MgSO₄, filtered and the solvent was removed under reduced pressure to give (1*S*)-2-fluoro-2-*p*-tolyl-ethanol-1-*d*₁¹⁴ as a clear liquid. The product was purified by flash column chromatography on silica gel (ethyl acetate/petroleum ether 40:60) (31 mg, 75%). ¹H NMR (500 MHz, CDCl₃) δ 7.18-7.08 (m, 4H), 5.45 (dd, *J* = 7.8 Hz, 48.6 Hz, 1H), 3.83 (dd, *J* = 7.3, 14.9 Hz, 0.46 H), 3.71 (d, *J* =

31.7 Hz, 0.54 H), 2.29 (s, 3H), 2.02 (bs, 1H). ^2H NMR (46 MHz, CHCl_3) δ 3.81 (d, $J = 7.6$ Hz).

***p*-Methylphenylacetaldehyde from (1*S*)-2-fluoro-2-*p*-tolyl-ethanol-1-*d*₁**



BF₃·OEt₂ (66 μL , 0.51948 mmol) was added to a solution of (1*S*)-2-fluoro-2-*p*-tolyl-ethanol-1-*d*₁ in dioxan under an argon atmosphere. The reaction mixture was stirred at room temperature for 4 hours. Saturated K₂CO₃ was added and the solution stirred for 10 minutes. The solution was dried with anhydrous K₂CO₃, filtered and the solvent removed under reduced pressure to give 4.7 as a colourless liquid (45% yield by ^1H NMR).

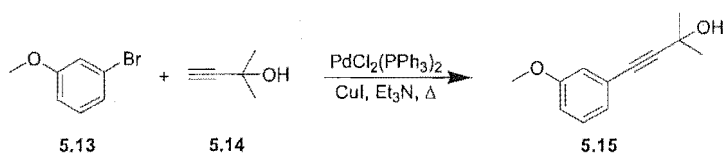
10.4 EXPERIMENTAL WORK DESCRIBED IN CHAPTER FIVE

$\text{PdCl}_2(\text{PPh}_3)_3$ ¹⁵



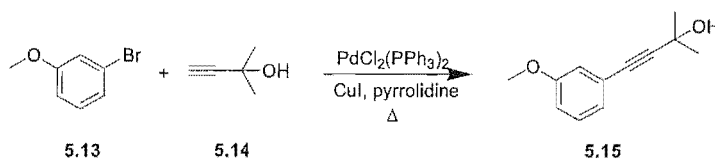
PdCl_2 (0.55 g) was added to a solution of PPh_3 (1.7123 g) and LiCl (0.2636 g) in dry methanol. The reaction mixture was heated at reflux for 3 hours. The yellow product was filtered and washed repeatedly with ether (2.0150 g, 93%).

2-Methyl-4-(3-methoxyphenyl)-3-butyne-2-ol in Et_3N at reflux



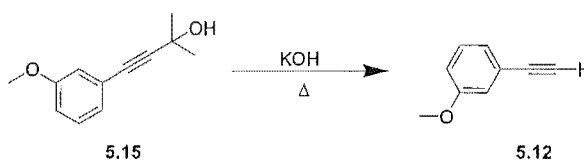
CuI (0.025 g, 0.119 mmol) and $\text{Pd}(\text{Ph}_3\text{P})_2$ (0.055 g, 0.071 mmol) were added to a solution of *m*-bromoanisole (0.4448 g, 2.38 mmol) and 2-methyl-3-butyn-2-ol (0.242 mL, 2.50 mmol) in Et_3N under a positive flow of Ar. The reaction was heated at reflux for 6.5 hours, cooled to room temperature and poured into saturated NH_4Cl (60 mL). The aqueous solution was extracted with ether and the organic extract washed with brine, dried (MgSO_4) and filtered. The solvent was removed under reduced pressure. The product was purified by flash column chromatography on silica gel (ethyl acetate / petroleum ether 1:2) to give 2-methyl-4-(3-methoxyphenyl)-3-butyne-2-ol as a colourless liquid (81.5 mg, 18%).

2-Methyl-4-(3-methoxyphenyl)-3-butyn-2-ol in pyrrolidine at reflux



CuI (0.052 g, 0.273 mmol) and $\text{PdCl}_2(\text{Ph}_3\text{P})_2$ (0.1052 g, 0.150 mmol) were added to a solution of *m*-bromoanisole (1.0313 g, 5.51 mmol) and 2-methyl-3-butyn-2-ol (0.641 mL, 6.61 mmol) in pyrrolidine (20 mL) under a positive flow of Ar. The reaction was heated at reflux for 4 hours, cooled to room temperature and poured into saturated NH_4Cl (120 mL). The aqueous solution was extracted with ether and the organic extract washed with brine, dried (MgSO_4) and filtered. The solvent was removed under reduced pressure. The product was purified by flash column chromatography on silica gel (ethyl acetate / petroleum ether 1:2) to give **5.15**¹⁶ as a colourless liquid (938 mg, 89%). ^1H NMR (500 MHz, CDCl_3) δ 7.20 (dd, $J = 7.8, 8.3$ Hz, 1H), 7.01 (m, 1H), 6.94 (m, 1H), 6.86 (m, 1H), 3.79 (s, 3H), 2.27 (s, 1H), 1.62 (s, 6H).

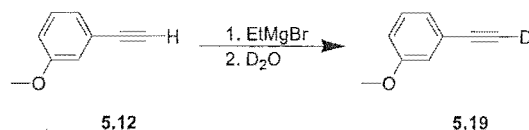
m-Methoxyphenylacetylene



KOH pellets were ground in a mortar and pestle under a lab atmosphere and allowed to absorb water from the atmosphere. The reaction did not work when the KOH was ground under an inert atmosphere in order to exclude water from the reaction. KOH (60 mg, 0.663 mmol) was added to a solution of 2-methyl-4-(3-methoxyphenyl)-3-butyn-2-ol (0.1682 g, 0.884 mmol) in toluene. The reaction mixture was heated at reflux for 3.5 hours, washed with water, dried (MgSO_4) and the solvent removed under reduced pressure. The product was purified by bulb to bulb distillation in a Kuguruhr apparatus to give **5.12**¹⁷ as a

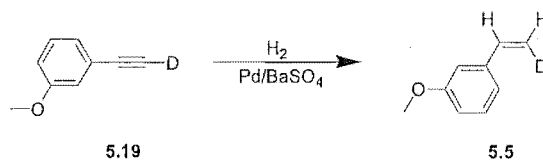
colourless liquid (91 mg, 78%). ^1H NMR (500 MHz, CDCl_3) δ 7.22 (dd, $J = 7.8, 7.8$ Hz, 1H), 7.08 (m, 1H), 7.02 (m, 1H), 6.89 (m, 1H), 3.79 (s, 3H), 3.06 (s, 1H).

m-Methoxyphenylacetylene-1- d_1



Bromoethane (5.79 mL, 77.4 mmol) in dry Et_2O (20 mL) was added dropwise to a rapidly stirring suspension of magnesium turnings (2.09g, 86.1 mmol) in dry Et_2O (20 mL) under N_2 . The reaction mixture was stirred at room temperature for two hours. 3-methoxyphenylethyne (0.9757 g, 8.4 mmol) dissolved in dry Et_2O (15 mL) was added dropwise and the reaction mixture was stirred at room temperature for 16 hours. The solution was cooled to 0°C and D_2O (2 mL) was added slowly and the reaction mixture stirred at room temperature for two hours. The solution was diluted with Et_2O and filtered. The filtered solids were washed with Et_2O , and the filtrates were combined and evaporated under reduced pressure to give a clear yellowish liquid¹⁷ (0.871 g, 89%). The product showed greater than 99% deuterium incorporation by ^1H NMR. ^1H NMR (500 MHz, CDCl_3) δ 7.23 (dd, $J = 7.8, 7.8$ Hz, 1H), 7.09 (m, 1H), 7.02 (m, 1H), 6.90 (m, 1H), 3.80 (s, 3H). ^2H NMR (CHCl_3) δ 3.08 (s).

m-Methoxystyrene-*cis*- β - d_1



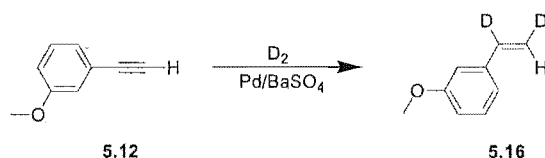
m-Methoxyphenylacetylene-1- d_1 (0.3785 g, 2.85 mmol) was added to quinoline (0.2 mL) and 10% Pd/BaSO_4 (35 mg) in pentane (10 mL), and stirred vigorously under an H_2 atmosphere for 30 minutes. The solids were removed by filtration, and the filtrate washed

with 1M HCl and H₂O, and dried with MgSO₄. The solvent was removed under reduced pressure to give a clear yellowish liquid¹⁸ (0.3685 g, 96%). ¹H NMR (500 MHz, CDCl₃) δ 7.25 (m, 1H), 7.00 (d, *J* = 7.3, 1H), 6.95 (m, 1H), 6.81 (m, 1H), 6.68 (m, 1H), 5.24 (d, *J* = 10.7 Hz), 3.82 (s, 3H). ¹³C NMR (75 MHz, CDCl₃) δ 159.7, 139.0, 136.6, 129.4, 118.8, 113.8 (t, *J*_{CD} = 23.3 Hz), 113.4, 111.5, 55.1. ²H NMR (46 MHz, CHCl₃) δ 5.81 (d, *J* = 2.3 Hz).

The reaction was carried out several times in order to determine the extent of reaction compared to the amount of dideuterated : trideuterated alkene:

Compound	alkyne : alkene : alkane (37 : 41 + 42 : 43)	dideuterated : trideuterated alkene (41 : 42)
2.155.1	0 : 44 : 56	14 : 86
2.157.1	0 : 45 : 55	27 : 73
2.161.1	0 : 85 : 15	70 : 30
2.158.1	0 : 97 : 3	75 : 25
2.159.1	50 : 50 : 0	95 : 5

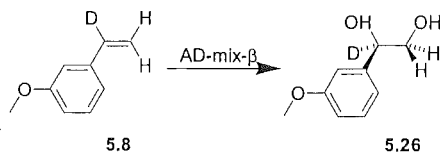
***m*-Methoxystyrene-*cis*-α,β-*d*₂**



m-Methoxyphenylacetylene-1-*d*₁ (0.1487 g, 1.13 mmol) was added to quinoline (0.1 mL) and 10% Pd/BaSO₄ (25 mg) in pentane (4 mL), and stirred vigorously under an D₂ atmosphere for 30 minutes. The solids were removed by filtration, and the filtrate washed with 1M HCl and H₂O, and dried with MgSO₄. The solvent was removed under reduced pressure to give a clear yellowish liquid¹⁸ (0.1473 g, 96%). ¹H NMR (500 MHz, CDCl₃) δ

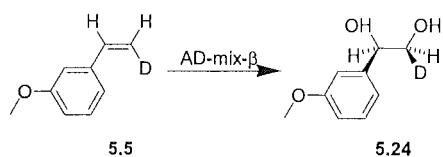
7.26-7.22 (m, 1H), 7.20-7.00 (m, 1H), 6.95 (m, 1H), 6.82-6.80 (m, 1H), 5.72 (s, 1H), 3.82 (s, 3H). ^2H NMR (46 MHz, CHCl_3) δ 6.76 (s, 1H), 5.31 (s, 1H).

(1*R*)-1-(3-Methoxyphenyl)-1,2-ethanediol-1-*d*₁



m-Methoxystyrene- α -*d*₁ (0.3385 g, 2.507 mmol) was added to a vigorously stirring solution of AD mix- β (3.51 g) in tertiary butyl alcohol (13 mL) and water (13 mL) at 0°C. The solution was stirred for 24 hours at 0°C. The reaction mixture was diluted with CH_2Cl_2 , the organic layer separated and the aqueous layer extracted with ethyl acetate. The solvent was removed under reduced pressure and flash chromatography on silica gel (ethyl acetate / petroleum ether 70 : 30) gave **5.26**⁴ as a colourless liquid (0.2403 g, 55%). $[\alpha]_{\text{D}}^{20} = -55.6$ (*c* 1.3, CHCl_3). ^1H NMR (500 MHz, CDCl_3) δ 7.28-7.25 (m, 1H), 6.93-6.92 (m, 2H), 6.85-6.82 (m, 1H), 3.80 (s, 3H), 3.73 (d, $J = 11.2$ Hz, 1H), 3.64 (d, $J = 11.2$ Hz, 1H), 2.54 (bs, 2H).

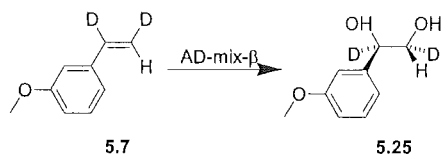
(1*R*),(2*S*)-1-(3-Methoxyphenyl)-1,2-ethanediol-2-*d*₁



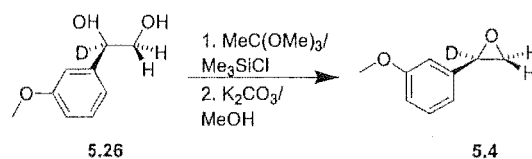
m-Methoxystyrene-*cis*- β -*d*₁ (0.240 g, 1.78 mmol) was added to a vigorously stirring solution of AD mix- β (2.65 g) in tertiary butyl alcohol (9.5 mL) and water (9.5 mL) at 0°C. The solution was stirred for 24 hours at 0°C. Sodium metabisulphite (2.8 g) was added and the solution was stirred at room temperature for 2 hours. The reaction mixture was diluted with CH_2Cl_2 , the organic layer separated and the aqueous layer extracted with ethyl

acetate. The solvent was removed under reduced pressure and flash chromatography on silica gel (ethyl acetate / petroleum ether 70 : 30) gave **5.24**⁴ as a colourless liquid (0.279 g, 92%). $[\alpha]_{20}^D = -49.2$ (c 1.1, CHCl_3) ^1H NMR (300 MHz, CDCl_3) δ 7.25-7.20 (m, 1H), 6.90-6.86 (m, 2H), 6.82-6.78 (m 1H), 4.72 (d, $J = 2.9$ Hz, 1H), 3.76 (s, 3H), 3.66 (d, $J = 2.9$ Hz, 1H), 3.40 (bs, 2H). ^2H NMR (46 MHz, CHCl_3) δ 3.56 (s).

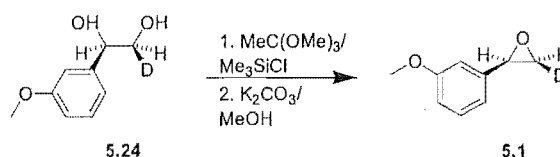
(1R),(2R)-1-(3-Methoxyphenyl)-1,2-ethanediol-1,2- d_2



m-Methoxystyrene-*cis*- β - d_1 (0.1473 g, 1.083 mmol) was added to a vigorously stirring solution of AD mix- β (1.52 g) in tertiary butyl alcohol (5.5 mL) and water (5.5 mL) at 0°C. The solution was stirred for 24 hours at 0°C. Sodium metabisulphite (1.5 g) was added and the solution was stirred at room temperature for 2 hours. The reaction mixture was diluted with CH_2Cl_2 , the organic layer separated and the aqueous layer extracted with ethyl acetate. The solvent was removed under reduced pressure and flash chromatography on silica gel (ethyl acetate / petroleum ether 70 : 30) gave **5.25**⁴ as a colourless liquid (0.139 g, 82%). ^1H NMR (500 MHz, CDCl_3) δ 7.30-7.26 (m, 1H), 6.94-6.93 (m, 2H), 6.86-6.84 (m, 1H), 3.82 (s, 1H), 3.65 (s, 1H), 1.98 (bs, 2H). ^2H NMR (46 MHz, CHCl_3) δ 4.76 (s, 1H), 3.73 (s, 1H).

(αR)-*m*-Methoxystyrene oxide- α - d_1 

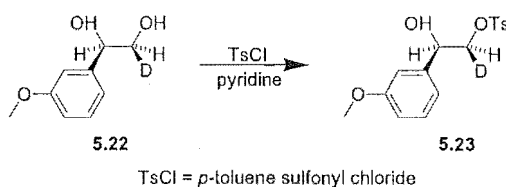
Trimethylsilyl chloride (0.179 mL, 1.19 mmol) was added to a stirring solution of trimethylorthoacetate (0.182 mL, 1.43 mmol) and (1*R*)-*p*-methoxyphenylethane-1,2-diol-1- d_1 (0.201 g, 1.43 mmol) in CH_2Cl_2 (20 mL) at 0°C. After 3.5 hours, the solvent was removed under reduced pressure and the residue dissolved in methanol (3 mL). K_2CO_3 (405 mg) was added and the mixture was stirred for 2 hours before the solvent was removed under reduced pressure. The residue was partitioned between H_2O and CH_2Cl_2 . The organic layer was separated and dried over $NaSO_4$, and the solvent evaporated under reduced pressure. The product was purified by flash column chromatography on silica gel (ether / pentane 10 : 90) to give a clear liquid (0.201 g, 93%). $[\alpha]_D^{20} = -13.9$ (c 1.3, $CHCl_3$) [lit.¹⁹ $[\alpha]_D^{24} +11.5$ (c 2.94, $CHCl_3$, ee >99%) for undeuterated *S* epoxide]. 1H NMR ($CDCl_3$, 500 MHz) δ 7.26 (t, $J = 7.8$ Hz, 1H), 6.89 (d, $J = 7.8$ Hz, 1H), 6.85 (m, 1H), 6.81 (m, 1H), 3.81 (s, 3H), 3.13 (d, $J = 5.9$ Hz, 1H), 2.78 (d, $J = 5.4$ Hz, 1H).

(αR),(βS)-*m*-Methoxystyrene oxide- β - d_1 

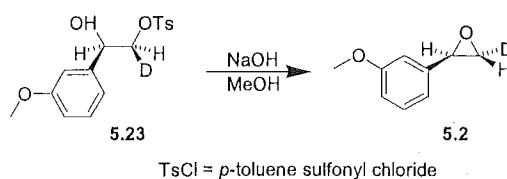
Trimethylsilyl chloride (0.179 mL, 1.19 mmol) was added to a stirring solution of trimethylorthoacetate (0.182 mL, 1.43 mmol) and (1*R*), (2*S*)-*m*-methoxyphenylethane-1,2-diol-2- d_1 (0.201 g, 1.43 mmol) in CH_2Cl_2 (20 mL) at 0°C. After 3.5 hours, the solvent was removed under reduced pressure and the residue dissolved in methanol (3 mL). K_2CO_3 (405 mg) was added and the mixture was stirred for 2 hours before the solvent was

removed under reduced pressure. The residue was partitioned between H₂O and CH₂Cl₂. The organic layer was separated and dried over NaSO₄, and the solvent evaporated under reduced pressure. The product was purified by flash column chromatography on silica gel (ether / pentane 10 : 90) to give a clear liquid¹⁹ (0.201 g, 93%). ¹H NMR (CDCl₃, 500 MHz) δ 7.26 (dd, J = 8.3, 7.3 Hz, 1H), 6.89 (d, J = 7.8 Hz, 1H), 6.85 (m, 1H), 6.81 (m, 1H), 3.84 (d, J = 3.9 Hz, 1H), 3.81 (s, 3H), 3.12 (d, J = 3.9 Hz, 1H). ²H NMR (CDCl₃, 46 MHz) δ 2.77 (s).

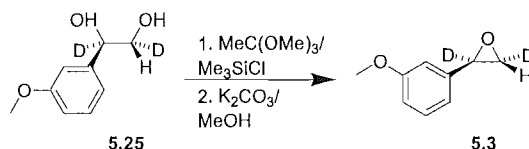
(1*R*),(2*S*)-1-(3-Methoxyphenyl)-2-(4-methylbenzenesulfonate)-1,2-ethandiol-2-*d*₁



p-Toluenesulfonyl chloride was purified as per Vogel prior to use. (1*R*),(2*S*)-*m*-Methoxyphenylethandiol-2-*d*₁ (205 mg, 1.21 mmol) was dissolved in pyridine (1.7 mL) under Ar. *p*-Toluenesulfonyl chloride (276.6 mg, 1.2 equivalents, 1.46 mmol) was added and the solution was stirred at room temperature for 18 hours. The reaction mixture was poured into 1N HCl and extracted with ether. The organic layer was washed with 1N HCl and water, dried (MgSO₄) and the solvent removed under reduced pressure. ¹H NMR (500 MHz, CDCl₃) δ 7.76 (d, J = 8.3, 2H), 7.33 (d, J = 8.3, 2H), 7.25 (d, J = 7.3 Hz, 2H), 6.87 (m, 2H), 4.95 (s, 1H), 4.13 (s, 1H), 3.79 (s, 3H), 2.55 (bs, 1H), 2.45 (s, 3H).

(αR),(βR)-*m*-Methoxystyrene oxide- β - d_1 

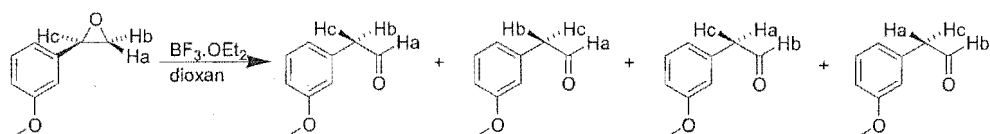
Crude tosylate was dissolved in dry methanol (8 mL) and cooled to -10°C in an ice/salt bath. NaOH (80 mg) dissolved in methanol (3 mL) was added dropwise and the solution stirred at -10°C for 3 1/2 hours. The reaction mixture was diluted with ether, and washed with H_2O . The organic layer was separated, dried (MgSO_4) and the solvent removed under reduced pressure. The epoxide was purified by flash chromatography on silica gel (10% ether / pentane). $[\alpha]_{\text{D}}^{20} = -14.2$ (c 1.2, CHCl_3) [lit.¹⁹ $[\alpha]_{\text{D}}^{24} +11.5$ (c 2.94, CHCl_3 , ee >99%) for undeuterated *S* epoxide]. ^1H NMR (CDCl_3 , 500 MHz) δ 7.26 (dd, $J = 7.8$, 7.8 Hz, 1H), 6.89 (d, $J = 7.3$ Hz, 1H), 6.85 (m, 1H), 6.81 (m, 1H), 3.84 (d, $J = 2.9$ Hz, 1H), 3.81 (s, 3H), 2.77 (d, $J = 2.4$ Hz, 1H).

(αR),(βR)-*m*-Methoxystyrene oxide- α,β - d_2 

Trimethylsilyl chloride (0.179 mL, 1.19 mmol) was added to a stirring solution of trimethylorthoacetate (0.182 mL, 1.43 mmol) and (1*R*)-*m*-methoxyphenylethan-1,2-diol-1- d_1 (0.201 g, 1.43 mmol) in CH_2Cl_2 (20 mL) at 0°C . After 3.5 hours, the solvent was removed under reduced pressure and the residue dissolved in methanol (3 mL). K_2CO_3 (405 mg) was added and the mixture was stirred for 2 hours before the solvent was removed under reduced pressure. The residue was partitioned between H_2O and CH_2Cl_2 . The organic layer was separated and dried over NaSO_4 , and the solvent evaporated under reduced pressure. The product was purified by flash column chromatography on silica gel

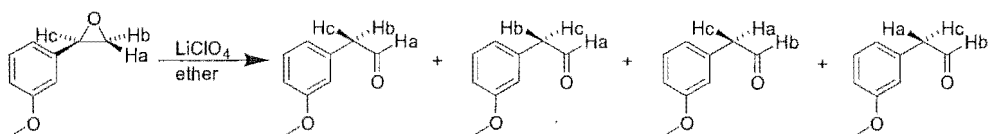
(ether / pentane 10 : 90) to give a clear liquid¹⁹ (0.201 g, 93%). ¹H NMR (CDCl₃, 500 MHz) δ 7.26 (dd, J = 7.8, 8.3 Hz, 1H), 6.89 (m, 1H), 6.85 (m, 1H), 6.81 (m, 1H), 3.80 (s, 3H), 3.77 (s, 1H). ²H NMR (CDCl₃, 46 MHz) δ 3.82 (s, 1H), 3.12 (s, 1H).

Rearrangement of epoxides with BF₃.OEt₂



BF₃.OEt₂ (5 μ L,) was added to a stirring solution of epoxide (0.12 μ L,) in 1,4 dioxan (5 mL) under an atmosphere of Ar. The reaction mixture was stirred at room temperature for 15 minutes, a saturated solution of K₂CO₃ (2 mL) was added and the solution was stirred for 30 minutes. Anhydrous K₂CO₃ was added and the solution was filtered and the solvent removed under reduced pressure.

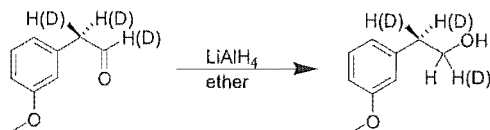
Rearrangement of epoxides with LiClO₄



LiClO₄ (1.55 g) was added to dry ether (3 mL, 5 M solution) at room temperature. Epoxide (15 μ L) was added and the solution left to stir for 18 hours at room temperature. The solution was washed with water, dried (MgSO₄) and the solvent was removed under reduced pressure. Formation of aldehyde was confirmed by ¹H NMR.

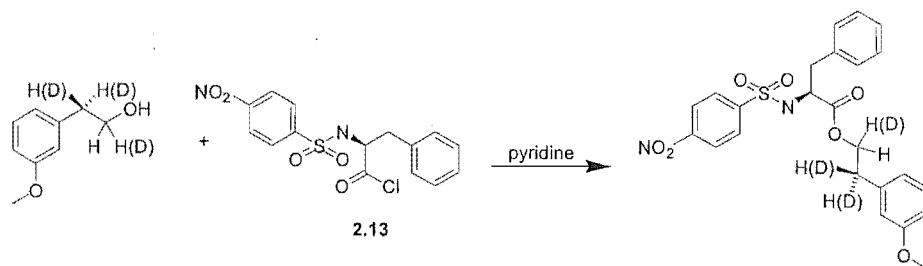
Analysis of rearrangement products

Reduction with LiAlH_4



The crude reaction product from the $\text{BF}_3 \cdot \text{OEt}_2$ catalysed rearrangement was dissolved in dry ether and LiAlH_4 (20 mg) was added. The suspension was stirred under Ar for 3 hours and sat. NH_4Cl was added dropwise until the LiAlH_4 residues formed a paste. The solution was dried (MgSO_4), filtered and the solvent was removed under reduced pressure.

Esterification



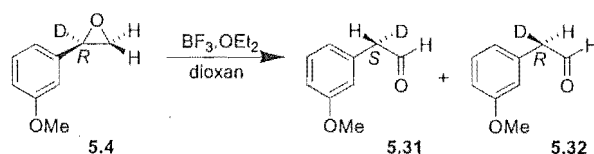
The crude reaction mixture from the LiAlH_4 reduction was dissolved in dry CH_2Cl_2 (5 mL), *N*-(4-nitrophenylsulfonyl)-L-phenylalanyl chloride (310 mg, 0.84 mmol) and dry pyridine (0.103 mL, 1.33 mmol) were added and the solution stirred at room temperature for 3 hours. The solution was washed with HCl (5 mL, 1M), saturated Na_2CO_3 (5 mL), dried over anhydrous Na_2SO_4 and the solvent removed on a rotary evaporator. The product was purified by flash column chromatography on silica gel (ethylacetate : petroleum ether).

NMR analysis with $\text{Yb}(\text{hfc})_3$ chiral shift reagent

$\text{Yb}(\text{hfc})_3$ was added portionwise to an NMR sample of 2-phenylethyl (*N*-(4-nitrophenylsulfonyl)-(*S*)-2-amino-3-phenylpropanoate in CDCl_3 until the signals for the two protons β - to the ester oxygen become resolved. The relative integral of the two peaks

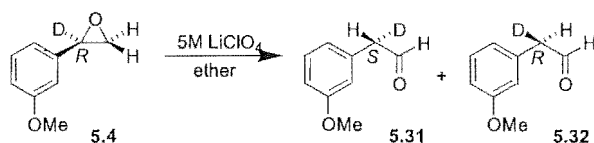
was obtained using a curve-fitting algorithm in the mathematical modeling software package MATLAB.

Rearrangement of (αR)-*m*-methoxystyrene oxide- α - d_1 with $\text{BF}_3 \cdot \text{OEt}_2$



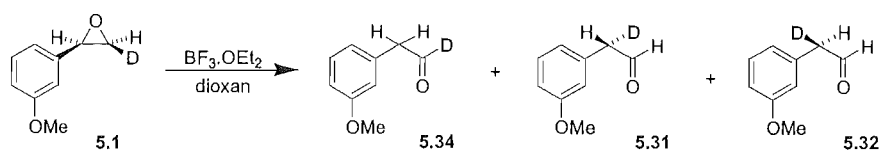
Reaction	H migration with retention of configuration (5.31)	H migration with inversion of configuration (5.32)
1	50%	50%
2	48%	52%
3	50%	50%

Rearrangement of (αR)-*m*-methoxystyrene oxide- α - d_1 with LiClO_4



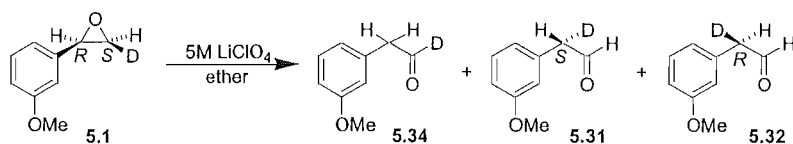
Reaction	H migration with retention of configuration (5.31)	H migration with inversion of configuration (5.32)
1	50%	50%
2	48%	52%
3	53%	47%

Rearrangement of (αR),(βS)-*m*-methoxystyrene oxide- β - d_1 with $\text{BF}_3 \cdot \text{OEt}_2$



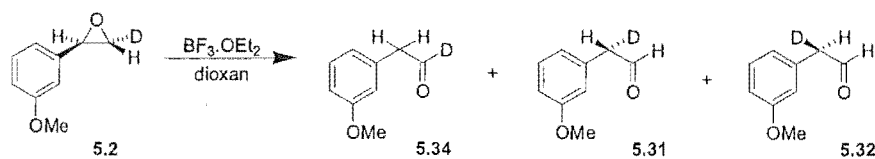
Reaction	H migration (5.34)	D migration with inversion of configuration (5.31)	D migration with retention of configuration (5.32)
1	71%	20%	9%
2	70%	24%	6%
3	70%	17%	13%

Rearrangement of (αR),(βS)-*m*-methoxystyrene oxide- β - d_1 with LiClO_4



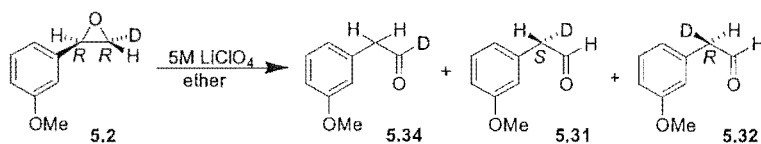
Reaction	H migration (5.34)	D migration with inversion of configuration (5.31)	D migration with retention of configuration (5.32)
1	73%	26%	1%
2	72%	28%	0%

Rearrangement of (αR),(βR)-*m*-methoxystyrene oxide- β - d_1 with $\text{BF}_3 \cdot \text{OEt}_2$



Reaction	H migration (5.34)	D migration with inversion of configuration (5.31)	D migration with retention of configuration (5.32)
1	71%	20%	9%
2	70%	24%	6%
3	70%	17%	13%

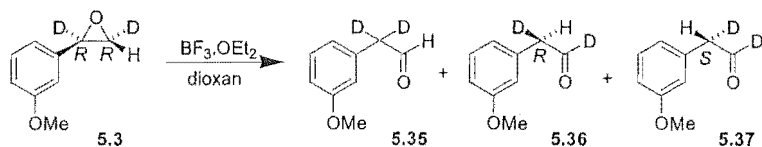
Rearrangement of (αR),(βR)-*m*-methoxystyrene oxide- β - d_1 with LiClO_4



Reaction	H migration (5.34)	D migration with inversion of configuration (5.31)	D migration with retention of configuration (5.32)
1	70%	5%	25%
2	67%	3%	28%
3	69%	3%	27%

Rearrangement of ($\alpha R, \beta R$)-*m*-methoxystyrene oxide- α, β - d_2 with $\text{BF}_3 \cdot \text{OEt}_2$

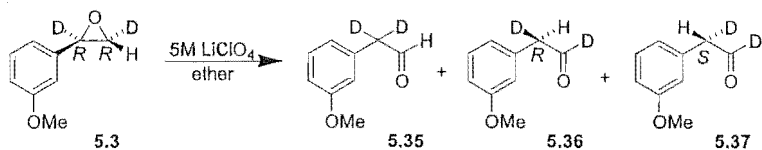
(Not adjusted for isomers).



Reaction	D migration (5.35)	H migration with inversion of configuration (5.36)	H migration with retention of configuration (5.37)
1	36%	41%	23%
2	38%	39%	23%
3	35%	42%	23%

Rearrangement of ($\alpha R, \beta R$)-*m*-methoxystyrene oxide- α, β - d_2 with LiClO_4

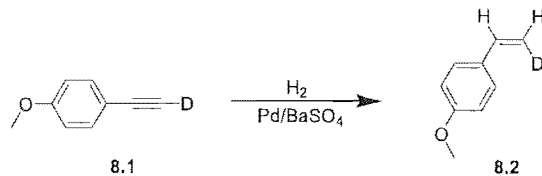
(Not adjusted for isomers).



Reaction	D migration (5.35)	H migration with inversion of configuration (5.36)	H migration with retention of configuration (5.37)
1	34%	53%	13%
2	32%	58%	10%
3	35%	53%	12%

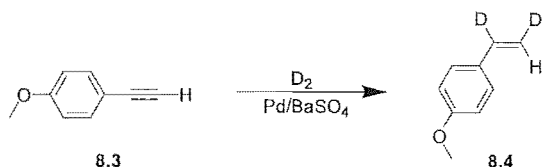
10.5 EXPERIMENTAL WORK DESCRIBED IN CHAPTER EIGHT

p-Methoxystyrene-*cis*- β - d_1



p-Methoxyphenyl acetylene-1- d_1 (1.069 g, 8.04 mmol) was added, under Ar to a suspension of Pd/BaSO₄ (0.14g) and quinoline (0.65 mL) in dry pentane (9 mL). The reaction mixture was stirred under an H₂ atmosphere for 2.5 hours. The solution was filtered and washed with 1N HCl and H₂O. The organic extracts were dried (MgSO₄) and the solvent removed under reduced pressure to give *p*-methoxystyrene-*cis*- β - d_1 ²⁰ as a yellowish liquid (1.07 g, 90% by ¹H NMR). ¹H NMR (500 MHz, CDCl₃) δ 7.35 (d, J = 8.3 Hz, 2H), 6.85 (m, 2H), 5.58 (d, J = 5.4 Hz, 1H), 3.81 (s, 3H).

p-Methoxystyrene-*cis*- α,β - d_2



p-Methoxyphenyl acetylene (0.3952 g, 2.99 mmol) was added, under Ar to a suspension of Pd/BaSO₄ (0.06g) and quinoline (0.2 mL) in dry pentane (3.5 mL). The reaction mixture was stirred under a D₂ atmosphere for 2 hours. The solution was filtered and washed with 1N HCl and H₂O. The organic extracts were dried (MgSO₄) and the solvent removed under reduced pressure to give *p*-methoxystyrene-*cis*- α,β - d_2 ²¹ as a yellowish liquid (0.3955 g, 97%). ¹H NMR (500 MHz, CDCl₃) δ 7.35 (d, J = 8.3 Hz, 2H), 6.85 (m, 2H), 5.58 (d, J = 5.4 Hz, 1H), 3.81 (s, 3H).

(1*R*),(2*S*)-1-(4-Methoxyphenyl)-1,2-ethanediol-2-*d*₂

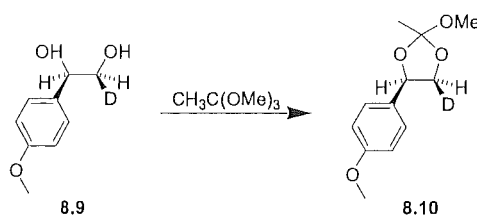
p-Methoxystyrene-*cis*- β -*d*₁ (0.55 g, 4.07 mmol) was added to a vigorously stirring solution of AD mix- β (5.72 g) in tertiary butyl alcohol (21 mL) and water (21 mL) at 0°C. The solution was stirred for 24 hours at 0°C. Sodium metabisulphite (6.1 g) was added and the solution was stirred at room temperature for 2 hours. The reaction mixture was diluted with CH₂Cl₂, the organic layer separated and the aqueous layer extracted with ethyl acetate. The solvent was removed under reduced pressure and the crude product was purified by recrystallisation from ethyl acetate / pet ether to give white crystals.²² (0.454 g, 66%). ¹H NMR (500 MHz, CDCl₃) δ 7.27 (d, *J* = 8.8 Hz, 2H), 6.88 (d, *J* = 8.8 Hz, 2H), 4.74 (d, *J* = 2.9 Hz, 1H), 3.80 (s, 3H), 3.68 (s, 1H), 2.86 (bs, 1H), 2.49 (bs, 1H). ²H NMR (46 MHz, CHCl₃) δ 3.62 (s).

(1*R*),(2*R*)-1-(4-Methoxyphenyl)-1,2-ethanediol-1,2-*d*₂

p-Methoxystyrene-*cis*- β -*d*₁ (0.2966 g, 2.18 mmol) was added to a vigorously stirring solution of AD mix- β (3.05 g) in tertiary butyl alcohol (11 mL) and water (11 mL) at 0°C. The solution was stirred for 24 hours at 0°C. Sodium metabisulphite (3.3 g) was added and the solution was stirred at room temperature for 2 hours. The reaction mixture was diluted with CH₂Cl₂, the organic layer separated and the aqueous layer extracted with ethyl acetate. The solvent was removed under reduced pressure and the crude product was

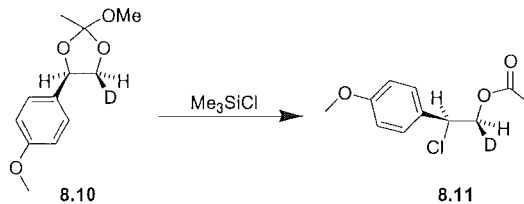
purified by recrystallisation from ethyl acetate / pet ether to give white crystals.²² (0.281 g, 76%). ²H NMR (46 MHz, CHCl₃) δ 4.70 (s, 1D), 3.62 (s, 1D).

2-Methoxy-2-methyl-4-(4-methoxy)phenyl-1,3-dioxolane

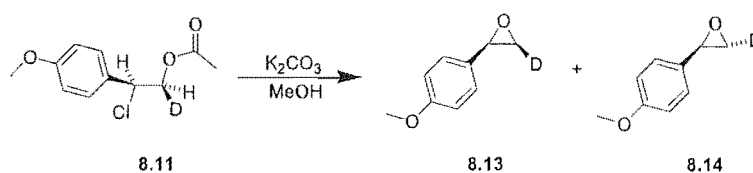


Trimethylorthoacetate (72 μL, 0.57 mmol) was added to a stirring solution of (1*R*),(2*S*)-1-(4-methoxyphenyl)-1,2-ethanediol-2-*d*₁ (80 mg, 0.47 mmol) in CH₂Cl₂ (6 mL). After 10 minutes, TLC showed reaction was complete.

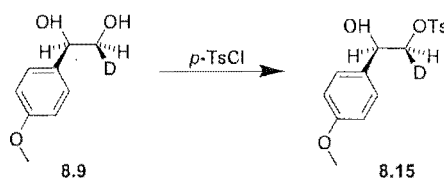
(2*S*)-2-chloro-2-(4-methoxyphenyl)-ethyl acetate-2-*d*₁



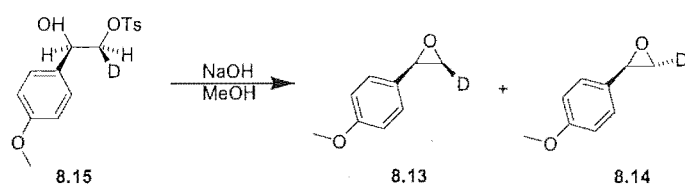
The reaction mixture from above was cooled to 0°C and trimethylsilyl chloride (72 μL, 0.57 mmol) was added. The solution was warmed to room temperature and stirred for 2 hours. The volatiles were evaporated under reduced pressure to give **8.11** as a yellow liquid. ¹H NMR (500 MHz, CDCl₃) δ 7.34-7.32 (m, 2H), 6.91-6.89 (m, 2H), 5.04 (d, *J* = 7.5 Hz, 1H), 4.44 (d, *J* = 7.5 Hz, 1H), 3.81 (s, 3H), 2.07 (s, 3H).

***p*-Methoxystyrene oxide from chloro acetate with K₂CO₃ in MeOH**

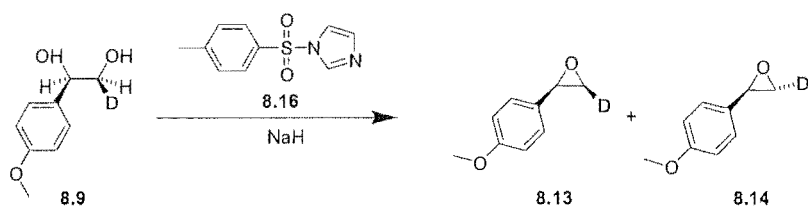
The crude reaction mixture from above was dissolved in methanol (1.5 mL) and K₂CO₃ (160 mg) was added. The reaction mixture was stirred at room temperature under Ar for 15 minutes and poured into water and extracted with ether. Yield of epoxide was 40% by NMR, a 2:1 mixture of deuterium *cis* : *trans* to the aromatic group.

(1*R*),(2*S*)-1-(4-Methoxyphenyl)-2-(4-methylbenzenesulfonate)-1,2-ethandiol-2-*d*₁

(1*R*,2*S*)-*p*-Methoxyphenylethandiol-2-*d*₁ (49.3 mg, 0.292 mmol) was dissolved in pyridine (0.4 mL) under Ar. *p*-Toluenesulfonyl chloride (67 mg, 0.353 mmol) was added and the solution was stirred at room temperature for 48 hours. The reaction mixture was poured into H₂O and extracted with CH₂Cl₂. The organic layer was washed with 1N HCl and water, dried (MgSO₄) and the solvent removed under reduced pressure²³ (80.6 mg, 85%).
¹H NMR (500 MHz, CDCl₃) δ 7.77 (d, *J* = 7.8 Hz, 2H), 7.33 (d, *J* = 8.3 Hz, 2H), 7.23 (d, *J* = 8.3 Hz, 2H), 6.86 (d, *J* = 7.8 Hz, 2H), 4.91 (d, *J* = 2.9 Hz, 1H), 4.08 (d, *J* = 2.4 Hz, 1H), 3.79 (s, 3H), 2.45 (s, 3H).

***p*-Methoxystyrene oxide from tosyl chloride with NaOH**

Crude tosylate was dissolved in methanol (1.5 mL) and cooled to -10°C in an ice/salt bath. NaOH (40 mg) in methanol (1.5 mL) was added and the reaction stirred for 3 hours. The reaction mixture was diluted with ether, and washed with H₂O. The organic layer was separated, dried (MgSO₄) and the solvent removed under reduced pressure. An 80% yield of epoxide was obtained (determined by ¹H NMR). Epoxide was a 4 : 1 mixture of *trans* : *cis* deuterated epoxide.

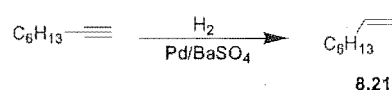
***p*-Methoxystyrene oxide from diol with NaH and tosyl imidazole**

(1*R*,2*S*)-*p*-Methoxyphenylethane-1,2-diol-2-*d*₁ (49.3 mg, 0.292 mmol) was added to NaH (60% dispersion in oil, 0.0227 g, washed with pentane to remove oil) in THF (2 mL) under N₂. After 1 hour *N*-*p*-tolylsulfonylimidazole (1 eq.) was added and the reaction mixture was stirred at room temperature for 1 hour and poured into H₂O. The aqueous layer was extracted with ether and the combined organic layers were dried (Na₂SO₄) and the solvent removed under reduced pressure to give *p*-methoxystyrene oxide as a yellowish liquid. 70% yield of epoxide as a 3.25 : 1 mixture of *trans* : *cis* deuterated epoxide, determined by ¹H and ²H NMR.

Methods of *p*-methoxystyrene oxide formation:

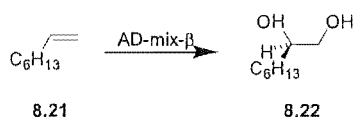
Method	Yield of epoxide	8.13 : 8.14
MeC(OMe) ₃ / Me ₃ SiCl	40%	2 : 1
TsCl / NaOH	85%	1 : 4
<i>N</i> -TsIm / NaH	70%	1 : 3.25

1-Octene



Pd on BaSO₄ (0.15 g) and quinoline (0.25 mL) in pentane (8 mL) were shaken under an H₂ atmosphere. 1-Octyne (1.3 mL) was added and the reaction mixture was shaken for 2 1/2 hours. The reaction mixture was washed with 1 N HCl, H₂O, dried (Na₂SO₄) and the solvent was removed under reduced pressure.²⁴ ¹H NMR (300 MHz, CDCl₃) δ 5.82 (m, 1H), 5.03 (m, 2H), 2.04 (m, 2H), 1.32 (m, 8H), 0.88 (t, *J* = 6.8 Hz, 3H).

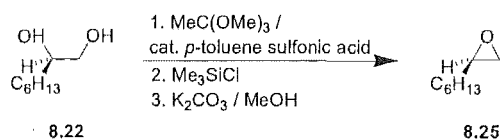
(2*R*)-1,2-Octandiol



AD-mix-β (4.9 g), K₂CO₃ (1.44 g) and K₂Fe(CN)₆ (3.43 g) were dissolved in a solution of H₂O (35 mL) and *tert* butanol (35 mL) and cooled to 0°C. 1-Octene (0.7925 g, 1.108 mL) was added and the reaction mixture was stirred vigorously for 16 hours. The solution was again cooled to 0°C and sodium metabisulphite (10.5 g) was added and the solution left to stir at room temperature for 2 hours. The reaction mixture was diluted with CH₂Cl₂ (30 mL), the organic layer separated and the aqueous layer was extracted with CH₂Cl₂. The organic extracts were combined, dried (Na₂SO₄) and the solvent removed under reduced

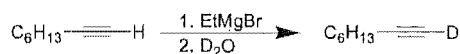
pressure.²⁵ ^1H NMR (300 MHz, CDCl_3) δ 3.69 (m, 1H), 3.64 (m, 1H), 3.44 (m, 1H), 1.98 (bs, 2H), 1.44 (m, 2H), 1.29 (m, 8H), 0.89 (t, $J = 6.8$ Hz, 3H).

(2*R*)-1-Octene oxide



Trimethyl orthoacetate (84 μL , 0.738 mmol) was added to a solution of (2*R*)-1,2-octandiol (90 mg, 0.615 mmol) and *p*-toluene sulfonic acid monohydrate (5 mg) in CH_2Cl_2 (1 mL). After stirring at room temperature for 1 hour, the volatiles were removed under reduced pressure and the residue placed under a high vacuum pump for 1 minute to remove methanol. The residue was taken up in CH_2Cl_2 (1 mL), chlorotrimethylsilane (109 mL, 1.03 mmol) was added and the solution was stirred for 18 hours. The volatiles were removed under reduced pressure and the residue taken up in methanol (1.5 mL) and K_2CO_3 was added. The reaction mixture was stirred for 5 hours and poured into NH_4Cl (7 mL) and extracted with CH_2Cl_2 . The organic extracts were dried (MgSO_4) and filtered and the solvent removed under reduced pressure to give **8.25**²⁶ as a yellowish liquid (78 mg, 82%). ^1H NMR (300 MHz, CDCl_3) δ 2.91 (m, 1H), 2.75 (dd, $J = 4.9, 7.4$ Hz, 1H), 1.48 (dd, $J = 4.9, 5.4$ Hz, 4H), 1.52 (m, 2H), 1.45 (m, 2H), 1.30 (m, 6H), 0.89 (t, $J = 6.8$ Hz, 3H).

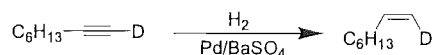
1-Octyne-1-*d*₁



Ethyl bromide (1.3 mL) in ether (2 mL) was added dropwise to a rapidly stirring suspension of magnesium (0.5 g) in ether (2 mL) under a nitrogen atmosphere. After the solution returned to room temperature, 1-octyne (0.35 mL, 0.1 equivalents) in ether was added dropwise and the reaction mixture was left to stir overnight. D_2O (1.3 mL) was added slowly and the resulting slurry was extracted with pentane. The organic extract was

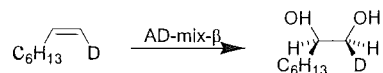
dried (Na_2SO_4) and the solvent removed under reduced pressure, giving 1-Octyne-1- d_1 ²⁷ as a colourless liquid. ^1H NMR showed greater than 95% D incorporation at C1. ^1H NMR (300 MHz, CDCl_3) δ 1.51 (m, 2H), 1.37 (m, 2H), 1.30 (m, 6H), 0.89 (t, $J = 6.8$ Hz, 3H).

1-Octene-*cis*- d_1

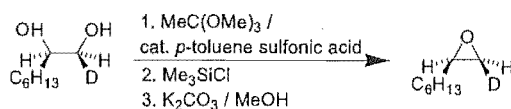


Pd on BaSO_4 (0.15 g) and quinoline (0.25 mL) in pentane (8 mL) were shaken under an H_2 atmosphere. 1-Octyne-1- d_1 (1.3 mL) was added and the reaction mixture was shaken for 2 hours. The reaction mixture was washed with 1 N HCl, H_2O , dried (Na_2SO_4) and the solvent was removed under reduced pressure.²⁴ ^1H NMR (300 MHz, CDCl_3) δ 5.80 (m, 1H), 4.91 (d, $J = 9.8$ Hz, 1H), 2.04 (m, 2H), 1.29 (m, 8H), 0.88 (t, $J = 6.8$ Hz, 3H).

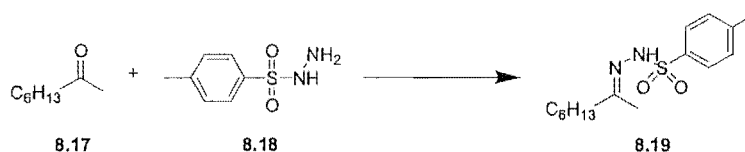
(1*S*),(2*R*)-1,2-Octandiol-1- d_1



AD-mix- β (4.9 g), K_2CO_3 (1.44 g) and $\text{K}_2\text{Fe}(\text{CN})_6$ (3.43 g) were dissolved in a solution of H_2O (35 mL) and *tert* butanol (35 mL) and cooled to 0°C . 1-Octene-*cis*- d_1 (0.7925 g, 1.108 mL) was added and the reaction mixture was stirred vigorously for 16 hours. The solution was again cooled to 0°C and sodium metabisulphite (10.5 g) was added and the solution left to stir at room temperature for 2 hours. The reaction mixture was diluted with CH_2Cl_2 (30 mL), the organic layer separated and the aqueous layer was extracted with CH_2Cl_2 . The organic extracts were combined, dried (Na_2SO_4) and the solvent removed under reduced pressure.²⁵ ^1H NMR (300 MHz, CDCl_3) δ 3.68 (s, 1H), 3.62 (s, 1H), 2.82 (bs, 2H), 1.43 (m, 2H), 1.27 (m, 8H), 0.88 (t, $J = 6.8$ Hz, 3H). ^2H NMR (46 MHz, CHCl_3) δ 3.33 (s).

(1*S*),(2*R*)-1-Octene oxide-1-*d*₁

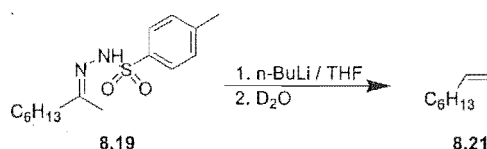
(1*S*,2*R*)-1,2-Octanediol-1-*d*₁ (0.1583 g), trimethyl orthoacetate (0.1368 mL) and *p*-toluene sulfonic acid monohydrate were dissolved in CH₂Cl₂ (3 mL). The reaction mixture was stirred at room temperature for 1 hour and the solvent removed under reduced pressure. The resulting residue was put under a high vacuum pump (0.07 torr) for 1 minute to remove methanol. The residue was dissolved in CH₂Cl₂ (3 mL) and chlorotrimethylsilane (0.191 mL) was added. The solution was stirred at room temperature for 16 hours. The solvent was removed under reduced pressure and the residue taken up in methanol (3 mL). K₂CO₃ (0.297 g) was added and the reaction mixture was stirred for 5 hours, poured into saturated NH₄Cl (7 mL) and extracted with CH₂Cl₂. The combined organic extracts were dried (Na₂SO₄) and the solvent removed under reduced pressure.²⁶ ¹H NMR (300 MHz, CDCl₃) δ 2.91 (m, 1H), 2.74 (d, *J* = 3.9 Hz, 1H), 1.48 (m, 4H), 1.30 (m, 6H), 0.89 (t, *J* = 6.8 Hz, 3H). ²H NMR (46 MHz, CHCl₃) δ 2.44 (s).

(1-Methylheptylidine)hydrazide-(4-methyl-benzene)sulfonic acid

4-Toluene sulfonylhydrazide (2.04 g, 11.0 mmol) was dissolved in refluxing dry methanol (11 mL). 2-Octanone (1.72 mL, 19.1 mmol) was added and the reaction mixture was stirred at reflux for two hours, before cooling to room temperature and placing in a fridge overnight. The white crystals were filtered and washed with cold methanol. Solvent was removed on a rotary evaporator, giving **8.19**²⁸ as white crystals (3.02 g, 93%). ¹H NMR (300 MHz, CDCl₃) δ 7.85 (m, 2H), 7.30 (d, *J* = 7.8 Hz, 2H), 2.43 (s, 3H), 2.19 (dd, *J* = 7.3,

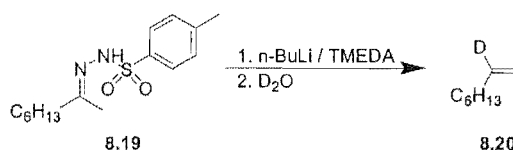
7.8 Hz, 2H), 1.90 (s, 1H), 1.75 (s, 3H), 1.42 (m, 2H), 1.20 (m, 6H), 0.85 (t, $J = 6.8$ Hz, 3H).

1-Octene



Tosyl hydrazone (0.289 g,) was dissolved in dry THF (10 mL) under Ar and the solution cooled to -78°C . Butyl lithium (2.5 mL,) was added dropwise. After 10 minutes stirring at -78°C the reaction mixture was warmed to 0°C and gas was evolved. After twenty minutes stirring at 0°C , D_2O (1.5 mL) was added dropwise and the reaction mixture warmed to room temperature and stirred for eight hours. The organic layer was separated, dried ($MgSO_4$) and solvent removed under reduced pressure, giving 1-octene. ^1H NMR indicated approximately 5% deuterium incorporation at C2.

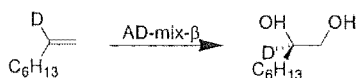
1-Octene-2- d_1



TMEDA was pre-dried with KOH pellets, before vigorous drying by refluxing with butyric anhydride for 2 hours, and fractional distillation under N_2 . Tosyl hydrazone was recrystallised from methanol. Tosyl hydrazone was dissolved in TMEDA (10 mL) under N_2 . The solution was cooled to -78°C and BuLi (1 M solution in THF, 5 mL) was added dropwise. After 4 hours stirring at room temperature, the reaction mixture was cooled to 0°C and D_2O (1 equivalent) was added. After 10 minutes a further 4 equivalents of D_2O were added. The solution was stirred at room temperature for 8 hours, poured into 1 N HCl (30 mL) and extracted with ether. The organic layer was washed with saturated Na_2CO_3 ,

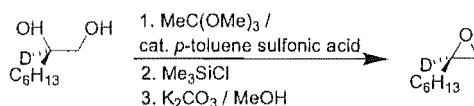
dried (MgSO_4) and the solvent removed under reduced pressure. The product was purified by flash chromatography on a silica column eluted with pentane to give 1-octene²⁴ as a colourless liquid (94% yield). ^1H NMR showed 86% deuterium incorporation at C2. ^1H NMR (300 MHz, CDCl_3) δ 4.98 (m, 1H), 4.92 (m, 1H), 2.04 (m, 2H), 1.28 (m, 8H), 0.88 (t, $J = 6.8$ Hz, 3H).

(2*R*)-1,2-Octandiol-2-*d*₁



AD- β (0.577 g), $\text{K}_3\text{Fe}(\text{CN})_6$ (0.506 g), K_2CO_3 (0.357 g) were dissolved in a 1 : 1 solution of H_2O / 2-methyl-2-propanol (20 mL) and the solution cooled to 0°C . 1-Octene-2-*d* (0.15 g, 1.3 mmol) was added, the solution was allowed to slowly return to room temperature and stirred for 40 hours. The reaction mixture was cooled to 0°C and sodium metabisulphite (1.2 g) was added, after warming to room temperature, the reaction mixture was stirred for one hour. CH_2Cl_2 (30 mL) was added and the organic layer separated. The aqueous layer was extracted three times with CH_2Cl_2 to give the title compound²⁵ as a yellow liquid (0.094 g, 50%). ^1H NMR (300 MHz, CDCl_3) δ 3.66 (d, $J = 10.7$ Hz, 1H), 3.43 (d, $J = 11.2$ Hz, 1H), 1.82 (bs, 2H), 1.43 (m, 2H), 1.27 (m, 8H), 0.88 (t, $J = 6.8$ Hz, 3H).

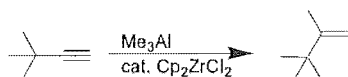
(2*R*)-1-Octene oxide-2-*d*₁



Trimethyl orthoacetate (0.173 mL, 1.35 mmol) was added to a solution of 1,2-octandiol-2-*d*₁ in CH_2Cl_2 at 0°C . Chlorotrimethylsilane (0.173 mL,) was added and the reaction mixture was stirred for 20 hours at room temperature. The solvent was removed under reduced pressure and the residue dissolved in methanol (10 mL), K_2CO_3 was added and the

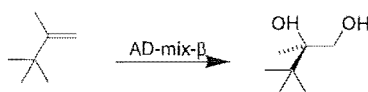
reaction mixture was stirred for 5 hours. The reaction mixture was partitioned between CH_2Cl_2 and H_2O , the organic layer was separated, dried (MgSO_4) and the solvent was removed under reduced pressure, giving 1-octene oxide-2- d^{26} as a yellow liquid. ^1H NMR (500 MHz, CDCl_3) δ 2.74 (d, $J = 5.4$ Hz, 1H), 2.46 (d, $J = 5.4$ Hz, 1H), 1.52 (m, 2H), 1.44 (m, 2H), 1.30 (m, 6H), 0.89 (t, $J = 6.8$ Hz, 3H).

2,3,3-Trimethyl-1-butene



Cp_2ZrCl_2 (0.157 g, 0.537 mmol) was dissolved in CH_2Cl_2 (10 mL) under N_2 . Me_3Al (5.1 mL, 10 mmol) was added and the solution stirred for 10 minutes at which point the solution went lime green. 3,3-Dimethyl-1-butyne (0.607 mL, 5 mmol) was added and the solution was stirred for 24 hours to give an orange solution. The reaction mixture was cooled to 0°C and H_2O was added dropwise. The solvent was removed by distillation and the product was purified by flash column chromatography on silica eluting with pentane to give (1*R*),(2*R*)-2,3,3-trimethyl-1-butene-1- d_1^{29} as a colourless liquid (332 mg, 67%). ^1H NMR (300 MHz, CDCl_3) δ 5.30 (s, 1H), 4.71 (s, 1H), 1.75 (s, 3H), 1.06 (s, 9H).

(2*R*)-2,3,3-Trimethyl-1,2-butandiol



2,3,3-Trimethyl-1-butene (0.198 g, 2.0 mmol) was added to a vigorously stirring solution of AD mix- β (2.8 g) in tertiary butyl alcohol (10 mL) and water (10 mL) at 0°C . The solution was stirred for 24 hours at 0°C . Sodium metabisulphite (3.0 g) was added and the solution was stirred at room temperature for 2 hours. The reaction mixture was diluted with CH_2Cl_2 , the organic layer separated and the aqueous layer extracted with ethyl acetate to give (2*R*)-2,3,3-trimethyl-1,2-butandiol³⁰ as a yellow liquid (0.186 g, 70%). ^1H NMR (300

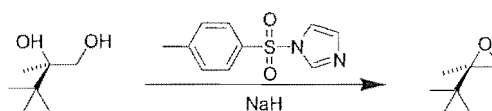
MHz, CDCl_3) δ 3.71 (d, $J = 10.7$ Hz, 1H), 3.44 (d, $J = 10.7$ Hz, 1H), 1.87 (bs, 2H), 1.20 (s, 3H), 0.96 (s, 9H).

N-*p*-Tolylsulfonylimidazole

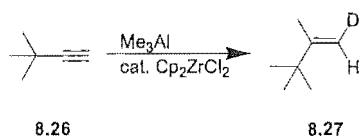


p-Toluenesulfonyl chloride (8.56 g, 46 mmol) was added in portions to a stirred solution of imidazole (6.12 g, 90 mmol) in dry CHCl_3 (66 mL). After stirring for 24 hours, the reaction mixture was filtered, washed with NaHCO_3 (40 mL) and water (40 mL). The organic extract was dried (NaSO_4) and the solvent removed under reduced pressure. The product formed crystals on standing overnight and was recrystallised from ethanol³¹ (9.19 g, 90%). ^1H NMR (300 MHz, CDCl_3) δ 8.01 (s, 1H), 7.83 (d, $J = 8.3$ Hz, 2H), 7.36 (d, $J = 8.3$ Hz, 2H), 7.29 (s, 1H), 7.08 (s, 3H), 2.44 (s, 3H).

(2*R*)-2,3,3-Trimethyl-1-butene oxide



(2*R*)-2,3,3-Trimethyl-1,2-butanediol (0.030 g, 0.227 mmol) was added to NaH (60% dispersion in oil, 0.0227 g, washed with pentane to remove oil) in THF (2 mL) under N_2 . After 1 hour *N*-*p*-tolylsulfonylimidazole (**9**) was added and the reaction mixture was stirred at room temperature for 1 hour and poured into H_2O . The aqueous layer was extracted with ether and the combined organic layers were dried (Na_2SO_4) and the solvent removed under reduced pressure to give (2*R*)-2,3,3-trimethyl-1-butene oxide³² as a yellowish liquid (22 mg, 84%). ^1H NMR (300 MHz, CDCl_3) δ 2.80 (m, 1H), 2.44 (d, $J = 4.4$ Hz, 1H), 1.29 (s, 3H), 0.95 (s, 9H).

2,3,3-Trimethyl-1-butene-trans-1-*d*₁

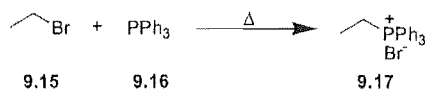
Cp_2ZrCl_2 (0.157 g, 0.537 mmol) was dissolved in CH_2Cl_2 (10 mL) under N_2 . Me_3Al (5.1 mL, 10 mmol) was added and the solution stirred for 10 minutes at which point the solution went lime green. 3,3-Dimethyl-1-butyne (0.607 mL, 5 mmol) was added and the solution was stirred for 24 hours to give an orange solution. The reaction mixture was cooled to 0°C and D_2O was added dropwise. The solvent was removed by distillation and the product was purified by flash column chromatography on silica eluting with pentane to give (1*R*),(2*R*)-2,3,3-trimethyl-1-butene-1-*d*₁²⁹ as a colourless liquid (332 mg, 67%). ^1H NMR (300 MHz, CDCl_3) δ 4.71 (s, 1H), 1.29 (s, 3H), 0.98 (s, 9H).

(1*R*),(2*R*)-2,3,3-Trimethyl-1,2-butandiol-1-*d*₁

2,3,3-Trimethyl-1-butene-trans-1-*d*₁ (0.198 g, 2.0 mmol) was added to a vigorously stirring solution of AD mix- β (2.8 g) in tertiary butyl alcohol (10 mL) and water (10 mL) at 0°C . The solution was stirred for 24 hours at 0°C . Sodium metabisulphite (3.0 g) was added and the solution was stirred at room temperature for 2 hours. The reaction mixture was diluted with CH_2Cl_2 , the organic layer separated and the aqueous layer extracted with ethyl acetate to give (1*R*),(2*R*)-2,3,3-trimethyl-1,2-butandiol-1-*d*₁³⁰ as a yellow liquid (0.186 g, 70%). ^1H NMR (300 MHz, CDCl_3) δ 3.69 (s, 1H), 1.82 (bs, 2H), 1.19 (s, 3H), 0.94 (s, 9H).

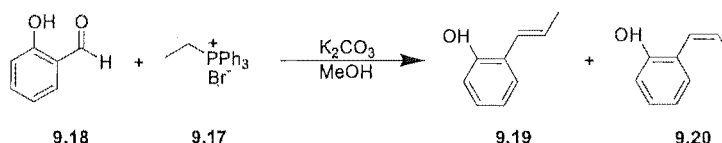
10.6 EXPERIMENTAL WORK DESCRIBED IN CHAPTER NINE

Ethyltriphenylphosphonium bromide



Bromoethane (1.2 equivalents) was added to a solution of triphenylphosphine (1 equivalent) in dry benzene (10 mL) at 0°C. The solution was heated at 60°C for 48 hours, and cooled to room temperature to give a white precipitate that was filtered and washed with cold benzene. (90%).

2-(1-Propenyl)phenol



Salicylaldehyde (9.59 mL, 90 mmol) was added to a stirring solution of ethyltriphenylphosphonium bromide (42.92g, 115.7 mmol) and potassium carbonate (18.66g, 135 mmol) in methanol (90 mL). The solution was stirred at room temperature for 4 hours, filtered and the solvent removed under reduced pressure. Distillation of the crude product under reduced pressure gave the title compound (7.994 g, 66%) as a 77 : 33 mixture of the E : Z isomers.³³ The E and Z isomers were separated by flash column chromatography on silver nitrate impregnated silica (see below for details). **E-2-(1-Propenyl)phenol** ¹H NMR (CDCl₃, 300 MHz) δ 7.29 (dd, *J* = 7.8, 1.5 Hz, 1H), 7.09 (m, 1H), 6.88 (m, 1H), 6.68 (dd, *J* = 7.8, 1.0 Hz, 1H), 6.58 (dd, *J* = 15.6, 1.5 Hz, 1H), 6.20 (m, 1H), 5.10 (s, 1H), 1.91 (dd, *J* = 6.6, 1.5 Hz, 3H). **Z-2-(1-Propenyl)phenol** ¹H NMR (CDCl₃, 300 MHz) δ 7.20-7.07 (m, 2H), 6.86 (m, 1H), 6.40 (d, *J* = 11.2 Hz, 1H), 6.04 (m, 1H), 5.04 (s, 1H), 1.72 (m, 3H).

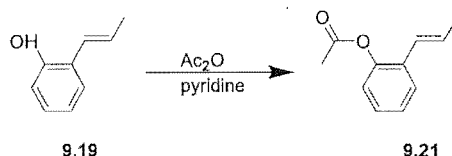
Separation of E and Z isomers of 2-(2-propenyl)phenol by flash chromatography on silver nitrate impregnated silica

Silver nitrate impregnated silica plates for TLC were prepared by dissolving AgNO_3 (2.0 g) in H_2O (5 mL). Alumina backed silica TLC plates were dipped in the solution and carefully dried with a heat gun (if too much heat is used to dry the plate, the silver is oxidised and the TLC plate turns black).

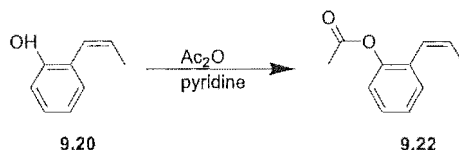
Silver nitrate impregnated silica was prepared by dissolving AgNO_3 (5.5 g) in distilled water (30 mL). The solution was added to silica (50 g) and ground with a mortar and pestle for 5 minutes. The silica was dried in an oven at 90°C for 16 hours and stored over P_2O_5 .

The E and Z isomers of 2-(2-propenyl)phenol were separated by flash chromatography on AgNO_3 impregnated silica using 10% ethyl acetate : 90% petroleum ether as the eluant. The E isomer came off the column first and was identified by its proton NMR coupling constant.

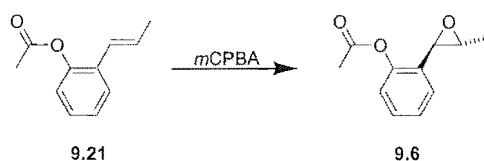
E-1-(2-Acetoxyphenyl)propene



E-2-(1-Propenyl)phenol (2.83 g,) was added to a solution of pyridine (7 mL) and acetic anhydride (4.2 mL) in CH_2Cl_2 under Ar. The reaction mixture was stirred at room temperature for 24 hours and the volatiles removed under reduced pressure. The residue was taken up in ethyl acetate and washed successively with H_2O , 1 N HCl, NaHCO_3 and brine. The organic layer was dried with MgSO_4 and the solvent removed under reduced pressure. The crude product was purified by flash chromatography on silica, with ethyl acetate-petroleum ether (10 : 90) as eluant.³⁴ (98%). ^1H NMR (CDCl_3 , 500 MHz) δ 7.49 (dd, $J = 7.3, 2.0$ Hz, 1H), 7.20 (m, 2H), 7.00 (dd, $J = 7.8, 1.5$ Hz, 1H), 6.39 (dd, $J = 15.5, 1.5$ Hz, 1H), 6.24 (m, 1H), 2.33 (s, 3H), 1.89 (dd, $J = 6.8, 1.5$ Hz, 3H).

Z-1-(2-Acetoxyphenyl)propene

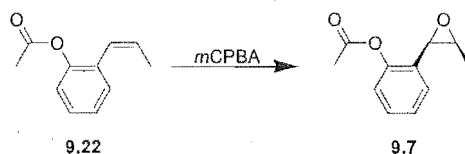
Z-2-(1-Propenyl)phenol (2.83 g,) was added to a solution of pyridine (7 mL) and acetic anhydride (4.2 mL) in CH_2Cl_2 under Ar. The reaction mixture was stirred at room temperature for 24 hours and the volatiles removed under reduced pressure. The residue was taken up in ethyl acetate and washed successively with H_2O , 1 N HCl, NaHCO_3 and brine. The organic layer was dried with MgSO_4 and the solvent removed under reduced pressure. The crude product was purified by flash chromatography on silica, with ethyl acetate-petroleum ether (10 : 90) as eluant.³⁴ (98%). ^1H NMR (CDCl_3 , 500 MHz) δ 7.33-7.18 (m, 3H), 7.05 (m, 1H), 6.30 (m, 1H), 5.85 (m, 1H), 2.27 (s, 3H), 1.77 (m, 3H).

E-1-(2-Acetoxyphenyl)propene oxide

70 % *m*CPBA (0.4047 g, 1.64 mmol) was added to a solution of E-1-(2-acetoxyphenyl)propene (0.200 g, 1.49 mmol) in CH_2Cl_2 (5 mL) at 0°C . The solution was warmed to room temperature and stirred for 16 hours, washed successively with saturated sodium metabisulfite (3 mL), 5% aqueous NaHCO_3 (5 x 3 mL) and water. The organic extracts were dried over Na_2SO_4 and the solvent was removed under reduced pressure. The product was purified by flash chromatography on silica with ethyl acetate-petroleum ether (20 : 80) as the eluant.³⁴ ^1H NMR (CDCl_3 , 500 MHz) δ 7.30 (m, 1H), 7.24 (m, 2H), 7.05 (m, 1H), 3.63 (d, J = 2.4 Hz, 1H), 2.95 (m, 1H), 2.34 (s, 3H), 1.43 (d, J = 4.9 Hz, 3H). ^{13}C

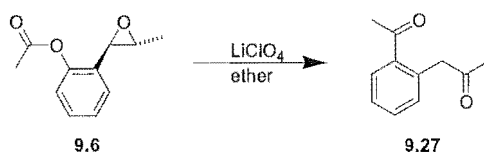
NMR (CDCl₃, 75 MHz) δ 169.1, 149.0, 130.0, 128.6, 126.3, 125.7, 121.9, 58.1, 55.1, 20.7, 12.8. IR (KBr disk) cm⁻¹ 2995.2, 1766.7, 1490.9, 1454.2, 1425.3, 1371.3, 1209.3, 1176.5.

Z-1-(2-Acetoxyphenyl)propene oxide



70 % *m*CPBA (0.4047 g, 1.64 mmol) was added to a solution of Z-1-(2-acetoxyphenyl)propene (0.200 g, 1.49 mmol) in CH₂Cl₂ (5 mL) at 0°C. The solution was warmed to room temperature and stirred for 16 hours, washed successively with saturated sodium metabisulfite (3 mL), 5% aqueous NaHCO₃ (5 x 3 mL) and water. The organic extracts were dried over Na₂SO₄ and the solvent was removed under reduced pressure. The product was purified by flash chromatography on silica with ethyl acetate-petroleum ether (20 : 80) as the eluant.³⁴ ¹H NMR (CDCl₃, 500 MHz) δ 7.32 (m, 2H), 7.26 (d, *J* = 7.3 Hz, 1H), 7.07 (d, *J* = 8.3 Hz, 1H), 4.00 (d, *J* = 4.4 Hz, 1H), 3.34 (m, 1H), 2.32 (s, 3H), 1.05 (d, *J* = 5.4 Hz, 3H).

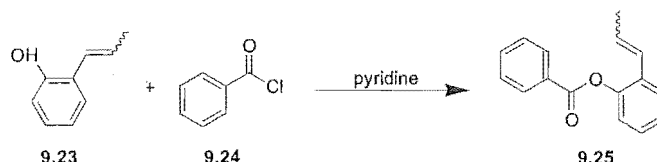
LiClO₄ promoted rearrangement of E-1-(2-acetoxyphenyl)propene oxide



E-1-(2-acetoxyphenyl)propene oxide (71.7 mg, 0.373 mmol) was added to a solution of LiClO₄ (2.1446 g) in ether (5 mL) at 0°C, under Ar. The reaction mixture was stirred at room temperature for 62 hours. The LiClO₄ was removed by repeated washing with water. The organic solution was dried with MgSO₄ and the solvent removed under reduced pressure to give **9.27**³⁵ (68 mg, 95%). ¹H NMR (CDCl₃, 500 MHz) δ 7.32 (m, 1H), 7.24

(m, 2H), 7.11 (m, 1H), 3.60 (s, 2H), 2.29 (s, 3H), 2.11 (s, 3H). ^{13}C NMR (CDCl_3 , 75 MHz) δ 205.6, 169.2, 149.2, 131.4, 128.6, 126.4, 122.7, 46.2, 28.9, 20.8. IR (KBr disk) cm^{-1} 2922.0, 1766.7, 1712.7, 1490.9, 1456.2, 1425.3, 1371.3, 1209.3, 1174.6.

Mixture of E and Z 2-(1-propenyl)phenyl benzoate



A roughly 2:1 mixture of *trans*- : *cis*-2-(2-propenyl)phenol (0.2718 g, 2.028 mmol) was added to a stirring solution of benzoyl chloride (0.313 g, 0.258 mmol) in pyridine (3 mL). The reaction mixture was stirred at room temperature for 48 hours, diluted with CH_2Cl_2 and washed successively with 1N HCl, saturated NaCO_3 and water. The organic extracts were dried with MgSO_4 and the solvent removed under reduced pressure. The product was purified by flash chromatography on silica (20 : 80 ethyl acetate / petroleum ether). ^1H NMR (CDCl_3 , 500 MHz) δ 8.23 (m, 4H), 7.65 (m, 2H), 7.54 (m, 5H), 7.39 (d, $J = 1.5$ Hz, 1H), 7.38-7.19 (m, 6H), 7.12 (m, 1H), 6.45 (m, 1H), 6.37 (m, 1H), 6.27 (m, 1H), 5.80 (m, 1H), 1.80 (m, 6H).

Mixture of E and Z 2-(1-epoxypropyl)phenyl benzoate



2-(1-Propenyl)phenyl benzoate (0.1572 g, 0.66 mmol) was added to *m*CPBA (0.2656g) in CH_2Cl_2 (10 mL) at 0°C . The reaction mixture was stirred at room temperature for 4 hours, washed with saturated sodium metabisulphite, 5% aqueous NaHCO_3 and water. The organic solution was dried with MgSO_4 and the solvent removed under reduced pressure,

giving a yellowish liquid (0.1676 g, 100%). **Trans-2-(1-epoxypropyl)phenyl benzoate** ^1H NMR (CDCl_3 , 300 MHz) δ 8.25-7.18 (m, 9H), 3.70 (d, $J = 2.0$ Hz, 1H), 2.99 (m, 1H), 1.34 (d, $J = 4.9$ Hz, 3H). **Cis-2-(1-epoxypropyl)phenyl benzoate** ^1H NMR (CDCl_3 , 300 MHz) δ 8.25-7.18 (m, 9H), 4.09 (d, $J = 4.4$ Hz, 1H), 3.29 (m, 1H), 1.09 (d, $J = 5.4$ Hz, 3H).

Rearrangement of 2-(1-epoxypropyl)phenyl benzoate with $\text{BF}_3 \cdot \text{OEt}_2$

$\text{BF}_3 \cdot \text{OEt}_2$ (500 μL) was added to benzoyl epoxide (0.1911 g) in dry ether (40 mL). The reaction mixture was stirred at room temperature for 2.5 hours, saturated K_2CO_3 (0.5 mL) was added to the stirring solution, followed by anhydrous K_2CO_3 . The solution was filtered and the solvent removed under reduced pressure. Analysis of the product by TLC showed that at least four compounds were present. ^1H NMR indicated the presence of some rearranged ketone.

¹ Coxon, James M.; Cambridge, James R. A.; Nam, Shayne G. C. *Org. Lett.* **2001**, 3, 4225-4227.

² Daquette, L. A.; Ra, C. S. *J. Org. Chem.* **1988**, 53, 4978.

³ De Luca, Lidia; Giacomelli, Giampaolo; Masala, Simonetta; Porcheddu, Andrea. *J. Org. Chem.* **2003**, 68, 4999-5001.

⁴ Moussou, P.; Archelas, A.; Baratti, J.; Furstoss, R. *J. Org. Chem.* **1998**, 63, 3532-3537.

⁵ Coxon, James M.; Cambridge, James R. A.; Nam, Shayne G. C. *Synlett* **2004**, 8, 1422-1424.

⁶ Liang, Jiang-Lin; Yuan, Shi-Xue; Huang, Jie-Sheng; Che, Chi-Ming. *J. Org. Chem.* **2004**, 69, 3610-3619.

⁷ Arisawa, Mitsuhiro; Ramesh, Namakkal G.; Nakajima, Makiko; Tohma, Hirofumi; Kita, Yasuyuki. *J. Org. Chem.* **2001**, 66, 59-65.

⁸ Iwasawa, Tetsuo; Tokunaga, Makoto; Obora, Yasushi; Tsuji, Yasushi. *J. Am. Chem. Soc.* **2004**, 126, 6554-6555.

⁹ Sivaguru, J.; Sunoj, Raghavan B.; Wada, Takehiko; Origane, Yumi; Inoue, Yoshihisa; Ramamurthy, Vaidhyanathan. *J. Org. Chem.* **2004**, 69, 6533-6547.

¹⁰ Driver, Tom G.; Woerpel, K. A. *J. Am. Chem. Soc.* **2004**, 126, 9993-10002.

¹¹ Moussou, P.; Archelas, A.; Baratti, J.; Furstoss, R. *J. Org. Chem.* **1998**, 63, 3532-3537.

¹² Tami, Kenichiro; Mitsudo, Koichi; Fujita, Kazuyoshi; Ohashi, Youichi; Yoshida, Junichi. *J. Am. Chem. Soc.* **2004**, 126, 11058-11066.

¹³ Moussou, P.; Archelas, A.; Baratti, J.; Furstoss, R. *J. Org. Chem.* **1998**, 63, 3532-3537.

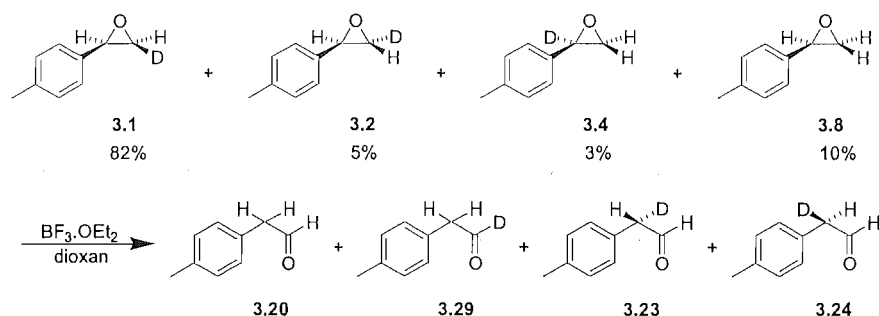
¹⁴ Aranda, G.; De Luze, H. *Org. Mag. Res.* **1972**, 4, 847-56.

-
- ¹⁵ Heck, R. F. *Palladium Reagents in Organic Synthesis*, Academic Press (1985).
- ¹⁶ Dulog, Lothar; Koerner, Bernd; Heinze, Juergen; Yang, Jianjun. *Liebigs Annalen* **1995**, *9*, 1663-71.
- ¹⁷ Li, Zhiping; Li, Chao-Jun. *J. Am. Chem. Soc.* **2004**, *126*, 11810-11811.
- ¹⁸ Utsunomiya, Masaru; Hartwig, John F. *J. Am. Chem. Soc.* **2004**, *126*, 2702-2703.
- ¹⁹ Schaus, S. E.; Brandes, B. D.; Larrow, J. F.; Tokunaga, M.; Hanson, K. B.; Gould, A. E.; Furrow, M. E.; Jacobson, E. N. *J. Am. Chem. Soc.* **2002**, *124*, 1307-1315.
- ²⁰ Vassilikogiannakis, Georgios; Hatzimarinaki, Maria; Orfanopoulos, Michael. *J. Org. Chem.* **2000**, *65*, 8180-8187.
- ²¹ Brown, John M.; Lloyd-Jones, Guy C. *J. Am. Chem. Soc.* **1994**, *116*, 866-78.
- ²² Doeblner, Christian; Mehlretter, Gerald M.; Sundermeier, Uta; Beller, Matthias. *J. Am. Chem. Soc.* **2000**, *122*, 10289-10297.
- ²³ Cho, Byung Tae; Kang, Sang Kyu; Shin, Sung Hye. *Tetrahedron: Asymmetry* **2002**, *13*, 1209-1217.
- ²⁴ Tsuchii, Kaname; Imura, Motohiro; Kamada, Nagisa; Hirao, Toshikazu; Ogawa, Akiya. *J. Org. Chem.* **2004**, *69*, 6658-6665.
- ²⁵ Paddon-Jones, Gregory C.; McErlean, Christopher S. P.; Hayes, Patricia; Moore, Christopher J.; Konig, Wilfried A.; Kitching, William. *J. Org. Chem.* **2001**, *66*, 7487-7495.
- ²⁶ Halland, Nis; Brauton, Alan; Bachmann, Stephan; Marigo, Mauro; Jorgensen, Karl Anker. *J. Am. Chem. Soc.* **2004**, *126*, 4790-4791.
- ²⁷ Takaki, Ken; Koshiji, Go; Komeyama, Kimihiro; Takeda, Mitsuhiro; Shishido, Tetsuya; Kitani, Akira; Takehira, Katsuomi. *J. Org. Chem.* **2003**, *68*, 6554-6565.
- ²⁸ Kabalka, George W.; Summers, S. Timothy. *J. Org. Chem.* **1981**, *46*, 1217-18.
- ²⁹ Renaud, Philippe; Ollivier, Cyril; Weber, Valery. *J. Org. Chem.* **2003**, *68*, 5769-5772.
- ³⁰ Ahmad, Saleem; Spengel, Steven H.; Barrish, Joel C.; DiMarco, John; Gougoutas, Jack. *Tetrahedron: Asymmetry* **1995**, *6*, 2893-4.
- ³¹ Pearson, William H.; Mans, Douglas M.; Kampf, Jeff W. *J. Org. Chem.* **2004**, *69*, 1235-1247.
- ³² Sassaman, Mark B.; Prakash, G. K. Surya; Olah, George A. *J. Org. Chem.* **1990**, *55*, 2016-18.
- ³³ Padwa, Albert; Straub, Christopher S. *J. Org. Chem.* **2003**, *68*, 227-239.
- ³⁴ Lattanzi, Alessandra; Senatore, Antonello; Massa, Antonio; Scettri, Arrigo. *J. Org. Chem.* **2003**, *68*, 3691-3694.
- ³⁵ Gal, J.; Folest, J. C.; Troupel, M.; Guittou, P.; Robin, Y. *New Journal of Chemistry* **1996**, *20*, 375-83.

Appendices

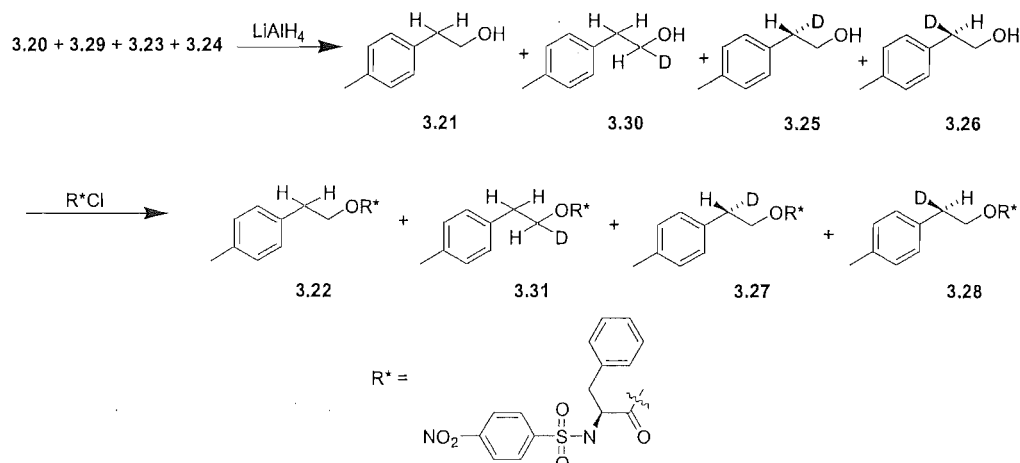
APPENDIX A - CALCULATION OF THE RATIO OF ALDEHYDES PRODUCED ON REARRANGEMENT OF β -MONO-DEUTERATED EPOXIDE

The ^1H and ^2H NMR integrals of the chiral ester formed from rearrangement product are used to determine the ratio of aldehydes produced in the epoxide rearrangement for β -deuterated epoxide by the method shown below. An example of the calculation is given for the $\text{BF}_3\cdot\text{OEt}_2$ catalysed rearrangement of enriched **3.1** (Scheme A.1).



Scheme A.1. $\text{BF}_3\cdot\text{OEt}_2$ catalysed rearrangement of enriched **3.1**.

The aldehyde products from the rearrangement were reduced and esterified with a chiral ester (Scheme A.2). The esters were analysed by ^2H NMR, to get the ratio of deuterium α : β to the ester oxygen and by ^1H NMR with $\text{Yb}(\text{hfc})_3$ chiral shift reagent to get the ratio of H_S : H_R hydrogen in the position β - to the ester oxygen (Table A.1).



Scheme A.2. Reduction and esterification of the epoxide rearrangement products.

Reaction	α ^2H NMR integral	β ^2H NMR integral	β H_S ^1H NMR integral	β H_R ^1H NMR integral
1	66.6	33.4	1	1.239

Table A.1. $\text{BF}_3 \cdot \text{OEt}_2$ catalysed rearrangement of **3.1**.

The ratio of esters **3.22**, **3.31**, **3.27** and **3.28** can be determined from the NMR data and is identical to the ratio of aldehydes **3.20**, **3.29**, **3.23** and **3.24**. Esters **3.22**, **3.31** and **3.28** contribute to the H_S proton signal, while **3.22**, **3.31** and **3.27** contribute to the H_R proton signal. The constant x is required to convert the ^1H NMR integral in arbitrary units into a fraction of total ester:

$$\mathbf{3.22} + \mathbf{3.31} + \mathbf{3.28} = 1x \quad (1)$$

$$\mathbf{3.22} + \mathbf{3.31} + \mathbf{3.27} = 1.239x \quad (2)$$

The amount of undeuterated ester is the same as the starting epoxide i.e. **3.22** = 10%. Only **3.31** has a deuterium α - to the ester oxygen and so the amount of **3.31** is obtained from the ^2H NMR integral, taking into account that 10% of the material is undeuterated: **3.31** = $66.6 \times 0.9 = 60\%$. Therefore **3.27** + **3.28** = 30%.

X can be determined by noting that the total number of hydrogen and deuterium atoms β -to the ester oxygen is 2:

$$1x + 1.239x + 0.3 = 2 \quad (3)$$

$$x = (2 - 0.30) / 2.239 = 0.7593 \quad (4)$$

The amount of **2.27** and **3.28** can then be obtained from (1), (2) and (4) above:

$$0.10 + 0.60 + \mathbf{3.28} = 1 * 0.7593$$

$$\mathbf{3.28} = 6\%$$

$$0.10 + 0.60 + \mathbf{3.27} = 1.239 * 0.7593$$

$$\mathbf{3.27} = 24\%$$

The amount of esters **3.22**, **3.31**, **3.27** and **3.28** and aldehydes **3.20**, **3.29**, **3.23** and **3.24** is given in Table A.2:

Reaction	3.20 (3.22)	3.29 (3.31)	3.23 (3.27)	3.24 (3.28)
1	10%	60%	24%	6%

Table A.2. Products from $\text{BF}_3 \cdot \text{OEt}_2$ catalysed rearrangement of enriched **3.1**.

APPENDIX B - CORRECTION FOR THE MINOR ISOMERS IN THE REARRANGEMENT OF β -MONO-DEUTERATED EPOXIDE

Methods for the synthesis of enriched β -mono-deuterated epoxide gave a mixture of epoxide deuterioisomers and undeuterated epoxide. For example, the synthesis of enriched **3.1** gave the following ratio of epoxides:

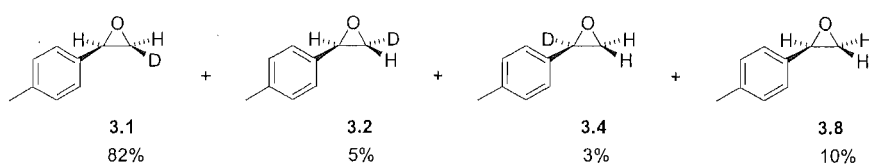


Figure B.1. Ratio of epoxides produced from synthesis of enriched **3.1**.

Aldehydes produced from the rearrangement of **3.2** and **3.4** must be subtracted from the reaction mixture in order to calculate the ratio of aldehydes that would be produced on rearrangement of a sample of pure **3.1**. Epoxide was rearranged with $\text{BF}_3 \cdot \text{OEt}_2$ and the rearrangement products were reduced, esterified and analysed by NMR (see Appendix A, Schemes A.1, A.2 and Table A.1).

The ratio of aldehydes produced in the $\text{BF}_3 \cdot \text{OEt}_2$ catalysed rearrangement of **3.2** and **3.4** is shown in Tables 3.12 and 3.6 respectively. The NMR signal produced by esters from the rearrangement of **3.2** and **3.4** is subtracted from values in Table A.1:

^2H NMR signal correction for the rearrangement of **3.4** (3.3% of deuterated epoxide):

Subtract 3.3% of epoxide giving rise to the β ^2H NMR signal:

$$\text{Corrected } \beta \text{ } ^2\text{H NMR integral} = 33.4 - 3.3 = 30.1$$

The relative ^2H NMR integral corrected for the presence of rearranged **3.4** is shown in Table B.1:

α ^2H NMR integral	β ^2H NMR integral
68.9	31.1

Table B.2. ^2H NMR integral of the rearrangement esters from the $\text{BF}_3\cdot\text{OEt}_2$ catalysed rearrangement of enriched **3.1**, corrected for the presence of **3.4**.

The ^2H NMR integrals are further corrected for the presence of rearranged **3.2** (See Chapter 3, Table 3.8). The integrals in Table B.1 are from the rearrangement of **3.1** and **3.2**. **3.2** accounts for 5.7% of **3.1+3.2**:

$$\text{Corrected } \alpha \text{ } ^2\text{H NMR integral} = 68.9\% - 0.057 \times 71.4\% = 64.8$$

$$\text{Corrected } \beta \text{ } ^2\text{H NMR integral} = 31.1\% - 0.057 \times 28.6\% = 29.5$$

The relative ^2H NMR integrals, corrected for rearranged **3.4** and **3.2** are shown in Table B.2:

α ^2H NMR integral	β ^2H NMR integral
68.7	31.3

Table B.2. ^2H NMR integral of the esters from rearrangement of enriched **3.1**, corrected for the products of rearranged **3.2** and **3.4**.

The ^1H NMR signal arising from rearranged **3.2** and **3.4** can be subtracted from the β H_S and H_R chiral shifted ^1H NMR integrals (44.6% : 55.4%) (Appendix A, Table A.1):

The integral for the ^1H NMR signal from esters **3.27** and **3.28** formed from rearrangement of **3.2** (Table 3.12) is subtracted from the data in Table A.1. 5% of the material is rearranged **3.2** and of this 6% gives **3.27** (contributing to the H_R signal) and 21% gives **3.28** (contributing to the H_S signal) (Table 3.12).

Corrected H_S 1H NMR signal = $44.6\% - 0.05 \times 21\% = 43.6\%$

Corrected H_R 1H NMR signal = $55.4\% - 0.05 \times 6\% = 55.1\%$

The H_S and H_R 1H NMR integrals for the rearrangement of enriched **3.1**, corrected for the presence of rearranged **3.2** are shown in Table B.3:

β H_S 1H NMR integral	β H_R 1H NMR integral
44.2	55.8

Table B.3. 1H NMR integrals for the products from rearrangement of enriched **3.1**, corrected for the presence of rearranged **3.2**.

The ratio of the β 1H NMR integrals can also be corrected for the presence of 3% of rearranged **3.4**. The ratio of esters **3.27** and **3.28** formed on rearrangement of **3.4** with $BF_3 \cdot OEt_2$ is shown in Table 3.6.

Corrected H_S 1H NMR signal = $44.2\% - 0.03 \times 47\% = 42.8\%$

Corrected H_R 1H NMR signal = $55.8\% - 0.03 \times 53\% = 54.2\%$

The final 1H NMR integrals for the rearrangement of a sample of pure **3.1** are shown in Table B.4:

β H_S 1H NMR integral	β H_R 1H NMR integral
44.1	55.9

Table B.4. 1H NMR integrals for the rearrangement of a sample of pure **3.1**.

The method outlined in Appendix A is used to obtain the ratio of esters/aldehydes that would be formed on rearrangement of a sample of pure **3.1** (Table B.5).

Reaction	H migration (3.29)	D migration with inversion of configuration (3.23)	D migration with retention of configuration (3.24)
1	69%	13%	18%

Table B.5. Ratio of aldehydes formed on the BF₃.OEt₂ catalysed rearrangement of pure 3.1.

The calculations were performed for each reaction automatically using an Excel spreadsheet.

APPENDIX C - CORRECTION FOR THE MINOR ISOMERS IN THE REARRANGEMENT OF α,β -*CIS*-DIDEUTERATED EPOXIDE

Synthesis of enriched α,β -*cis*-dideuterated epoxide gave a mixture of deuterioisomers:

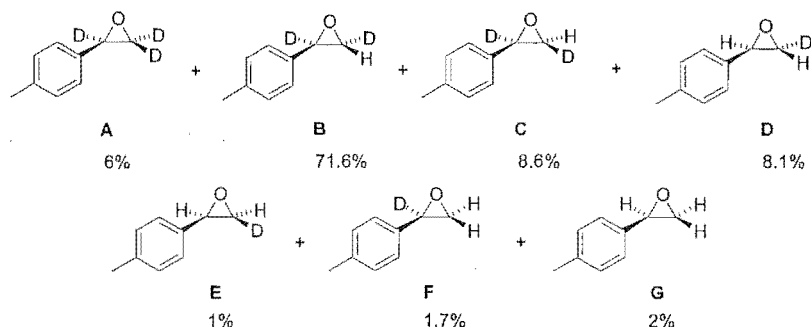


Figure C.1. Isomers from the synthesis of enriched **3.3**.

$\text{BF}_3 \cdot \text{OEt}_2$ catalysed rearrangement of the above mixture of epoxides gives the following mixture of aldehydes:

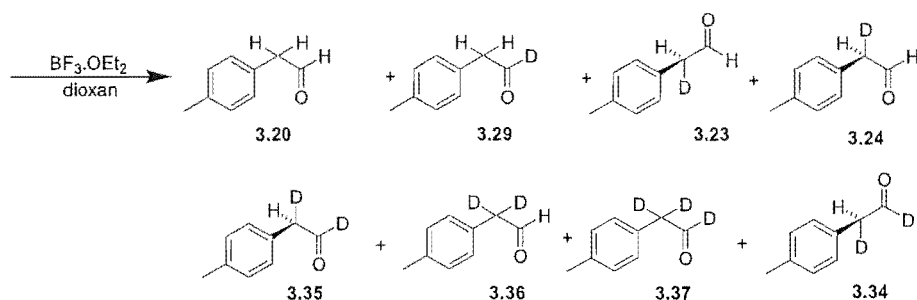
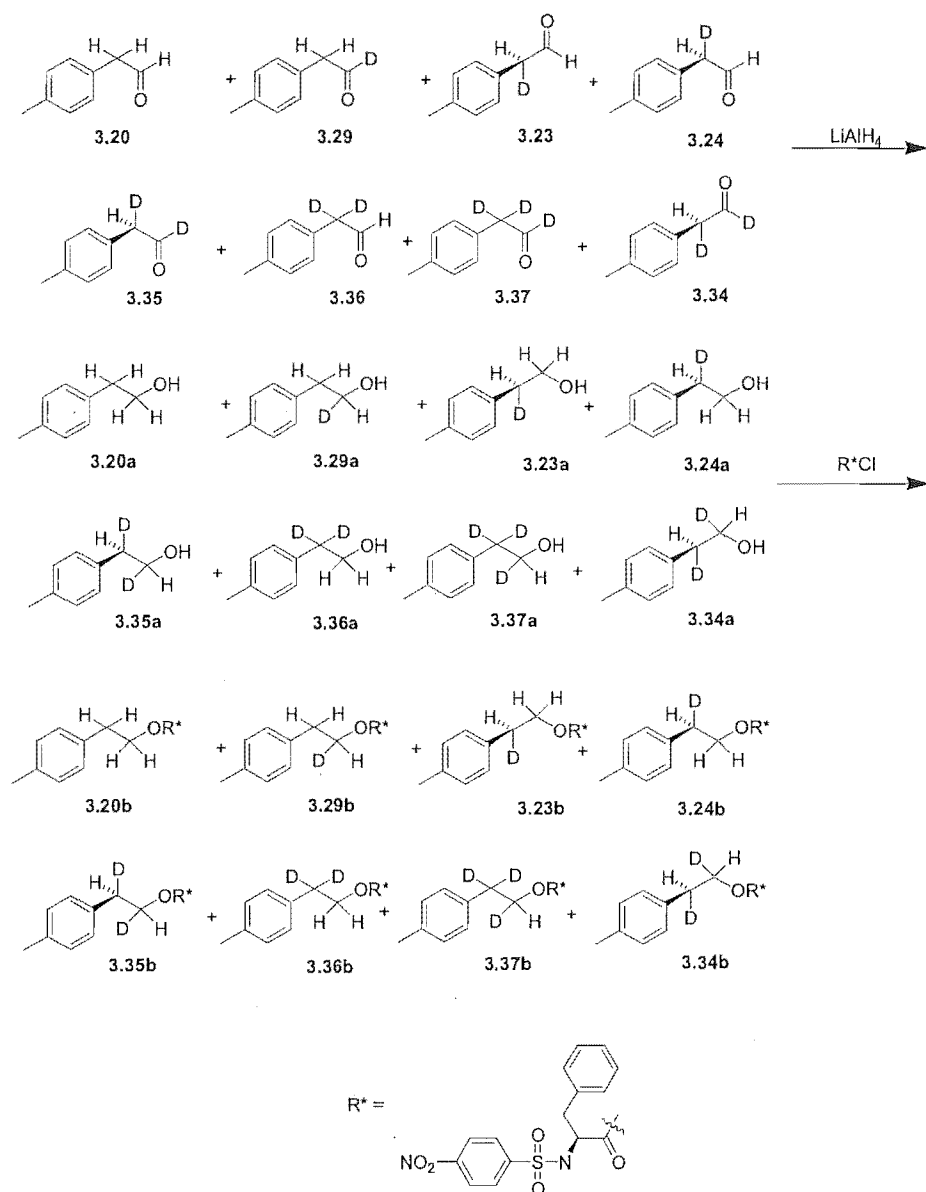


Figure C.2. Aldehydes produced by the $\text{BF}_3 \cdot \text{OEt}_2$ catalysed rearrangement of enriched **3.3**.

The aldehydes were reduced to alcohols and reacted with *N*-(4-nitrophenylsulfonyl)-*S*-phenylalanyl chloride to give chiral esters that were analysed by ^2H NMR and ^1H NMR spectroscopy in the presence of $\text{Yb}(\text{hfc})_3$ chiral shift reagent as described previously:



Scheme C.3. Reduction and esterification of the rearrangement products of enriched **3.3**.

^2H and chiral shifted ^1H NMR spectroscopy on the esters gave the following integral ratios for reaction 1:

α ^2H NMR integral	β ^2H NMR integral	β H_S ^1H NMR integral	β H_R ^1H NMR integral
1	1.8	3.03	1

Table C.1. Ratio of ^2H and ^1H NMR integrals obtained from ester derived from the $\text{BF}_3\cdot\text{OEt}_2$ rearrangement products of enriched **3.3**.

It is assumed that the ratio of esters **3.20b-3.34b** is the same as the ratio of aldehydes **3.20-3.34**. The ratio of aldehydes that would be produced on rearrangement of a sample of pure **3.3** is obtained by the method outlined below.

A parameter x is calculated that can be used to convert the ^2H NMR integrals, in arbitrary units into a number deuterium atoms in aldehyde (It has been shown that no deuterium is lost in the rearrangement, so the amount of deuterium in the aldehyde is the same as the amount of deuterium in epoxide):

$$\begin{aligned} (\% \alpha \text{ } ^2\text{H}) * x + (\% \beta \text{ } ^2\text{H}) * x &= 3 * (\% \mathbf{3.32}) + 2 * (\% \mathbf{3.3}) + 2 * (\% \mathbf{3.33}) + (\% \mathbf{3.2}) + (\% \mathbf{3.1}) + (\% \mathbf{3.4}) \\ 66.6x + 33.4x &= 3 * 6 + 2 * 72 + 2 * 9 + 8 + 1 + 2 \\ x &= 67.57 \end{aligned}$$

Where $\% \mathbf{3.1}$, $\% \mathbf{3.2}$ etc are the % of epoxide deuterioisomers **3.1** and **3.2** etc.

The deuterium signal coming from rearrangement of the minor isomers is subtracted from both the α and β ^2H NMR signal:

Let $\text{rng} \mathbf{3.1} = 0.3$, the amount of deuterium migration on rearrangement of epoxide deuterated *cis* to the aryl group from rearrangement of **3.1**.
And $\text{rng} \mathbf{3.2} = 0.27$, the amount of deuterium migration on rearrangement of epoxide deuterated *trans* to the aryl group from rearrangement of **3.2**.

$$\alpha \text{ } ^2\text{H signal from rearranged } \mathbf{3.4} = 1 * x - (\%A + \%C * (1 - \text{rng3.1}) + \%D * (1 - \text{rng3.2}) + \%E * (1 - \text{rng3.1})) = 1 * 67.57 - (6 + 8.6 * (1 - 0.3) + 8.1 * (1 - 0.27) + 1 * (1 - 0.3)) = 48.9$$

$$\beta \text{ } ^2\text{H signal from rearranged } \mathbf{3.4} = 1.8 * x - (2 * \%A + \%C * (1 + \text{rng3.1}) + \%D * \text{rng3.2} + \%E * \text{rng3.1} + \%F) = 1.8 * 67.57 - (2 * 6 + 8.6 * (1 + 0.3) + 8.1 * 0.27 + 1 * 0.3 + 1.7) = 94.3$$

The fraction of deuterium that has migrated is therefore:

$$D_{\text{migr}} = 1 - (2 / (48.9 + 94.3)) / 48.9 = 0.32$$

A correction is then made to the signal for the prochiral β - protons. The signal arising from compounds formed from rearrangement of the minor isomers determined based on the selectivity observed in the rearrangement of **3.1** and **3.2**. This is then subtracted from the overall signal.

A parameter z is determined to convert the integral in arbitrary units into a fraction of ester (aldehyde) present.

$$z = ((1 - D_{\text{migr}}) * \%B + (1 - \text{rng3.1}) * \%C + (1 + (1 - \text{rng3.2})) * \%D + (1 + (1 - \text{rng3.1})) * \%E + \%F + 2 * \%G) / (\beta \text{ H}_S \text{ } ^1\text{H NMR integral} + \beta \text{ H}_R \text{ } ^1\text{H NMR integral}) = 18.96$$

From rearrangement of **3.1**, **3.2**, and **3.4**, the facial selectivity for migration of the deuterium *cis* to the aryl group, *trans* to the aryl group and the overall selectivity for migration can be determined:

Fraction *cis* D migration with inversion (from **3.1**), $cisD_{\text{migr}} = 0.67$

Fraction *trans* D migration with inversion (from **3.2**), $transD_{\text{migr}} = 0.22$

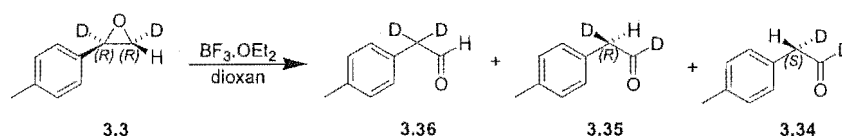
Overall facial selectivity for H migration (from **3.4**), $H_{\text{migr}} = 0.53$

Subtracting the signal arising from rearrangement of the minor isomers:

$$\beta H_{inv} = (\beta H_S \text{ } ^1\text{H NMR integral}) * z - ((1 - \text{rng3.1}) * \text{transD}_{migr} * \%C + (1 - \text{rng3.2} * \text{transD}_{migr}) * \%D + (1 - \text{rng3.1} * \text{cisD}_{migr}) * \%E + H_{migr} * \%F + \%G) = 3.03 * 18.96 - ((1 - 0.3) * 0.22 * 8.6 + (1 - 0.27 * 0.22) * 8.1 + (1 - 0.3 * 0.67) * 1 + 0.53 * 1.7 + 2) = 44.76$$

$$\beta H_{retn} = (\beta H_R \text{ } ^1\text{H NMR integral}) * z - ((1 - \text{rng3.1}) * (1 - \text{transD}_{migr}) * \%C + (1 - \text{rng3.2} * (1 - \text{transD}_{migr})) * \%D + (1 - \text{rng3.1} * (1 - \text{cisD}_{migr})) * \%E + (1 - H_{migr}) * \%F + \%G) = 1 * 18.96 - ((1 - 0.3) * (1 - 0.22) * 8.6 + (1 - 0.27 * (1 - 0.22)) * 8.1 + (1 - 0.3 * (1 - 0.67)) * 1 + (1 - 0.53) * 1.7 + 2) = 4.175$$

These are the NMR signals that would be obtained on rearrangement of a sample of pure **3.3**. The aldehyde produced from rearrangement of a sample of pure **3.3** that would give rise to these signals can then be calculated:



Scheme C.4. Rearrangement of a sample of pure **3.3**.

$$\mathbf{3.36} \text{ (D migration)} = D_{migr} = 0.32$$

$$\mathbf{3.35} \text{ (H migration with inversion of configuration)} = (1 - D_{migr}) * (\beta H_{inv} / (\beta H_{inv} + \beta H_{retn})) = (1 - 0.32) * (44.76 / (44.76 + 4.175)) = 0.61$$

$$\mathbf{3.34} \text{ (H migration with retention of configuration)} = (1 - D_{migr}) * (\beta H_{retn} / (\beta H_{inv} + \beta H_{retn})) = (1 - 0.32) * (4.175 / (44.76 + 4.175)) = 0.07$$

The uncorrected NMR data for the $\text{BF}_3 \cdot \text{OEt}_2$ and LiClO_4 catalysed rearrangements of enriched **3.3** are shown below:

Reaction	α ^2H NMR integral	β ^2H NMR integral	β H_S ^1H NMR integral	β H_R ^1H NMR integral
1	1	1.8	3.03	1
2	1	1.9	2.25	1
3	1	1.7	2.53	1

Table C.2. NMR data for the esters from the $\text{BF}_3\cdot\text{OEt}_2$ catalysed rearrangement of **3.3**.

Reaction	α ^2H NMR integral	β ^2H NMR integral	β H_S ^1H NMR integral	β H_R ^1H NMR integral
1	1	2.0	3.35	1
2	1	2.0	4.63	1
3	1	2.4	3.00	1

Table C.3. NMR data for the esters from the LiClO_4 catalysed rearrangement of **3.3**.